Investigating Mechanisms of Reductive Chlorinated Hydrocarbon Degradation with Compound-Specific Isotope Analysis

Dissertation

der Mathematisch-Naturwissenschaftlichen Fakultät

der Eberhard Karls Universität Tübingen

zur Erlangung des Grades eines

Doktors der Naturwissenschaften

(Dr. rer. nat.)

vorgelegt von

M. Sc. Benjamin Matthäus Heckel

aus Füssen

Tübingen

2017

Gedruckt mit Genehmigung der Mathematisch-Naturwissenschaftlichen Fakultät der Eberhard Karls Universität Tübingen.

Tag der mündlichen Qualifikation:	25.01.2018
Dekan:	Prof. Dr. Wolfgang Rosenstiel
1. Berichterstatter:	Prof. Dr. Martin Elsner
2. Berichterstatter:	Prof. Dr Stefan Haderlein
3. Berichterstatter:	Prof. Dr. Lynn Kamerlin

Dank

In erster Linie möchte ich meinem Doktorvater Prof. Dr. Martin Elsner danken für die hervorragende Betreuung über die letzten 3 Jahre. Sein Optimismus, Engagement sowie die kreativen und äußerst hilfreichen mechanistischen Diskussionen haben sehr zum Gelingen dieser Arbeit beigetragen. Zudem ließen das tolle Forschungsumfeld und die hervorragende Laborausstattung keine Wünsche offen.

Ich bedanke mich außerdem bei Herrn Prof. Dr. Stefan Haderlein für die Zweitbetreuung und sehr hilfreichen Kommentare innerhalb des Thesis Committees.

I am very grateful to Prof. Dr. Kristopher McNeill for his helpful ideas and his support during my stay in Zürich. Thanks also to Dr. Vivian Lin for the help and warm welcome in Zürich.

Weiterer Dank gilt:

Den Ingenieuren/ Technikern Harald Lowag, Ramona Brejcha und Martina Höche für die Hilfe bei technischen Problemen und wertvolle Unterstützung, was die Laborarbeit deutlich erleichtert hat.

Meinen Bürokollegen Benno und Christina für die tolle Atmosphäre, die amüsanten Gespräche und deren stete Hilfe. Den momentanen und ehemaligen Kollegen aus der Isotopenchemie Gruppe Armin, Heide, Alex, Aileen, Marina, Medhi, Sviatlana und Kankana für die hilfreiche Zusammenarbeit. Zudem bedanke ich mich bei Judith und Anne für die unterhaltsamen Kaffeekränzchen, die mir den Arbeitsalltag verschönert haben.

Aus ganz Herzen danke ich meinen Eltern Wilhelm und Angela für den unendlichen Rückhalt und die Unterstützung, die Sie mir in jeglicher Form zukommen ließen. Meinen Geschwistern Miriam, Dominik und seiner Freundin Nici, die in jeder Situation hinter mir stehen und immer für mich da sind. Klarissa für ihre Liebe, Unterstützung und Rückhalt, wodurch Sie mir die Zeit in München wesentlich verschönert hat.

Table of Contents

ZUSAMMENFASSUNG I

SUMMARY III

1. GENERAL INTRODUCTION - 1 -

1.1 WATER CONTAMINATION BY ORGANIC CHEMICALS - 1 -

1.2 IDENTIFICATION OF THE REACTION MECHANISM WITH COMPOUND SPECIFIC ISOTOPE ANALYSIS - 3 -

1.2.1 REDUCTIVE DEHALOGENATION – STATE OF ART - 3 -

1.2.2 CONCEPT OF CSIA - 3 -

1.2.3 MULTI ELEMENT ISOTOPE ANALYSIS - 5 -

1.3 OBJECTIVES - 6 -

2. COMPOUND-SPECIFIC CHLORINE ISOTOPE ANALYSIS OF TETRACHLOROMETHANE AND TRICHLOROMETHANE BY GC-IRMS VS. GC-QMS: METHOD DEVELOPMENT AND EVALUATION OF PRECISION AND TRUENESS - 9 -

2.1. ABSTRACT - 10 -

2.2. INTRODUCTION - 11 -

2.3. EXPERIMENTAL SECTION - 13 -

2.3.1. CHEMICALS - 13 -

2.3.2. ABIOTIC DEGRADATION OF CCL_4 WITH SODIUM FORMATE - 13 -

2.3.3. ABIOTIC DEGRADATION OF $CHCL_3$ WITH CAST IRON AT PH 12 - 13 -

2.3.4. STABLE CARBON ISOTOPE ANALYSIS BY GC-C-IRMS - 14 -

2.3.5. STABLE CHLORINE ISOTOPE ANALYSIS BY GC-IRMS IN MUNICH - 15 -

2.3.6. CONCENTRATION AND STABLE CHLORINE ISOTOPE MEASUREMENTS WITH GC-QMS - 16 -

2.3.7. EVALUATION OF CHLORINE ISOTOPE DATA - 17 -

2.4. RESULTS AND DISCUSSION - 20 -

2.4.1. ACQUISITION PARAMETERS FOR GC-QMS ANALYSIS - 20 -

2.4.2. AMOUNT DEPENDENCY ("LINEARITY") OF CHLORINE ISOTOPE ANALYSIS OF CCL_4 BY GC-QMS AND GC-IRMS - 21 -

2.4.3. AMOUNT DEPENDENCY ("LINEARITY") OF CHLORINE ISOTOPE ANALYSIS OF $CHCL_3$ BY GC-IRMS - 23 -

2.4.4. AMOUNT DEPENDENCY ("LINEARITY") OF CHLORINE ISOTOPE ANALYSIS OF $CHCL_3$ BY GC-QMS. - 25 -

2.4.5. TRUENESS OF CHLORINE ISOTOPE ANALYSIS OF CCl_4 AND $CHCl_3$ BY GC-QMS AND GC-IRMS - 27 -
2.5. CONCLUSION - 30 -
3. REDUCTIVE OUTER-SPHERE SINGLE ELECTRON TRANSFER IS AN EXCEPTION RATHER THAN THE RULE IN NATURAL AND ENGINEERED CHLORINATED ETHENE DEHALOGENATION - 33 -
3.1. ABSTRACT - 34 -
3.2. INTRODUCTION - 35 -
3.3. MATERIALS & METHODS - 39 -
3.3.1. CHEMICALS - 39 -
3.3.2. REACTIONS IN WATER - 39 -
3.3.3. REACTIONS IN AN ORGANIC SOLVENT - 40 -
3.3.4. ANALYTICAL METHODS - 41 -
3.4. RESULTS AND DISCUSSION - 42 -
3.4.1. AQUEOUS REDUCTIVE OS-SET REAGENTS INDUCED CHLORINE ISOTOPE EFFECTS IN CHLOROFORM, BUT NOT IN CHLORINATED ETHENES - 42 -
3.4.2. CHLORINE ISOTOPE EFFECTS WERE PARTLY RECOVERED WHEN CHLORINATED ETHENES WERE REACTED WITH OS-SET REAGENTS IN AN ORGANIC SOLVENT - 44 -
3.4.3. OUR OBSERVATIONS ARE CONSISTENT WITH A DISSOCIATIVE OS-SET IN CHLORINATED ALKANES COMPARED TO A STEPWISE PROCESS IN CHLORINATED ETHENES - 45 -
3.4.4. SYSTEMATICALLY DIFFERENT ISOTOPE FRACTIONATION TRENDS SUGGEST THAT OS-SET IS NOT A COMMON MECHANISM IN NATURAL AND ENGINEERED CE REDUCTIVE DEHALOGENATIONS - 50 -
3.5. CONCLUSION - 53 -
4. CHLORINATED ETHENE REACTIVITY WITH VITAMIN B12 IS GOVERNED BY COBALAMIN CHLOROETHYLCARBANIONS AS CROSSROADS OF COMPETING PATHWAYS - 55 -
4.1. ABSTRACT - 56 -
4.2. INTRODUCTION - 57 -
4.3. MATERIALS & METHODS - 62 -
4.3.1. CHEMICALS - 62 -
4.3.2. KINETICS, ISOTOPE EFFECTS AND PRODUCT FORMATION IN DEHALOGENATION OF CHLORINATED ETHENES BY VITAMIN B_{12} AT DIFFERENT PH - 62 -
4.3.3. EXPERIMENTS TO DETECT COMPLEX FORMATION BETWEEN VITAMIN B12 AND TCE BY DIRECT INJECTION-MASS SPECTROMETRY (DI-MS) AND ANALYSIS OF MASS BALANCE DEFICITS - 62 -

4.3.4. Analytical Methods - 63 -
4.4. Results and Discussion - 63 -
4.4.1. Isotope effects and reactivity trends indicate different reaction mechanisms for PCE and cis-DCE - 63 -
4.4.2. Isotope effects and reactivity trends indicate a pH-dependent mechanistic shift in reaction of TCE - 65 -
4.4.3. pH-dependent product distribution supports a mechanistic shift in TCE transformation - 68 -
4.4.4. Mass balance deficits indicate formation of reversible and irreversible Vitamin B_{12} - TCE complexes - 69 -
4.4.5. High resolution mass spectra give evidence of cob(II)alamin chloroalkyl and chlorovinyl complexes - 71 -
4.4.6. Experimental evidence is not consistent with initial electron transfer (either inner- or outer sphere) - 72 -
4.4.7. The occurrence of two pathways cannot be explained by alkyl cob(I)alamin complexes as common intermediates - 73 -
4.4.8. Cobalamin carbanions as key intermediates can explain experimental observations - 75 -
4.4.9. Implications for reactivity and product formation in biodegradation of chlorinated ethenes - 78 -
4.5. Conclusion - 81 -
5. GENERAL CONCLUSIONS - 83 -
APPENDIX - 89 -
A. Carbon and Chlorine Isotope Fractionation Patterns Associated with Different Engineered Chloroform Transformation Reactions - 89 -
B. Supporting Information of Chapter 2 - 101 -
B.1. Experimental section - 101 -
C. Supporting Information of Chapter 3 - 103 -
C.1. Experimental section - 103 -
C.2. Results and Discussion - 107 -
D. Supporting Information of Chapter 4 - 111 -
D.1. Materials & Methods - 111 -
D.2. Results and Discussion - 117 -
ABBREVIATIONS - 127 -
REFERENCES - 131 -

Zusammenfassung

Chlorierte Kohlenwasserstoffe, wie chlorierte Methane und Ethene, sind in großen Mengen hergestellte chemische Produkte, die regelmäßig als giftige Schadstoffe in der Umwelt detektiert werden. Sanierungsmaßahmen verwenden oft die reduktive Dechlorierung durch Bakterien oder reduzierende Chemikalien. Jedoch beobachtet man bei Organismen häufig, dass der Abbau bei toxischen Zwischenprodukten stoppt und keine vollständige Dechlorierung erreicht wird. Bisher ist der Grund dafür nicht bekannt. Aufklärungsversuche mit mechanistischen Studien und Interpretationen waren nicht aufschlussreich, da zuletzt mehrere Mechanismen für den Abbau in Frage kommen konnten. Aus diesem Grund wurde in dieser Arbeit die substanzspezifische Isotopenanalytik, ein viel versprechender Ansatz zur Identifikation von Reaktionsmechanismen, mit chemischen Modelsystemen kombiniert, um reduktive Abbaumechanismen zu identifizieren.

Die Chlorisotopenanalytik für chlorierte Ethene wurde im Jahr 2006 etabliert und wird seitdem regelmäßig eingesetzt, um das Schicksal dieser Substanzen im Grundwasser zu untersuchen und Reaktionsmechanismen zu identifizieren. Allerdings gab es bisher keine etablierte und geprüfte Methode zur Messung der Chlorisotope von chlorierten Methanen. Daher wurde im ersten Teil dieser Arbeit eine Methode zur Chlorisotopenanalytik für Tetrachlormethan und Trichlormethan für Gas-Chromatographie – quadrupole Massenspektrometrie (GC-qMS) und Gas-Chromatographie – Isotopenverhältnis Massenspektrometrie (GC-IRMS) entwickelt. Beide Methoden wurden auf Präzision und Richtigkeit der Werte miteinander verglichen. Somit war es zum ersten Mal möglich, Informationen von Kohlenstoff- und Chlorisotopen zu kombinieren und einen Doppel-Element Isotopen Plot für den reduktiven Trichlormethan Abbau zu generieren.

Die direkte Untersuchung des Abbaumechanismus von chlorierten Ethenen durch Organismen erweist sich als sehr schwierig, da eine Vielzahl von Prozessen in dem Abbau involviert wie Diffusion durch die Zelle, Bindung am Enzym etc., welche die Interpretation des Mechanismus verkomplizieren. Aus diesem Grund werden häufig vereinfachte Modelsysteme (wie Abbau von chlorierten Ethenen durch reine Enzyme oder nur den Cofactor wie z.B. Vitamin B12) gewählt, um den Mechanismus zu untersuchen. In dieser Arbeit wurde der enzymatische Cofaktor Vitamin B12 (welcher das aktive Zentrum in allen bisher identifizierten reduktiven Dehalogenasen bildet) als Modelsystem gewählt.. Trotz vieler Studien mit diesem Modelsystem, konnte der für den Abbau verantwortliche

Reaktionsmechanismus noch nicht aufgedeckt werden. Basierend auf diesen Ergebnissen und den vorgeschlagenen Reaktionsmechanismen für dieses System (1. Outer-Sphere oder Inner-Sphere Ein-Elektronen-Transfer 2. Nucleophile Substitution 3. Nucleophile Addition), wurden zuerst die Isotopenfraktionierung des Outer-Sphere Ein-Elektronen-Transfer (OS-SET) für Tetra-, Tri- und *cis*-Dichlorethen (PCE, TCE und *cis*-DCE) untersucht. Die OS-SET Reaktion wurde mit verschiedenen Ein-Elektronen-Transfer Reagenzien (z.B. CO_2 Radikal Anionen) in Wasser und organischen Lösungsmittel simuliert. Bei den durchgeführten Reaktionen wurde keine Chlorisotopenfraktionierung festgestellt, was den OS-SET für die Reaktion von chlorierten Ethenen mit Organismen und Vitamin B12 ausschließt, sondern auch darauf hinweist, dass der OS-SET Mechanismus ebenfalls für die reduktive Dechlorierung von chlorierten Ethenen durch nullwertiges Eisen nicht überwiegt. In letzter Instanz konnte durch Messung von Kohlenstoff- und Chlorisotopeneffekten ein unterschiedlicher Mechanismus für die Reaktion von PCE und *cis*-DCE mit Vitamin B12 aufgedeckt werden, sowie ein sich verändernder Mechanismus für den TCE Abbau in Anhängigkeit vom pH-Wert. Basierend auf Kohlenstoff-, Chlor- und Wasserstoffisotopeneffekten, pH abhängiger Reaktionskinetik und der Produkteversteilung des TCE Abbaus, konnte ein Reaktionsmechanismus nachgewiesen werden, der zwei mögliche Reaktionswege beinhaltet 1. Addition-Eliminierung 2. Addition-Protonierung. Durch Defizite in der Massenbilanz konnten irreversible und reversible Cobalamin-Substrat Komplexe und durch hochauflösende Massenspektroskopie mögliche Strukturen von Chloralkyl- und Chlorvinylkomplexen detektiert werden. Die experimentellen Daten führten schließlich zu dem Ergebnis, dass der initiale Elektronen-Transfer oder die Bildung von Alkyl- oder Vinylkomplexen nicht der Schnittpunkt der beiden Reaktionspfade ist. Hingegen konnte gezeigt werden, dass Cobalamin-Chlorcarbanionen die Schlüsselspezies darstellen. Durch die Eliminierung von Chlorid bilden diese Vinylkomplexe (was die Kinetik und Produkteverteilung bei hohen pH-Wert erklärt) und durch Protonierung weniger reaktive Alkylkomplexe (was wiederum die Kinetik und Produkteverteilung bei niedrigen pH-Wert erklärt). Des Weiteren deuten starke Indizien darauf hin, dass PCE nur über Addition-Eliminierung reagiert und *cis*-DCE nur über Addition-Protonierung. Bei Übertragung dieser Mechanismen auf Biosysteme würde dies implizieren, dass Enzyme, die über Addition-Eliminierung reagieren, kein *cis*-DCE abbauen können, was auch eine mögliche Erklärung dafür liefert, weshalb der Abbau oft bei *cis*-DCE stoppt

Summary

Chlorinated hydrocarbons, such as chlorinated methanes and ethenes, are large-scale industrial products and frequently detected in the environment as toxic contaminants. As remediation approach the reductive dechlorination through bacteria or reducing agents is commonly applied. However, for organisms it is often observed that the degradation stops at toxic intermediates and no full dechlorination is achieved. The reason why degradation stops is not understood so far and even the elucidation with mechanistic experiments and interpretation were ultimately not successful because until today multiple reaction mechanisms are plausible candidates for the degradation. Therefore, compound specific isotope analysis, a promising tool for identifying reaction mechanisms was combined with chemical model systems to identify the reductive dechlorination mechanisms in this thesis.

Chlorine isotope measurement for chlorinated ethenes (CEs) became accessible in 2006 and is frequently used to follow the fate of CEs in groundwater and to identify their reaction mechanisms. However, an established and verified method for chlorine isotope measurement of chlorinated methanes was not available. Therefore, in first instance, a method for chlorine isotope analysis of tetrachloromethane and trichloromethane was realized for Gas Chromatography - quadropol Mass Spectrometry (GC-qMS) and Gas Chromatography - Isotope Ratio Mass Spectrometry (GC-IRMS) and both methods were compared in points of precision and trueness. Thus, for the first time it became possible to combine information from carbon and chlorine isotope values to form a dual element isotope plot for reductive trichloromethane degradation.

Direct investigation of the reaction mechanism of chlorinated ethene degradation by organisms is no simple task, because processes like diffusion through the cell membrane or binding at the enzyme complicate the interpretation of the mechanism. Therefore, often simplified model systems such as degradation of chlorinated ethenes by pure enzymes or the enzymatic cofactor vitamin B12 are used. The enzymatic cofactor vitamin B12 (which lies at the heart of practically all reductive dehalogenases identified to date) was chosen as model system for this thesis. . Despite numerous studies which investigated this model system, the prevailing mechanism still remains elusive. Based on these results and the suggested reaction mechanisms for this system (1. Outer-Sphere or Inner-Sphere Single Electron Transfer 2. Nucleophilic Substitution 3. Nucleophilic Addition), first the isotope fractionation of the Outer-Sphere Single Electron Transfer (OS-SET) mechanism was investigated for tetra-, tri and cis-dichloroethene. The OS-SET reaction was simulated using different single electron

transfer reagents (e.g. CO_2 radical anions) in water and organic solvent. Through the absence of chlorine isotope effects the OS-SET reaction for CEs by organism and vitamin B12 could be ruled out and furthermore it was indicated that the OS-SET reaction does not prevail for reductive dechlorination of CEs by zero valent iron (ZVI).

In last instance, carbon and chlorine isotope effects revealed a mechanistic shift for PCE ($\varepsilon^{37}Cl$ = -4.0‰) and *cis*-DCE ($\varepsilon^{37}Cl$ = -1.5‰) reaction with vitamin B12 and a pH dependent shift for TCE (from $\varepsilon^{37}Cl$ = -5.2‰ at pH 12 to $\varepsilon^{37}Cl$ = -1.2‰ at pH 5). Based on carbon-, chlorine- and hydrogen isotope effects, pH-dependent shifts in reaction rates and TCE product distribution the existence of two possible pathways (1. addition-elimination, 2. addition-protonation) was narrowed down. Reversible and irreversible cobalamin-substrate association was detected by mass balance deficits, whereas possible structures of chloroalkyl and chlorovinyl cobalamin complexes could be analyzed by high-resolution mass spectrometry. By combining experimental evidence it was revealed that initial electron transfer or alkyl or vinyl complexes as crossroads of both pathways are not consistent with experimental observations. In contrast, the formation of cobalamin chlorocarbanions is supported as key intermediates, where chloride elimination produces vinyl complexes (explaining rates and products of TCE at high pH) and protonation generates less reactive alkyl complexes (explaining rates and products of TCE at low pH).

Furthermore, circumstantial evidence indicates that PCE reacts only via addition-elimination and *cis*-DCE only via addition-protonation. Transferring these results into biosystems implies that enzymes which react via the addition-elimination cannot degrade *cis*-DCE. Finally this fact can provide a possible answer why degradation often stops at the step of *cis*-DCE.

Declaration according to § 5 Abs. 2 No. 8 of the PromO of the Faculty of Science

-Share in publications done in team work-

List of Publications:

1. Heckel, B.; Rodríguez-Fernández, D.; Torrentó, C.; Meyer, A.; Palau, J.; Domènech, C.; Rosell, M.; Soler, A.; Hunkeler, D.; Elsner, M.; Compound-specific Chlorine Isotope Analysis of Tetrachloromethane and Trichloromethane by GC-IRMS vs. GC-qMS: Method Development and Evaluation of Precision and Trueness, *Anal. Chem.* **2017**, 89, 3411−3420
2. Heckel, B.; Cretnik, S.; Kliegman, S.; Shouakar-Stash, O.; McNeill, K.; Elsner, M.; Reductive Outer-sphere Single Electron Transfer Is an Exception Rather than the Rule in Natural and Engineered Chlorinated Ethene Dehalogenation, *Environ. Sci. Technol.* **2017**, 51, 9663−9673
3. Heckel, B.; McNeill, K.; Elsner, M.; Chlorinated Ethene Reactivity with Vitamin B12 Is Governed by Cobalamin Chloroethylcarbanions as Crossroads of Competing Pathways, *ACS Catal.* **2018**, 8, 3054−3066

Nr.	**Accepted for publication yes/no**	**Number of all authors**	**Position of the candidate in list of authors**	**Scientific ideas of candidate (%)**	**Data generation by candidate (%)**	**Analysis and Interpretation by candidate (%)**	**Paper writing by candidate (%)**
1	yes	10	1	60-70	90	80-90	80
2	yes	6	1	80	70	90	55
3	yes	3	1	60-70	100	70-80	55

1.

General Introduction

1.1 Water contamination by organic chemicals

The worldwide growing demand for water supply is one of the most challenging tasks for next generations. On the one hand, a growing population increases the demand for clean water and on the other hand, increasing pollution of water through organic chemicals further aggravate water scarcity problem [1]. Chlorinated hydrocarbons are one of the major types of contaminants. These chemicals are used as dry cleaning agents, softeners for plastic, solvents and refrigerants [2, 3]. Two of the most prominent pollutants in this group are chlorinated methanes and ethenes (CEs). Considering them as inert and unproblematic led to improper handling and industrial disposal, resulting in thousands of hazardous waste sites worldwide. In the priority list of hazardous substances from 2015 of the U.S. Environmental Protection Agency three of these chemicals are ranked in the top twenty (vinyl chloride (4); trichloromethane (11); trichloroethene (16)) [4, 5].

Their toxic nature originates from their chlorine substituents which make them reactive towards metabolic bioactivation and are the cause for their mutagenic property [6]. Through complete dehalogenation non-toxic hydrocarbons can be produced, what was intriguingly observed in groundwater ecosystems. Stepwise dechlorination of these substances was detected by microorganisms which use chlorinated hydrocarbons as electron acceptor what is called "dehalorespiration" [7]. In this process chlorine is stepwise substituted by hydrogen (hydrogenolysis; Figure 1). However, only few organisms can achieve complete dehalogenation to non-toxic end products, often they stop at the step of *cis*-dichloroethene (*cis*-DCE) or vinyl chloride (VC)[8] for chlorinated ethenes and at dichloromethane for chlorinated methanes [9-11]. This fact aggravates the problem of contamination because *cis*-DCE and VC are more toxic than their parent compound. In general remediation of CEs can be approached with different technologies. One possibility is the addition of dehalogenating bacteria (bioaugmentation); a second one is the enhancement of the dehalogenation activity of organisms through addition of organics (biostimulation) [12]. Beside the degradation of chlorinated ethenes by organisms, the installation of permeable reactive barriers of zero valent iron (ZVI) is a broadly implemented removal technology. Reducing CEs by ZVI is very efficient and operates, beside the stepwise hydrogenolysis, with vicinal ß-elimination as a second reduction pathway, [13-15]. However, the incomplete removal can still be observed with these remediation approaches. Therefore, the identification of the reaction mechanism is of great interest, to understand why complete dehalogenation is not achieved and how it can be improved.

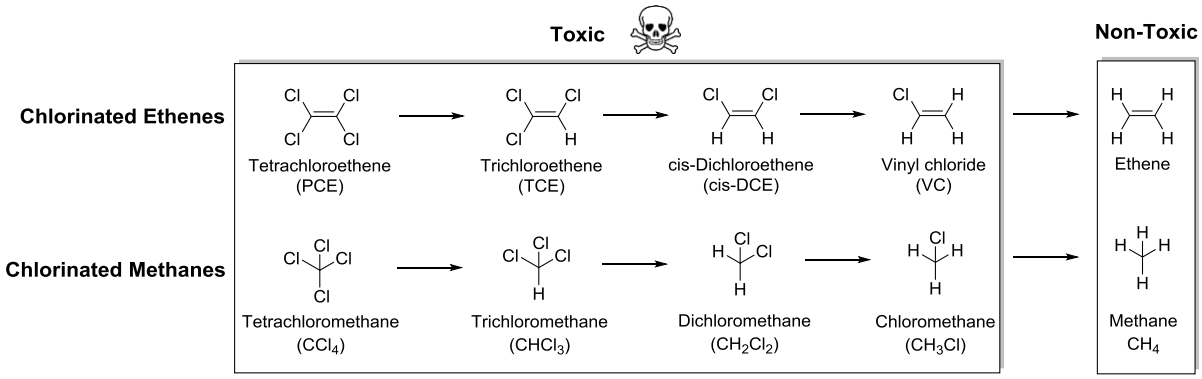

Figure 1. Stepwise reductive dechlorination of chloroethenes and chloromethanes by hydrogenolysis

1.2 Identification of the reaction mechanism with compound specific isotope analysis

1.2.1 Reductive dehalogenation – state of art

To improve remediation strategies in order to achieve complete detoxification of contaminated sites, great interest is directed towards the reaction mechanism of reductive dehalogenation. Therefore, in recent years this aim was addressed by a lot of studies using pure organisms, enrichment cultures, purified dehalogenase enzymes, coenzyme Vitamin B12 and chemical model systems which mimic such dehalogenation reactions. Numerous investigations focused on the enzymatic cofactor vitamin B12 which is present in almost all reductive dehalogenases identified to date [16]. Nevertheless, the reaction mechanisms are still incompletely understood. However, measuring multi element isotope effects of particular elements (e.g. $^{37}Cl/^{35}Cl$, $^{13}C/^{12}C$, $^{2}H/^{1}H$) is an emerging approach which has the potential to close this knowledge gab.

1.2.2 Concept of CSIA

Measuring kinetic isotope effects (KIE) can provide the information which is necessary to identify a reaction mechanism. Heavy and light isotopes show an unequal reaction behavior which can be expressed through the KIE (Equation 1). Primary isotope effects are observed through the difference in reaction rates of molecules containing heavy (e.g. ^{13}C) and light isotopes (e.g. ^{12}C). The mass difference of these isotopologues affects the vibration energies what leads to different zero point energies (ZPEs). Consequently, different activation energies are necessary to reach the transition state.

$$\left(\frac{^{l}k}{^{h}k}\right) = KIE \qquad (1)$$

Here ^{l}k and ^{h}k are the reaction rate of light and heavy isotopologues. Furthermore, secondary isotope effects can also be detected at atoms next to the reaction position which do not directly take part in the chemical reaction. But their mass also has an effect on the

vibrational energies. Degradation reactions typically cause normal KIE effects which means that light isotopes react faster than heavy ones. However, there are also observations were heavy isotopes reacted faster what resulted in an inverse isotope effect [17]. Through the reflection of these transition state properties, KIEs make it possible to pinpoint reaction mechanisms.

The changes in isotopic composition can be analyzed through coupling of a gas chromatograph with an isotope ratio mass spectrometer (GC-IRMS). Analytical advances[18-20] made it possible to measure compound-specific isotope ratios of single chlorinated compounds (e.g., PCE, TCE) at their natural isotopic abundance in chemical model reactions and natural samples. At natural abundance such isotope ratios ($^{13}C/^{12}C$, $^{37}Cl/^{35}Cl$ and $^{2}H/^{1}H$) are expressed as difference relative to an international reference material by the delta notation:

$$\delta^{13}C = \frac{(^{13}C/^{12}C_{Sample} - ^{13}C/^{12}C_{S\tan dard})}{^{13}C/^{12}C_{S\tan dard}} \quad (2)$$

$$\delta^{37}Cl = \frac{(^{37}Cl/^{35}Cl_{Sample} - ^{37}Cl/^{35}Cl_{S\tan dard})}{^{37}Cl/^{35}Cl_{S\tan dard}} \quad (3)$$

$$\delta^{2}H = \frac{(^{2}H/^{1}H_{Sample} - ^{2}H/^{1}H_{S\tan dard})}{^{2}H/^{1}H_{S\tan dard}} \quad (4)$$

$$\Delta\delta^{13}C = \delta^{13}C - \delta^{13}C_{initial} \quad (5)$$

$$\Delta\delta^{37}Cl = \delta^{37}Cl - \delta^{37}Cl_{initial} \quad (6)$$

$$\Delta\delta^{2}H = \delta^{2}H - \delta^{2}H_{initial} \quad (7)$$

Here, the isotope ratios of international reference standard ($^{13}C/^{12}C_{Standard}$) and sample ($^{13}C/^{12}C_{Sample}$) and the isotope values at the beginning of a reaction ($\delta^{13}C_{inital}$) and a given time-point ($\delta^{13}C$) are used, respectively. As international reference standards, Vienna Pee Dee Belemite (VPDB) is used for carbon and Standard Mean Ocean Chloride (SMOC) for chloride. Through these standards, isotope measurements in different laboratories can be compared on an absolute scale. According to the Rayleigh equation [21], isotope effects can be evaluated using the change of isotope values at natural abundance [22].

$$\delta^{13}C = \delta^{13}C_{initial} + [\varepsilon_C \cdot \ln f] \quad (8)$$

In Equation 8 f expresses the concentration at a given time-point divided through the concentration at the beginning. ε_C is the resulting enrichment factor which symbolizes the difference in transformation rates of light and heavy isotopes of a molecule and which is equivalent to a compound specific KIE. Analogous equations are valid for chlorine and hydrogen using ^{37}Cl and ^{35}Cl or ^{2}H and ^{1}H in equation 8.

1.2.3 Multi element isotope analysis

Trough combining the isotope changes of two elements dual element isotope plots can be formed (e.g. $\lambda = \Delta\delta^{13}C/\Delta\delta^{37}Cl$). These plots combine the information of two elements and provide an even more robust interpretation of reaction mechanisms. Interpreting the isotopic information from one element can lead to wrong conclusions because the information can be biased, if aside the chemical reaction a reaction cascade with rate limiting steps is involved. These masking effects could be caused by diffusion through cell membranes or the binding of the substrate to an enzyme. Conclusively, the observed enrichment factor wouldn't reflect the isotope effects generated by the reaction mechanism. Adding the isotopic information of a second element can avoid this problem because masking would influence the apparent kinetic isotope effects (AKIE) of both elements to the same extent. Therefore, the dual element plot would still reflect the characteristics of the reaction mechanism.

In order to enable the dual element isotope analysis for chlorinated ethenes or methanes, methods had to be invented for chlorine and hydrogen measurements, beside the already existing method for carbon which is well described by W.A. Brand [23]. For chlorine isotope analysis the "online" measurement was developed by Shouakar Stash et al. [18] what made the laborious offline preparation unnecessary[24] and enabled the direct measurement of chlorinated compounds. Here, chlorinated ethenes are directly transferred from the gas chromatograph into the IRMS and molecule fragments of chlorinated ethenes are measured with sensitive detectors (Faraday cups) which were adapted to these mass fragments (e.g. $C_2Cl_2^+$ for PCE and $C_2HCl_2^+$ for TCE). For chlorinated methanes (tetrachloromethane and trichloromethane) such a method was developed during the time of this thesis. The method itself is described in Chapter 2. A method for hydrogen isotope measurements of chlorinated hydrocarbons was developed in 2013 by Shouakar Stash et al. and Kuder et al. [25, 26]. For this

approach a chromium reactor was invented which enabled the conversion of chlorinated hydrocarbons to H_2 without the formation of HCl which is corrosive and was the biggest hindrance for these measurements. Afterwards this method was improved and intensively tested by Renpenning et al.[20]

1.3 Objectives

CSIA is a promising tool to identify the reaction mechanism of biodegradation of chlorinated methanes and ethanes. However, until recently it was only possible to measure carbon isotope values for chlorinated methanes because chlorine and hydrogen measurements were not invented. That made the identification of reaction mechanisms more difficult because information for only one element was available.

In chapter 2 of this thesis a method for chlorine isotope analysis of tetrachloromethane and trichloromethane was realized for the Gas Chromatography - quadrupol Mass Spectrometry (GC-qMS) and the IRMS and both methods were compared in points of precision and trueness. Furthermore, the developed GC-qMS methods were tested in an interlaboratory comparison between Munich and Neuchâtel. This method also forms the basis for a related study that is provided in the Appendix A1 but does not form part of this thesis: it was possible for the first time to create dual element isotope slopes for oxidative and reductive trichloromethane degradation and to investigate isotope fractionation for three different mechanisms: oxidative C-H bond cleavage using heat-activated persulfate, reductive C−Cl bond cleavage by cast zero-valent iron (ZVI) and transformation under alkaline conditions at pH 12.

The work presented in chapter 3 and 4 aims to identify the reaction mechanism of reductive dehalogenation of chlorinated ethenes by the coenzyme vitamin B12 (cobalamin) and by organisms, which still remains elusive until today. Furthermore, the question should be answered: “Why does biodegradation often stop at the step of cDCE or VC?” Dual element isotope analysis in combination with a simplified model system is used to achieve this goal. Direct investigation of the reaction mechanism of chlorinated ethene degradation by organism is no simple task, because processes like diffusion through the cell membrane, binding at the enzyme etc. complicate the interpretation of the mechanism. Therefore, often simplified model systems are used such as degradation of chlorinated ethenes by pure

enzymes or the enzymatic cofactor vitamin B12 Depending on isotope data Cretnik at al. 27 pin-pointed, that degradation of chlorinated ethenes by vitamin B12 is an optimal model system to investigate the mechanism. Three reaction mechanisms are suggested for the reductive dehalogenation of chlorinated ethenes by vitamin B12: 1. Outer-sphere or inner-sphere Single electron transfer (OS- or IS-SET) 2. nucleophilic substitution (inner sphere reaction) and 3. nucleophilic addition (inner sphere reaction).

In chapter 3 outer-sphere single electron transfer (OS-SET) reagents were used to simulate an OS-SET in water and organic solvent. The changes of isotopic composition were monitored. The results of dual element isotope analysis (carbon and chlorine) were compared to reported dual element isotope slopes from reactions of organisms, enzymes and vitamin B12. Besides, the results are compared to previous zero valent iron experiments because for this system either an IS- or OS-SET is supposed. Finally, an explanation was provided why different isotope values are observed for the OS-SET in organic solvent and water, and the question was answered whether an OS-SET is observed in biodegradation or degradation by zero valent iron

To pin-point which reaction mechanism is responsible for the reductive dehalogenation of chlorinated ethenes, further experiments with pure vitamin B12 and chlorinated ethenes (PCE, TCE and cis-DCE) were conducted (chapter 4). Changing the initial pH value in combination with dual element isotope analysis for the reaction of vitamin B12 with PCE and cis-DCE revealed different reaction mechanisms for PCE and cis-DCE. Subsequently, experiments with TCE from pH value 5 to 12 were conducted, where combining dual element isotope analysis with determination of intermediates by UV-VIS and high-resolution mass spectrometry enabled us to identify the reaction mechanisms of PCE, TCE and cis-DCE degradation by vitamin B12. Furthermore, we included results and interpretations from numerous previous studies to verify the reaction mechanisms. Finally, we were able to provide an answer to the question: “Why does biodegradation often stop at the step of cDCE or VC?”.

2.

Compound-specific Chlorine Isotope Analysis of Tetrachloromethane and Trichloromethane by GC-IRMS vs. GC-qMS: Method Development and Evaluation of Precision and Trueness

Benjamin Heckel, Diana Rodríguez-Fernández, Clara Torrentó, Armin Meyer, Jordi Palau, Cristina Domènech, Mònica Rosell, Albert Soler, Daniel Hunkeler, Martin Elsner, *Anal.Chem.* **2017**, 89, 3411−3420 DOI: 10.1021/acs.analchem.6b04129

2.1. ABSTRACT

Compound-specific chlorine isotope analysis of tetrachloromethane (CCl_4) and trichloromethane ($CHCl_3$) was explored by both, gas chromatography – isotope ratio mass spectrometry (GC-IRMS) and GC – quadrupole MS (GC-qMS), where GC-qMS was validated in an interlaboratory comparison between Munich and Neuchâtel with the same commercial GC-qMS instrument. GC-IRMS measurements analyzed CCl isotopologue ions, whereas GC-qMS analyzed the isotopologue ions CCl_3, CCl_2, CCl (of CCl_4) and $CHCl_3$, $CHCl_2$, CHCl (of $CHCl_3$), respectively. Lowest amount dependence (good linearity) was obtained (i) in H-containing fragment ions where interference of ^{35}Cl- to ^{37}Cl-containing ions was avoided; (ii) with tuning parameters favoring one predominant rather than multiple fragment ions in the mass spectra. Optimized GC-qMS parameters (dwell time 70 ms, 2 most abundant ions) resulted in standard deviations of 0.2‰ ($CHCl_3$) and 0.4‰ (CCl_4) which are only about twice as large as 0.1‰ and 0.2‰ for GC-IRMS. To compare also the trueness of both methods and laboratories, samples from CCl_4 and $CHCl_3$ degradation experiments were analyzed and calibrated against isotopically different reference standards for both CCl_4 and $CHCl_3$ (two of each). Excellent agreement confirms that true results can be obtained by both methods provided that a consistent set of isotopically characterized reference materials is used.

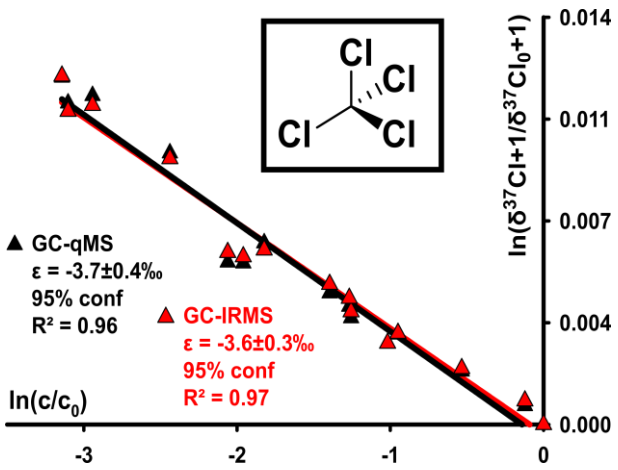

2.2. Introduction

Chlorinated methanes such as trichloromethane ($CHCl_3$) and tetrachloromethane (CCl_4) have been used as dry cleaning agents, solvents and for the production of chlorofluorocarbons. As a consequence of accidents and inadvertent handling, spills of these chemicals have led to groundwater and soil contaminations. Because of their potential to cause cancer and chronic diseases, both compounds have received attention as notorious legacy chemicals at contaminated sites.[27, 28]

To characterize on-site contamination, and to explore best remediation strategies, compound-specific isotope analysis (CSIA) offers the possibility to distinguish chemically identical contamination sources by their isotope values, and to quantify transformation of chlorinated solvents by the observation of degradation-induced changes in these isotope ratios [29, 30]. While the ability to derive both lines of evidence is limited if isotope ratios of only one element are measured, the possibilities of CSIA are magnified when analyzing isotopic information from several elements.[31-34] Specifically, as shown for chlorinated ethylenes, analysis of carbon and chlorine isotopes makes it possible to create dual element isotope plots offering the opportunity to distinguish sources more confidently, to detect degradation and, importantly, to investigate different transformation mechanisms [35-42]. For CCl_4 and $CHCl_3$ this perspective became achievable by the introduction of viable approaches for compound-specific chlorine isotope analysis of organic compounds [43-45]. Traditionally, the analysis of chlorine isotopes does not only require dedicated instrumentation, but also time-demanding offline preparation, such as analyte conversion to CH_3Cl [18, 46]. Subsequently, CH_3Cl can be measured on a dual-inlet gas isotope ratio mass spectrometer (DI-IRMS). This so-called offline method for chlorine isotope analysis was established by Holt et al.[24] Another possibility is the conversion to cesium chloride for thermal ion mass spectrometry analysis [47], or the atomization of compounds in an inductively coupled plasma followed by multi-collector MS[48, 49]. A breakthrough for compound-specific chlorine isotope analysis by continuous flow ("online") measurements without laborious offline preparation was accomplished by Shouakar Stash et al.[18] and Sakaguchi-Soder et al. [50]. Chlorine isotope analysis was performed on original target analyte molecules of tetrachloroethylene (PCE) and trichloroethylene (TCE) eluting from gas chromatographic separation. Measurements rely on molecular ions, or fragment ions, generated in the ion source of an IRMS[18] or qMS[50].

In 2010 Aeppli et al.[51] obtained chlorine isotope ratios for PCE, PCP and DDT using this GC-qMS approach. To improve the qMS measurements of PCE and TCE Jin et al. [52] optimized the method and compared different evaluation schemes. Palau et al. investigated for the first time 1,2-dichloroethane[37] and 1,1,1-trichloroethane[53]. Chlorine isotope measurements for $CHCl_3$ were reported, but not yet systematically validated by Breider and Hunkeler [54]. Hitzfeld et al.[55] and Renpenning et al.[56] introduced yet an alternative and potentially improved strategy to measure chlorine, bromine and sulfide isotopes. In their studies, GC separation was followed by H_2-induced high temperature conversion (HTC) to HCl, HBr or H_2S, respectively and subsequent qMS[55] or IRMS[56] analysis. While this approach represents a universal strategy irrespective of target compound structure, memory effects and short reactor lifetimes are presently reported to limit HTC applications.[56] Consequently, analyses of unconverted target analytes by GC-IRMS [18] or GC-qMS [50] are the current methods of choice. They represent an emerging opportunity for field studies and mechanistic investigations that is far from being explored. Specifically, current applications are restricted for several reasons. On the one hand, parameters for GC-qMS and GC-IRMS analyses must be carefully validated for each new target compound[19] and the choice of adequate analyte / fragment ions to achieve optimum performance (sensitivity, linearity) in isotope analysis is still an open question. [52] On the other hand, interlaboratory comparisons show that the use of two isotopically distinct isotopic reference materials of each target compound are necessary to ensure comparable results in different laboratories[19, 37, 57]. Comparisons between the performance of GC-qMS and GC-IRMS using the same reference materials are highly desirable, yet limited to few comparative studies[19, 37].

In this study we, therefore, optimized, and carefully evaluated, compound-specific chlorine isotope analysis for two new important target compounds - $CHCl_3$ and CCl_4 - by both, GC-IRMS and GC-qMS, with a particular focus on the comparison of precision and trueness for both approaches. Also, we focused on the question whether rules of thumb can be derived to choose the best analyte / fragment ions for optimum performance (sensitivity, linearity) of isotope analysis. We evaluated the performance using reference material with independently determined isotope ratios, as well as with samples from degradation experiments to investigate if measured shifts in isotope ratios and enrichment factors are consistent among methods. In addition, GC-qMS methods were validated in an interlaboratory comparison between Munich and Neuchâtel.

2.3. Experimental section

2.3.1. Chemicals

All chemicals in this study were used as received: $CHCl_3$ (Fluka), CCl_4 (Panreac), sodium formate (HCOONa, Merck), cast iron (92% Gotthart Maier Metallpulver GmbH), dibasic anhydrous sodium phosphate (Na_2HPO_4, Panreac AppliChem)**,** sodium hydroxide (NaOH, Baker), hydrochloric acid (HCl, 32 wt. %, Sigma-Aldrich).

2.3.2. Abiotic Degradation of CCl_4 with Sodium Formate

Ten microliters of CCl_4 were dissolved in 35 mL of degassed ultrapure water by vigorous stirring for 24 hours in a 40 mL vial. The reaction was started inside an anoxic chamber with the addition of 1 g sodium formate. The vial was closed with a mininert valve (Supelco) and constantly stirred with a magnetic stir plate. Seven samples were taken over a time course of 7 hours. For each time point 0.5 mL were removed from the reaction mixture, diluted in 7 mL hydrogen peroxide solution (1%) and 1 mL subsamples were immediately taken from this solution to analyze concentrations and chlorine isotope values. One experimental replicate was performed with 2 g instead of 1 g sodium formate and was analyzed in the same way.

2.3.3. Abiotic Degradation of $CHCl_3$ with Cast Iron at pH 12

The cast iron was washed with 0.1 M HCl for an hour, rinsed and dried overnight to activate the surface[58]. The surface of the activated iron was determined by the BET (Brunauer-Emmett-Teller) method as 1.624±0.007 m^2g^{-1}. Forty-two milliliter vials (20 reaction vials, 12 blank vials) were wrapped in aluminum foil to inhibit photoreaction and 2 g of cast iron were added to each vial. Subsequently, a buffer solution of pH 12 was added until nearly no headspace was left. To start the reaction, pure $CHCl_3$ was added to reach a concentration of 100 mg/L. During the whole reaction vials were placed on a horizontal shaker (IKA KS 260 BASIC, Stanfen, Germany). Samples were taken over 9 days and for each time point one vial was sacrificed. To stop the reaction, 0.2 µm filtration and subsequent neutralization by

acetic acid was done. Samples were frozen[59] in 10 mL vials until analyses for concentrations, carbon and chlorine isotope ratios.

2.3.4. Stable Carbon Isotope Analysis by GC-C-IRMS

Carbon isotope analyses of $CHCl_3$ were performed in the Centres Científics i Tecnològics at the Universitat de Barcelona (CCiTUB) according to the method described elsewhere [60] by using a Thermo Finnigan Trace GC Ultra instrument coupled via a GC-Isolink interface to a Delta V Advantage isotope ratio mass spectrometer (Thermo Scientific GmbH, Bremen, Germany). The GC was equipped with a Supelco SPB-624 column (60 m × 0.32 mm × 1.8 µm, Bellefonte, PA, USA). The GC program started at 60 °C for 5 min, the GC was heated to 165 °C at a rate of 8 °C/min, then heated to 220 °C at 25 °C/min and finally held at 220 °C for 1 min. A split ratio of 1:5 was used at an injector temperature of 250 °C. Helium (5.o) served as a carrier gas (2.2 mL min^{-1}). The chlorinated methanes were extracted from aqueous samples by automated headspace solid-phase micro-extraction (HS-SPME) using a 75 µm Carboxen-PDMS fiber (Supelco, Bellefonte, PA, USA) and a TriPlus™ autosampler equipped with a SPME holder (Thermo Fisher Scientific, Waltham, USA). Samples were extracted at a constant agitation rate (600 rpm) for 20 minutes at 40°C. After extraction, the SPME fibers were desorbed at 250°C for 5 minutes in the GC injector. The analytical uncertainty (2σ) of carbon isotopic measurements never exceeded ±0.5‰. A pulse of CO_2 as monitoring gas was introduced at the beginning and at the end of each run. For carbon, the monitoring gas had been calibrated beforehand so that values are stated relative to the international reference material Vienna Pee Dee Belemnite (VPDB) on the international per mille scale. Moreover, several $CHCl_3$ aqueous control standards were prepared daily at the same concentration range than the samples from a pure in-house standard of known carbon isotopic composition ($\delta^{13}C$) and analyzed on the same days as the samples to ensure accuracy of the isotopic measurements and to correct slight carbon isotopic fractionation induced by the HS-SPME preconcentration technique [61]. The $\delta^{13}C$ of this pure $CHCl_3$ standard (-48.96 ± 0.04‰) was determined previously using a Flash EA1112 (Carlo-Erba, Milano, Italy) elemental analyzer (EA) coupled to a Delta C IRMS (Thermo Fisher Scientific, Bremen, Germany) through a Conflo III interface (Thermo Finnigan, Bremen, Germany) using six international reference materials (NBS 19, IAEA-CH-6, USGS40, IAEA-600, IAEA-CH-7, L-SVEC) with respect to the VPDB standard, according to Coplen

et al. [62]. All the controls injected together with the present samples had an average $CHCl_3$-$\delta^{13}C$ value of -50.0 ± 0.3‰ (n = 15).

2.3.5. Stable Chlorine Isotope Analysis by GC-IRMS in Munich

GC-IRMS analysis of CCl_4 and $CHCl_3$ was conducted by recording the masses m/z = 47 and 49 (CCl fragment), which correspond to half of the masses for which the IRMS instrument is specifically configured (98: dichloroethene molecular ion; 94: double dechlorinated tetrachloroethene fragment ion). The GC-IRMS system (Thermo Scientific) consisted of a Trace GC that was connected via a transfer line to a MAT 253 IRMS equipped with a dual inlet system. The gas chromatograph was operated with He carrier gas (5.0) at 1.4 mL/min and contained a 30 m VOCOL column (Supelco) with 0.25 mm inner diameter and a film thickness of 1.5 µm. The GC program started at 60 °C for 2 min, followed by a temperature ramp of 8 °C/min to 165 °C and of 25 °C/min to 220 °C (held for 1 min). One milliliter gas phase was injected from 10 mL headspace vials that contained 1 mL of aqueous sample and that had previously been equilibrated for 5 min at 40 °C. Injection was performed in split mode (1:10 split ratio) at 220 °C through a split/splitless injector. No difference was observed in isotope values obtained with a split ratio of 1:10 compared to 1:20 (data not shown).

To provide an anchor between individual measurements, pulses of a monitoring gas of CCl_4 and $CHCl_3$ were introduced via the dual inlet system at the beginning and the end of each measurement. Monitoring gas was never adjusted to sample concentration, but instead the amount dependency ("linearity") of isotope measurements was carefully investigated using external standards (see below). In addition, to convert delta values relative to the international reference Standard Mean Ocean Chloride (SMOC), a two-point calibration was performed with external standards of CCl_4 and $CHCl_3$. These external standards were placed into daily measurement sequences in the following way. At the beginning of a sequence, ten injections of the first standard and four injections of the second standard were performed with different headspace volumes. This resulted in a series of amplitudes that allowed evaluating the linearity of the method and, if necessary, performing an amplitude correction. After that, duplicate measurements of both standards were introduced after every ten sample injections to enable a drift correction accounting for slow outgassing of the CCl_4 monitoring

gas from the reference bellow of the IRMS. The measurement sequence was, finally, concluded by quadruplicate measurements of both standards with the same concentration and headspace volumes. Values of the external standards (after amplitude and drift correction) were plotted against their values on the SMOC scale and sample measurements were evaluated using the intercept and the slope of this regression (again, after amplitude and drift correction). The chlorine isotope signatures ($\delta^{37}Cl$) of the external CCl_4 standards were +1.98±0.1‰ (n=2) and -4.11±0.07‰ (n=2), as characterized in the University of Delaware (Newark, USA) and those of the external $CHCl_3$ standards were -3.02±0.17‰ (n=17) and -5.4±0.3‰ (n=8), as characterized in Waterloo (Isotope Tracer Technologies Inc., Waterloo, Canada), in both cases by IRMS after conversion to CH_3Cl[24].

2.3.6. Concentration and Stable Chlorine Isotope Measurements with GC-qMS

GC-qMS measurements for analysis of CCl_4 and $CHCl_3$ concentrations and chlorine isotope values were performed in Munich (GC-qMS-1) and Neuchâtel (GC-qMS-2). A summary of instrument parameters in the GC-qMS-1 and GC-qMS-2 setups can be found in the Supporting Information of Chapter 2 (Table B1). The isotope data from both qMS were also corrected by a two-point calibration with the external standards mentioned above. For each run, four samples of both standards with the same concentration were measured at the beginning, two after every ten measurements and again four at the end to enable a drift correction. In contrast to GC-IRMS, an amplitude ("linearity") correction was not necessary, because we did not observe an amount-dependency (for further discussion see the Results section below). The data acquisition frequency was chosen such that 15-25 data points are obtained across the chromatographic peaks (Agilent GC/MSD ChemStation and Instrument Operation – Course Number H4043A Volume I, page 100). This requires around 3 measurement cycles/second corresponding to a total scan time for each cycle of around 300ms. A suitable dwell time is then obtained by dividing this time interval by the number of ions (n) analyzed. Reasonable dwell times were calculated in milliseconds.

$$\text{dwell time} = \frac{300}{n+1} \quad (1)$$

In this study, the dwell time was varied around this typical value.

2.3.7. Evaluation of chlorine isotope data

Instrument isotope values for chlorine and carbon measurements by IRMS were in a first step derived from the instrument's software, where samples were evaluated relative to a monitoring gas in each run. For the calculation of chlorine isotope values equation 2 was used:

$$\delta^{37}Cl_{compound} = \frac{(^{37}Cl/^{35}Cl)_{compound} - (^{37}Cl/^{35}Cl)_{ref}}{(^{37}Cl/^{35}Cl)_{ref}} = \frac{R_t}{R_{ref}} - 1 \quad (2)$$

where values are given in per mille For example, a value of 10 ‰ indicates that a substance contained 10 per mille (or one percent) more $^{37}Cl/^{35}Cl$ than the compound to which it was compared. An analogous equation applies with $^{13}C/^{12}C$ for carbon.

For chlorine isotope measurements by GC-qMS-1, we tested settings with different numbers of ion pairs and different dwell times (i.e., 2, 4 and 6 ions and dwell times between 40 and 100). The molecular ion peaks and fragment ion peaks of CCl_4 and $CHCl_3$ are shown in Figure 1. The masses 119/117, 84/82 and 49/47 were chosen for CCl_4 and 120/118, 85/83 and 49/47 for $CHCl_3$. For the evaluation of selected-ion monitoring (SIM) measurements relying on only two ions we chose the peak intensities of the two most abundant fragment ions (m/z 83 and 85) for $CHCl_3$ and (m/z 117, 119) for CCl_4. These ioncouples correspond to the isotopologue pairs ($[^{35}Cl_2{}^{12}CH]^+$ and $[^{35}Cl^{37}Cl^{12}CH]^+$) and ($[^{35}Cl_3{}^{12}C]^+$ and $[^{35}Cl_2{}^{37}Cl^{12}C]^+$), respectively[51]. The isotope ratio was obtained from the ratio of these isotopologues according to Eq. 3 and 4 [63].

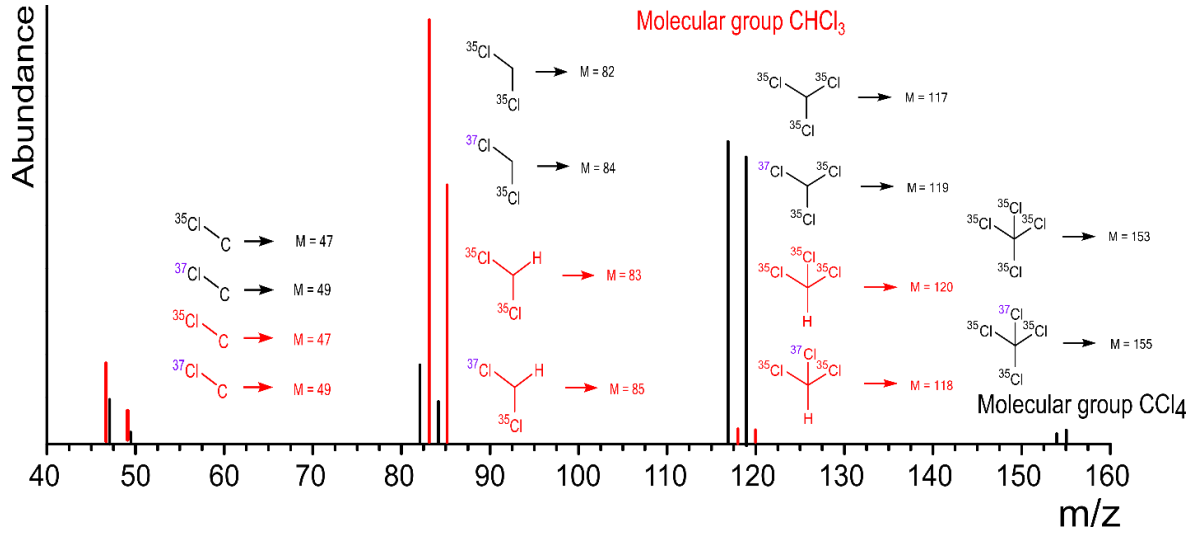

Figure 1. Mass spectra of the isotopologue ion peaks of CCl_4 (in black) and $CHCl_3$ (in red) in analysis by GC-qMS

For the fragment ions m/z 83 and 85 of $CHCl_3$ the equation applies

$$R = \frac{^{37}Cl}{^{35}Cl} = \frac{^{37}\mathrm{p}}{^{35}\mathrm{p}} = \frac{k}{(n-k+1)} \cdot \frac{^{37}Cl_{(k)}\,^{35}Cl_{(n-k)}}{^{37}Cl_{(k-1)}\,^{35}Cl_{(n-k+1)}} = \frac{1}{2} \cdot \frac{^{85}I}{^{83}I} \qquad (3)$$

where ^{37}p and ^{35}p are the probabilities of encountering ^{37}Cl and ^{35}Cl, n is the number of Cl atoms in the fragment (here: 2), k is the number of ^{37}Cl isotopes in the "heavy" isotopologue (here: 1), $^{37}Cl_{(k)}{}^{35}Cl_{(n-k)}$ and $^{37}Cl_{(k-1)}{}^{35}Cl_{(n-k+1)}$ represent the isotopologues containing k and (k−1) heavy isotopes (here: $[^{35}Cl^{37}Cl^{12}CH]^+$ and $[^{35}Cl_2{}^{12}CH]^+$), respectively, and I indicates the ion peak intensities. An analogous equation applies to the fragment ions m/z 117 and 119 ($[^{35}Cl_2{}^{37}Cl^{12}C]^+$ and $[^{35}Cl_3{}^{12}C]^+$ of CCl_4, respectively):

$$R = \frac{^{37}Cl}{^{35}Cl} = \frac{^{37}\mathrm{p}}{^{35}\mathrm{p}} = \frac{k}{(n-k+1)} \cdot \frac{^{37}Cl_{(k)}\,^{35}Cl_{(n-k)}}{^{37}Cl_{(k-1)}\,^{35}Cl_{(n-k+1)}} = \frac{1}{3} \cdot \frac{^{119}I}{^{117}I} \qquad (4)$$

with n=3 and k=1. Values calculated this way were subjected to a calibration with the external standards as described above (measured values of standards were plotted against their values on the SMOC scale, sample measurements were subsequently evaluated using the intercept and the slope of this regression). Resultant values were reported in the δ-notation in parts per thousand relative to the international Standard Mean Ocean Chloride (SMOC) standard.

In contrast, for evaluation of the 4 and 6 ion settings for CCl_4 and $CHCl_3$ the modified multiple ion method was used[52] . Eq. 5 and 6 show the corresponding expressions for $CHCl_3$

4 ions:

$$R_{CHCl_3} = a \cdot R_{F1}^{CHCl_3} + b \cdot R_{F2}^{CHCl_3}$$

$$a = \frac{I_{85}+I_{83}}{(I_{85}+I_{83})+(I_{49}+I_{47})}$$

$$b = \frac{I_{49}+I_{47}}{(I_{85}+I_{83})+(I_{49}+I_{47})} \quad (5)$$

6 ions:

$$R_{CHCl_3} = a \cdot R_{M}^{CHCl_3} + b \cdot R_{F1}^{CHCl_3} + c \cdot R_{F2}^{CHCl_3}$$

$$a = \frac{I_{120}+I_{118}}{(I_{120}+I_{118})+(I_{85}+I_{83})+(I_{49}+I_{47})}$$

$$b = \frac{I_{85}+I_{83}}{(I_{120}+I_{118})+(I_{85}+I_{83})+(I_{49}+I_{47})}$$

$$c = \frac{I_{49}+I_{47}}{(I_{120}+I_{118})+(I_{85}+I_{83})+(I_{49}+I_{47})} \quad (6)$$

where R_M is the isotope ratio of the molecular group, R_{F1} of fragment 85/83 and R_{F2} of the fragment 49/47 (Eq. 3). For a quantitative evaluation of degradation experiments, isotopic enrichment factors (ε) were determined according to the Rayleigh equation [21, 64]

$$\ln\left(\frac{\delta^{37}Cl+1}{\delta^{37}Cl_0+1}\right) = \varepsilon \cdot lnf \quad (7)$$

where $\delta^{37}Cl_0$ is the chlorine isotope value at time zero, $\delta^{37}Cl$ is the chlorine isotope value at time *t* and *f* is the residual fraction of the substrate (i.e. the concentration at time *t* divided through the concentration at time zero).

The isotopic enrichment factor expresses the difference in reaction rates of molecules containing light and heavy isotopes, respectively, where a value of, e.g., -3.5‰ indicates that heavy isotopologues reacted by 3.5‰ more slowly than light isotopologues.

2.4. Results and Discussion

2.4.1. Acquisition Parameters for GC-qMS Analysis

A crucial parameter for chlorine isotope measurements on a GC-qMS is the optimum configuration in SIM mode. On the one hand, instrument fluctuations and also "isotope swings" (i.e., changing isotope values over a chromatographic peak) are better accounted for when measurements jump quickly back and forth between masses. On the other hand, each mass is analyzed more precisely when recorded over a longer time. Finally, different masses can be selected to derive isotope values (see Figure 1). In a first step it was, therefore, our aim to find the optimal choice of ions and dwell times. As described in detail above, we evaluated the most abundant ions method (equation 3 and 4) plus dwell times of 100, 70 or 50 ms, on the one hand, and the multiple ion method (equation 5 and 6) for 4 and 6 ions with dwell times of 60 ms and 40 ms, respectively, on the other hand. For each configuration 25 identical aqueous samples with concentrations of 1-5 mg/L were measured and the resultant standard deviations were plotted in Figure 2A (after two-point calibration against the international standard SMOC to convert instrument readings into per mille units of the δ-scale). This plot of precision versus instrument configuration showed that the recording of 2 ions with a dwell time of 70 ms gave most precise results for both CCl_4 and $CHCl_3$, with a low standard deviation of around 0.35 per mille. Consequently, we used this setting for all subsequent evaluations in GC-qMS-1. In Neuchâtel (GC-qMS-2), the method already established for $CHCl_3$ by Breider and Hunkeler[27], using the two most abundant ions and 50 ms as dwell time, was followed.

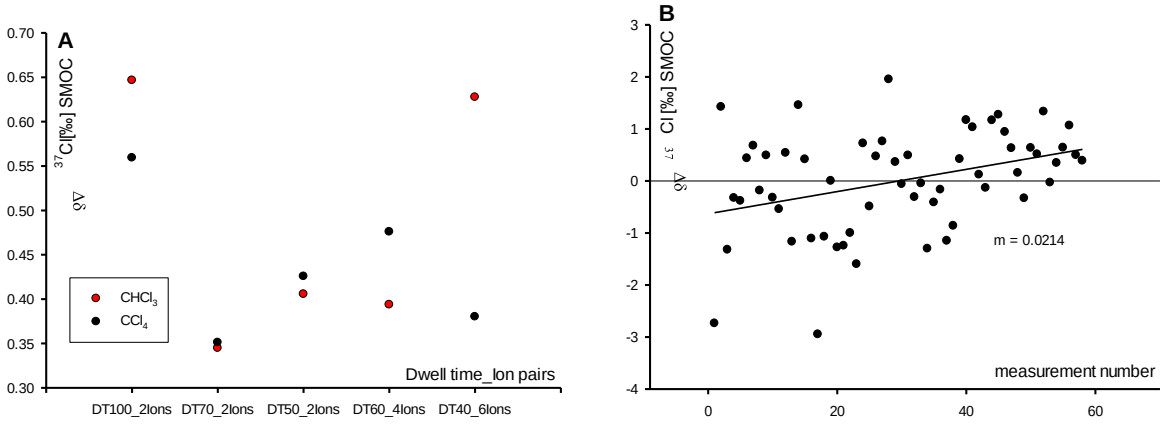

Figure 2. (A) Standard deviation (n=25) of $\delta^{37}Cl$ of CCl_4 and $CHCl_3$ with different ion pair/dwell time settings measured on GC-qMS-1. Delta values (in per mille) are calibrated against SMOC (B) $\delta^{37}Cl_{CCl4}$ measurements with dwell times of 70 ms and 2 ions in per mil and calibrated against SMOC, indicating a small drift over time for CCl_4 in GC-qMS-1.

Figure 2B gives an example of CCl_4 standard measurements over time (60 measurements in a range of 1 to 25 mg/L) showing a small drift, which occurs with increasing measurement number. We observed such a shift in nearly all measurements and a corresponding drift correction was applied, both in GC-qMS-1 as well as in GC-IRMS measurements. To this end, a linear regression similar to Figure 2B was performed from external standards analyzed along the sequence. Subsequently, the regression parameters were used to correct isotope values of samples.

2.4.2. Amount Dependency ("Linearity") of Chlorine Isotope Analysis of CCl_4 by GC-qMS and GC-IRMS

To determine the precision of CCl_4 measurements on the GC-IRMS instrument, we analyzed 70 standards in a range of 0.03 to 2.6 mg/L. Even at the lowest amplitude (100 mV) CCl_4 measurements had a standard deviation of only ±0.6‰ (n=10) and at signals greater than 1 V a very small standard deviation of ±0.1‰ (n=60) was accomplished (Figure 3A). No amount dependency of the trueness (i.e., the target value) was detected, which is consistent with results obtained previously with chlorinated ethylenes on the GC-IRMS system[65]. Figure 3B shows the precision of CCl_4 measurements by GC-qMS.

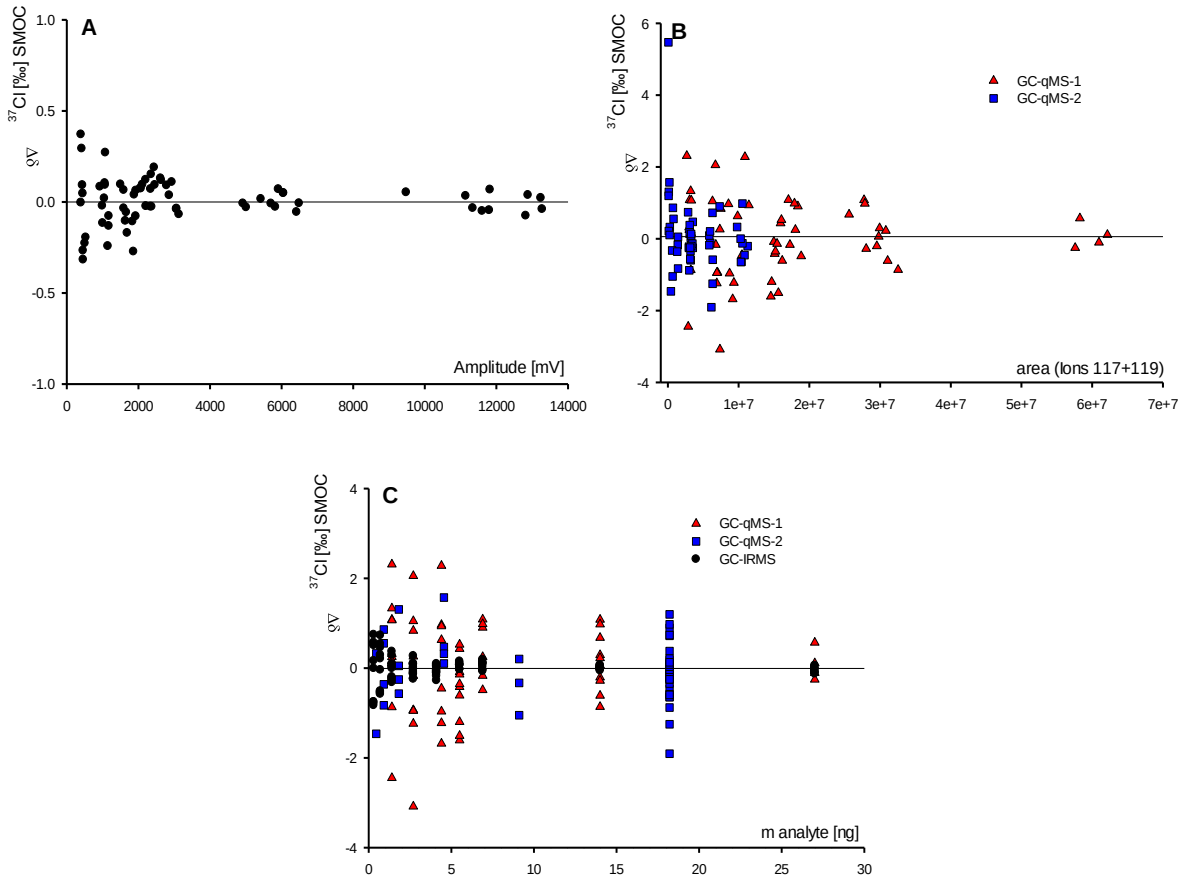

Figure 3. (A) Precision of chlorine isotope measurements vs. signal amplitude of CCl_4 measured by GC-IRMS (70 data points). (B) Precision of chlorine isotope measurements of CCl_4 on GC-qMS-1 and GC-qMS-2 in dependence on signal intensity, where $\delta^{37}Cl_{CCl4}$ (calibrated to SMOC scale) of the two most abundant ions are plotted against area (from 119 + 117 ions; qMS-1 - 58 data points; GC-qMS -2- 50 data points) (C) Comparison of the precision of chlorine isotope analysis by GC-IRMS vs.GC- qMS-1 and GC-qMS-2 in dependence on the mass of analyte (CCl_4) on column.

For signals of small areas below 10 million TIC (Total Ion Count), chlorine isotope values of GC-qMS-1 measurements showed a rather low precision (±3‰). Above an area of 30 million, in contrast, standard deviations of ±0.6 to 0.4‰ (n=13) were obtained, which represent an excellent precision for a GC-qMS[65]. In support of these data, an inter-laboratory comparison using the same type of GC-qMS gave identical results in Neuchâtel for the GC-qMS-2 (Figure 3B). Therefore, even though standard deviations (i.e., the precision) were clearly affected by the injected amount, the target value (i.e., the trueness) appeared to be hardly amount-dependent in both laboratories. This is in remarkable contrast to previous

TCE measurements with GC-qMS[65], where the concentrations of external standards had to be adjusted to sample concentrations for accurate chlorine isotope analysis by GC-qMS. To compare the precision of GC-IRMS and GC-qMS, the same standard and concentration range (on-column amounts) was measured on the three instruments (Figure 3C). Here, the x axis displays the amount of analyte that, after accounting for the split flow in the injector, reaches the chromatographic column and is measured at the ion source. This amount is also reflected in the signal amplitudes of Figures 3A and 3B.

2.4.3. Amount Dependency ("Linearity") of Chlorine Isotope Analysis of $CHCl_3$ by GC-IRMS

Chlorine isotope measurements of $CHCl_3$ by GC-IRMS were conducted identically, meaning that, like for CCl_4, also the fragment masses 49 and 47 were recorded on the GC-IRMS (corresponding to $[^{12}C^{37}Cl]^+$ and $[^{12}C^{35}Cl]^+$ in both cases). Figure 4A shows that – in contrast to CCl_4 – for $CHCl_3$ a strong amount-dependency of isotope values was observed, which could be taken into account by an amplitude correction. We attribute this observation to the fact that, besides the fragment $[^{12}C^{37}Cl]^+$, also the fragment $[^{13}C^{1}H^{35}Cl]^+$ fell on the detector cup that analyzed the mass 49 (Figure 4B). Therefore, as the number of ions increased, also the probability of collisions increased so that more H atoms were stripped from the $[^{13}C^{1}H^{35}Cl]^+$ fragment and were transferred to other ions (which were not analyzed) and therefore the interference by $[^{13}C^{1}H^{35}Cl]^+$ decreased. The phenomenon is well-known from H-measurements where hydrogen atoms are transferred to H_2 molecules creating ions of the mass H_3^+ that are detected together with $[^{2}H^{1}H]^+$. In both cases the probability of H transfer increases with the amount of analyte molecules in the ion source. However, while in the case of hydrogen, more collisions create more H_3^+ ions and, hence, increase the interference, in the case of $CHCl_3$ more collisions decreased the number of $[^{13}C^{1}H^{35}Cl]^+$ ions so that the interference became smaller. For hydrogen isotope measurements, the problem is circumvented by a linear correction of the amount-dependency, i.e., determination of a (positive) H_3-factor. Following an analogous strategy, we introduced an amplitude correction with a negative factor to take into account the amount-dependency of the interference by $[^{13}C^{1}H^{35}Cl]^+$. This amplitude correction did not require additional analytical effort because external standards needed to be measured anyways and an injection of different amount of

headspace from the same standard was sufficient to calibrate for the amount-dependency according to Figure 4A (see Experimental Part above).

Our hypothesis of this "crossover interference" (where ions containing a light isotope (^{35}Cl) contributed to the mass of a heavy isotope (^{37}Cl)) is confirmed by analysis of the fragment masses 50 and 48 of $CHCl_3$, which did *not* show a mass dependency between 2000 to 12000 mV. Figure 4B illustrates the underlying reason: unlike in the case of mass 49 and 47, there is no possibility for ions containing ^{35}Cl to contribute to the mass recorded for ions containing heavy isotopes, $^{37}Cl^{12}CH$ (note that ^{2}H is of too low abundance for $^{35}Cl^{13}C^{2}H$ to make a difference). Since in the case of chloroform, the sensitivity of measurements of the masses 50 and 48 was 2.5 times lower and standard deviation was worse compared to masses 49 and 47 we nevertheless decided against measurements of the masses 50 and 48 and rather performed an amplitude correction on the masses 49 and 47. Figure 5B illustrates the resulting linearity demonstrating that – after correction - excellent accuracy could be obtained.

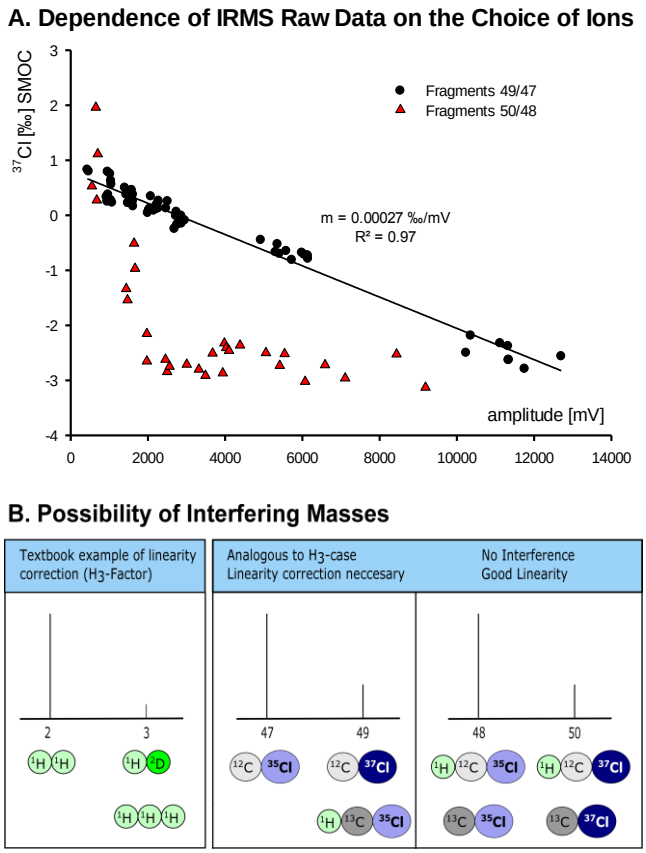

Figure 4. (A) Chlorine isotope values of $CHCl_3$ in dependence on increasing amplitudes on the GC-IRMS (Fragments 49/47 – 60 data points; Fragments 50/48 – 30 data points). (B) "Crossover interference" where ions containing a light isotope (^{35}Cl or ^{1}H) contribute to the mass of a heavy isotope (^{37}Cl or ^{2}H). This interference is dependent on intermolecular proton transfer in the ion source of the GC-IRMS and, hence, amount-dependent. Such interference is possible for the masses m/z = 3 ($^{1}H_3^+$ vs. $^{1}H^{2}H$, left) and m/z = 49 ($^{37}Cl^{12}C$ vs. $^{35}Cl^{13}C^{1}H$, center), but not for mass 50 (right).

2.4.4. Amount Dependency ("Linearity") of Chlorine Isotope Analysis of $CHCl_3$ by GC-qMS.

To accomplish a similar method comparison of GC-IRMS and GC-qMS as for CCl_4, $CHCl_3$ standards were measured again by both GC-qMS instruments in Munich and Neuchâtel (Figure 5A). As in the case of CCl_4, standard deviations were amount-dependent ranging from ±1.0‰ (low concentrations of 0.24-0.36 mg/L, n=20) to ±0.4‰ (higher concentrations of 1.2-2.4 mg/L, n=15). On the one hand, the low standard deviations for GC-qMS are remarkable. On the other hand, however, Figure 5B illustrates that GC-IRMS still showed better precision, especially when on-column amounts of samples became smaller.

In contrast to the amount-dependency of precision, no amount-dependency was observed for the trueness of chlorine isotope values of CCl_4 and $CHCl_3$ on both GC-qMS (Figure 3B and 5A). This can partly be explained by the fact that masses of fragment ions of the type $CHCl_x^+$ were analyzed, where "crossover interferences" as in Figure 4B can be avoided. However, amount dependencies of mean values did occur on some instruments in previous analysis of TCE[19] despite the fact that also there, only the fragments with hydrogen atoms were measured (e.g TCE mass 97/95 "$C_2HCl_2^+$") and not those without (e.g TCE mass 96/94 "$C_2Cl_2^+$"). It is important to understand the reasons for this poor linearity, but since "crossover interferences" are not a possible explanation, Figure 5C explores an additional factor.

Expected isotope fractionation trends in Figure 5C predict that the isotope ratios of molecular and fragment ions should be more stable if the respective ion pair is the predominant one in a given mass spectrum: i.e., to the very left of the reactant (molecular ion) curve, or to the very right of the product (fragment ion) curve. The reason is that these are the locations where the slope of the isotope fractionation graph is shallowest (i.e., least sensitive to changes in the extent of fragmentation). Indeed, we found that the relative peak intensities in mass spectra differed significantly between chlorinated methanes and TCE (Figure 5C). Measuring all three compounds with the same ion source settings showed for each chlorinated methane mainly one fragment, but three fragments of similar intensity for TCE. Hence, the "lesson learned" from this observation is that instruments should be tuned for either soft ion source settings which preserve mainly the original molecule or for strong ion source fragmentation which ideally leads to one predominant fragment.

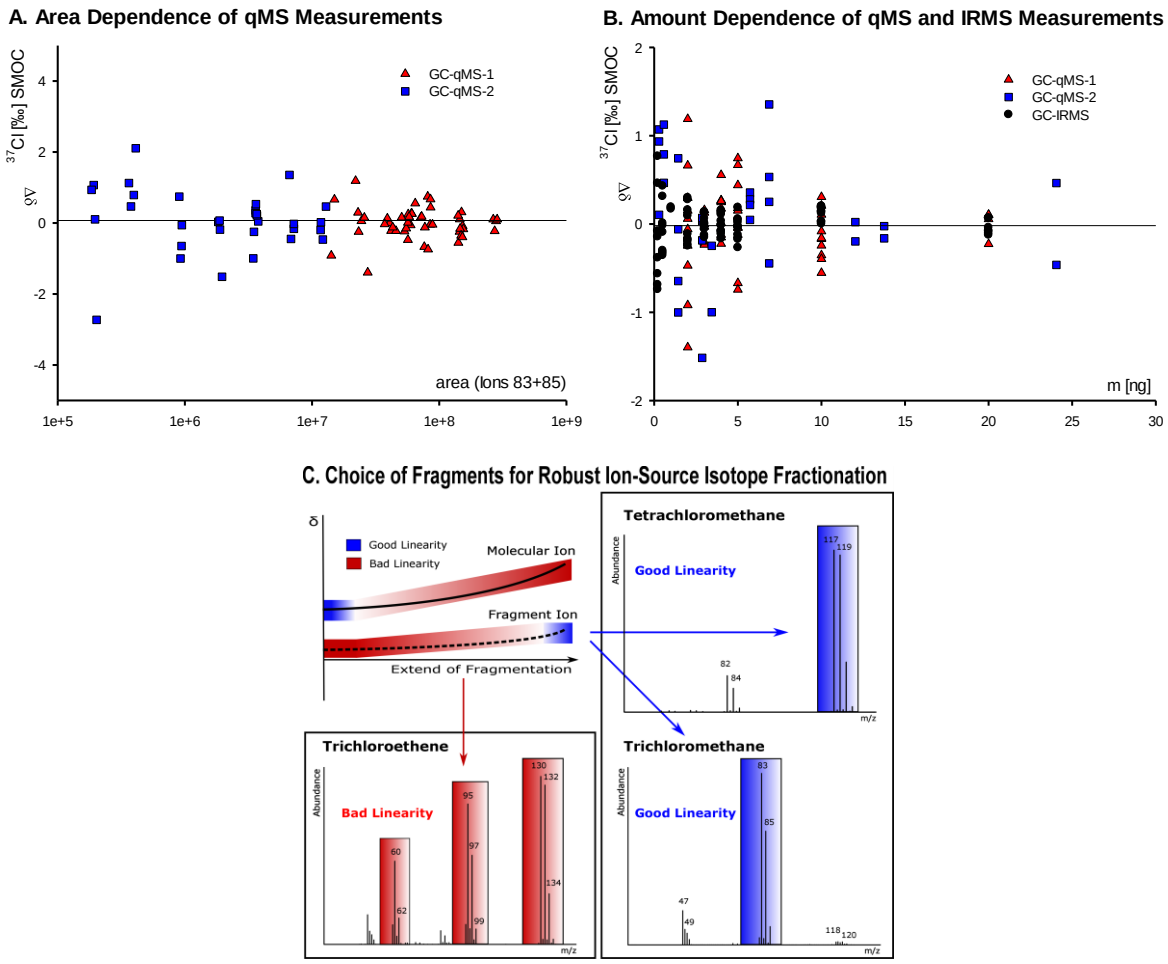

Figure 5. (A) Interlaboratory comparison of $CHCl_3$ measurements on GC-qMS-1 and GC-qMS-2, where the $\delta^{37}Cl_{CHCl3}$ (calibrated to SMOC scale) of the two most abundant ions are plotted against area (from 83 + 85 ions) readings (GC-qMS-1 51 data points; GC-qMS-2 - 32 data points). (B) Comparison of the precision of chlorine isotope analysis by GC-IRMS (after amplitude correction) vs. both GC-qMS in dependence on the mass of analyte ($CHCl_3$) on column (IRMS -60 data points). (C) Expected isotope fractionation trends of molecular and product ions (see, e.g., ref. [66]) predict that isotope values are not amount dependent if one kind of ion predominates (either parent or product). Mass spectra of $CHCl_3$ and CCl_4 illustrate that, indeed, CCl_4 gives almost exclusively rise to the fragment of mass m/z = 117/119/121 and $CHCl_3$ almost exclusively to that of m/z = 83/85. This contrasts with ionization of TCE, where several fragments of similar intensity are formed under identical tune settings.

2.4.5. Trueness of Chlorine Isotope Analysis of CCl_4 and $CHCl_3$ by GC-qMS and GC-IRMS

While Figures 3, 4 and 5 illustrate the methods' performances in terms of precision, the trueness requirements of both methods can only be tested with samples that include a range

of isotope values. Therefore, for each substance one degradation experiment was conducted. CCl_4 was reduced with sodium formate and $CHCl_3$ with zero-valent iron. Both reactions gave rise to pronounced chlorine isotope fractionation, which is a necessary precondition for reliable investigations of trueness over a representative range of δ values. Figure 6A shows changes in isotope values during the degradation of CCl_4 with sodium formate determined by GC-qMS-1. The Figure illustrates the importance of a two-point standard calibration. On the one hand, without an external standard that projects instrument values on the international SMOC scale, the start isotope value would be wrong by 5‰ precluding comparisons between laboratories. On the other hand, however, the data show that a two-point calibration is important to quantify changes in isotope values relative to this starting value, as demonstrated by a difference of 0.5‰ in the enrichment factor ε_{Cl} (Figure 6A). The underlying reason for this is illustrated in Figure 6B which shows isotope data obtained from degradation experiments for CCl_4 and $CHCl_3$. In this Figure, uncorrected "instrument" chlorine isotope values determined by GC-qMS are plotted against corrected ones by a two-point calibration relative to SMOC. The deviation of the slopes from unity and the differences between compounds and laboratories strongly emphasize the need of calibration by two characterized compound-specific isotope standards for chlorine isotope measurements. The effect is particularly pronounced for $CHCl_3$, where the isotope values would be strongly overestimated without a standard correction (m(Munich) = 1.6 and m(Neuchâtel) = 1.9). These slopes show even small variations between measurement days (or sequence number, Figure 6C) over a period of half a year for CCl_4 and two years for $CHCl_3$. For CCl_4 the average slopes were 0.91±0.03 in Munich and 1.06±0.02 in Neuchâtel, whereas for $CHCl_3$ average slopes were 1.6±0.2 and 1.8±0.2, respectively. With a two-point calibration, in turn, reliable results were obtained by GC-qMS for CCl_4, as evidenced by the strong agreement of GC-qMS-1 versus GC-IRMS results shown in Figure 7A, indicating that excellent trueness can be achieved by both methods. Good agreement was also accomplished for $CHCl_3$ degradation with iron, as shown in Figure 7 where results of chlorine isotope measured on both instruments were combined with carbon isotope values analyzed by GC-C-IRMS in a dual element isotope plot. Very good agreement of linear regressions performed on GC-qMS vs. GC-IRMS – both regarding the slope and 95% confidence intervals – confirms that both methods are able to deliver precise and true results.

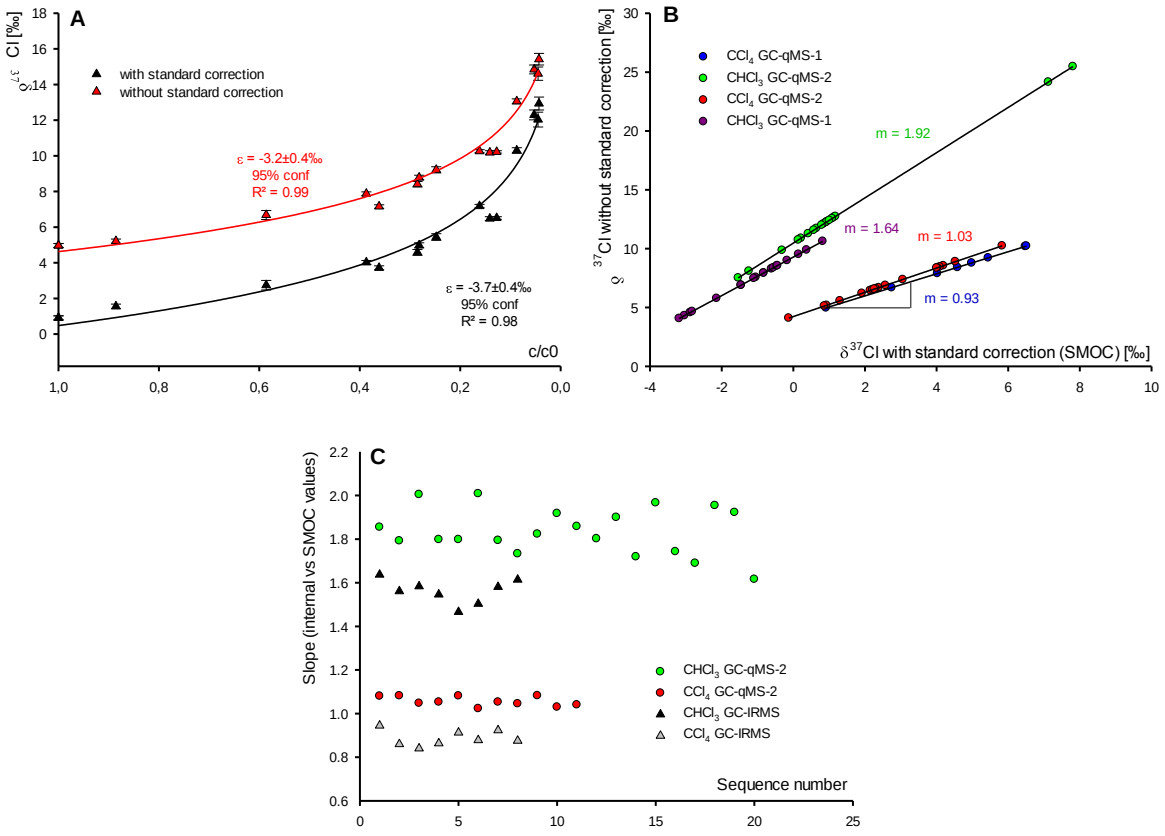

Figure 6. (A) CCl_4 degradation with sodium formate measured at the GC-qMS-1. (Four measurements were conducted for each data point.) Calibration of isotope values by external standards is not only necessary to fix the start chlorine isotope value to the SMOC scale, but also to obtain true enrichment factors. (B) Comparison of chlorine isotope values of $CHCl_3$, and CCl_4 from degradation experiments determined with and without correction in two different sequences from GC-qMS-2 and GC-qMS-1. (C) Plot of slope vs sequence number for CCl_4 and $CHCl_3$ from Munich and Neuchâtel shows small variations for different measurement days over long periods.

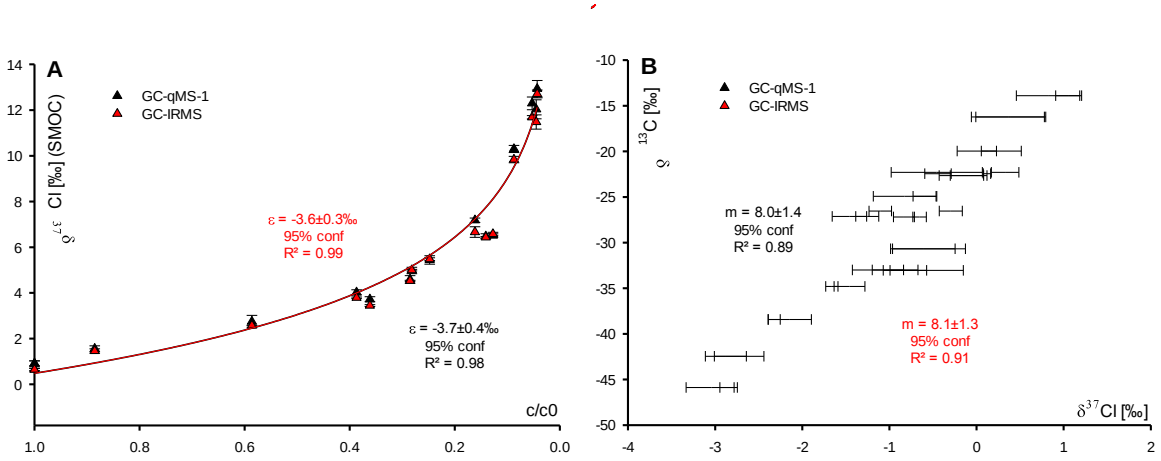

Figure 7. (A) Comparison of $\delta^{37}Cl_{CCl4}$ results against remaining fraction in sodium formate experiments from GC-IRMS and GC-qMS-1 after two-point calibration. (Four measurements were conducted for each data point) (B) Dual element isotope plot of $CHCl_3$ degradation with metallic iron at pH 12 and comparison of regressions from GC-qMS-1 and GC-IRMS chlorine isotope measurements. (Four measurements were conducted for each data point).

2.5. Conclusion

With its enabling role for dual element isotope studies, compound-specific chlorine isotope analysis can greatly increase the identification of groundwater contamination sources and the elucidation of pollutant transformation pathways, and the dual element approach may be a game changer in the assessment of contaminated sites. However, chlorine CSIA has been validated for only a handful of compounds, and systematic method comparisons have been rare. This study contributes to closing this gap by validating, on the one hand, the method for $CHCl_3$ and CCl_4 as important environmental contaminants. On a more fundamental (and general) level, it highlights factors that may lead to strong amount dependence (poor linearity) of chlorine isotope values: (i) protonation of ions containing ^{13}C and ^{35}Cl that may contribute to the mass off ^{37}Cl ions; and (ii) deviation from "ideal" fragmentation conditions where multiple fragment ions rather than one predominant ion are formed. This insight will be valuable to guide future method developments also for other target compounds. On the other hand, our study systematically addresses the question of trueness: whether accurate results are obtained by different methods (GC-qMS vs. GC-IRMS) in different laboratories. Our results show indeed that measurements of $CHCl_3$ and CCl_4 on a GC-qMS are a very

promising alternative if no GC-IRMS is available. Especially at higher concentrations (1.2-2.4 mg/L) isotope measurements with a low standard deviation and a high trueness can be obtained ($\Delta\delta^{37}Cl$ = 0.2-0.6‰). In turn, the possibility to measure chlorine isotope values of $CHCl_3$ and CCl_4 on a GC-IRMS can provide the extra precision that may be critical to distinguish different sources of groundwater contaminations, and to detect the onset of degradation in field samples. Finally, our results stress the importance of a two-point calibration with compound-specific chlorine isotope standards bracketing a range of different chlorine isotope values. For true results, the need must, therefore, be addressed for standards with large differences in chlorine isotope values.

3.

Reductive Outer-sphere Single Electron Transfer Is an Exception Rather than the Rule in Natural and Engineered Chlorinated Ethene Dehalogenation

Benjamin Heckel, Stefan Cretnik, Sarah Kliegman, Orfan Shouakar-Stash, Kristopher McNeill, Martin Elsner; *Environ. Sci. Technol.* **2017**, 51, 9663−9673

DOI: 10.1021/acs.est.7b01447

3.1. ABSTRACT

Chlorinated ethenes (CEs) such as perchloroethylene, trichloroethylene and dichloroethylene are notorious groundwater contaminants. Although reductive dehalogenation is key to their environmental and engineered degradation, underlying reaction mechanisms remain elusive. Outer-sphere reductive single electron transfer (OS-SET) has been proposed for such different processes as Vitamin B_{12}-dependent biodegradation and zero-valent metal-mediated dehalogenation. Compound-specific isotope effect ($^{13}C/^{12}C$, $^{37}Cl/^{35}Cl$) analysis offers a new opportunity to test these hypotheses. Defined OS-SET model reactants (CO_2 radical anions, S^{2-}-doped graphene oxide in water) caused strong carbon (ε_C = -7.9‰ to -11.9‰), but negligible chlorine isotope effects (ε_{Cl} = -0.12‰ to 0.04‰) in CEs. Greater chlorine isotope effects were observed in $CHCl_3$ (ε_C = -7.7‰, ε_{Cl} =-2.6‰), and in CEs when the exergonicity of C-Cl bond cleavage was reduced in an organic solvent (reaction with arene radical anions in glyme). Together, this points to dissociative OS-SET (SET to a σ* orbital concerted with C-Cl breakage) in alkanes compared to stepwise OS-SET (SET to a π* orbital followed by C-Cl cleavage) in ethenes. The non-existent chlorine isotope effects of chlorinated ethenes in all aqueous OS-SET experiments contrast strongly with pronounced Cl isotope fractionation in all natural and engineered reductive dehalogenations reported to date suggesting that OS-SET is an exception rather than the rule in environmental transformations of chlorinated ethenes.

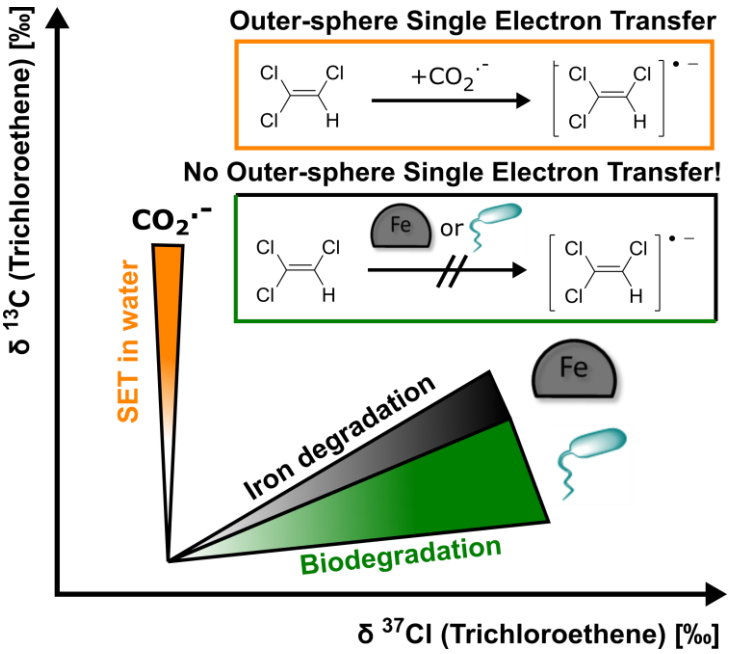

3.2. Introduction

Groundwater contamination by chlorinated ethenes is a prominent environmental problem of our time. Left by a legacy of improper handling and disposal, these compounds are among the most commonly found groundwater contaminants[67]. While they are resistant to degradation, they are susceptible to reductive dehalogenation under reducing conditions [68]. Most groundwater remediation schemes therefore aim at removing these contaminants under anoxic conditions, either through enhanced natural biodegradation[69], or by installing trenches of reactive granular metal, in particular zero-valent iron[70, 71]. These reactions, unfortunately, do not always lead to complete dehalogenation/detoxification. Biotransformation sequentially replaces the chlorine substituents by hydrogen atoms (hydrogenolysis) so that perchloroethylene (PCE) and trichloroethene (TCE) are converted to more problematic *cis*-dichloroethene (*cis*-DCE) and vinyl chloride (VC) before non-toxic ethene is formed.[8] Dehalogenation with zero-valent metal also shows release of problematic daughter compounds, but involves a parallel vicinal-dichloro elimination pathway where two chlorine substituents are removed, offering a more direct avenue to benign end products.[14] The underlying reasons for these different reaction pathways have eluded researchers for years.[72] Electrons must clearly be transferred in some form since less halogenated, more reduced daughter compounds are formed. The nature of this electron transfer (ET), however, has been subject of debate. Following a convention from transition metal chemistry [73], inner-sphere-electron transfer (IS-SET) is conceptualized to occur if electrons are transferred between chemically associated electron donors and electron acceptors (i.e., the CE). [74] By contrast, outer-sphere-electron transfer (OS-SET) takes place if the donor and acceptor are not associated through a chemical bond during ET. [75] In OS-SET, electrons are transferred over some distance, usually from the highest occupied molecular orbital (HOMO) of the electron donor (or a conduction band of an electron-donating metal) into the lowest unoccupied molecular orbital (LUMO) of the electron acceptor (the CE). These concepts of non-adiabatic outer-sphere SET and adiabatic inner-sphere SET have been treated in comprehensive textbooks[76] and reviews [77], but are intrinsically difficult to pinpoint in environmental transformations.

To elucidate the underlying mechanism of biotransformation, numerous studies have focused on cob(I)alamin (Vitamin B_{12})[78], the co-factor present in almost all reductive dehalogenases

identified to date [16]. Inner-sphere reaction has been proposed in the form of nucleophilic addition or nucleophilic substitution reactions by cob(I)alamin with the chlorinated ethene[78]. By contrast, single electron transfer (either inner or outer-sphere) was proposed based on the detection of trichlorovinyl radicals in reaction of TCE with Vitamin B_{12} [79-81]. Both hypotheses are supported by recent insight from crystal structures of the first heterologously expressed dehalogenases [82-84]. Studies either favor outer-sphere SET, both for the reductive dehalogenase VcrA from *Dehalococcoides mccartyi* Strain VS [82] and the reductive dehalogenase PceA from *Sulfurospirillum multivorans* (based on a distance of 5.8 Å between Co(II) and TCE) [84]. Alternatively, an inner-sphere mechanism by attack of Co at the halogen atom is proposed based on the detection of direct Co-Br interactions in the reductive dehalogenase NpRdhA of *Nitratireductor pacificus*.[83]

Competing mechanistic hypotheses have also been proposed for CE transformation by zero-valent metals. Besides "indirect" reactions with by-products of iron corrosion such as activated hydrogen or Fe(II), direct electron transfer at the metal surface (or from a conducting metal oxide layer) is commonly invoked. [70, 85, 86] Inner-sphere ET in the form of complexes at the metal surface was proposed based on reactivity trends [14] and computational calculations [87, 88], whereas (OS)-SET transfer has been invoked based on the consideration that metals likely transfer electrons one at a time and that metals in aqueous solution are covered by a passive oxide layer [70, 89]. OS-SET would also be consistent with the observation that most CE dehalogenation rates correlate with redox potentials derived from LUMOs and one-electron reduction potentials (linear free energy relationships, LFERs)[90]. However, such LFERs may arise owing to different mechanisms[91] so that they cannot uniquely answer the questions of underlying reaction chemistry: which bonds are broken in the chlorinated ethenes, in what order are they broken, and by attack of what reaction partner? Therefore, even though recent research has explored LFERs (or quantitative structure activity relationships, QSARs) as pragmatic approaches to forecast transformation rates in the environment ([92] and refs cited therein), a fundamental understanding of underlying chemical reaction mechanisms – the knowledge that is crucial to tailor the transformation chemistry of remediation schemes – has so far eluded researchers.

Multiple element ($^{37}Cl/^{35}Cl$, $^{13}C/^{12}C$) isotope effect measurements are currently emerging as a potential approach to close this gap[35, 38, 42, 93, 94]. Analytical advances[18, 19] have made it possible to measure compound-specific isotope ratios of single chlorinated ethene

compounds (e.g., PCE, TCE) at their natural isotopic abundance in chemical model reactions and natural samples. At natural abundance, such isotope ratios $^{13}C/^{12}C$ and $^{37}Cl/^{35}Cl$ are expressed as difference relative to an international reference material:

$$\delta^{13}C = \frac{(^{13}C/^{12}C_{Sample} - ^{13}C/^{12}C_{S\,tan\,dard})}{^{13}C/^{12}C_{S\,tan\,dard}} \quad (1)$$

$$\delta^{37}Cl = \frac{(^{37}Cl/^{35}Cl_{Sample} - ^{37}Cl/^{35}Cl_{S\,tan\,dard})}{^{37}Cl/^{35}Cl_{S\,tan\,dard}} \quad (2)$$

$$\Delta\delta^{13}C = \delta^{13}C - \delta^{13}C_{initial} \quad (3)$$

$$\Delta\delta^{37}Cl = \delta^{37}Cl - \delta^{37}Cl_{initial} \quad (4)$$

where $^{13}C/^{12}C_{Sample}$ and $^{13}C/^{12}C_{Standard}$ are the isotope ratios of sample and international reference standard, whereas $\delta^{13}C_{inital}$ and $\delta^{13}C$ and are isotope values at the beginning of a transformation and a given time point, respectively. To determine isotope effects, these values are subsequently evaluated according to the Rayleigh equation[21], which corresponds to analogous equations from chemistry [95,96] for the case that isotope ratios are measured at natural abundance[22]

$$\delta^{13}C = \delta^{13}C_{initial} + [\varepsilon_C \cdot \ln f] \quad (5)$$

Here *f* is the residual fraction of the substrate in a closed system (i.e. the concentration at time point *t* divided through the concentration at time point zero). The resultant isotopic enrichment factor ε_C is the equivalent of a compound-specific kinetic isotope effect: it expresses the difference in reaction rates of molecules containing light and heavy isotopes, respectively. For example, a value of -9‰ indicates that heavy isotopologues (with the label randomly distributed across the molecule) reacted 9‰ (0.9%) more slowly than light isotopologues. This corresponds to a compound-specific kinetic isotope effect of $^{12}k/^{13}k$ = 1.009. Equivalent expressions are valid for the evaluation of chlorine isotope effects.[63]

Similar to classical position-specific isotope effect studies from (bio)chemistry [96, 97], compound-specific isotope effects reflect underlying transition states and, therefore, represent an yes yet underexplored sensitive tool for distinguishing different reaction mechanisms. Mechanistic distinction is easiest when isotope values of two elements are

plotted against each other, because the slope (here: $\lambda = \Delta\delta^{13}C/\Delta\delta^{37}Cl \approx \varepsilon_C/\varepsilon_{Cl} \approx (1-{}^{12}k/{}^{13}k)/(1-{}^{35}k/{}^{37}k)$) represents the compound-specific isotope effects of the two elements relative to each other [98, 99]. In recent years, an increasing number of studies have reported compound-specific isotope effects ε_C, ε_{Cl} and $\lambda \approx \varepsilon_C/\varepsilon_{Cl}$ of chlorinated ethenes in biodegradation [35, 38, 42, 100-103], dehalogenation by Vitamin B_{12} [35, 36], and transformation by zero-valent iron [13, 94]. This data, however has offered only limited mechanistic insight until today because it did not include isotope effect reference data for defined OS-SET reactions.

To close this knowledge gap, we conducted outer-sphere SET reactions in water and in an organic solvent, and measured associated changes in carbon, chlorine and hydrogen isotope values of chlorinated ethenes. To facilitate OS-SET in water, we employed two systems: CO_2 radical anions[104] and graphene oxide that had been doped with electrons from a sodium sulfide solution[105]. CO_2 radical anions transfer an electron to form stable CO_2, whereas graphene oxide shuttles electrons and protons from the donors (sulfide and water) to the acceptor (the chlorinated ethene)[106-108]. In the organic solvent, dimethoxyethane (glyme), OS-SET was modeled with radical anions of naphthalene and pyrene, which readily transfer an electron to regain their aromaticity[109]. All reagents have in common that they are not conducive to direct (inner-sphere) bond interactions and are, therefore, regarded as outer-sphere single electron transfer agents.[109] To probe for differences in OS-SET between chlorinated alkenes and alkanes, an additional experiment investigated the reaction of CO_2 radical anions with chloroform. Finally, to test the hypothesis that OS-SET is a common mechanism in different environmental dehalogenation reactions, we compared our results to reported values for multi-element isotope fractionation of chlorinated ethenes from dehalogenation by vitamin B_{12}, by dehalogenating bacteria, and by iron metal. To measure for the first time hydrogen isotope fractionation in TCE by reaction with iron metal, also a complementary experiment with nanoscale zero valent iron (nZVI) was conducted.

3.3. Materials & Methods

3.3.1. Chemicals

A list of all chemicals is provided in the supporting information of chapter 3.

3.3.2. Reactions in Water

3.3.2.1. Reactions with CO_2 Radical Anions

To prepare reactions of CO_2 radical anions with PCE, TCE, *cis*-DCE and $CHCl_3$, 40 mL vials were filled with 38 mL of deoxygenized water containing the respective chlorinated target compound (10 µL, corresponding to between 0.09 mmol to 0.13 mmol) together with sodium formate (1.2 g,17.5 mmol). Vials were kept closed and anoxic, were stirred (300 rpm) and heated to 80°C. To start the reaction, one milliliter of sodium persulfate dissolved in deoxygenized water (70 mg; 0.29 mmol) was injected to trigger formation of CO_2 radical anions according to:

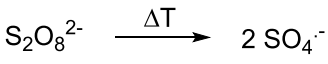

(6)

(7)

At selected time points, samples of the reaction solution (0.3 mL) were taken and injected into an 8 mL-vial containing a H_2O_2 solution (7 mL, 0.5 %) so that CO_2 radical anions were quenched and the reaction was stopped. From these 8 mL-vials, samples were withdrawn for analysis of substrate concentrations, as well as for carbon, chlorine and hydrogen isotope analysis. Concentrations were measured immediately after quenching and 24 hours later to ensure that there was indeed no further reaction of the chlorinated target compounds after quenching (e.g., with remaining CO_2 radical anions or through reaction with hydroxyl radicals formed according to

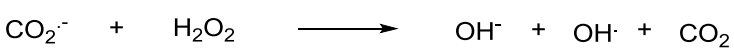

(8)

Furthermore, a control was run with PCE and sodium persulfate, but without sodium formate to exclude that isotope values were influenced by a parallel reaction of PCE with sodium persulfate. (data shown in Supporting Information). Three identical replicates were conducted for each experiment.

3.3.2.2. Reactions with Graphene Oxide in the Presence of Sodium Sulfide

Reactions were conducted in 40 mL-vials containing solid sodium sulfide (2.4 g, 30.7 mmol) and a graphene oxide solution (0.4 mL, 2000 mg/L). To start the reaction, 38 mL of a PCE stock solution (2.3 mM, 0.09 mmol) containing TRIS (Tris(hydroxymethyl)-aminomethane) (500 mg, 4.1 mmol) at pH 7, was injected. The reaction was conducted on a stir plate at 25°C in an anoxic chamber with an atmosphere of 97% N_2 and 3% H_2. Over 60 days, fourteen samples of 0.5 mL were taken and injected into 8 mL-vials containing a H_2O_2 solution (7 mL, 0.5%) to stop the reaction. From these 8 mL-vials samples were withdrawn for subsequent analysis of substrate concentrations, as well as for carbon, chlorine and hydrogen isotope analysis. To complement the experiment at pH 7, a reaction of PCE (1.2 mM) was performed in exactly the same way at pH 2 with the exception that no TRIS buffer was used and that 6 samples were taken over 8 days.

3.3.3. Reactions in an Organic Solvent

3.3.3.1. Reactions with Radical Anions of Naphthalene and Pyrene

For a detailed description see the Supporting Information. All modifications were conducted in an anoxic glovebox. Radical anion solutions were prepared from solutions of naphthalene or pyrene through reaction with sodium metal in glyme. Solutions were filtered and added to stock solutions of PCE and TCE at six different concentrations so different degrees of CE degradation were achieved. To enable headspace analysis of the chlorinated target compounds, aliquots of the completed reaction mixtures were subsequently added to deionized water from where chlorinated analytes could partition into the headspace.

Headspace samples were withdrawn for subsequent analysis of substrate concentrations, as well as for carbon and chlorine isotope analysis.

3.3.4. Analytical Methods

A detailed description of concentration analysis as well as isotope measurements (carbon and chlorine) is provided in the supporting information. Briefly, concentrations were measured by gas chromatography-mass spectrometry (GC-MS) and isotope values by gas chromatography – isotope ratio mass spectrometry (GC-IRMS). For $^{13}C/^{12}C$ analysis separated analyte peaks were online combusted to CO_2[110] whereas $^{37}Cl/^{35}Cl$ analysis was conducted on intact CE isotopologue molecules[18, 19].

3.4. Results and Discussion

3.4.1. Aqueous Reductive OS-SET Reagents Induced Chlorine Isotope Effects in Chloroform, but not in Chlorinated Ethenes

CO_2 radical anions were generated *in situ* by oxidation of sodium formate by sulfate radicals according to Eq. 7 Consistent with their low reduction potential ($CO_2/CO_2^{\cdot-}$: -1.9 V)[111] they induced rapid transformation of chlorinated ethenes and $CHCl_3$, corresponding to a total duration of experiments of between 13 min and 60 min for the CEs and 30 min for $CHCl_3$ (see Supporting Information). Despite similarly rapid kinetics, isotope effects showed pronounced differences between CEs and $CHCl_3$, as illustrated in Figure 1a-c. While carbon isotope effects could be observed in both substances, as expressed by the carbon isotope enrichment factors of -11.9‰ +/- 1.0‰ for TCE (11.9‰) and -17.7‰ +/- 0.8‰ for $CHCl_3$ (Figure 1a), chlorine isotope effects were only observed for $CHCl_3$ (-2.6‰ +/- 0.2‰) and not for TCE (0.04‰ +/- 0.03‰) (Figure 1b). This disparity is visually represented in the dual-element isotope plot of TCE and $CHCl_3$ of Figure 1c. Since isotope effects in $CHCl_3$ are expressed for both elements, they result in a finite slope for $CHCl_3$ of $\lambda = \Delta\delta^{13}C/\Delta\delta^{37}Cl = 6.7 \pm 0.4 \approx \varepsilon_C/\varepsilon_{Cl}$. By contrast, due to the absence of chlorine isotope effects in TCE, the dual-element isotope slope of TCE was close to infinity. The same trend was observed not only for TCE, but also for PCE and cis-DCE (Figure 1c, Table 1). To further confirm the absence of chlorine isotope effects in the reaction of CEs by OS-SET reagents in water, a second experiment was conducted with PCE, graphene oxide and sodium sulfide in aqueous solution at pH 7 and pH 2. TCE was formed as main product clearly demonstrating the occurrence of reductive dehalogenation. Even though transformation of PCE by doped graphene oxide was much slower than with CO_2 radical anions (duration over two months), the isotope effect results were consistent: Figure 1d shows the occurrence of carbon isotope effects, but no change in chlorine isotope values (Figure C3 and C4 Appendix). Taken together, these results are consistent with OS-SET to the chlorinated alkane $CHCl_3$ that is concerted with C-Cl bond cleavage so that a chlorine isotope effect could be observed. In contrast, OS-SET to the chlorinated ethenes is consistent with a stepwise – or at least asynchronous – process that involved C-Cl bond cleavage only after the rate-determining step so that chlorine isotope effects were not observable.

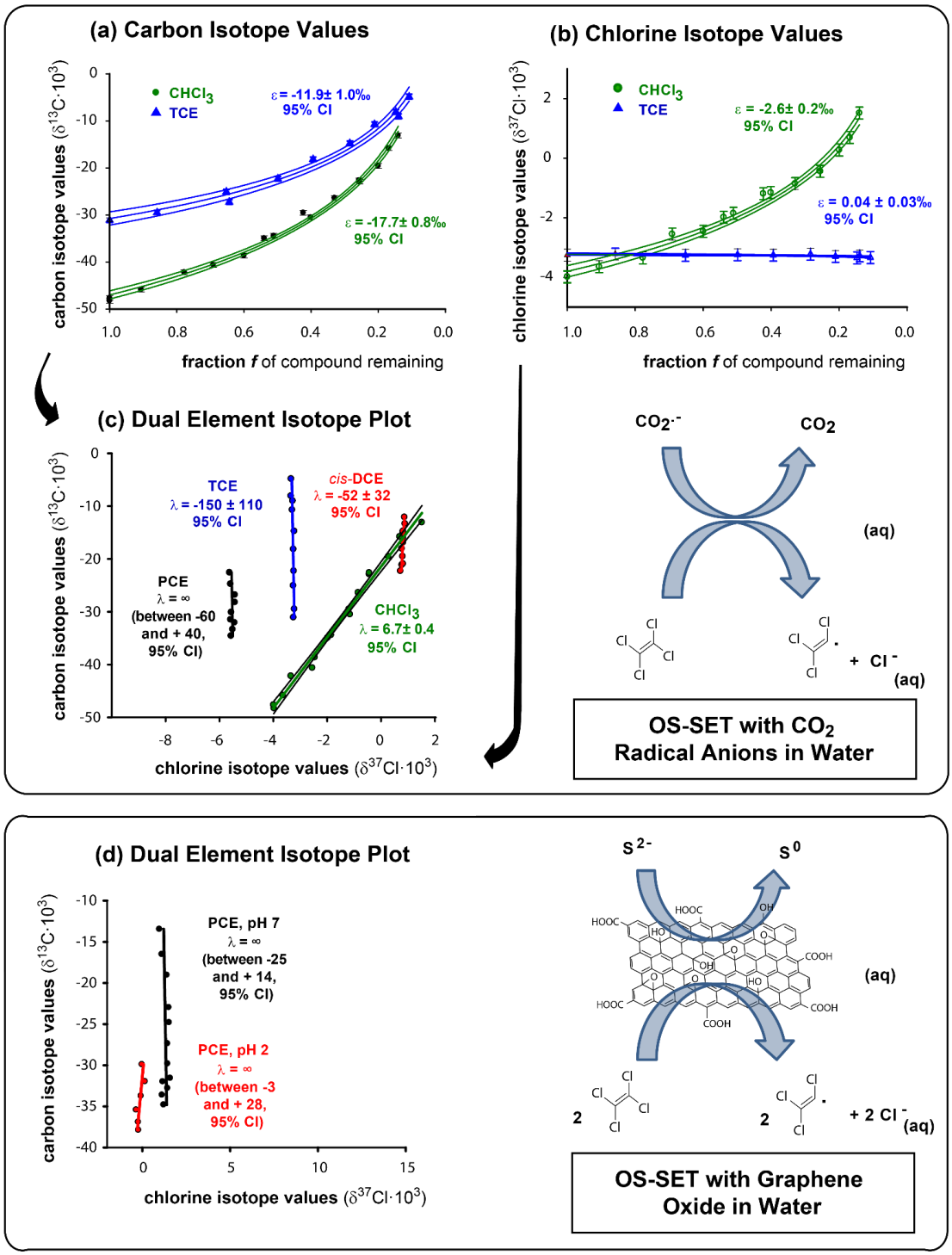

Figure 1. Model reagents for OS-SET in water caused chlorine isotope effects in chloroform, but not in chlorinated ethenes. Isotopic enrichment factors of carbon (a) and chlorine (b) for TCE and $CHCl_3$ in reaction with CO_2 radical anions were obtained by fitting experimental data according to Equation 5. The dual-element isotope slope in panel (c) – where changes in carbon isotope values are plotted against changes in chlorine isotope values – is an alternative way to visualize the presence of carbon, but the absence of chlorine isotope effects in different chlorinated ethenes. Panel (d) shows that the same absence of chlorine isotope effects was also observed for reaction of PCE with

graphene oxide as alternative OS-SET reagent. Error bars correspond to the analytical uncertainty (±0.5‰ for carbon, ±0.2‰ for chlorine isotope analysis). Regressions are represented together with their 95% confidence intervals.

3.4.2. Chlorine Isotope Effects Were Partly Recovered when Chlorinated Ethenes Were Reacted with OS-SET Reagents in an Organic Solvent

The finding that C-Cl bond cleavage in chlorinated ethenes was not concerted / synchronous with OS-SET in our aqueous experiments raises the question whether chlorine isotope effects can be recovered by slowing down C-Cl bond cleavage so that it becomes (partially) rate-limiting. Since a large component of the driving force of aqueous dehalogenation reactions is the high Gibbs enthalpy that is released due to chloride solvation [112], additional experiments were conducted with OS-SET reagents in an organic solvent. Figure 2 shows dual-element isotope slopes for reaction of (a) PCE and (b) TCE with OS-SET model reactants (naphthalene and pyrene radical anions) in glyme. Also here, the SET reactions resulted in steep slopes $\lambda = \Delta\delta^{13}C/\Delta\delta^{37}Cl \approx \varepsilon_C/\varepsilon_{Cl}$ for both PCE and TCE, indicative of large carbon isotope effects of between ε_C = -10.5‰ +/- 1.7‰ and -27.0‰ +/- 4.0‰ (Table 1). In contrast to SET reactions in water, however, we did observe small changes in chlorine isotope values (ε_{Cl} = -0.7‰ +/- 0.2‰ to -2.5‰ +/- 0.3‰, Table 1) indicating that C-Cl bond cleavage became at least partially rate-limiting so that chlorine isotope effects were recovered.

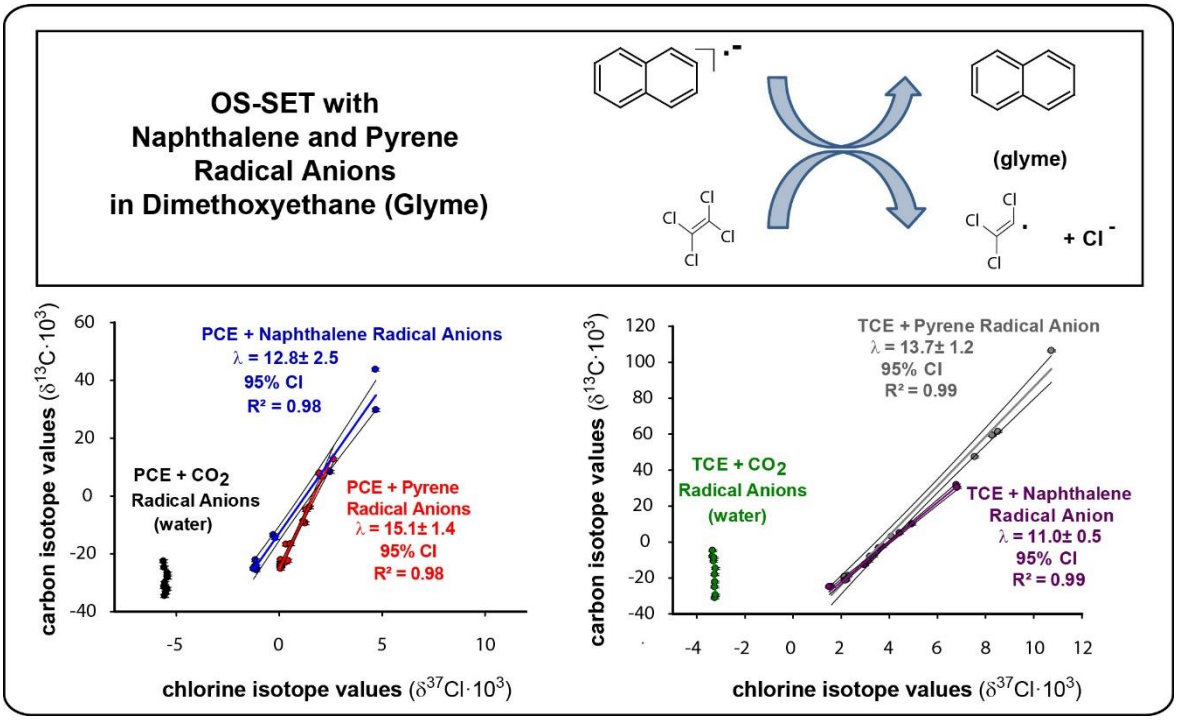

Figure 2. OS-SET reagents caused small chlorine isotope effects when chlorinated ethenes were brought to reaction in the organic solvent glyme. Dual-element isotope plots show carbon and chlorine isotope effects in reaction of (a) PCE and (b) TCE with radical anions of pyrene and naphthalene in glyme compared to reactions of the same substances with CO_2 radical anions as OS-SET reagents in water. Error bars correspond to the analytical uncertainty (±0.5‰ for carbon, ±0.2‰ for chlorine isotope analysis). Regressions are represented together with their 95% confidence intervals.

3.4.3. Our Observations Are Consistent with a Dissociative OS-SET in Chlorinated Alkanes Compared to a Stepwise Process in Chlorinated Ethenes

A mechanistic model explaining our results must take into account (1) the different chlorine isotope effects in $CHCl_3$ and chlorinated ethenes when reacting with OS-SET reagents and (2) the observation that chlorine isotope effects of chlorinated ethenes were partly recovered when the OS-SET was conducted in an organic solvent.

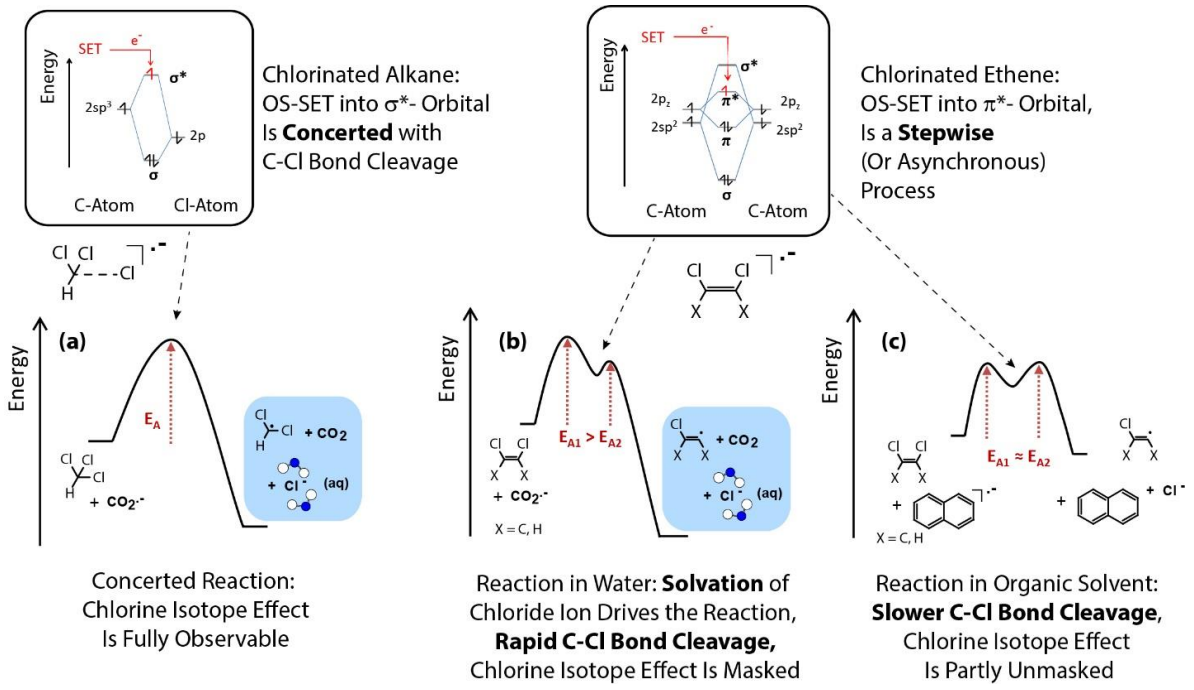

Figure 3: Mechanistic hypothesis of a concerted dissociative OS-SET in chlorinated alkanes versus a stepwise (or asynchronous) process in chlorinated ethenes. Energy diagrams are sketched together with molecular orbitals of the chlorinated compounds. They illustrate (a) the transfer of an electron into the σ* orbital of the C-Cl bond of a chlorinated alkane ($CHCl_3$) compared to (b) a SET into the π* orbital of the C-C bond of a chlorinated ethenel. Both reactions are driven downhill by the Gibbs enthalpy of solvation of the chloride ion in water. In contrast, panel (c) sketches OS-SET to chlorinated ethenes in an organic solvent where the driving force of C-Cl bond cleavage is reduced by the absence of this solvation energy.

Addressing the first point, the different chlorine isotope effects in reactions of $CHCl_3$ and CEs can be rationalized from their electronic structures, where the LUMO orbitals are a σ* and π* orbital, respectively. Adding an electron to the σ*-orbital in $CHCl_3$ is believed to cause immediate (i.e., concerted) carbon-chlorine bond cleavage (Figure 3a)[113]. By contrast, addition of an electron to the π*-orbital of the CEs causes a weakening of the π-π bond, but not necessarily immediate bond cleavage. Indeed, the non-existent chlorine isotope effect in chlorinated ethenes strongly suggests that the chlorine atom was cleaved in a subsequent step (Figure 3b). Hence, we hypothesize that OS-SET into a σ*-orbital of $CHCl_3$ leads to a concerted reaction, whereas OS-SET into a π*-orbital of chlorinated ethenes involves a stepwise (or asynchronous) reaction.

Considering the second point, a possible explanation for the observation that CE chlorine isotope effects were partly recovered when OS-SET was conducted in an organic solvent is

provided by Figure 3b and 3c. According to our hypothesis of a stepwise process the transformation would involve two activation barriers: one barrier (E_{A1}) for the transfer of an electron into the π*-orbital of the chlorinated ethene and a second barrier (E_{A2}) for subsequent cleavage of the C-Cl bond. As discussed above, solvation of the chloride ion in water is strongly exergonic [112]. In line with Hammond's postulate,[114] this lowers the second activation barrier (E_{A2}) (Figure 3b). In an organic solvent, by contrast, the driving force is lower so that the height of the second activation barrier (E_{A2}) is less reduced compared to the first (E_{A1}) (Figure 3c). A strong driving force of the second step will cause practically all intermediate CE radical anions to react onwards to form products so that hardly any molecule partitions back to the reactant side (Figure 3b). Hence, the chlorine isotope effect from C-Cl bond cleavage in E_{A2} will not be observable in the reactant. This masking / demasking of kinetic isotope effects is expressed by mathematical expressions for an apparent kinetic isotope effect in a two-step reaction: [98]

$$\varepsilon^{apparent} = \frac{k_{-1}}{k_{-1}+k_2}\cdot\left(\varepsilon_1^{equ}+\varepsilon_2^{kin}\right)+\frac{k_2}{k_{-1}+k_2}\cdot\varepsilon_1^{kin} \qquad (9)$$

where k_{-1} and k_2 are the reaction rates of intermediate CE radical anions back to reactant and onward to product. ε_1^{kin} and ε_1^{equ} are kinetic / equilibrium isotope effects of the OS-SET in step 1 (non-zero for carbon, zero for chlorine) whereas ε_2^{kin} is the kinetic isotope effect of the C-Cl bond cleavage in step 2 (non-zero for both carbon *and* chlorine). Equations equivalent to 9 are well established expressions in the chemical[96], biochemical[115] and biogeochemical[116] literature (see ref. [98] and references cited therein). Substitution of the rate constants k_{-1} and k_2 by the respective Arrhenius equations $k_i = A_i\cdot\exp\left\{-\frac{(E_{Ai})}{R\cdot T}\right\}$ and multiplication of numerator and denominator by $\frac{1}{A_1}\cdot\exp\left\{\frac{(E_{A1})}{R\cdot T}\right\}\cdot\frac{1}{A_2}\cdot\exp\left\{\frac{(E_{A2})}{R\cdot T}\right\}$ gives the expression[98]

$$\varepsilon^{apparent} = \frac{\left(\frac{1}{A_2}\cdot\exp\left\{\frac{E_{A2}}{R\cdot T}\right\}\right)}{\frac{1}{A_1}\cdot\exp\left\{\frac{(E_{A1})}{R\cdot T}\right\}+\frac{1}{A_2}\cdot\exp\left\{\frac{(E_{A2})}{R\cdot T}\right\}}\cdot\left(\varepsilon_1^{equ}+\varepsilon_2^{kin}\right)+\frac{\left(\frac{1}{A_1}\cdot\exp\left\{\frac{E_{A1}}{R\cdot T}\right\}\right)}{\frac{1}{A_1}\cdot\exp\left\{\frac{(E_{A1})}{R\cdot T}\right\}+\frac{1}{A_2}\cdot\exp\left\{\frac{(E_{A2})}{R\cdot T}\right\}}\cdot\varepsilon_1^{kin} \qquad (10)$$

where A is the pre exponential factor of the Arrhenius equation, R is the universal gas constant, T is the absolute temperature, E_{A1} is the energy difference between reactant state and transition state one and E_{A2} the energy difference between reactant state and transition state two (see Figure 3). The equation expresses the same phenomenon as derived above: that the apparent kinetic isotope effect is a weighted average of the isotope effects of each step, where the weight is given by the height of the respective activation barriers. In water (Figure 3b) the apparent kinetic isotope effect of the reaction of TCE with CO_2 radical anions is, therefore, hypothesized to reflect the OS-SET of the first step (ε_C = -11.9‰; ε_{Cl} = 0.03‰) whereas in glyme (Figure 3c) the reaction of TCE with naphthalene radical anions likely represents a weighted average of both steps (ε_C = -27.0‰; ε_{Cl} = -2.5‰).

Our hypothesis of a concerted mechanism for chloroform and a stepwise mechanism for chlorinated ethenes is in accordance to electrochemical observations of Jean-Michel Savéant[117-120] . By cyclic voltammetry they could determine, that results for the symmetric factor α strongly supports the concerted mechanism for chlorinated methanes[118], whereas the attractive interaction between the caged fragments (D_{CF}) for chlorinated ethenes is too high for a concerted mechanism, favoring a stepwise mechanism[118, 121].

Finally, it was determined that the strength of the reduction potential, what is significant different for CO_2 radical anions and the graphene/sodium sulfide reaction, had no appeal on the intrinsic isotope effect of chlorinated ethenes because k_{-1} (Equation 9) is not affected by reduction of the activation energy by stronger reductive OS-SET reagents[122]

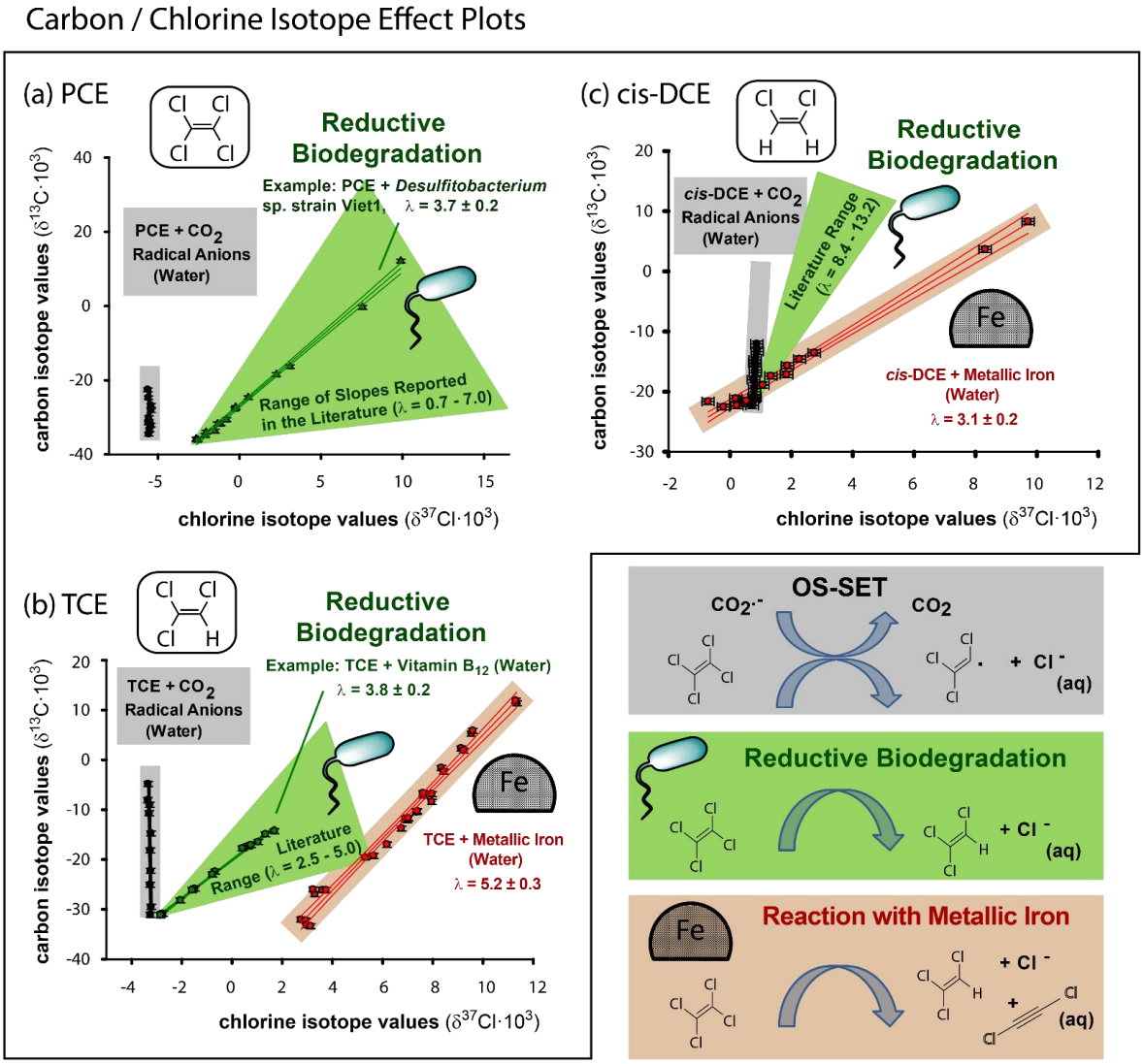

Figure 4. Multi-element isotope effects of chlorinated ethenes in natural and engineered reductive dehalogenation are systematically different from reductive OS-SET in water. Dual-element isotope plots of carbon and chlorine in OS-SET reaction with CO_2 radical anions (this study) are compared to data for biodegradation of PCE (panel a) by *Desulfitobacterium* sp. strain Viet1 [101], to data for transformation of TCE (panel b) with Vitamin B_{12} [35] and metallic iron [94], and to data for transformation of *cis*-DCE (panel c) with metallic iron [94]. Shaded areas illustrate trends of isotope fractionation for OS-SET (grey), metallic iron (pink) and biodegradation (green) from published literature studies (see Table 1). Data for carbon and hydrogen dual-element isotope effects which were measured specifically for this study are shown in Figure 4d. Error bars correspond to the analytical uncertainty (±0.5‰ for carbon, ±0.2‰ for chlorine, ±5‰ for hydrogen isotope analysis). Regressions are represented together with their 95% confidence intervals.

3.4.4. Systematically Different Isotope Fractionation Trends Suggest that OS-SET Is Not a Common Mechanism in Natural and Engineered CE Reductive Dehalogenations

In Figure 4, multi-element isotope effect trends of PCE and TCE from the OS-SET experiments with CO_2 radical anions are compared to literature data on reductive biodegradation and on dehalogenation by zero-valent iron. Example data on natural and engineered transformations (biodegradation of PCE by *Desulfitobacterium* sp. strain Viet1, reductive dehalogenation of TCE by Vitamin B_{12}, transformation of TCE with metallic iron) are shown together with shaded areas representing literature values reported to date. The literature data includes experiments with mixed cultures, pure strains, isolated reductive dehalogenases and purified corrinoids, as listed in Table 1. Even though Figure 4 does illustrate some isotope effect variability in natural and engineered reductive dehalogenation, the combined data still clearly cluster outside the range of our OS-SET experiments in water. The distinguishing feature is the presence of chlorine isotope fractionation in all reactions of PCE, TCE and *cis*-DCE with organisms or zero valent iron reported to date, compared to the total absence of a chlorine isotope effect with OS-SET reagents in our experiments. This is particularly true in cases in which both ε_C and ε_{Cl} are so large that they reflect intrinsic isotope effects of the reaction rather than binding isotope effect of substrate-enzyme association (see Table 1). This combined data, therefore, indicates that OS-SET reaction mechanisms are an exception rather than the rule in natural biodegradation or engineered reactions with zero valent iron. In further support of this statement, are great differences of the predictions and experimental data of rate constants of PCE and TCE reduction by either electron transfer or by vitamin B12 and dehalogenases determined by Constantin et al[121]. Indicating a more intimate interaction between the substrate and the electron donor where the chlorinated ethene enters the cobalt coordination sphere, supporting an inner-sphere rather than outer-sphere mechanism.

Table 1: Literature overview of results from dual-element (C, Cl) isotope studies targeting reductive dehalogenation of PCE, TCE and *cis*-DCE in biodegradation and metallic iron-mediated transformation. Values are stated together with their 95% confidence intervals.

	ε_C [‰]	ε_{Cl} [‰]	dual-element isotope trend [$\lambda \approx \varepsilon_C / \varepsilon_{Cl}$]	references
OS-SET in an organic solvent				
PCE pyrene	-10.5±1.7	-0.7±0.2	15.1±1.4	this study
PCE naphthalene	-15.4±1.5	-1.5±0.1	12.8±2.5	this study
TCE pyrene	-26.5±2.6	-1.9±0.1	13.7±1.2	this study
TCE naphthalene	-27.0±4.0	-2.5±0.3	11.0±0.5	this study
OS-SET in water				
PCE CO_2 radical anions	-7.6±0.8	0.04±0.12	∞ (-11.3±47)	this study
PCE graphene oxide/sodium sulfide pH 7	-9.3±0.9	0.05±0.18	∞ (-10.6±24.5)	this study
PCE graphene oxide/sodium sulfide pH 2	-7.9±1.4	-0.3±0.3	∞ (12.4±15.7)	this study
TCE CO_2 radical anions	-11.9±1.0	0.04±0.03	∞ (148.5±112.2)	this study
cis-DCE CO_2 radical anions	-10.5±0.7	-0.12±0.06	∞ (51.5±32.1)	this study
$CHCl_3$ CO_2 radical anions	-17.7±0.8	-2.6±0.2	6.7±0.4	this study
Reductive biodegradation of PCE				
Desulfitobacterium sp. strain Viet1	-19.0±0.9	-5.0±0.1	3.7±0.2	Cretnik et al. 2014[101]
Enrichment culture dominated by *Desulfitobacterium aromaticivorans* UKTL*	-5.6±0.7	-2.0±0.5	2.8	Wiegert et al. 2013[42]
Sulphurospirillum spp. enrichment culture harboring PceA-TCE*	-3.6±0.2	-1.2±0.1	2.7±0.3	Badin et al. 2014[102]
Sulphurospirillum . enrichment culture harboring PceA-DCE*	-0.7±0.1	-0.9±0.1	0.7±0.2	Badin et al. 2014[102]
Reductive dehalogenase from *Sulphurospirillum multivorans* (norpseudo-B12)*	-1.4±0.1	-0.6±0.2	2.2±0.5	Renpenning et al. 2014[36]
Reductive dehalogenase from *Sulphurospirillum multivorans* (nor-B12)*	-1.3±0.1	-0.4±0.1	2.8±0.5	Renpenning et al. 2014[36]
Norpseudo-B12 (purified cofactor)	-25.3±0.8	-3.6±0.4	6.9±0.7	Renpenning et al. 2014[36]
Nor-B12 (purified cofactor)	-23.7±1.2	-4.8±0.9	5.0±0.8	Renpenning et al. 2014[36]

Cyano-B12 (purified cofactor)	-22.4±0.8	-4.8±0.2	4.6±0.2	Renpenning et al. 2014[36]
Dicyanocobinamid (purified cofactor)	-25.2±0.5	-3.4±0.4	7.0±0.8	Renpenning et al. 2014[36]
Reductive biodegradation of TCE				
Geobacter lovleyi	-12.2±0.5	-3.6±0.1	3.3±0.1	Cretnik et al. 2013[35]
Desulfitobacterium hafniense Y51	-9.1±0.6	-2.7±0.6	3.4±0.2	Cretnik et al. 2013[35]
	-8.6±0.0	-2.6±0.2	3.2±0.2	Buchner et al. 2015[103]
	-8.8±0.2	-2.4±0.2	3.4±0.2	Buchner et al. 2015[103]
	-9.0±0.2	-3.1±0.3	2.8±0.3	Buchner et al. 2015[103]
	-9.0±0.2	-2.6±0.1	3.5±0.2	Buchner et al. 2015[103]
Dehalococcoides (two species)	-16.4±1.5	-3.6±0.3	4.5	Kuder et al. 2013[38]
Enrichment culture dominated by *Desulfitobacterium aromaticivorans* UKTL	-8.8±2.0	-3.5±0.5	2.5	Wiegert et al. 2013[42]
Reductive dehalogenase from *Sulphurospirillum multivorans* (norpseudo-B12)	-20±0.5	-3.7±0.2	5.3±0.3	Renpenning et al. 2014[36]
Reductive dehalogenase from *Sulphurospirillum multivorans* (nor-B12)	-20.2±1.1	-3.9±0.6	5±0.8	Renpenning et al. 2014[36]
Norpseudo-B12 (purified cofactor)	-18.5±2.8	-4.2±0.8	4.5±0.8	Renpenning et al. 2014[36]
Nor-B12 (purified cofactor)	-15.1±2.7	-3.9±1.0	3.7±0.3	Renpenning et al. 2014[36]
Dicyanocobinamid (purified cofactor)	-16.5±0.7	-3.9±0.5	4.2±0.6	Renpenning et al. 2014[36]
Cyano-Vitamin B12 (purified cofactor)	-15±2.0	-3.2±1.0	4.4±0.7	Renpenning et al. 2014[36]
Cyano-Vitamin B12 (purified cofactor)	-16.1±0.9	-4.0±0.2	3.8±0.2	Cretnik et al. 2013[35]
Cobaloxime (chemical model reactant)	-21.3±0.5	-3.5±0.1	6.1±0.2	Cretnik et al. 2013[35]
Reduction by metallic iron	-14.9±0.9	-2.6±0.2	5.2±0.3	Audí-Miró et al.2013[94]
Reduction by metallic iron	-12.4	-3.0	4.2	Lojkasek-Lima et al. 2012[13]
Reductive biodegradation of *cis*-DCE				
Mixed culture harboring *Dehalococcoides*	-26.8	-3.2	8.4	Kuder et al. 2013[38]
Mixed culture harboring *Dehalococcoides*	-18.5±1.8	-1.6±0.1	11.6	Abe et al. 2009[93]
Mixed culture harboring *Dehalococcoides*	-18.5±1.3	-1.4±0.2	13.2	Abe et al. 2009[93]
Reduction by metallic iron	-20.5±1.8	-6.2±0.8	3.1±0.2	Audí-Miró et al.2013[94]

* entries with a star indicate cases in which observable ε_c are so small that they likely reflect isotope effects of substrate-enzyme association etc. in addition to those of the intrinsic (bio)chemical reaction.

3.5. Conclusion

Pinpointing detailed chemical reaction mechanisms in complex natural and engineered transformations is intrinsically difficult. Methods employed to characterize electron transfer encounter complexes in laboratory experiments – spectral elucidation, or even X-ray structure analysis[77] – are not accessible in natural environments. Yet it is this knowledge about the manner and order of chemical bond cleavage that provides the key to understanding subsequent transformation pathways leading to problematic vs. benign daughter products in remediation schemes. This study takes advantage of a new opportunity – multi-element isotope effect analysis of organic compounds at natural isotopic abundance – to evaluate whether outer-sphere single electron transfer, a mechanism that has frequently been invoked, but not been proven, is involved in natural and engineered reductive dehalogenation reactions.

Experiments with chemical model reactants made it possible to derive a consistent mechanistic explanation for the absence of chlorine isotope effects in chlorinated ethene transformation by aqueous OS-SET reagents. Our results indicate the occurrence of a stepwise OS-SET (SET to a π^* orbital followed by C-Cl cleavage) in chlorinated ethenes compared to a dissociative OS-SET (SET to a σ^* orbital concerted with C-Cl breakage) in chlorinated alkanes (Figure 3). Building on this mechanistic understanding, the consistent *absence* of chlorine isotope effects in aqueous OS-SET could be compared to the consistent *presence* of chlorine isotope effects in all biodegradation studies and in all metallic iron-mediated dehalogenation reactions of PCE and TCE reported to date (Figure 4). The discrepancy strongly suggests that OS-SET is an exception rather than the rule in natural and engineered reductive dehalogenation reactions. This result is relevant to guide future research on the organic reaction chemistry of environmental reductive dehalogenations. Our results indicate that product formation cannot necessarily be derived from chlorinated vinyl radicals resulting from initial outer-sphere electron transfer, and that reactivity cannot necessarily be predicted from Marcus theory of outer-sphere non-adiabatic ET [75]. Instead, our results point to inner-sphere interactions, consistent with organometallic reactions at metal surfaces and in reductive dehalogenases which still warrant exploration. Future research should be directed at characterizing the underlying reaction chemistry of chlorinated ethene degradation. Together with the recent structural elucidation of reductive

dehalogenases, the new opportunity of multi-element isotope effect analysis at natural isotopic abundance may enable pursuit of this goal

.

4.

Chlorinated Ethene Reactivity with Vitamin B12 Is Governed by Cobalamin Chloroethylcarbanions as Crossroads of Competing Pathways

Benjamin Heckel, Kristopher McNeill, Martin Elsner; *ACS Catal.* **2018**, 8, 3054−3066

DOI: 10.1021/acscatal.7b02945

4.1. ABSTRACT

Chlorinated ethenes are toxic groundwater contaminants. While they can be dechlorinated by microorganisms, reductive dehalogenases and their corrinoid cofactor, biochemical reaction mechanisms remain unsolved. This study uncovers a mechanistic shift revealed by contrasting compound-specific carbon ($\varepsilon^{13}C$) and chlorine ($\varepsilon^{37}Cl$) isotope effects between perchloroethene, PCE ($\varepsilon^{37}Cl$ = -4.0‰) and *cis*-dichloroethene, *cis*-DCE ($\varepsilon^{37}Cl$ = -1.5‰), and a pH-dependent shift for trichloroethene, TCE (from $\varepsilon^{37}Cl$ = -5.2‰ at pH 12 to $\varepsilon^{37}Cl$ = -1.2‰ at pH 5). The existence of different pathways is supported also by pH-dependent shifts in reaction rates, TCE product distribution and hydrogen isotope effects. Mass balance deficits revealed reversible and irreversible cobalamin-substrate association, whereas high-resolution mass spectrometry narrowed down possible structures to chloroalkyl and chlorovinyl cobalamin complexes. Combined experimental evidence is inconsistent with initial electron transfer or alkyl or vinyl complexes as crossroads of both pathways. In contrast, it supports cobalamin chlorocarbanions as key intermediates from which Cl^- elimination produces vinyl complexes (explaining rates and products of TCE at high pH), whereas protonation generates less reactive alkyl complexes (explaining rates and products of TCE at low pH). Multielement isotope effect analysis holds promise to identify these competing mechanisms also in real dehalogenases, microorganisms and even contaminated aquifers.

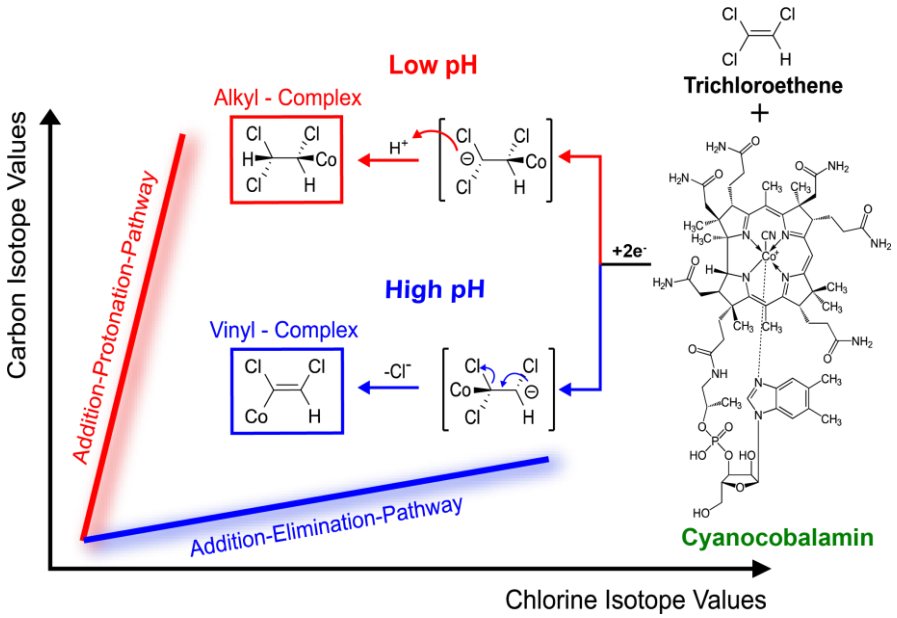

4.2. Introduction

Chlorinated ethenes are important chemical intermediates, degreasing and dry cleaning agents, and they rank among the most frequent groundwater contaminants [123]. They can enter the subsurface through accidents and improper handling. Because of their high density and low water solubility, they tend to accumulate as pure phase pools at the confining layer of aquifers leading to long-lasting groundwater contaminations. Highly chlorinated ethenes are rather persistent under oxic conditions, but are conducive to biotic reductive dehalogenation in anoxic zones of aquifers.[68] Natural or engineered biodegradation does not always achieve complete dehalogenation, however. [8] Biodegradation involves sequential replacement of chlorine by hydrogen so that perchloroethene (PCE) and trichloroethene (TCE) are transformed to more problematic *cis*-dichloroethene (*cis*-DCE) and vinyl chloride (VC), before harmless ethene is formed. While some microorganisms of the genus *Dehalococcoides* are able to achieve complete dehalogenation, most microorganisms stop at the stage of *cis*-DCE or VC [69]. This raises the question for the underlying (bio)chemical degradation mechanism and why transformation frequently stops at the stage of these more problematic daughter compounds. The key must lie in the reaction chemistry of cobalamin (Vitamin B_{12}) since this enzymatic cofactor lies at the heart of practically all reductive dehalogenases (Rdases) identified to date[124]. The importance of the lower axial ligand at the Co center was highlighted in dechlorination with *Dehalococcoides mccartyi*, where amendment with a 5,6-dimethylbenzimidazole base resulted in complete cis-DCE, whereas amendment with other ligands did not.[125] In contrast, crystal structures of Rdases from *Sulfurospirillum multivorans* and *Nitratireductor pacificus* suggest that this base is not even ligated with the Co center[83, 84, 126]. Despite this evidence and much research on putative reaction intermediates of cobalamine and its functional mimics (cobaloxime, tetraphenylporphyrin cobalt (TPP)Co), [78, 127-133] and despite even the first elucidation of reductive dehalogenase enzyme structures,[82-84] a consistent picture of the underlying reaction biochemistry of chlorinated ethenes has still not be pinpointed. Three different reductive dechlorination mechanisms have been brought forward [78]: 1. (inner sphere) nucleophilic addition [134]; 2. electron transfer (either inner-[83, 135-137] or outer-sphere[84,79, 126, 138]; 3. (inner-sphere) nucleophilic substitution [78, 139]

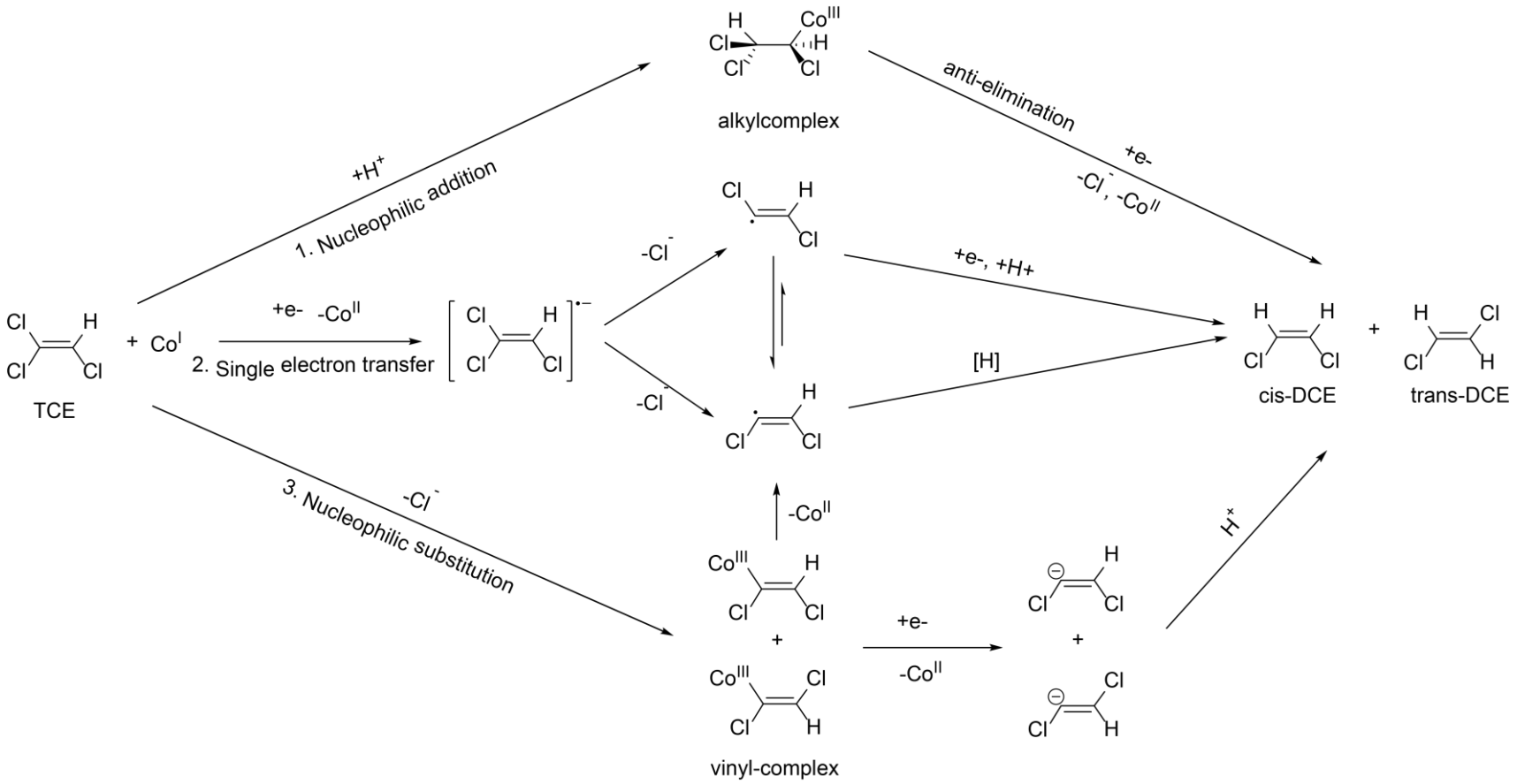

Scheme 1. Suggested reaction mechanisms for reductive dehalogenation of TCE. 1) Nucleophilic addition; 2) Single electron transfer; 3) Nucleophilic substitution. Here, "$-e^-$, $+H^+$" indicate an electron transfer followed by protonation, whereas "[H]" indicates abstraction of a hydrogen atom.

The nucleophilic addition and substitution pathways are motivated by the observation of pH-dependent reaction kinetics[134], by the detection of alkyl and vinyl Vitamin B_{12} complexes from (low resolution) mass spectrometry[79, 140], and by the observation that typical product spectra are obtained from synthesis and subsequent reaction of such intermediates [78, 79, 132, 140, 141]. Conversely, the hypothesis of single electron transfer is based on the detection of trichlorovinyl radicals during the reaction of vitamin B_{12} with TCE[79, 80, 131, 138, 141]. Furthermore, studies of the reductive dehalogenase PceA from *Sulfurospirillum multivorans*[84, 126] favor an outer-sphere single electron transfer (OS-SET) based on a Co(II)-to-TCE distance of 5.8 Å. EPR evidence for a direct interaction of the halogen atom and Co in reductive dehalogenation of aromatic phenols by the reductive dehalogenase NpRdhA of *Nitratireductor pacificus* supports an inner-sphere SET mechanism [83]; DFT-based computational calculations simulated this mechanistic scenario also for chlorinated ethenes [137]. Conversely, the absence of such EPR observations in reductive dehalogenation of PCE by PceA from *Sulfurospirillum multivorans* was interpreted as evidence for an outer-sphere SET mechanism [126]. An inner-sphere two-electron transfer *via* a halogenophilic substitution, finally, has been proposed for halogenated aromatic compounds (not shown in Scheme 1) [135].

The difficulty in coming up with a coherent mechanistic picture for even the simplest model of reductive biotransformation – chlorinated ethene reduction by Vitamin B_{12} – presents, therefore, a major obstacle in advancing our understanding of reaction mechanisms in dehalogenases, or even whole organisms. The research need exists for additional experimental evidence to integrate existing observations in a coherent mechanistic picture, to subsequently transfer such insight from model systems to real environmental systems, and to demonstrate, thereby, that the same reaction mechanisms prevail in enzymes, or real organisms.

Multiple element compound-specific isotope effect analysis (CSIA) of chlorinated ethenes offers an underexplored opportunity from geochemistry [142] to answer both questions and to close the gap between mechanistic insight from model systems, enzymes and organisms[116]. Isotope ratios of carbon ($^{13}C/^{12}C$), chlorine ($^{37}Cl/^{35}Cl$) and hydrogen ($^{2}H/^{1}H$) can be measured at their natural isotopic abundance (i.e., without isotope label) in samples taken along a (bio) chemical reaction and can be expressed as difference relative to an international reference.

$$\delta^{13}C = \frac{(^{13}C/^{12}C_{Sample} - ^{13}C/^{12}C_{\mathrm{Re}\,ference})}{^{13}C/^{12}C_{\mathrm{Re}\,ference}} \quad (1)$$

$$\Delta\delta^{13}C = \delta^{13}C - \delta^{13}C_{initial} \quad (2)$$

Here, ($^{13}C/^{12}C_{Reference}$) and sample ($^{13}C/^{12}C_{Sample}$) are the isotope ratios of an international reference and of the sample, and $\delta^{13}C$ and $\delta^{13}C_{initial}$ are isotope values of samples taken at a given time point and at the beginning of the reaction, respectively. Recent analytical advances [18, 20, 65] have made it possible to analyze such isotope ratios also for chlorine ($^{37}Cl/^{35}Cl$) and hydrogen ($^{2}H/^{1}H$) in chlorinated ethenes; analogous equations apply for these elements. Compound-specific isotope effects are subsequently evaluated for each element according to [21, 22]

$$\delta^{13}C = \delta^{13}C_{initial} + \left[\varepsilon^{13}C \cdot \ln f\right] \quad (3)$$

where f is the fraction of reactant remaining and $\varepsilon^{13}C$ is the so-called enrichment factor which expresses the difference in transformation rates of light and heavy isotopologues and which is equivalent to a compound-specific kinetic isotope effect $^{12}k/^{13}k$. Specifically, a value, e.g., of $\varepsilon^{13}C$ = -10‰ means that molecules containing ^{13}C react by 10 per mille – or one percent – slower than those with ^{12}C corresponding to a compound-average kinetic isotope effect of $^{12}k/^{13}k$ = 1.01. For chlorine and hydrogen analogous expressions are valid [63]. When plotting changes in isotope ratios of two elements against each other, a dual element isotope plot is obtained. Its slope $\lambda = \Delta\delta^{13}C/\Delta\delta^{37}Cl \approx \varepsilon^{13}C/\varepsilon^{37}Cl \approx (^{12}k/^{13}k - 1)/(^{35}k/^{37}k - 1)$ expresses the magnitude of isotope effects of different elements relative to each other and is, therefore, a sensitive tool to distinguish different reaction mechanisms [53, 98, 99, 143, 144]. Indeed, a recent computational study brought forward in this journal suggests that dual element isotope analysis may provide the key evidence necessary to distinguish different mechanisms of chlorinated ethene reduction by Cob(I)alamin.[139] However, even though several studies have recently determined compound-specific isotope effects of carbon[35, 36, 42, 103], chlorine[35, 36, 42, 103] and even hydrogen[38] for chlorinated ethenes in reductive dehalogenation by Vitamin B_{12}, enzymes and bacteria [35, 36, 42, 100-103], interpretations remain inconclusive: the variability of isotope effects has not been systematically investigated; observed isotope effects have not been combined with "classical" mechanistic

probes such as reactivity trends, detection of intermediates, etc. Finally, the approach has not been pursued to rationalize product formation (e.g., why reactions often stop at the stage of *cis*-DCE).

With the aim to derive a consistent mechanistic picture for the conflicting mechanisms of Scheme 1, this study, therefore, combines all available lines of evidence: reactivity trends and multielement (C, H, Cl) isotope effects of chlorinated ethenes with different molecular structures (PCE, TCE, *cis*-DCE); detection of intermediates by high-resolution mass spectrometry, radical trap experiments and mass balance deficit analysis; and, changes in the relative contribution of various pathways upon changes in reaction conditions (pH between 5 and 12). The mechanistic insights gained from this study are then explored for their ability to explain reactivity trends and product formation, and to answer why biodegradation of chlorinated ethenes often stops at *cis*-DCE or VC.

4.3. Materials & Methods

4.3.1. Chemicals

A list of all chemicals is provided in the Supporting Information of Chapter 4.

4.3.2. Kinetics, isotope effects and product formation in dehalogenation of chlorinated ethenes by Vitamin B_{12} at different pH

For a detailed description see the Supporting Information. Briefly, a pH-specific buffer solution (pH between 5 to 12) was prepared, degassed with nitrogen and PCE, TCE or *cis*-DCE were added in an anoxic glovebox. In parallel, titanium(III)chloride was dissolved in water, the solution was degassed with nitrogen, sodium citrate was added and the pH adjusted. The reaction was started by combining the chlorinated ethene solution, the Ti(III)citrate solution and Vitamin B_{12} to give concentrations of about 1 mM chlorinated ethene, between 15 μM and 325 μM Vitamin B_{12} and about 25 mM Ti(III) citrate. Reactions were conducted in the dark. Samples for concentration, carbon- and chlorine isotope measurements were removed at selected time-points either by headspace sampling with a pressure lock syringe or by taking liquid samples in which the reaction was stopped through hydrogen peroxide addition.

4.3.3. Experiments to detect complex formation between Vitamin B12 and TCE by direct injection-mass spectrometry (DI-MS) and analysis of mass balance deficits

To capture intermediates, experiments at different pH were conducted with stoichiometric amounts of pre-reduced vitamin B_{12} and without Ti(III) as bulk reductant. Mass balance deficits were determined as the difference between (a) initial TCE; (b) remaining TCE; (c) volatile products (not observed under stoichiometric conditions); (d) reversibly associated TCE that could be recovered by exhaustive sparging of the solution. A detailed description is provided in the Supporting Information.

4.3.4. Analytical Methods

A detailed description of concentration-, isotope analysis (carbon, chlorine and hydrogen) and high resolution mass spectrometry is provided in the Supporting Information. Briefly, concentrations were analyzed by gas chromatography-mass spectrometry (GC-MS) and isotope values by gas chromatography coupled to an isotope ratio mass spectrometer (GC-IRMS). $^{13}C/^{12}C$ and $^{2}H/^{1}H$ ratios were determined after peak separation and combustion to CO_2[145] or reduction to H_2[56] respectively, whereas $^{37}Cl/^{35}Cl$ ratios were determined after gas chromatographic separation by direct analysis of intact CE isotopologue molecules[18, 19].

4.4. Results and Discussion

4.4.1. Isotope effects and reactivity trends indicate different reaction mechanisms for PCE and cis-DCE

To probe for the occurrence of different transformation mechanisms as hypothesized in Scheme 1 and brought forward in previous studies[79, 134], Vitamin B_{12}-catalyzed dehalogenation was investigated for the chlorinated ethenes PCE and *cis*-DCE with titanium citrate as bulk reductant at different pH (6.5 to 11). Increasing pH values resulted in opposing reactivity trends for PCE and *cis*-DCE, where 2nd order rate constants (derived for S = PCE, TCE, *cis*-DCE and catalyst = Vitamin B_{12} according to $d[S]/dt = -k \cdot [S] \cdot [catalyst]$) increased for PCE (pH 6.5: k= 115 ± 15 $(M\ catalyst)^{-1} \cdot s^{-1}$; pH 9: k= 176 ± 14 $(M\ catalyst)^{-1} \cdot s^{-1}$; pH 11: k= 270 ± 41 $(M\ catalyst)^{-1} \cdot s^{-1}$) whereas they decreased for *cis*-DCE (from pH 6.5: k= 0.03 ± 0.006 $(M\ catalyst)^{-1} \cdot s^{-1}$ over pH 9: k= 0.0008 ± 0.0002 $(M\ catalyst)^{-1} \cdot s^{-1}$ to pH 11: hardly any degradation at all). The greater rate constants of PCE compared to *cis*-DCE agree perfectly with those of previous studies (e.g. PCE pH 9.0 k= 155 ± 21 $M^{-1} \cdot s^{-1}$; *cis*-DCE pH 9.0 k= 0.0006 ± 0.0001 $M^{-1} \cdot s^{-1}$)[134]. Conversely, the different nature of *relative* reactivity (trends of decreasing rates of PCE at lower pH vs. increasing rates of cis-DCE) indicate the occurrence of different underlying reaction mechanisms.

In agreement with these opposing reactivity trends, also carbon and chlorine isotope effects showed pronounced differences between the two compounds. Large carbon and small chlorine isotope effects were detected for *cis*-DCE ($\varepsilon^{13}C$ = -28.4‰ ± 1.1‰; $\varepsilon^{37}Cl$ = -1.5‰ ± 0.2‰; Figure 1a & b), whereas reaction of Vitamin B_{12} with PCE resulted in smaller carbon but much greater chlorine isotope effects ($\varepsilon^{13}C$ = -16.6‰ ± 2.7‰ to -17.0‰ ± 1.2‰; $\varepsilon^{37}Cl$ = -4.0‰ ± 0.4‰ to -4.2‰ ± 0.4‰; Figure 1a & b). (Note that these differences cannot be explained by the number of chlorine atoms in the molecules: when taking into account a "dilution" by non-reacting positions[22], the discrepancy in intrinsic chlorine isotope effects (2·(-1.5‰) = -3‰ vs. 4·(-4‰) = -16‰) would be even more pronounced). The trend is also represented in the dual element isotope plot of Figure 1c, where the small chlorine isotope effects in reaction of *cis*-DCE resulted in a steep slope of $\lambda = \Delta\delta^{13}C/\Delta\delta^{37}Cl$ = 18.2 +/- 2.2, whereas the larger chlorine isotope effects in PCE gave rise to a much flatter slope (λ = 3.9 +/- 0.4 to 4.2 +/- 0.3). The pH value of the reaction solution had no influence on the carbon and chlorine isotope effects of PCE. Taken together, both lines of evidence point to different reaction mechanisms in the reductive dehalogenation of PCE vs. *cis*-DCE. The increasing reaction rates of PCE with increasing pH can be explained with the increasing reduction potential of titanium(III) citrate[146] and – consequently – a higher steady-state concentration of Co^{I} (where we have considered that the redox potential of Co^{I} does not change above pH 4.7[147, 148]). The opposite trend for *cis*-DCE, in contrast, indicates that its reactivity must be governed by a different underlying mechanism and that the reaction rate of this mechanism is accelerated by the presence of H^{+}. Further, the strong chlorine isotope effect in PCE indicates that a C-Cl bond must be cleaved in the rate-determining step of PCE dehalogenation, whereas the small chlorine isotope effect (in conjunction with a large carbon isotope effect) in *cis*-DCE indicates that a different chemical step involving carbon, but not chlorine atoms was rate-determining in reduction of *cis*-DCE.

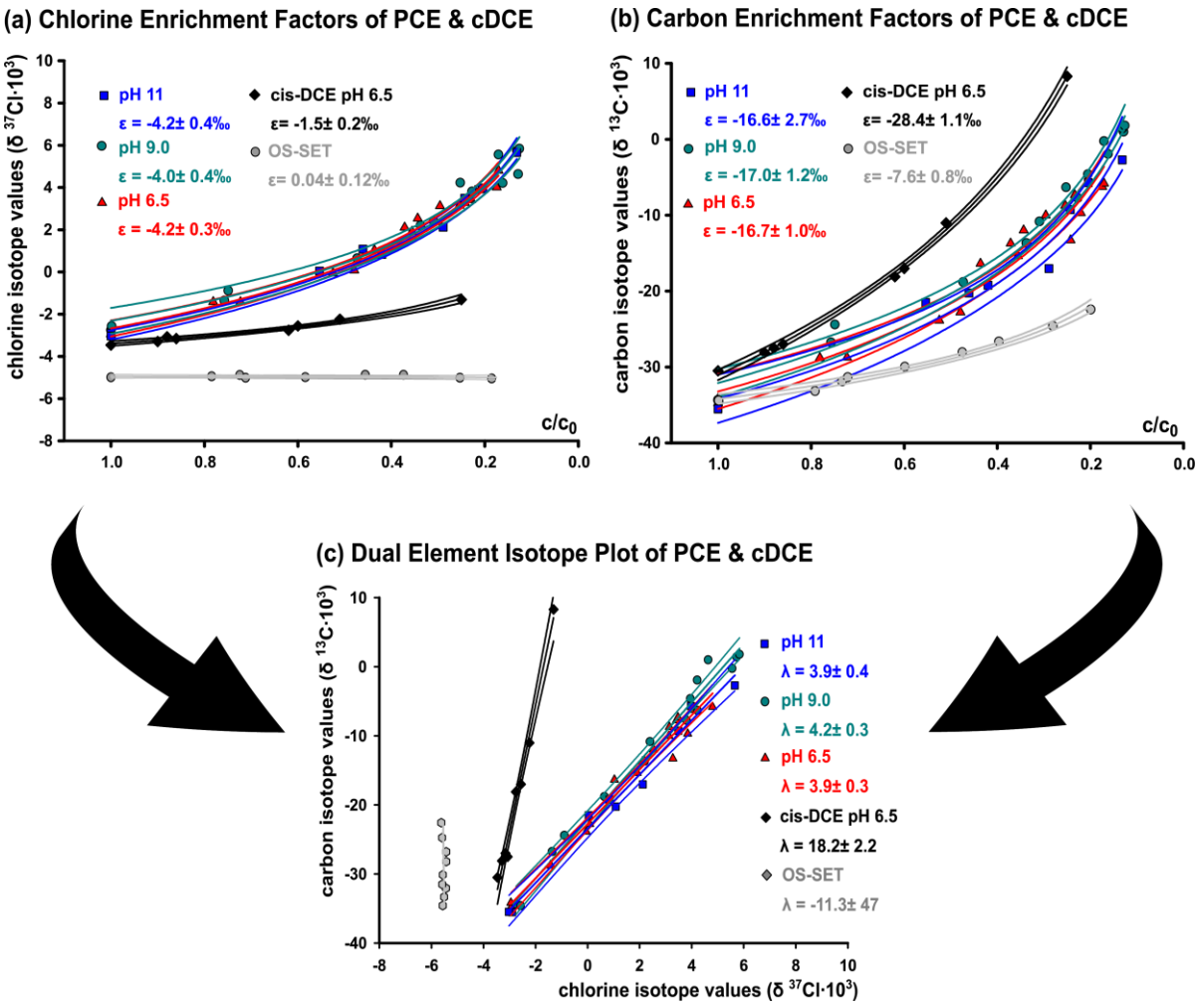

Figure 1: Different carbon vs. chlorine isotope effects in reaction of PCE and *cis*-DCE with Vitamin B_{12}. Isotopic enrichment factors ε of chlorine (a) and carbon (b) for PCE and *cis*-DCE in reaction with Vitamin B_{12} were obtained according to Equation 3 by fitting changes in isotope values against the remaining fraction of substrate. (c) The different trends in isotope effects are represented in the dual element isotope plot which combines carbon and chlorine isotope values from the reaction of Vitamin B_{12} with PCE and *cis*-DCE.

4.4.2. Isotope effects and reactivity trends indicate a pH-dependent mechanistic shift in reaction of TCE

To further probe for the observed pH-dependency in reductive chlorinated ethene dehalogenation by Vitamin B_{12}, experiments were conducted with TCE between pH 5 and 12. TCE contains one dichlorovinylidene group (=CCl_2) like in PCE and one chlorovinylidene group (=CHCl) like in *cis*-DCE, and its redox potential (CHCl=$CCl_{2(aq)}$ +

$2e^- + H^+ \rightarrow CHCl=CHCl_{(aq)} + Cl^-_{(aq)}$; -0.67 V vs. the standard hydrogen electrode) has been computed to lie between PCE ($CCl_2=CCl_{2(aq)} + 2e^- + H^+ \rightarrow CHCl=CCl_{2(aq)} + Cl^-_{(aq)}$;; -0.60 V) and *cis*-DCE ($CHCl=CHCl_{(aq)} + 2e^- + H^+ \rightarrow CH_2=CHCl_{(aq)} + Cl^-_{(aq)}$;; -1.012 V)[112]. The reactivity trend of TCE was analogous to PCE: a decrease in pH resulted in a reduction of TCE reaction rates, where the decline was particularly drastic below pH 8 (Figure 2f). Remarkably, this trend was also accompanied by a change in observable TCE chlorine isotope effects, where the change was again particularly pronounced at pH 8 (Figure 2e). While carbon isotope effects showed only a small variation ($\varepsilon^{13}C$ = -15.8‰ ± 0.9‰ to -17.5‰ ± 1.0‰; Figure 2a) chlorine isotope effects of TCE decreased dramatically from $\varepsilon^{37}Cl$ = -5.2‰ ± 0.4‰ at pH 11 to $\varepsilon^{37}Cl$ = -1.2‰ ± 0.1‰ at pH 5 (Figure 2b, e). The observed carbon isotope enrichment factors $\varepsilon^{13}C$ are consistent with those of previous studies [35, 36, 149-151]. Variation of chlorine isotope enrichment factors, $\varepsilon^{37}Cl$, in contrast, was much greater than previously observed [35, 36, 149-151] indicating a hitherto unrecognized shift to a different reaction mechanism in the reduction of TCE. This shift is also visualized in the dual element isotope plot of Figure 2e, where the slope $\lambda = \Delta\delta^{13}C/\Delta\delta^{37}Cl$ increased with decreasing pH (from λ = 3.3 +/- 0.1 to 12.4 +/- 1.4; Figure 2e).

The large chlorine isotope effect at high pH is indicative of a mechanism that involves C-Cl bond cleavage. In contrast, the small chlorine isotope effect at low pH indicates a different mechanism which, like in the case of *cis*-DCE, does not involve C-Cl bond cleavage in the rate-determining step and which is accelerated by the presence of $[H^+]$. The role of protonation in this mechanistic shift is emphasized by an additional experiment conducted with Vitamin B_{12} in deuterated water at pH 9.0, which resulted in the greatest chlorine isotope effect ($\varepsilon^{37}Cl$ = -6.8‰ +/- 0.4‰; Figure 2b) and the smallest slope (λ = 2.8 +/- 0.2; Figure 2c) of all observations. Hence, the lower reaction rate of D^+ ions slowed down the alternative pathway to the same, or an even greater extent, than a smaller concentration of H^+ ions imposed by the change of pH. Such a change in mechanism is further supported by carbon/hydrogen dual element isotope fractionation trends (Figure 2d) where also different slopes with changing pH are detected (for further discussion see below).

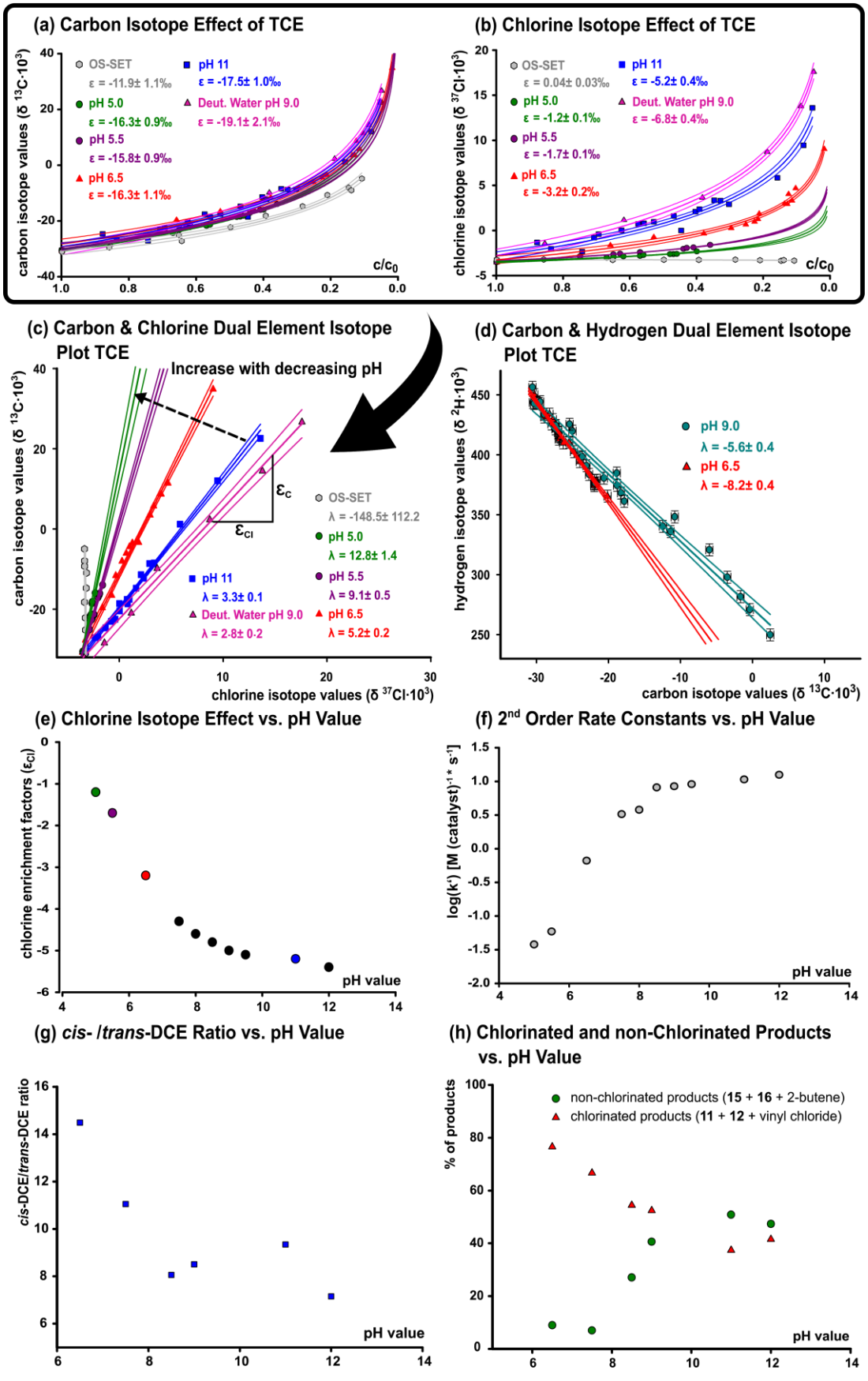
(a) Carbon Isotope Effect of TCE
carbon isotope values (δ 13C·10³)
c/c0
OS-SET
ε = -11.9± 1.1‰
pH 11
ε = -17.5± 1.0‰
pH 5.0
ε = -16.3± 0.9‰
Deut. Water pH 9.0
ε = -19.1± 2.1‰
pH 5.5
ε = -15.8± 0.9‰
pH 6.5
ε = -16.3± 1.1‰
(b) Chlorine Isotope Effect of TCE
chlorine isotope values (δ 37Cl·10³)
c/c0
OS-SET
ε = 0.04± 0.03‰
pH 11
ε = -5.2± 0.4‰
pH 5.0
ε = -1.2± 0.1‰
Deut. Water pH 9.0
ε = -6.8± 0.4‰
pH 5.5
ε = -1.7± 0.1‰
pH 6.5
ε = -3.2± 0.2‰
(c) Carbon & Chlorine Dual Element Isotope Plot TCE
Increase with decreasing pH
carbon isotope values (δ 13C·10³)
chlorine isotope values (δ 37Cl·10³)
εC
εCl
OS-SET
λ = -148.5± 112.2
pH 5.0
λ = 12.8± 1.4
pH 5.5
λ = 9.1± 0.5
pH 11
λ = 3.3± 0.1
Deut. Water pH 9.0
λ = 2·8± 0·2
pH 6.5
λ = 5.2± 0.2
(d) Carbon & Hydrogen Dual Element Isotope Plot TCE
hydrogen isotope values (δ 2H·10³)
carbon isotope values (δ 13C·10³)
pH 9.0
λ = -5.6± 0.4
pH 6.5
λ = -8.2± 0.4
(e) Chlorine Isotope Effect vs. pH Value
chlorine enrichment factors (εCl)
pH value
(f) 2nd Order Rate Constants vs. pH Value
log(k') [M (catalyst)-1 * s-1]
pH value
(g) cis- /trans-DCE Ratio vs. pH Value
cis-DCE/trans-DCE ratio
pH value
(h) Chlorinated and non-Chlorinated Products vs. pH Value
% of products
non-chlorinated products (15 + 16 + 2-butene)
chlorinated products (11 + 12 + vinyl chloride)
pH value

Figure 2: Trends in TCE chlorine isotope effects and observed product ratios indicate a change in the dechlorination mechanism with Vitamin B_{12}. Isotope enrichment factors of carbon (a) and chlorine (b) for TCE in reaction with Vitamin B_{12} were obtained by fitting changes of isotope values against the remaining fraction of TCE substrate according to Equation 3. (Data on OS-SET are from ref [59]). (c) pH dependent variation in carbon and chlorine isotope effects of TCE represented in a carbon/hydrogen dual element isotope plot, (d) pH dependent variation carbon and hydrogen isotope effects of TCE represented in a carbon/hydrogen dual element isotope plot. (e) Changes of chlorine isotope enrichment factors of TCE with pH (note that a more negative value indicates a stronger isotope effect). (f) Changes in 2nd order rate constants of TCE with pH. (g) *cis*-DCE-to-*trans*-DCE ratio versus pH. (h) Formation of chlorinated and non-chlorinated products versus pH (where numbers (**11**, **12**, **15** and **16**) correspond to structures in Scheme 2).

The results of the two sets of experiments with PCE / *cis*-DCE (Figure 1) and with TCE (Figure 2) are strikingly consistent. Both give evidence of different reaction mechanisms which are reflected by a different magnitude of chlorine isotope effects, and both have in common that the mechanistic path that is associated with a small chlorine isotope effect is accelerated by H^+.

4.4.3. pH-dependent product distribution supports a mechanistic shift in TCE transformation

Figures 2h and 2g demonstrate that this mechanistic dichotomy is also reflected in the pattern of TCE product distribution. Identical products, but drastic changes in their quantity were found between high and low pH values (Figure D2a and b), which is consistent with, but exceeds previous observations by Glod et al.[79] Degradation of TCE at pH 6 resulted in around 80% chlorinated products while less than 15% non-chlorinated products were formed (remaining TCE 2%). In contrast, over 50% non-chlorinated products, mainly ethene, and less than 40% chlorinated products were produced at high pH (remaining TCE 5%). Figure 2g further shows that even the *cis*- to *trans*-DCE ratio changed significantly with pH. It has been recognized that the preference of *cis*- over *trans*-DCE may derive from different intermediates [101, 109, 141, 152] and that the exact ratio of *cis*- over *trans*-DCE may serve as indicator of competing mechanisms [109]. Hence, our data suggests that different intermediates were involved as precursors to these isomers depending on pH. Experiments with d_7-isopropanol[80], finally, yielded more deuterated *cis*- and *trans*-DCE at pH 6.5 than at pH 9

revealing a greater steady-state concentration of dichlorovinyl radicals at pH 6.5 (Figure D2c). While such radicals have previously been taken as evidence of an initial SET mechanism [79, 138], they may alternatively also derive from decomposition of intermediate cobalamin vinyl complexes (see Scheme 1). Therefore, even though we reproduced in our study the observation of previous studies and were able to trap such radicals (Figure D2c), we conclude that they cannot provide conclusive evidence about the initial reaction step at this point.

4.4.4. Mass balance deficits indicate formation of reversible and irreversible Vitamin B_{12} - TCE complexes

To probe for reaction intermediates associated with either mechanism, experiments were conducted in the absence of Ti(III) citrate so that putative cob(I)alamin – TCE complexes would not be further reduced, but could be captured by targeted analysis. To this end, cob(III)alamin was pre-reduced with zinc and the pure cob(I)alamin was subsequently added to stoichiometric amounts of TCE in water at pH 3 and 11. These extreme pH values were chosen to probe for the putative endmember mechanisms. Besides TCE, no other volatile compounds were detected. To probe for reversibly formed complexes from cob(I)alamin and TCE, the mass balance deficit was determined between TCE concentrations sampled from the headspace of reaction vials and TCE concentrations sampled through exhaustive extraction of aqueous samples by Purge and Trap (P&T) at the same time point. Whereas headspace analysis gave the concentration of TCE in equilibrium with any reversible complexes, P&T analysis determined the maximum amount of TCE that could extracted from these equilibria. In both cases measurements were calibrated with standards treated in an identical way. In the presence of Vitamin B_{12}, calibrated P&T concentrations were much higher than headspace concentrations (Figure 3a and 3b). This reveals the formation of reversibly formed TCE-cobalamine complexes in which TCE was captured, and from which it could be extracted. Besides this reversible complex formation, an additional mass balance deficit was observed. Since no other products were detected, any mismatch must be attributable to the presence of Vitamin B_{12}. We, therefore, attribute this deficit to additional irreversible cob(I)alamin – TCE complex formation. Figure 3a and 3b, moreover, illustrate a pronounced pH dependence of the associated kinetics. Whereas formation of both complexes

was fast at high pH, at low pH reversible complexes were also produced, but transformation into irreversible complexes was much slower.

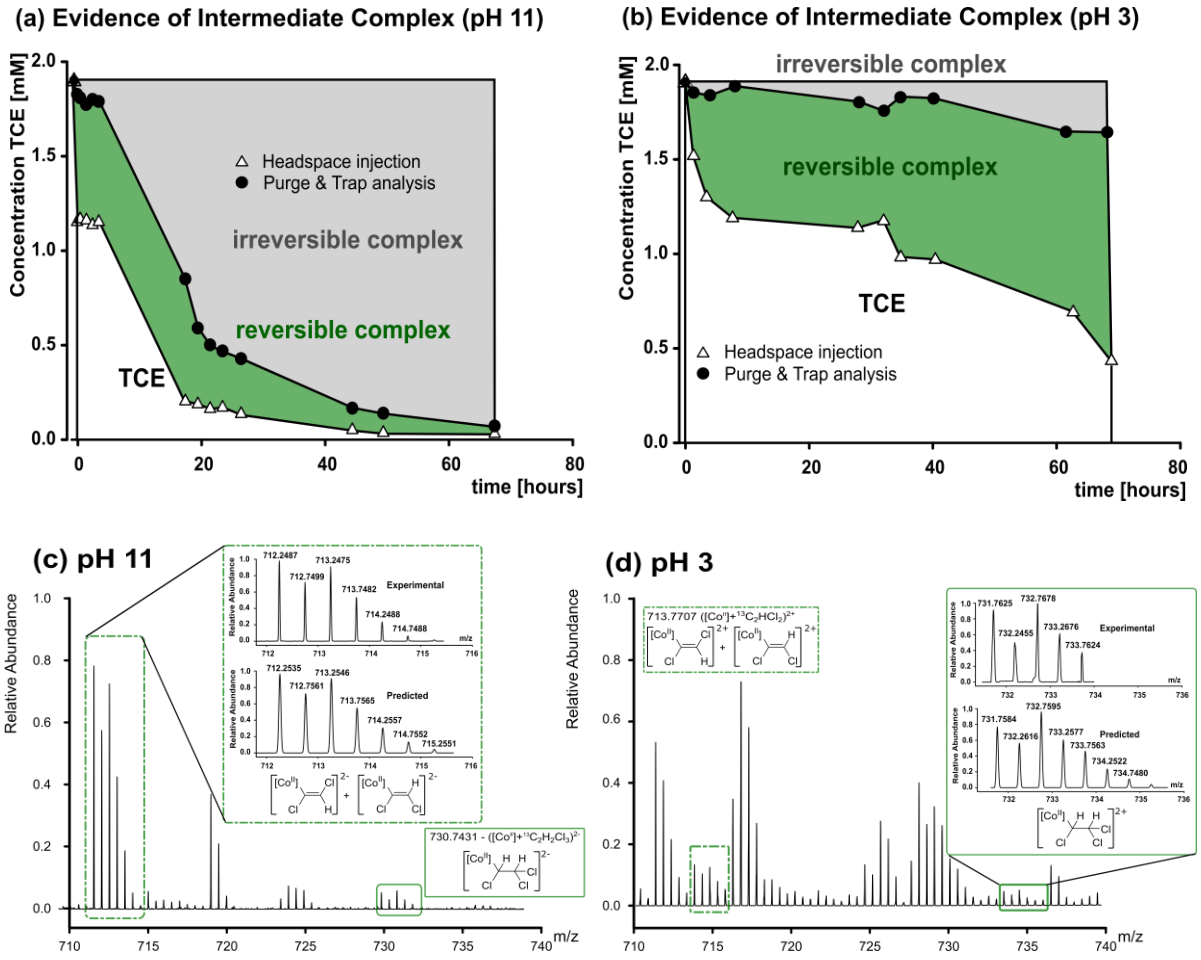

Figure 3. Evidence of reversible and irreversible complex formation (a, b) and complementary evidence of cob(II)alamin chlorovinyl- and chloroalkyl-complexes high-resolution mass spectra (c, d). Stoichiometric amounts of TCE and pre-reduced cob(I)alamine were brought to reaction at pH 11 (panel a) and pH 3 (panel b). The mass balance deficit between equilibrium TCE concentrations (from headspace analysis) and exhaustive extraction of TCE (from purge & trap analysis) gives the concentration of reversibly formed TCE-cob(I)alamin complexes. The remaining mass balance deficit is interpreted as evidence of irreversibly formed TCE-Cobalamin complexes. High resolution mass spectra of the reaction products from doubly ^{13}C-labeled TCE with Vitamin B_{12} at pH value 11 (panel c, measurement in double negative mode) and 2 (panel d, measurement in double positive mode). Note that the spectra are recorded in double positive or double negative mode so that a difference in m/z of 0.5 corresponds to a difference in one atomic mass unit. Complete mass spectra are provided in the supporting information (D4a, b)

4.4.5. High resolution mass spectra give evidence of cob(II)alamin chloroalkyl and chlorovinyl complexes

To further explore the chemical nature of these complexes, UV-Vis (Figure D3a and b) and high resolution MS (Figure 3c, d and D4 a, b) measurements were conducted. At both pH values reduction of cob(III)alamin to cob(I)alamin resulted in a shift of the absorption maximum from 370 nm to 390 nm, consistent with trends previously established by Glod et al.[79] Hence, the reaction of TCE and cob(I)alamin caused the disappearance of the signal at 390 nm and formation of maxima at 310 and 470 nm, which originate from cob(II)alamin complexes [79, 131, 153] Both pH-values triggered these changes indicating that either high pH or low pH enabled the formation of a complex from TCE and cob(I)alamin.

High resolution mass spectra from direct injection of reaction solutions into an Orbitrap mass spectrometer were obtained in double negative mode at pH 11 (Figure 3c) and in double positive mode at pH 2 (Figure 3d). In both cases TCE labeled with two ^{13}C atoms was brought to reaction with pre-reduced cob(I)alamine. Mass spectra of chlorinated alkyl-, vinyl and acetylene complexes of cob(II)alamin were observed at both pH values, and in addition spectra of chlorinated C_4-complexes at pH 2. Assessing the relative contribution of alkyl vs. vinyl vs. acetylene complexes in dependence on pH is difficult, because elimination of HCl in the electrospray ion source can convert one type into the other so that the mass spectra do not necessarily reflect proportions of solution chemistry. Even so, strong agreement between experimental and predicted mass spectra at 712.2 m/z and 730.2 m/z (high pH, Figure 3c) and at 713.7 m/z and 731.7 m/z (low pH, Figure 3d) could substantiate the formation of vinyl- and alkyl-cob(II)alamin-complexes from direct addition of cob(I)alamin to TCE (Figure 3a and b). These results are consistent with, but exceed previous observations by Lesage et al.[140] who employed low instead of high resolution mass spectrometry, and who detected chlorinated vinyl-complexes, chlorinated C_4-complexes and non-chlorinated alkyl complexes, but not chlorinated alkyl-complexes.

4.4.6. Experimental evidence is not consistent with initial electron transfer (either inner- or outer sphere)

The combined experimental evidence from reactivity trends, isotope effects, product distribution and detection of intermediates can serve to test and discard current mechanistic hypotheses (Scheme 1). A direct electron transfer (ET) as initial step (either inner or outer sphere) is an unlikely scenario for the following reasons. In the mechanism prevailing with TCE at low pH an ET would be inconsistent with reactivity trends: whereas the low pH-mechanism was *accelerated* with decreasing pH, an ET would be *slowed down* with decreasing pH owing to the decreasing redox potential of Ti(III)citrate[146]. In the mechanism prevailing with TCE at high pH, in turn, an outer sphere-SET can be excluded, because the large chlorine isotope effects of this study (Figure 2) are inconsistent with the small, or even non-existent chlorine isotope effects observed in outer sphere-SET of chlorinated ethenes in water (grey lines in Figure 2) [59]. This conclusion is consistent with work of Costentin et al.[118, 120] who observed that electrochemical rate constants of PCE and TCE via SET differed strongly from those involving vitamin B_{12} and reductive dehalogenases, respectively, ruling out an SET scenario for these catalysts and calling for more intimate reactant-catalyst interactions. This leaves inner sphere-ET as remaining possible ET at high pH. An inner sphere interaction of cob(I)alamin with a halogen atom, as suggested by Payne et al. for bromobenzenes [83], cannot involve an unoccupied d-orbital of Co^{I}. Instead, an occupied orbital of cob(I)alamin must attack the anti-binding orbital of the Cl-C bond resulting in a homolytic or heterolytic cleavage producing vinyl radicals or vinyl anions, as suggested by recent computational predictions [136, 137]. This, however, would be in contradiction to our observation of irreversibly, and even reversibly formed cob(I)alamin-TCE complexes as key intermediates in reaction with TCE (Figures 3 and D2c). If vinyl radicals and/or anions were formed, they would have to combine quantitatively with free cobalamin to generate such complexes. This is an unlikely scenario considering the difficulty in the synthetic preparation of vinyl-cobalamin complexes through this route[78, 79, 132, 140, 141] and considering how readily these radicals or carbanions can abstract $H^{\bullet}$ or H^{+}, respectively, from surrounding molecules in solution. The corresponding products (*cis*-DCE and *trans*-DCE), however, where not observed in the experiment of Figure 3a, b. Hence, electron transfer (either inner- or outer sphere) is not a likely scenario for the initial step of TCE reduction by vitamin B_{12}.

4.4.7. The occurrence of two pathways cannot be explained by alkyl cob(I)alamin complexes as common intermediates

Nucleophilic addition of cob(I)alamin leads to alkyl complexes (upper path in Figure 1), which were indeed observed by mass spectrometry (Figure 3c, d), which are consistent with the observation of reversible complex formation – no C-Cl bond is cleaved, all steps are reversible – (Figure 3a, b) and which can explain the absence of chlorine isotope effects at low pH (Figure 2). To explain vinyl complexes, on the other hand, a one-step nucleophilic substitution in analogy to S_N2 reactions (Scheme 1), is an unlikely scenario at a sp^2 carbon center so that Rappoport[154] suggested an addition-elimination or addition-protonation with consecutive ß-elimination as summarized in Scheme 2. This raises the question whether the mechanistic shift observed in our experiments can be explained by a common addition-protonation mechanism with alkyl complexes (**4** and isomers) as key intermediates (as suggested by Pratt and van der Donk [141]) which may either be further reduced to dichloroethenes (**11**, **12**) or may undergo ß-elimination of HCl to form vinyl complexes (**7**, **8** and isomers). Such a role of alkyl complexes at the crossroads of competing pathways, however, can be excluded for the following reasons. On the one hand, this mechanism alone cannot explain the changes in mechanism (and isotope effects) with pH, since both pathways would involve $[H^+]$. On the other hand, it cannot explain the observed product distribution. Reduction of alkyl cob(II) alamin complexes, as brought forward by Pratt and van der Donk[141] would lead to 1,1,-DCE in the case of a 1,1,2-trichloroalkyl-cobalamin complex (i.e., the intermediate originating from protonation of intermediate **3**). This is in disagreement with the observation that 1,1-DCE was hardly observed experimentally (see Figure D2b). Alternatively, if a cobalamin vinyl intermediate was formed by elimination of HCl from the cobalamin alkyl complex **4**, this would lead to a 1,1-dichlorovinyl intermediate implying again that 1,1-DCE should be the predominant product. (Note that in comparison, the 1,1,2-trichloroalkyl-cobalamin complex originating from protonation of **3** would be much less reactive towards elimination of HCl.) Hence, we conclude that rather than alkyl cobalamin complexes, the competing pathways observed in this study must involve a different common intermediate.

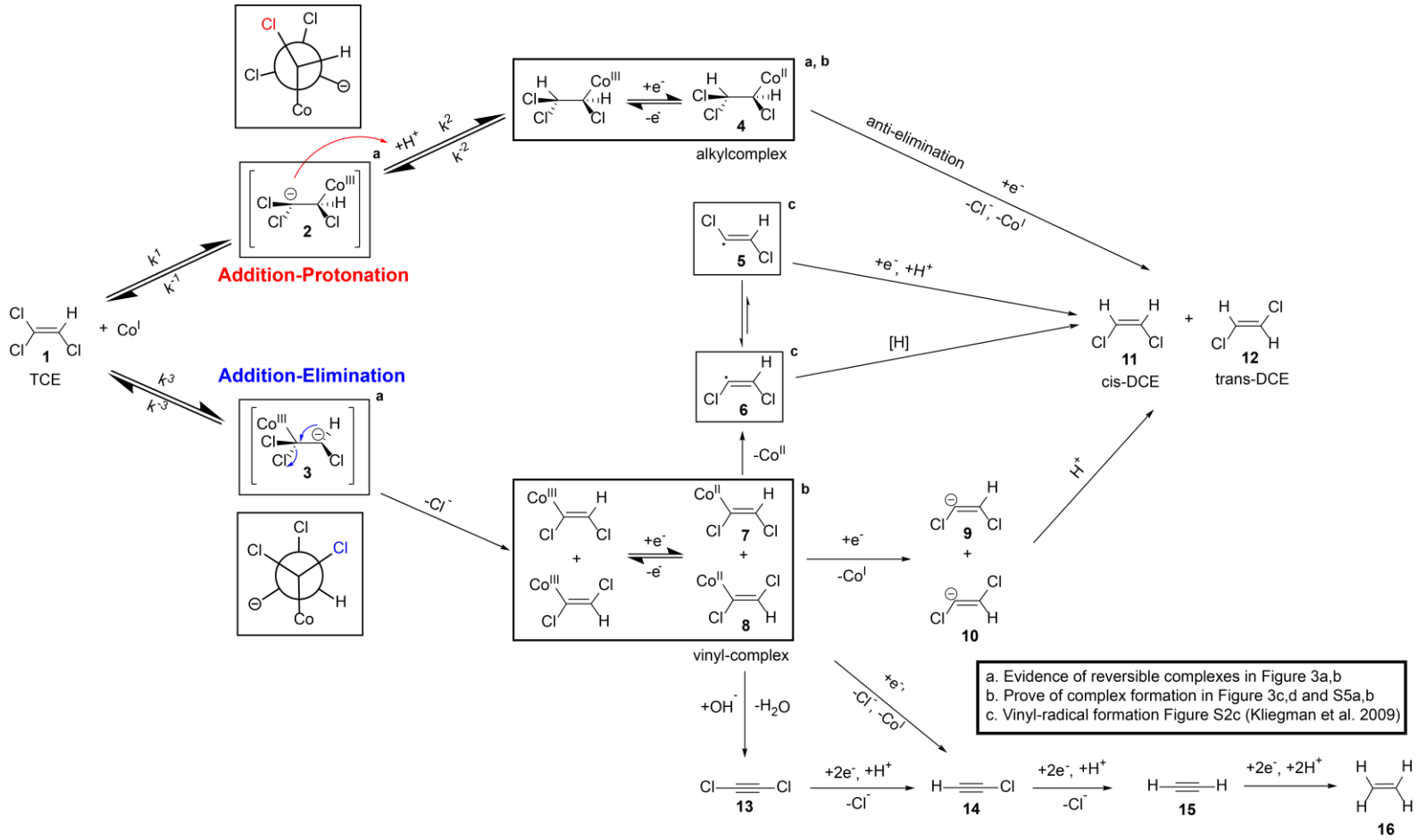

Scheme 2. Integrating mechanism for competing pathways of chlorinated ethene dehalogenation by Vitamin B_{12} The mechanism accommodates evidence from pH-dependent isotope effects (Figure 1 and 2), chlorinated ethene-Vitamin B_{12} complexes (Figure 3) (c), pH- dependent product formation (Figure 2g, h). Here, "$-e^-$, $+H^+$" indicate an electron transfer followed by protonation, whereas "[H]" indicates abstraction of a hydrogen atom. A more detailed Scheme illustrating the reaction paths at high and low pH separately is provided in Scheme D1 and D2 in the Supporting Information

4.4.8. Cobalamin carbanions as key intermediates can explain experimental observations

Given that we could rule out electron transfer, chlorovinyl complexes and chloroalkyl complexes as crossroads of competing pathways, Scheme 2 leaves carbanion complexes **2** and **3** as remaining possibility. Nucleophilic addition of Cob(I)alamin leads to either **2** or **3**. Both carbanions can either be protonated (addition-protonation), or eliminate Cl^- (addition-elimination), and they can explain practically all observations of this and previous studies, as laid out in the following.

Reversible and irreversible complex formation (Figure 3a, b). Scheme 2 uses structural information from Figure 3c, d to interpret the observation of reversible and irreversible complex formation in Figure 3. Formation of cobalamin alkyl complexes (e.g., **4**) only involves reversible steps and is, therefore, overall reversible, whereas C-Cl bond cleavage makes formation of cobalamin chlorovinyl complexes (**7, 8**) irreversible. Hence, Scheme 2 can explain our experimental observations of Figure 3 if chloroalkyl cobalamines are taken to be the reversibly formed cobalamine complexes, whereas chlorovinyl cobalamines represent irreversibly formed complexes.

Absence of 1,1-DCE. Practically no 1,1-DCE was observed (Figure D2b) implying that the carbanion **2** is almost exclusively protonated, whereas the carbanion **3** eliminates Cl^- to form dichlorovinyl complexes, as observed by mass spectrometry (Figure 3c, d). To explain this selectivity on the carbanion level, conformations may be considered in a similar way as computed for alkyl cobalamines in Pratt and Van Der Donk [141]. As sketched in Scheme 2, the energetically favored conformation in intermediate **3** is expected to position the negative charge exactly antiperiplanar to one of the two chlorine atoms facilitating Cl^- elimination and leading to cobalamin vinyl complexes **7**, **8**. In contrast, Scheme 2 illustrates that intermediate **2** is expected to maximize the Co-C-Cl angle (115.6° [141]) to minimize interaction of the chlorine atom with the corrin ring. Consequently, the negative charge is no longer positioned antiperiplanar to the C-Cl bond so that elimination is slowed and protonation is favored in comparison. Hence, carbanion **2** may indeed be expected to be protonated to alkyl cobalamine, whereas carbanion **3** would eliminate Cl^- to form vinyl cobalamine.

Mechanistic shift / change in chlorine isotope effects with pH (Figure 2). According to Scheme 2 and Scheme D1, low pH makes protonation of **2** (k_2) rapid because of high [H^+] concentrations, whereas it makes deprotonation of **4** (k_{-2}) slow because of low [OH^-] concentrations – likely slower than subsequent reduction so that TCE becomes "trapped" in the alkyl complex **4** (but can, in the absence of a reduction agent, still be recovered by P&T, see Figure 3). This can explain the small chlorine isotope effects observed at low pH, because no C-Cl bond cleavage is involved in the protonation. At high pH, in contrast, protonation of **2** is slower (by a factor of 10^6 between pH 5 and 11), whereas deprotonation of **4** is faster (also by a factor of 10^6 between pH 5 and 11) so that **2** can dissociate back to TCE (Figure D5). Subsequently, (sterically hindered) attack of cob(I)alamin can take place at the other, geminal (=CCl_2) position of TCE to form **3** in a reversible reaction. Intermediate **3**, in turn, may eliminate chloride forming **7** and **8**, as discussed above. Since all reaction steps prior to Cl^- elimination are reversible, the pronounced chlorine isotope effect of this C-Cl bond cleavage can be observed in the substrate TCE at high pH.

Slow reaction of chloroalkyl cobalamine complexes (Figure 3). The observation that reversibly formed chloroalkyl cobalamine complexes were only slowly further reduced (Figure 3b, Figure D2b) can be explained by the decreased reduction potential of titanium citrate at low pH.[146] Furthermore, Pratt and van der Donk suggested that the alkyl-complex must first convert from the preferred "base on" (E^0 = -1.78 V vs NHE) to the "base off" configuration (E^0 = -0.94 V vs NHE) to be reduced.[141] In contrast, the observation that irreversibly formed cobalamin vinyl complexes were quickly further transformed (Figure 3a, Figure D2a) is consistent with predictions of Pratt and van der Donk that their homolytic cleavage (0.27 V vs NHE[155]) is rapid leading to vinyl radicals and chlorovinyl anions (Scheme 2). This can explain the higher mass balance deficit at low vs. high pH, since more of the TCE was caught up in slowly reacting cobalamin alkyl complexes (Figure 3, Figure D2).

Product distribution trends with pH (Figure 2g, h, Figure D2). According to Scheme 2 and Scheme D2, high pH favors the formation of cobalamin vinyl complexes **7** and **8** (Figure 3c, d). Scheme 2 further illustrates that their subsequent reaction can produce both chlorinated and non-chlorinated products as observed in Figure 2h (**11**, **12**, **15** and **16**). In contrast, low pH favors reversible formation of the alkyl complex, which only reacts to chlorinated products, again consistent with observations of Figure 3b. Scheme 2 also highlights that the

same products – *cis*-DCE (**11**) and *trans*-DCE (**12**) – are expected to origin from different possible intermediates (alkyl cobalamin complexes vs. radicals or carbanions) explaining the pH dependency of *cis*-DCE/*trans*-DCE ratios observed in Figure 2g. Finally, Scheme 2 delineates how chlorovinyl-radicals **5**, **6** or -anions **9**, **10** can be formed from cobalamin chlorovinyl complexes. On the one hand chlorovinyl-radicals **5**, **6** can react to *cis*- or *trans*-DCE through reduction of a second electron, possibly provided from titanium citrate, and subsequent protonation. On the other hand the can form *cis*- or *trans*-DCE by abstraction of a hydrogen atom from surrounding molecules. This can explain why radicals could be trapped with d_7-isopropanol in our and previous studies, where they were inadvertently interpreted as evidence of an initial single electron transfer mechanism.[79-81, 134, 155, 156]. The competing pathways of Scheme 2 can also explain why only a finite proportion of products from TCE carried the deuterium label from radical traps in a previous study[80]; the other part was likely formed *via* the addition-protonation pathway of Scheme 2 which does not involve radicals. Finally, at lower pH the lifetime of these radicals (and, hence the probability of trapping them) increases with the decreasing reduction potential of titanium citrate[146] explaining why more deuterated dichloroethenes were trapped at pH 6.5 than at pH 9 (Figure D2c). In contrast, negligible amounts of trapped products - as observed for *cis*-DCE and VC by Glod et al. [134]- would be expected if the reaction was completely dominated by the addition-protonation pathway.

Hydrogen isotope effects (Figure 2d, Figure D1). Inverse hydrogen isotope effects were observed indicating that TCE with ^{1}H reacted more slowly than with ^{2}H. Such secondary inverse hydrogen isotope effects were previously observed in biodegradation of TCE [38] and are a hallmark of a change from sp^2 to sp^3 hybridization leading to a more cramped coordination environment around the C-H bond and thus stiffer bending vibrations [95, 157]. Our observation that stronger inverse hydrogen isotope effects were observed at pH 6.5 (ε_H = +130‰ ± 14‰) compared to pH 9.0 (ε_H =+98‰ ± 6‰) are indeed consistent with a more cramped coordination environment in the transition state to cobalamin alkyl complexes as opposed to smaller inverse hydrogen isotope effects in the formation of carbanions. Therefore, also hydrogen isotope effects support the mechanistic picture of Scheme 2.

4.4.9. Implications for reactivity and product formation in biodegradation of chlorinated ethenes

Our results suggest that the dual element (C, Cl) isotope plot of TCE (Figure 2) is a sensitive indicator of these competing pathways (addition-elimination at high pH vs. addition-protonation at low pH) and may even allow estimating their relative contribution (Figure D6). When transferring this insight to data of PCE and *cis*-DCE, Figure 1c suggests that PCE is mainly degraded *via* an addition-elimination reaction, whereas *cis*-DCE reacts *via* the addition-protonation pathway. According to Scheme 2, the differences in reactivity – and, hence, the question why *cis*-DCE and VC are less reactive than TCE and PCE – may be traced back to cobalamin carbanions as key intermediates. PCE contains two dichlorovinylidene groups ($=CCl_2$) giving rise to conformations analogous to intermediate **2**, whereas *cis*-DCE contains two chlorovinylidene groups (=CHCl) groups leading to conformations like in intermediate **3**. The addition-protonation pathway is consistent with the mechanism originally brought forward for *cis*-DCE and VC by Glod et al.[79], whereas for TCE and PCE a single electron transfer mechanism has been favored until now [83, 84, 135]. Notably, Scheme 2 can also explain why 1,1-DCE showed a thousand-fold higher reactivity and much higher proportions of trapped radicals than *cis*-DCE or *trans*-DCE in ref [134]: unlike *cis*-DCE or *trans*-DCE, the compound 1,1-DCE contains a $=CCl_2$ group, which makes it amenable to the addition-elimination pathway. Hence, in a similar way as recently suggested by Ji et al.[139], this study could indeed bring forward evidence from multielement isotope analysis to pinpoint different reaction mechanisms of chlorinated ethenes with Vitamin B_{12} - even though we arrive at slightly different mechanistic picture involving an addition-elimination pathway instead of a concerted nucleophilic substitution.

4.4.10. Relevance for enzymatic and bacterial biodegradation of chlorinated ethenes

This raises the question whether the same approach can be used to transfer mechanistic insight to real-world systems like enzymes or dehalogenating organisms. Can reaction mechanisms be compared even though cofactor-catalysis is much slower than with enzymes, although added Vitamin B_{12} exceeds environmental concentrations, and despite extreme pH

values? Theory predicts that comparable isotope effects are obtained as long as the manner and order of bond changes in the chlorinated ethene is similar – irrespective of reaction rates, or reaction partners. In other words, a reaction in solution at extreme pH may mimic protonation / deprotonation in an enzymatic pocket, whereas transformation at neutral pH may mimic an enzyme reaction in the absence of such a functionality. Still, intrinsic isotope effects may potentially be modulated by (i) the diffusion of substrates inside the enzyme core, (ii) interactions with amino acid residues, (iii) the position of the lower ligand of Vitamin B_{12} (base-on vs. base-off), as well as (iv) the necessity of products (i.e., the less chlorinated product and the chloride ion) to diffuse out of the enzymatic pocket.

First insight on the influence of such complicating factors can be derived from a recent study by Renpenning et al. on carbon and chlorine isotope effects with the reductive dehalogenase (RDase) PceA from *Sulfurospirillum multivorans* [36]. This PceA is one of the best characterized RDases to date. It contains a cave-like enzyme structure which introduces substrates in a specific orientation to the active center hypothesized to facilitate OS-SET [84, 126]. Isotope effects in PCE catalysis by the enzyme PceA were indeed much smaller than with vitamin B_{12} suggesting that diffusion into the enzyme channel was partially rate-determining for this highly reactive substrate [36]. Similarly small isotope effects were obtained with whole organisms by Badin et al. [102], whereas isotope effects with *Desulfitobacterium* sp. strain Viet1 [101] were fully expressed and agree perfectly with those of the present study ($\lambda = \Delta\delta^{13}C/\Delta\delta^{37}Cl = 3.8 \pm 0.2$ vs. $\lambda = 3.9$ to 4.2). Dual element isotope trends of PCE, finally, were slightly different in reaction with corrinoids that contained an axial base (nor-B_{12} ; cyano-B_{12}, $\lambda = 4.6$ to 5.0), compared to corrinoids without (dicyanocobinamid , $\lambda = 7.0$) [36].

In contrast to these differences observed with PCE, observed isotope effects of TCE are remarkably consistent in enzyme catalysis by PceA from *Sulfurospirillum multivorans*. Dual element isotope trends with pure corrinoids (both "nor-B_{12}" and "norpseudo-B_{12}) were similar to those of the present study and earlier investigations [35, 38] with λ values clustering between 3.7 and 4.5, confirming that the axial base does not play a decisive role. The corresponding λ values in enzymatic catalysis by PceA (both "nor-B_{12}" and "norpseudo-B_{12}), $\lambda = 5.0$ and 5.3, were indistinguishable within error from those of the corrinoids . Figure 4 plots these experimental data together with the trends obtained in this study with Vitamin B_{12}, and with isotope effect trends for OS-SET model reagents.

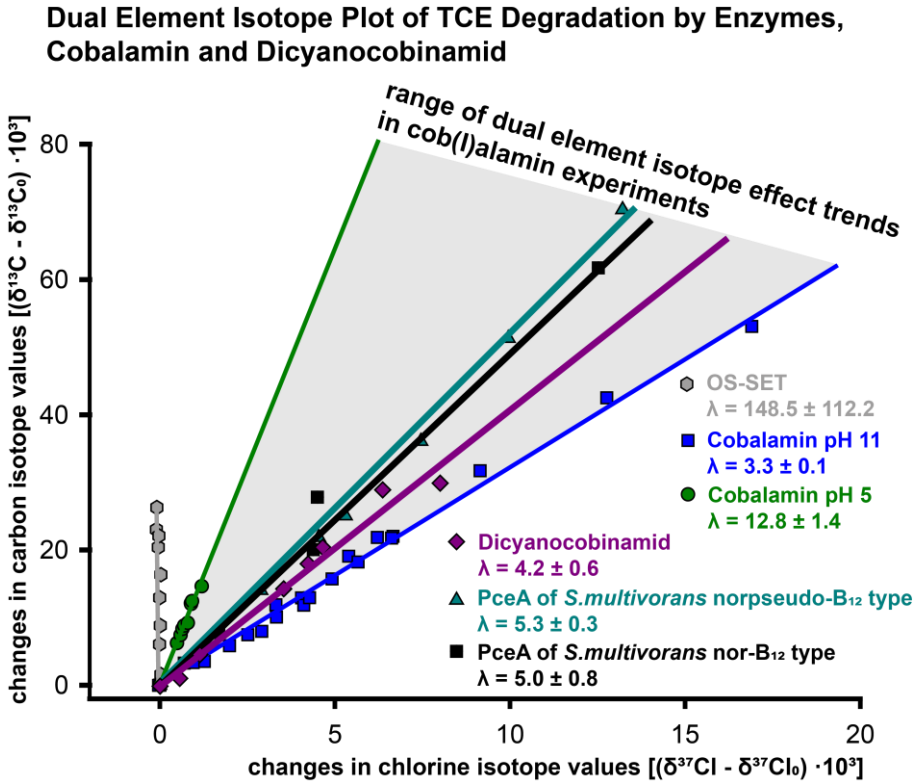

Figure 4. Trends of dual element isotope effects of TCE in enzymatic catalysis by PceA of *Sulfurospirillum multivorans* (data from Renpenning et al.[36]) compared to reaction with Vitamin B_{12} at different pH (this study), dicyanocobinamid (data from Renpenning et al.[36]) and model reagents for outer sphere-single electron transfer (data from Heckel et al.[158]).

Figure 4 illustrates that all isotope effect studies with corrinoids and enzymes share pronounced chlorine isotope effects, in contrast to non-existent chlorine isotope effects observed with aqueous outer-sphere single electron transfer agents [158]. Based on this evidence, we have recently concluded that outer-sphere electron transfer is an exception rather than the rule in natural and engineered reductive dehalogenation reactions[158], consistent with independent conclusions brought forward by Saveant and coworkers [121]. This conclusion certainly applies to the mechanism of PCE and TCE with Vitamin B_{12} in this study, and Figure 4 suggests it should also apply to the reaction of TCE with PceA from *Sulfurospirillum multivorans* – despite recent evidence for an OS-SET [126]. We, therefore, hypothesize that an OS-SET is not at work in the PceA of *Sulfurospirillum multivorans*, but favor instead an addition-elimination mechanism as laid out in Scheme 2.

Still, we caution that Figure 4 expresses the degree to which C-Cl bond cleavage occurs in the rate-determining step of the reaction. In a similar way as the steep slope λ with vitamin B_{12} reflects the addition-protonation mechanism with little involvement of C-Cl cleavage,

the steep slope in the OS-SET mechanism reflects a stepwise mechanism where SET occurs into the π* orbital of the chlorinated ethene so that subsequent C-Cl bond cleavage is decoupled. While absent in water, we observed that chlorine isotope effects could partly be recovered with OS-SET agents in organic solvents[158]. Hence, if the enzyme environment (i) keeps the reactants long enough together to reverse the ET before C-Cl bond cleavage and (ii) in addition, lets the majority of substrate molecules escape from the enzyme pocket as unreacted substrate *even after the ET has occurred and has been reversed* (otherwise the chlorine isotope effect of the transition state of C-Cl bond cleavage would not be observed!) this would still leave room for an OS-SET mechanism as hypothetical, but rather unlikely scenario.

4.5. Conclusion

Pinpointing the reaction mechanism of reductive dechlorination of chlorinated ethenes in natural transformations is intrinsically difficult. For experiments with the enzymatic cofactor vitamin B_{12} this study combines evidence from reaction rates, product formation, isotope effects and trapped intermediates to bring forward a reaction mechanism which supports all available observations to date. Our results indicate that after forming an intermediate complex of vitamin B_{12} and a chlorinated ethene (PCE, TCE and *cis*-DCE) two reaction pathways are possible 1. addition-elimination or 2. addition-protonation. To answer the question why reductive degradation of chlorinated ethenes often stops at the stage of *cis*-DCE or VC, the integrating mechanism of Scheme 2, therefore, bears the potential to provide consistent answers. Our experiments with TCE suggest that the chloroalkyl cobalamin intermediates of the addition-protonation pathway are of lower reactivity than the chlorovinyl cobalamin intermediates of the chlorovinyl cobalamin pathway offering a potential explanation for the persistence of the respective substrates (*cis*-DCE, VC) at contaminated sites.

The question remains whether these characteristic trends of competing mechanisms (addition-elimination / addition-protonation) can also be identified in reductive dehalogenases, or real microorganisms. As discussed above, recently reported isotope effects in TCE transformation with the enzyme PceA from *Sulfospirillum multivorans*[36], and similar trends with whole microorganisms[35, 38, 42, 101] hold promise to bridge this gap, and they

suggest an addition-elimination mechanism. Conversely, further studies will be required to investigate whether first data on *cis*-DCE and VC transformation may potentially be indicative of an addition-protonation mechanism[100]. The characteristic dual element isotope trends of Figures 1 and 2 clearly highlight multiple-element isotope analysis as a new opportunity to bridge the gap and to demonstrate that a mechanism characterized in the reaction flask also occurs on the enzyme level in microorganisms – or at contaminated sites. Labelled compounds are not required since isotope analysis is conducted at natural isotopic abundance. Hence, the stage is set for studies in more complex systems such as whole proteins or microorganisms, to use multi element isotope effect measurements to probe for the mechanistic dichotomy – addition-elimination vs. addition-protonation – brought forward in this contribution.

5.

General Conclusions

Dechlorination reactions of chlorinated methanes and ethenes are important transformation processes in the environment, and it is essential to get a better understanding of the reaction mechanisms at work. Compound-specific Stable Isotope Analysis (CSIA) is an emerging approach, what can achieve this task, especially in combination with other analytical methods what was clearly illustrated in this thesis.

In the first part, we introduced chlorine isotope analysis of tetrachloromethane and trichloromethane for the GC-qMS and GC- IRMS and created the first dual element isotope slope of trichloromethane degradation by ZVI (Chapter 2). Based on this method, chlorine isotope effects of trichloromethane in reaction with different reagents could be determined (Appendix A1). Dual element isotope plots allowed a clear distinction and interpretation of the prevailing reaction mechanisms and provided first reverence systems for future studies. Such information can be essential for decisive interpretation of field assessments, where the ε values allow an estimation of the extent of degradation by using induced abiotic remediation strategies. Based on this method and the recently introduced hydrogen isotope analysis for chlorinated hydrocarbons the foundation is laid to get more insights into the abiotic and biotic degradation of chlorinated methanes. Recent studies already used carbon

isotope analysis to investigate trichloromethane degradation by *Dehalobacter*-containing subcultures, which were functionally and phylogentically almost identical and observed strongly varying carbon isotope enrichments (ε_C (*Dehalobacter* strain UNSWDHB) = -4.3 ‰[159]; ε_C (*Dehalobacter* strain CF) = -27.5 ‰[160]). The strong carbon isotope effects from *Dehalobacter* CF indicate a C-Cl bond cleavage in the rate determine step, corresponding to Torrentó et al (Appendix A1). Subsequently also pronounced chlorine isotope should be expected. In contrast, small carbon isotope effects from *Dehalobacter* UNSWDHB imply no C-Cl bond cleavage in the rate determining step. Therefore, a previous rate limiting process could be involved which masked the carbon and chlorine isotope effects, e.g. irreversible binding at the enzyme. However, information gained from one element is limited and cannot completely answer why these almost identical strains result in total different isotope effects. Hence, the introduced chlorine isotope analysis for trichloromethane could be the key to identify the cause of the different isotope effects and could reveal more insights into the reaction behavior of chlorinated methanes and these two strains.

Identifying the reaction mechanism of chlorinated ethene degradation by vitamin B12 was another important goal of this thesis (Chapter 3 & 4). First, the absence of chlorine isotope effects was discovered by experiments of chlorinated ethenes with OS-SET reagents in combination with dual element isotope effect analysis. By comparing dual element isotope slopes of the OS-SET reactions with biodegradation and degradation by ZVI the OS-SET reaction was excluded as prevailing reaction mechanism for natural and engineered chlorinated ethene dehalogenation. Second, isotope analysis of degradation experiments with PCE and *cis*-DCE at different pH values revealed a different reaction mechanism for both substrates. Third, TCE reactions with vitamin B12 at varying pH value (pH value 5-12) exposed by isotope analysis a different reaction mechanism at high and low pH value. At last, UV-VIS and high-resolution mass-spectrometry disclosed reversible as well as alkyl and vinyl complex formation of the reaction of TCE and vitamin B12 at stochiometric amounts. Combining the isotopic and kinetic information of the TCE experiments with detection of intermediates enabled a more detailed interpretation of the results from CE degradation by vitamin B12 at different pH values. Finally, identifying an integrating reaction mechanism containing two pathways (1. addition-elimination 2. addition-protonation) became possible. Experimental evidence revealed, that initial electron transfer or alkyl or vinyl complexes as crossroads of both pathways are inconsistent. In contrast, the

formation of cobalamin chlorocarbanions is supported as key intermediates, where chloride elimination produces vinyl complexes (explaining rates and products of TCE at high pH) and protonation generates less reactive alkyl complexes (explaining rates and products of TCE at low pH). By transferring these observations into biological systems it was hypothesized that enzymes which react only via addition-elimination can degrade PCE and TCE, however, they cannot degrade *cis*-DCE. Consequently, the reaction would stop at the step of *cis*-DCE. This observation provides a possible answer to the question: "Why does degradation often stop at the step of *cis*-DCE or VC?"

However, beside these deep insights into the reaction mechanism of vitamin B12 with chlorinated ethenes, several questions which remain elusive:

1. *The reaction mechanism of VC*. This thesis could provide reaction mechanisms of PCE, TCE and *cis* DCE degradation by vitamin B12. However, it still remains elusive whether the highly toxic VC is degraded by the addition-elimination or addition-protonation or totally different reaction mechanism? Glod et al.[134] observed that corresponding to the reaction rate of *cis*-DCE, the rate of VC is decreasing with increasing pH value. Consequently, the addition-protonation might also be the underlying reaction mechanism. Measuring the isotope effects for VC is possible for carbon and hydrogen, however the decisive chlorine isotope effects analyzes is not feasible at the moment because there are no existing chlorine isotope standards for VC. Therefore, determining the intermediate formation as it was illustrated in Chapter 4 could be one way to identify the reaction mechanism of VC degradation by vitamin B12.
2. *The reaction mechanism of 1,1-DCE.* Analogous to vinyl chloride the reaction mechanism for 1,1-DCE degradation is still not clear. On the hand first evidence of decreasing reaction rates with increasing pH value observed by Glod et al.[134] as well as the energetic favored attack at the carbon atom with no chlorine atoms ($H_2C=$) strongly indicate the addition-protonation as responsible reaction mechanism. On the other hand, high radical formation which is observed for 1,1-DCE degradation is opposing the suggested mechanism. Glod et al.[134] proposed a possible reaction mechanism including steps which leave several questions: (a) possible elimination of chloride by the negative charge located at the same carbon atom? (b) the reaction rate is accelerating with decreasing pH, however no pH dependent step is involved in the suggested reaction mechanism). Here, also the non-existing chlorine isotope standards complicate the

disclosure of the mechanism. Hence, the determination of intermediates could also be helpful to reveal more of the 1,1.DCE degradation.

3. *The reaction mechanism in microorganism and enzymes*. Another question remains whether the addition-elimination and/ or the addition-protonation are the prevailing reaction mechanism in microorganisms or enzymes. Therefore, transferring the CE and vitamin B12 results into biological systems has to be the next step to test our hypothesized reaction mechanisms. Pinpointing chemical reaction mechanisms in complex natural transformations is intrinsically difficult because reactivity trends are often not conclusive – organisms typically depend on microbial growth and enzyme expression rather than reflecting the biochemical reaction. Furthermore, product distribution is also not very helpful because generally only one dehalogenated product is observed (e.g. TCE → *cis*-DCE). Multi-element isotope effect analysis has possibility to bridge this gap because it allows comparison of complex biological systems with simplified chemical systems by forming dual element isotope plots from information of two or more elements. Consequently, reactions in more complex systems such as enzymes or organisms have to be the next step.

Overall this work demonstrates the possibilities of CSIA what is already frequently applied in field assessments and since recent years as tool to identify reaction mechanism. However, the full potential of CSIA is still not used especially in organic and inorganic chemistry. In Chapter 3 and 4 we clearly illustrated, that isotopic measurement of multiple elements at natural abundance delivers important insights into the reaction mechanism of small molecules. However, this possibility is hardly used and strongly underestimated in organic and inorganic chemistry. Analyzing the KIEs of hydrogen by using molecules labeled with deuterium has already been crucial for mechanistic advances in C-H activation chemistry[161, 162] , the reverse oxidative addition[163], hydrogen transfer reactions[164-167], ß-elimination reactions[168, 169], C-C coupling reactions (e.g. Sonogashira- , Heck reaction)[170-173], cycloisomerization[174-176] ,cycloadditions[177, 178] and reactions of carbene complexes[179, 180]. However, several reaction mechanisms are still incompletely understood, in particular interactions of organic substrates with metal complexes (e.g. Sonogashira reaction which is one of the most important and widely used sp^2–sp carbon–carbon bond formation reactions in organic synthesis [181, 182]) or metal surfaces (Chapter 3). Beside isotopic information from hydrogen, the analysis of carbon, nitrogen and oxygen isotopes could provide important

insights whether reacting bonds are broken or not and if it's a concerted or stepwise reaction mechanism, what is not always clear (e.g. oxidative addition[183]). This possibility is now available because analytical advances have made it possible to measure compound-specific isotope ratios at natural abundance what renders the application of labeled atoms redundant. Combining isotope analysis with frequently used analytical methods in organic chemistry such as kinetic analysis, NMR-, mass- or laser-spectroscopy owns great potential to get a deeper understanding of chemical reactions and can simplify their interpretation. Following, the stage is set to unleash the full potential of CSIA of multiple elements.

Appendix

A. Carbon and Chlorine Isotope Fractionation Patterns Associated with Different Engineered Chloroform Transformation Reactions

Environmental Science & Technology

Article

pubs.acs.org/est

Carbon and Chlorine Isotope Fractionation Patterns Associated with Different Engineered Chloroform Transformation Reactions

Clara Torrentó,*[,†,‡] Jordi Palau,[†,‡] Diana Rodríguez-Fernández,[‡] Benjamin Heckel,[§] Armin Meyer,[§] Cristina Domènech,[‡] Mònica Rosell,[‡] Albert Soler,[‡] Martin Elsner,[§,⊥] and Daniel Hunkeler[†]

[†]Centre for Hydrogeology and Geothermics, Université de Neuchâtel, 2000 Neuchâtel, Switzerland

[‡]Grup de Mineralogia Aplicada i Geoquímica de Fluids, Departament de Mineralogia, Petrologia i Geologia Aplicada, Facultat de Ciències de la Terra, Martí Franques s/n, Universitat de Barcelona (UB), 08028 Barcelona, Spain

[§]Institute of Groundwater Ecology, Helmholtz Zentrum München, 85764 Neuherberg, Germany

[⊥]Chair of Analytical Chemistry and Water Chemistry, Technical University of Munich, Marchioninistrasse 17, D-81377 Munich, Germany

Supporting Information

ABSTRACT: To use compound-specific isotope analysis for confidently assessing organic contaminant attenuation in the environment, isotope fractionation patterns associated with different transformation mechanisms must first be explored in laboratory experiments. To deliver this information for the common groundwater contaminant chloroform (CF), this study investigated for the first time both carbon and chlorine isotope fractionation for three different engineered reactions: oxidative C−H bond cleavage using heat-activated persulfate, transformation under alkaline conditions (pH ∼ 12) and reductive C−Cl bond cleavage by cast zerovalent iron, Fe(0). Carbon and chlorine isotope fractionation values were −8 ± 1‰ and −0.44 ± 0.06‰ for oxidation, −57 ± 5‰ and −4.4 ± 0.4‰ for alkaline hydrolysis (pH 11.84 ± 0.03), and −33 ± 11‰ and −3 ± 1‰ for dechlorination, respectively. Carbon and chlorine apparent kinetic isotope effects (AKIEs) were in general agreement with expected mechanisms (C−H bond cleavage in oxidation by persulfate, C−Cl bond cleavage in Fe(0)-mediated reductive dechlorination and $E1_{CB}$ elimination mechanism during alkaline hydrolysis) where a secondary $AKIE_{Cl}$ (1.00045 ± 0.00004) was observed for oxidation. The different dual carbon-chlorine ($\Delta\delta^{13}C$ vs $\Delta\delta^{37}Cl$) isotope patterns for oxidation by thermally activated persulfate and alkaline hydrolysis (17 ± 2 and 13.0 ± 0.8, respectively) vs reductive dechlorination by Fe(0) (8 ± 2) establish a base to identify and quantify these CF degradation mechanisms in the field.

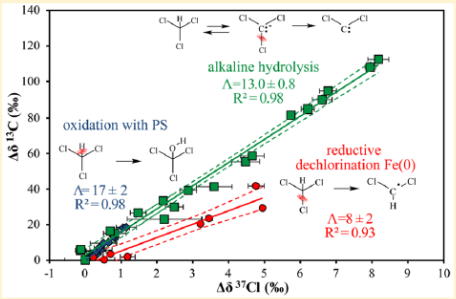

1. INTRODUCTION

Chloroform (CF) is both an anthropogenic environmental contaminant widely distributed around the world as well as a natural compound formed in various aquatic and terrestrial environments.[1−3] CF of anthropogenic origin has been extensively used as degreasing agent and as a precursor to Teflon and various refrigerants and was historically used in medicine as anesthetic. It is formed as oxidation byproduct during drinking water treatment[4] and may form as a daughter product of carbon tetrachloride (CT) dehalogenation at contaminated sites. As a result, CF is one of the most frequently detected volatile organic compounds (VOCs) in groundwater.[5] Taking into account its high ecotoxicity,[6] CF prominently ranks among the halogenated VOCs on the Agency for Toxic Substances and Disease Registry priority list of hazardous substances.[7]

Aerobic and anaerobic cometabolic biodegradation processes of CF have been described.[8] However, CF cometabolic degradation is restricted by several environmental factors such as the presence of other specific compounds that inhibit CF degradation, the availability of the substrate or the toxicity of derived metabolites.[8] Reductive dechlorination of CF via dehalorespiration by two *Dehalobacter* sp. strains (CF50 and UNSWDHB) and one *Desulfitobacterium* sp. strain (PR) has recently been described in laboratory studies[9−14] and proposed as anaerobic bioremediation strategy. However, this strategy is only applicable to contaminated sites in the absence of its parent compound, i.e. CT, which has been shown to strongly inhibit CF dehalorespiration in an enrichment culture containing *Dehalobacter* spp.[15] In turn, CF itself is a strong inhibitor of chlorinated ethene- or ethane-degrading cultures even when present at low concentrations.[16,17] These interdependencies make the remediation of sites contaminated with

Received: February 6, 2017
Revised: May 2, 2017
Accepted: May 9, 2017
Published: May 9, 2017

ACS Publications © XXXX American Chemical Society

DOI: 10.1021/acs.est.7b00679
Environ. Sci. Technol. XXXX, XXX, XXX−XXX

several chlorinated compounds particularly challenging so that multiple-stage remediation strategies are warranted in which inhibitors like chloromethanes are removed upfront.

Abiotic reactions bear potential to accomplish such an initial removal. Naturally occurring iron-bearing minerals like goethite and iron sulfide under low-redox environments have been demonstrated to be involved in the reductive dechlorination of CF.[18] However, due to the very restricted natural attenuation conditions for CF and its complex distribution in the subsurface as a dense nonaqueous phase liquid (DNAPLs), more efficient engineered remediation strategies have been proposed to increase CF removal in the environment. As a result of the high oxidation state of carbon in CF, its degradation by in situ chemical oxidation (ISCO) is in general much less effective than for chlorinated ethenes using common oxidants such as permanganate, iron-activated persulfate (PS), ozone, hydrogen peroxide, or Fenton's Reagent.[19] However, thermally activated PS was recently shown to be a better option for efficient CF oxidation with the advantage that under thermal activation, the strongly oxidizing sulfate radical and other reactive intermediates (i.e., hydroxyl radicals, or reducing radicals such as superoxide radicals, $O_2^{\bullet-}$) can be generated at neutral pH.[20−23]

Alternatively, CF alkaline hydrolysis has recently been proposed as a remediation technology based on its occurrence in drainage trenches filled with concrete-based construction wastes.[24] For the sustainable use of this new remediation strategy, identifying and assessing the performance of CF degradation reaction by alkaline hydrolysis, as well as understanding the underlying mechanism, is important.

Finally, CF reductive dechlorination by zerovalent metals has been studied only at laboratory scale.[25−29] Nevertheless, this remediation strategy has been successfully proven at field sites contaminated by chlorinated ethenes using permeable reactive barriers with micro/macro-scale Fe(0)[30,31] or Fe(0) nanoparticle injection.[32,33]

Improved methods are needed to delineate the relative efficacy of the above-mentioned CF remediation approaches in the field. During the last decades, compound-specific isotope analysis (CSIA) has evolved as a tool to monitor transformation reactions and to quantify the progress of natural and enhanced remediation of organic contaminants.[34,35] Molecules with light isotopes in the reactive position typically react slightly faster than molecules containing the heavy ones leading to a kinetic isotope effect (KIE). As a consequence, the heavier isotopes (e.g., ^{13}C and ^{37}Cl) usually become enriched in the remaining substrate. For a given reaction, quantification of the extent of contaminant transformation based on stable isotope ratios requires the experimental determination of isotopic fractionation (ε, see Materials and Methods).[36]

Isotopic fractionation values for transformation reactions need to be known for very practical reasons: (i) to understand what changes in isotope values can be expected in the field at all, and whether this holds promise to qualitatively detect degradation; (ii) to understand what mechanism lies behind the isotope effect, in order to subsequently chose an appropriate ε value for quantification in the field.

In order to gain insight into the underlying reaction mechanism, apparent kinetic isotope effects (AKIEs) can be derived from determined ε values taking into account which of the atoms in the target molecule are expected to be present at the reactive position. Comparison of the observed AKIEs to the theoretical maximum KIEs ("semiclassical Streitwieser Limits") associated with breakage of chemical bonds, enables interpretation of occurring transition state(s) of a bond cleavage in terms of (i) primary isotope effects affecting the atoms present in the reacting bond, (ii) secondary isotope effects affecting atoms located adjacent to the reacting position.[37,38] Often, however, it is uncertain whether additional factors exert an influence on observable isotope fractionation such as (iii) masking due to rate-limitation in mass transfer, and (iv) superimposed isotope effects of multiple reaction steps typical of enzyme catalysis or multistep chemical reactions.[39−42] When observable isotope fractionation of a single element varies between experiments, it is, therefore, often uncertain whether this is due to a different mechanism, or whether these other factors are responsible. Dual-element isotope plots, that is, graphs in which changes in isotope values of one element are plotted against those of a second offer a more reliable distinction between reaction mechanisms than ε values alone.[35,39,43−50]

Such information can be highly valuable in field situations. Nondestructive abiotic natural processes, such as sorption, volatilization or diffusion strongly affect concentrations of a contaminant, but generally do not cause significant isotopic fractionation.[51−57] Temporal or spatial shifts in isotope ratios, in contrast, are highly indicative of degradation and can, therefore, better monitor the success of remediation strategies at contaminated sites than mass balances alone.[58] Dual (or multi) isotope patterns, finally, can even be used to derive the relative contribution of different reaction mechanisms and then to quantify the efficiency of each of them in the field—provided that ε values of these processes have previously been characterized in laboratory experiments.[59−64]

Reported carbon isotope effects during CF transformation are, however, scarce in the literature. Chan et al.[11] reported a carbon isotope fractionation value of $-27.5 \pm 0.9‰$ during dehalorespiration of CF by a mixed culture containing *Dehalobacter* sp. strain CF50. In comparison, a much lower ε_C value of $-4.3 \pm 0.4‰$ was reported by Lee et al.[29] for the same dechlorination reaction by a mixed consortium containing another *Dehalobacter* sp. strain, UNSWDHB, whereas isotope fractionation in CF abiotic reductive dechlorination by microsized Fe(0) was found to be indistinguishable from that of the first experiment ($-29 \pm 2‰$). Significantly, larger carbon isotopic fractionation was observed for CF alkaline hydrolysis at pH ranging from 11.8 to 12.7 ($-53 \pm 3‰$).[24] To the best of our knowledge, chlorine isotope fractionation during any CF transformation mechanism has not been reported so far. Specifically, understanding whether different reaction mechanisms lead to characteristic patterns in dual C−Cl isotope plots is still limited even for chlorinated ethenes[46,47,62] and, to our knowledge, is currently nonexistent for chlorinated methanes. Hence, there is a need to explore dual element CSIA for defined reactions under controlled laboratory conditions to pave the path for the interpretation of isotope data in field studies.

Therefore, the goal of this study was to determine carbon and, for the first time, chlorine isotope fractionation patterns for different transformation processes of CF in important abiotic engineered reactions in order to explore the ability of CSIA to identify these processes at field sites. The selected chemical reactions were: oxidative C−H bond cleavage by radicals produced from PS activation, alkaline hydrolysis of chloroform at pH 12 and C−Cl bond cleavage in reductive dechlorination by cast milli-sized Fe(0).

DOI: 10.1021/acs.est.7b00679
Environ. Sci. Technol. XXXX, XXX, XXX−XXX

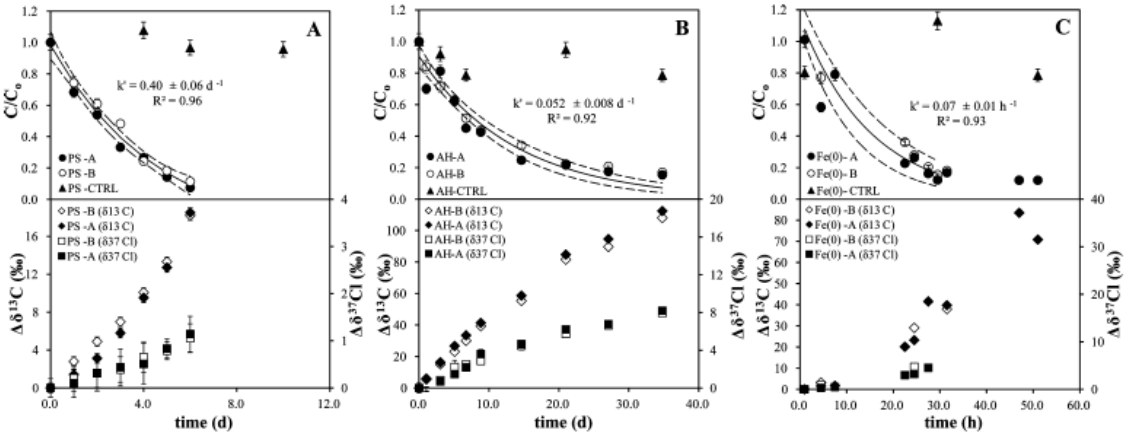

Figure 1. CF degradation kinetics (upper panels) and changes in C and Cl isotope ratios (lower panels) during oxidation by thermally activated PS with an initial PS/CF molar ratio of 40/1 (A), alkaline hydrolysis (B) and dechlorination by Fe(0) (C). Data from duplicate experiments (A and B parallel series) and from control (CTRL) experiments are shown. In the upper panels, the error bars show the uncertainty in of C/C_0, calculated by error propagation including uncertainty in concentration measurements. In some cases, error bars are smaller than the symbols. k′ values were obtained from curve fittings according to eq SI4 (see Figure S1). Fits were conducted with liner regressions in Sigma Plot 10.0 for Windows. Dashed lines represent 95% CI of regression. For CF dechlorination with Fe(0), k′ was calculated omitting data after 30 days when the disappearance of CF almost stopped. In the lower panels, error bars of individual data points indicate standard deviations of the measurements. In most cases, error bars are smaller than the symbols.

2. MATERIAL AND METHODS

2.1. Experimental Setup. All the experiments were conducted in duplicate using glass vials completely filled with aqueous solution without headspace to avoid partitioning of chlorinated volatile compounds into the gas phase. For the experiments with heat-activated PS and alkaline hydrolysis, 21 mL vials sealed with PTFE-coated rubber stoppers and aluminum crimp seals were used, whereas the Fe(0) experiments were performed using 42 mL clear glass vials capped with PTFE-coated rubber stoppers and plastic screw caps. A list of chemicals and additional experiment details is available in the Supporting Information (SI).

For the thermally activated PS experiments, the vials were filled with a pH 7 buffer solution and 0.5 mL of solutions with variable concentrations of PS were added to achieve initial PS-to-CF-molar ratios of 5/1, 10/1, or 40/1. The vials were placed in a thermostatic water bath at 50.0 ± 0.5 °C and the reaction was initiated by the addition of 0.5 mL of an aqueous CF (99%, Sigma-Aldrich) stock solution containing 2100 mg L^{-1} to achieve initial concentrations of 50 mg L^{-1}. The experiments lasted for 10 h and samples for analysis were collected at different time intervals. At each sampling time, the vials were removed from the water bath and immediately placed in an ice bath to quench the reaction by chilling. Samples were stored in the dark at 4 °C until analysis. Losses of CF due to volatilization and/or sorption were accounted for in control experiments set up in an identical manner except for the addition of PS.

CF alkaline hydrolysis experiments were performed at room temperature (~25 °C) in a pH 12 buffer solution and the vials were covered with aluminum foil to avoid photocatalyzed oxidation of CF. The reaction was initiated by the addition of 0.5 mL of the CF (99%, Sigma-Aldrich) stock solution to reach initial theoretical concentrations of 50 mg L^{-1}. The experiments started at different times to achieve reaction times varying from 0 to 35 days. After 35 days from the earliest prepared vials, all the vials were sacrificed at the same time. An appropriate volume of 0.1 M acetic acid was added to the vials to neutralize the solution to pH 6 and quench the alkaline hydrolysis reaction. Samples were stored in the dark at 4 °C until analysis. Control experiments with unbuffered deionized water were also performed.

For the Fe(0) experiments, 2 g of milli-sized cast iron (1.624 ± 0.007 m^2 g^{-1}) were added to each 42 mL vial to reach a surface concentration of 77 m^2 L^{-1}. Afterward the vials were filled with a pH 6.6 buffer solution and the reaction was initiated by the addition of the CF pure phase (99%, Alfa Aesar) to reach initial theoretical concentrations of 100 mg L^{-1}. The vials were covered with aluminum foil to avoid photocatalyzed oxidation of CF and were rotated on a horizontal shaker (IKA KS 260 BASIC, Stanfen, Germany) at 200 rpm. Control experiments without iron were also carried out. The experiments were performed at room temperature (~25 °C) and they lasted 51 h. Reactions were stopped by filtration through 0.2 μm filters at different time intervals and samples for analysis were stored frozen in 10 mL vials covered with aluminum foil.

2.2. Analytical Methods. Detailed descriptions of analytical methods are available in the SI. Briefly, concentration measurements of chlorinated compounds were performed by headspace (HS) using GC/MS as explained elsewhere,[24] except for the samples from Fe(0) experiments for which GC/TOF/MS was used. Chloride anion concentrations were analyzed by high-performance liquid chromatography. Carbon isotope analyses of CF and some detectable volatile daughter products were performed using two different GC/IRMS systems located at the University of Neuchâtel (GC/IRMS-1)[50] and at the Scientific and Technological Centers of the University of Barcelona (GC/IRMS-2).[24] Chlorine isotope CF analyses were performed using a GC/qMS system from the University of Neuchâtel as explained elsewhere[66] or a GC/IRMS system from the Institute of Groundwater Ecology of the Helmholtz

DOI: 10.1021/acs.est.7b00679
Environ. Sci. Technol. XXXX, XXX, XXX−XXX

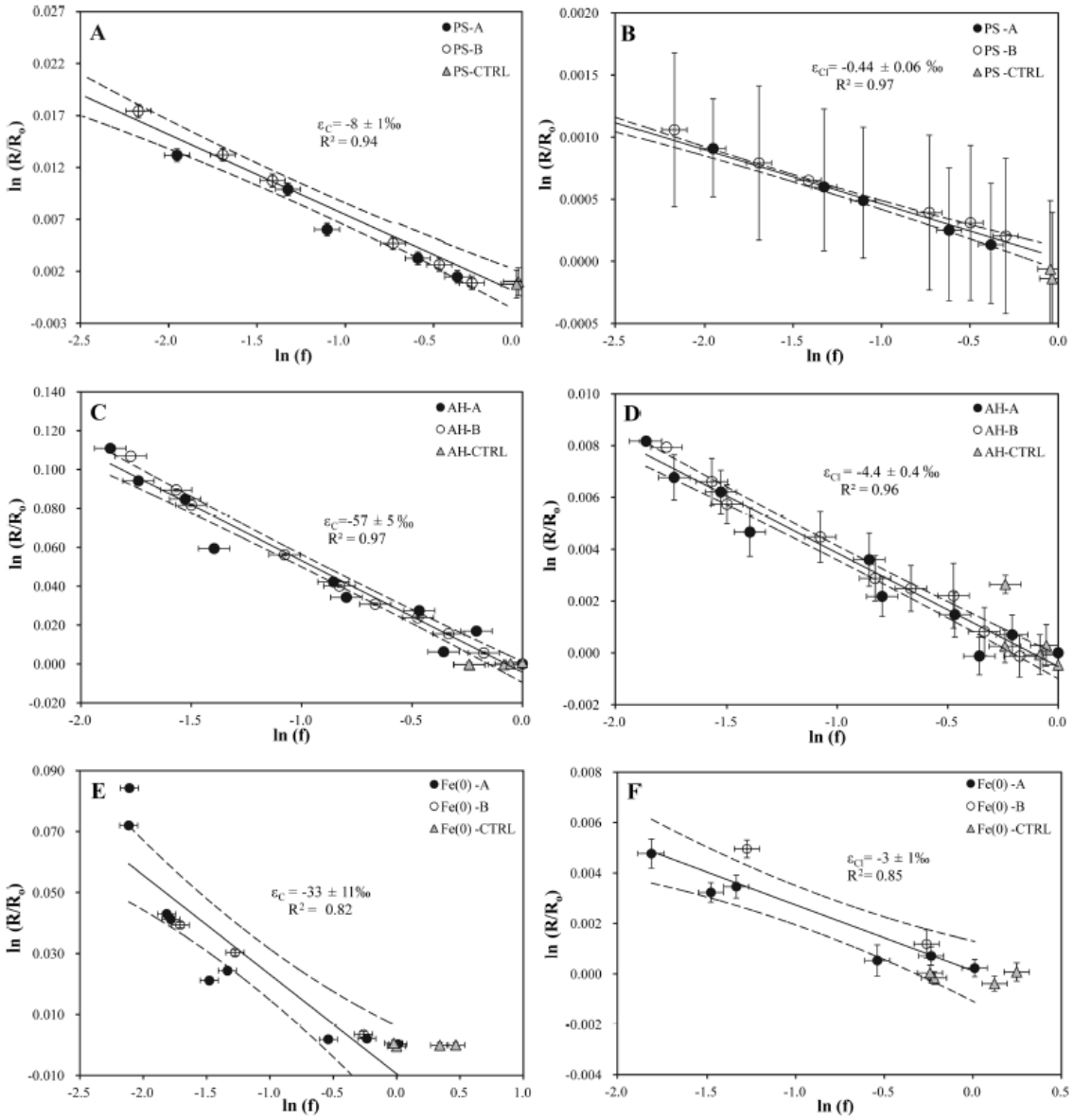

Figure 2. Logarithmic plots according to Rayleigh eq (eq 1) of carbon (left panels) and chlorine (right panels) isotope ratios during CF oxidation by thermally activated PS (A and B), alkaline hydrolysis (C and D) and dechlorination by Fe(0) (E and F). Data from duplicate experiments were used for estimating ε_C and ε_{Cl}. Dashed lines represent 95% CI of the linear regression. Error bars display the uncertainty calculated by error propagation including uncertainties in concentration and isotope measurements. In some cases, error bars are smaller than the symbols.

Zentrum München (GC/IRMS-3). An interlaboratory comparison demonstrating excellent agreement between the two analytical methods is provided in Heckel et al.[67]

2.3. Isotope Data Evaluation. Bulk carbon and chlorine ε values were obtained from the slope of the linearized Rayleigh equation for a closed system:[36]

$$\ln\left(\frac{\delta_t + 1}{\delta_0 + 1}\right) = \varepsilon \times \ln f \quad (1)$$

where δ_0 and δ_t are isotope values in the beginning (0) and at a given time (t), respectively, and f is the fraction of substrate remaining at time t. Isotope signatures were reported in per mil (‰) using the delta notation relative to international standards, that is, Vienna PeeDee Belemnite for carbon ($\delta^{13}C_{VPDB}$) and the international Standard Mean Ocean Chloride (SMOC) for chlorine ($\delta^{37}Cl_{SMOC}$):

$$\delta(\text{in‰}) = (R/R_{std} - 1) \quad (2)$$

DOI: 10.1021/acs.est.7b00679
Environ. Sci. Technol. XXXX, XXX, XXX−XXX

where R and R_{std} are the isotope ratios of the sample and the standard, respectively.

Errors given for ε values are the 95% confidence intervals (CI) of the slope of the regression line in the Rayleigh plots.

The apparent kinetic isotope effects (AKIEs) were calculated to evaluate the intrinsic isotope effect of the bond cleavage (see equations in the SI).

For dual C−Cl isotope plots, the slope of the correlation trend was determined by linear regression and the uncertainty corresponds to the 95% CI.

3. RESULTS AND DISCUSSION

3.1. Carbon and Chlorine Isotope Fractionation. Changes in CF concentration and C and Cl isotope ratios of CF during degradation by the three different mechanisms are shown in Figure 1. No CF degradation was observed in the experimental controls (without adding PS, Fe(0) or at neutral pH in the case of the hydrolysis reaction) for any of the three studied reactions. Measured concentrations in all the samples from the control experiments were always higher than 80% of the initial CF concentration (Figure 1). Accordingly, no significant changes in $\delta^{13}C$ and $\delta^{37}Cl$ isotope values were detected in the control experiments. In the rest of the experiments, a normal isotope effect was observed for both carbon and chlorine. The isotope results of combined experimental replicates, which were highly consistent for each experimental system, were used to derive C and Cl isotope fractionation values by the use of Rayleigh plots (Figure 2 and SI Figure S3). Further details on kinetics data evaluation, comparison with previous studies and product yields are provided in the SI.

PS Oxidation. The initial carbon and chlorine isotope composition remained constant (−42 ± 1‰ and −3.1 ± 0.2‰, respectively, both $n = 4$) in the control experiments (SI Figure S3A, B). Around 90% of CF removal was observed after 6 days in the PS experiments with an initial PS/CF molar ratio of 40/1 (Figure 1A). In contrast, only 30% and 20% of CF degradation were accomplished after 7 days with initial molar ratios of 10/1 and 5/1, respectively (SI Figure S1). Therefore, isotope ratios were determined only in those samples from the experiments with an initial PS to CF molar ratio of 40/1. Carbon isotope fractionation during oxidation with PS has been shown to be independent of the PS/contaminant molar ratio for chlorinated ethenes and 1,1,1-trichloroethane.[68,69] Carbon isotope composition exhibited an enrichment of $^{13}C/^{12}C$ up to $\delta^{13}C$ values of −23.8 ± 0.5‰, which resulted in an ε_C value of −8 ± 1‰ (Figure 2A). Compared to carbon, a much smaller shift in $^{37}Cl/^{35}Cl$ was observed (Figure 1A), resulting in $\delta^{37}Cl$ values up to −1.9 ± 0.4‰ (SI Figure S3AB). An ε_{Cl} of −0.44 ± 0.06‰ was obtained (Figure 2B). Neither carbon nor chlorine isotope fractionation associated with this reaction have been reported so far. The pH was kept at circumneutral values (7.0 ± 0.2) during the course of the experiment. This reaction followed pseudo-first-order kinetics with a k′ of 0.40 ± 0.06 d^{-1} ($R^2 = 0.96$, SI Figure S1). Neither PS consumption nor sulfate production were monitored along the experiments. Chloride concentrations released into solution were measured at the end of the experiment and accounted for between 95% and 110% of the total theoretical CF dechlorination yield, which was calculated assuming release of all the three chlorine atoms. Neither products nor intermediates were detected by headspace GC/MS analysis during the course of the experiments.

Alkaline Hydrolysis. Carbon and chlorine isotope values remained constant (−41.8 ± 0.5‰ and −2.6 ± 0.4‰, respectively, both $n = 5$) in control vials at neutral pH. Under alkaline conditions (the pH remained constant 11.84 ± 0.03 over the duration of the experiment), a 85% decrease in CF concentration within approximately 35 days was observed (Figure 1B). Alkaline hydrolysis induced a significant isotope effect, resulting in $\delta^{13}C$ and $\delta^{37}Cl$ values up to +70.6 ± 0.3‰ and +5.7 ± 0.4‰, respectively, after 85% CF removal (SI Figure S3C, D). An ε_C of −57 ± 5‰ (Figure 2C) and ε_{Cl} of −4.4 ± 0.4‰ (Figure 2D) were determined. So far, the only reported carbon isotope fractionation value for CF alkaline hydrolysis was −53 ± 3‰ at a pH range from 11.9 to 12.7,[24] which is comparable, within uncertainty, to that obtained in the present study. Carbon isotope fractionation is therefore independent of the pH in the tested range (from 11.8 to 12.7). To our knowledge chlorine isotope fractionation for this reaction has not been reported up to now. The reaction followed pseudo-first-order kinetics ($R^2 = 0.92$, SI Figure S1) with a k′ of 0.052 ± 0.008 d^{-1}, which is in agreement with a previously reported rate constant of 0.047 ± 0.004 d^{-1} obtained at a similar pH 11.9 ± 0.1.[24] No particular attempts were made to identify potential products of CF degradation, such as carbon monoxide (CO), formate (HCO_2^-), and chloride (Cl^-). In our previous work, excellent chlorine balances were achieved in similar experiments, indicating that CF was completely dehalogenated without accumulation of chlorinated intermediates.[24]

Fe(0) Dechlorination. CF in the controls without Fe(0) at pH 6.3 ± 0.2 did not show any changes in carbon and chlorine isotope composition ($\delta^{13}C = -47.8 \pm 0.5‰$, $n = 4$ and $\delta^{37}Cl = -3.2 \pm 0.2‰$, $n = 6$, respectively). In the presence of millisized Fe(0), CF isotope signatures of both elements showed significant changes leading up to values of $\delta^{13}C$ = +35.9 ± 0.5‰ and $\delta^{37}Cl$ = +1.7 ± 0.1‰, respectively, after 84% CF removal (SI Figure S3E, F). Isotope fractionation values of $\varepsilon_C = -33 \pm 11‰$ and $\varepsilon_{Cl} = -3 \pm 1‰$ were determined (Figure 2E and F). The obtained ε_C was not significantly different from ε_C of −29 ± 2‰ reported recently after 50% of CF dechlorination by commercial microsized Fe(0).[29] Chlorine isotope fractionation associated with this reaction has not been reported yet. The pH did not vary significantly over the duration of the experiment (6.2 ± 0.2). The degradation kinetics followed a pseudo-first-order rate law at the beginning of the reaction but after 30 h the disappearance of CF almost stopped (Figure 1C). For Fe(0)-mediated dechlorination of chlorinated ethenes, iron surface passivation due to reactive site saturation by iron hydroxide precipitates has been suggested as the cause of increased reaction half-lives and deviations from pseudo-first-order kinetics at later stages of a reaction.[70] The obtained k′ was 0.07 ± 0.01 h^{-1} ($R^2 = 0.93$, SI Figure S1), which corresponds to a k_{SA} of 2.1 ± 0.4 × 10^{-2} L m^{-2} d^{-1} (see SI).

DCM and free chloride were detected as final products in Fe(0) experiments, whereas no compounds different from CF appeared in the control experiments without iron. The yield of DCM, defined as the moles of product formed per mole of CF transformed ($DCM_t/(CF_0 - CF_t)$, where subscripts 0 and t indicate initial time and different sampling times, respectively) ranged from 0 to 2.4% over time, showing that accumulation of DCM only accounted for a small fraction of the initial CF. DCM was depleted in ^{13}C compared to the initial isotopic composition of the substrate (CF). DCM showed a trend toward higher $\delta^{13}C$ values, reflecting the enrichment trend of

DOI: 10.1021/acs.est.7b00679
Environ. Sci. Technol. XXXX, XXX, XXX−XXX

Table 1. Carbon and Chlorine Isotope Fractionation (ε_C and ε_{Cl}, Respectively), Apparent Kinetic Isotope Effects ($AKIE_C$ and $AKIE_{Cl}$, Respectively) and Dual Isotope Slopes ($\Lambda = \Delta\delta^{13}C/\Delta\delta^{37}Cl$) Values Obtained for the Three Studied CF Transformation Pathways: Oxidation with Thermally-Activated PS, Alkaline Hydrolysis and Fe(0)-Based Reductive Dechlorination[a]

experiment	reaction mechanism	ε_{bulkC} (‰)	R^2	$AKIE_C$	ε_{bulkCl} (‰)	R^2	$AKIE_{Cl}$	Λ
persulfate	oxidative C−H bond cleavage	−8 ± 1	0.94	1.008 ± 0.001	−0.44 ± 0.06	0.97	1.00045 ± 0.00004[b]	17 ± 2
alkaline hydrolysis	$E1_{CB}$ elimination	−57 ± 5	0.97	1.061 ± 0.006	−4.4 ± 0.4	0.96	1.0133 ± 0.0004	13.0 ± 0.8
Fe(0)	reductive dechlorination by C−Cl bond cleavage	−33 ± 11	0.82	1.034 ± 0.012	−3 ± 1	0.85	1.008 ± 0.001	8 ± 2

[a]The uncertainty of ε, AKIE and Λ values corresponds to the 95% CI. In all cases, $AKIE_C$ was calculated using $x = z = 1$ in eq SI6. For both alkaline hydrolysis and dechlorination by Fe(0), $AKIE_{Cl}$ was calculated using $x = z = 3$ as all C−Cl bonds are equivalent and compete for reaction. For oxidation with PS, as there is not primary chlorine isotopic effect, the secondary $AKIE_{Cl}$ was also calculated by eq SI6 using in this case $x = 3$ and $z = 1$ because no specific bond containing Cl is broken, and there is, therefore, no intramolecular competition for this bond. [b]secondary isotope effect.

the CF from which it was formed (SI Figure S3E). The DCM-related isotope fractionation $\varepsilon^{C}_{substrate\rightarrow product}$ was estimated as −19 ± 3‰ using the fitting parameter, $D(\delta^{13}C) = +13 \pm 2‰$ ($R^2 = 0.62$) (see equations in the SI). This discrepancy between the product-related and the substrate-related isotope fractionations ($\varepsilon^{C}_{CF\rightarrow DCM} = -19 \pm 3‰$ vs $\varepsilon_C = -33 \pm 11‰$) is likely attributable to the formation of other products including isotope-sensitive branching from the parent compound or intermediates, such as a dichloromethyl radical (SI Figure S4), to DCM.[71] However, due to the lack of DCM isotope signatures at early stages of reaction, such interpretations must be conducted with caution.

3.2. Mechanistic Considerations. For further elucidation of the reaction mechanism, AKIE values were calculated using eq SI6, to characterize the isotope effect of the cleavage of the chemical bond at the reactive positions. Table 1 summarizes the obtained results and proposed reaction pathways for the three studied reactions are shown in Figure 3 and discussed in detail in the SI.

The $AKIE_C$ for the oxidation reaction was 1.008 ± 0.001, which is within the range of reported carbon AKIEs for oxidative C−H bond cleavage for both abiotic (1.008−1.015) and microbial oxidation reactions (1.001−1.044) (SI Table S2), indicating that the observed fractionation was dominated by the KIE associated with oxidative cleavage of a C−H bond. A similar $AKIE_C$ value (1.008) was obtained for 1,1,1-TCA oxidation by thermally activated PS[65] from which it was suggested that the first reaction step was the rupture of the C−H bond and the abstraction of the hydrogen atom from the molecule by the attack of any of the radicals formed after persulfate activation.[65,72,73] The secondary $AKIE_{Cl}$ estimated in the present experiments (1.00045 ± 0.00004) also points to an oxidative reaction, where there is not initial C−Cl bond cleavage and thus a primary chlorine kinetic isotope effect is not expected. A reaction pathway involving the cleavage of the C−H as the rate-limiting step is proposed (Figure 3A and SI). In order to track more confidently the proposed mechanism, hydrogen isotope fractionation during CF oxidation with thermally activated PS might be further measured.

During alkaline hydrolysis, CF is abiotically dechlorinated to carbon monoxide and formate.[74,75] A stepwise elimination mechanism ($E1_{CB}$) has been proposed for this reaction.[24,74,76,77] This mechanism consists of the rapid, reversible, base-catalyzed deprotonation of the molecule with the formation of a trichloromethyl carbanion ($:CCl_3^-$), followed by the rate-determining unimolecular loss of a chloride ion to produce the reactive intermediate dichlorocarbene (CCl_2), which is then rapidly transformed into carbon monoxide and formate (SI Figure S4). If this is the case, as the deprotonation

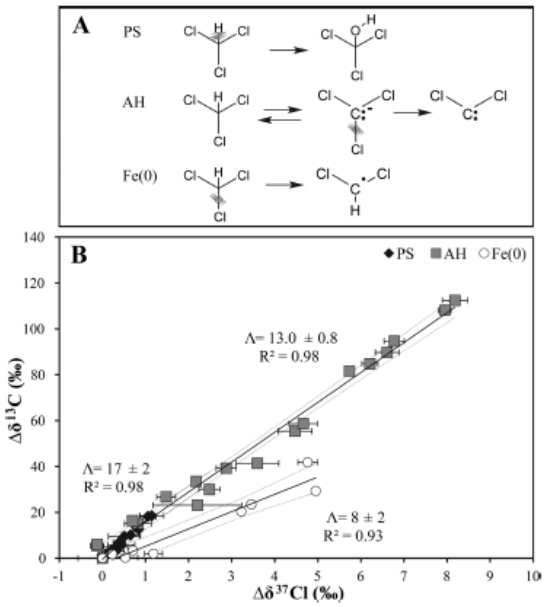

Figure 3. (A) Proposed reaction pathways for CF degradation by the three studied reactions. More details are given in the SI. (B) Dual C−Cl isotope plot for CF degradation by the three studied pathways: oxidation by thermally activated PS (PS), alkaline hydrolysis (AH) and dechlorination by Fe(0) (Fe(0)). Data from duplicate experiments were combined. Lines are linear regressions of the data sets with 95% CI (dashed lines). Error bars show uncertainty in isotope measurements. Note that error bars of $\delta^{13}C$ values are smaller than the symbols.

step is reversible and the loss of a chloride ion is the rate-determining step, both carbon and chlorine primary isotope effects in the CF molecule are expected during this process. In the present experiments, an $AKIE_C$ of 1.061 ± 0.006 was obtained for alkaline hydrolysis, which is consistent with the Streitwieser limit for a primary carbon KIE in C−Cl bonds (1.057, SI Table S2)[37,78] and is equivalent, within the given 95% CI, to the value previously found by Torrentó et al.[24] (1.056 ± 0.003). The $AKIE_{Cl}$ was calculated as 1.0133 ± 0.0004, which is equal to the maximum expected KIE_{Cl} for cleavage of a C−Cl bond (1.013, SI Table S2),[37] indicating the involvement of a C−Cl bond. In principle, the Cl kinetic isotope effect estimated in the present study is, therefore, consistent with the occurrence of a carbanion mechanism

DOI: 10.1021/acs.est.7b00679
Environ. Sci. Technol. XXXX, XXX, XXX−XXX

(Figure 3A) but also with a C−Cl bond cleavage via a concerted one-step S_N2 nucleophilic substitution mechanism. Nevertheless, based on energy considerations, the $E1_{CB}$ mechanism seems more plausible for this reaction (see the SI for further discussion). Further deuterium-exchange experiments might be performed to confirm the existence of a carbanion intermediate as a way to further corroborate the occurrence of the stepwise elimination mechanism.[79]

In the case of reductive dechlorination by Fe(0), an $AKIE_C$ of 1.034 ± 0.012 was obtained, which is similar to the value of 1.030 ± 0.007 obtained by Lee et al.[29] and within the $AKIE_C$ range for the reductive cleavage of C−Cl bonds reported in the literature (1.003−1.060) (SI Table S2). In fact, most $AKIE_C$ values for reductive dehalogenation fall in the range of 1.027 and 1.033, which corresponds to about 50% bond cleavage when considering a Streitwieser limit for a C−Cl bond of 1.057 for complete bond cleavage in an infinitely late transition state.[80] Regarding $AKIE_{Cl}$, a value of 1.008 ± 0.001 was calculated, which is also about 50% of the Streitwieser limit for KIE_{Cl} in C−Cl bonds (1.013).[37] Similar $AKIE_{Cl}$ values, ranging from 1.008 to 1.016 for abiotic reductive dechlorination and from 1.004 to 1.011 for biotic reductive dechlorination, have been previously reported for chlorinated methanes, ethenes and ethanes (SI Table S2). Therefore, both C and Cl-AKIEs pointed to cleavage of a C−Cl bond in the first rate-limiting step, which is compatible with the two-step pathway that is commonly hypothesized for this reaction (see SI). The first step may, for example, involve the transfer of a single electron from the metal surface causing the removal of a chlorine atom and the formation of a dichloromethyl radical ($\cdot CHCl_2$) (Figure 3A).

3.3. Dual Element Isotope Plot. Figure 3B shows the dual C−Cl isotope plot for the reactions of this study. A linear correlation between $\Delta\delta^{13}C$ and $\Delta\delta^{37}Cl$ was observed for the three studied transformation mechanisms ($r^2 \geq 0.92$). A comparison of the slopes ($\Lambda = \Delta\delta^{13}C/\Delta\delta^{37}Cl$) for the regression lines was performed by analysis of covariance (ANCOVA). Statistical significance was accepted at the $p < 0.05$ level. There is no significant statistical difference between oxidation by thermally activated persulfate (17 ± 2) and alkaline hydrolysis (13.0 ± 0.8) slopes (ANCOVA, $p = 0.2$). In contrast, these results differ significantly (ANCOVA, $p < 0.0001$) from the slope observed during CF reductive dechlorination by Fe(0) (8 ± 2).

Hence, although different mechanisms are involved in CF degradation by oxidation by thermally activated PS (cleavage of a C−H bond) and by alkaline hydrolysis (cleavage of a C−Cl bond), the obtained Λ values for both degradation reactions are not significantly different. This may be explained by considerations for carbon and chlorine isotope effects. *Carbon.* As expected, the obtained $AKIE_C$ value for CF degradation by oxidation with heat-activated PS is smaller than for alkaline hydrolysis. The higher the mass of the bonding partner, the greater is typically the primary kinetic isotope effects.[37] Hence it can be explained that carbon isotope fractionation associated with C−Cl bond cleavage is greater than in C−H bond cleavage since the carbon atom is bound to a heavier atom (chlorine vs hydrogen). *Chlorine.* This difference, however, is matched by similar differences in chlorine isotope fractionation. On the one hand, C−Cl bond cleavage involves a primary $AKIE_{Cl}$, which is clearly greater than a secondary $AKIE_{Cl}$ next to a reacting C−H bond. On the other hand, this primary $AKIE_{Cl}$ is "diluted" in ε_{Cl} due to the intramolecular competition between three chemically equivalent C−Cl bonds (z = 3 in eq SI6), whereas the simultaneous secondary $AKIE_{Cl}$ of three Cl atoms are not diluted (z = 1). By coincidence, the interplay of these factors results in a similar reduction of carbon as of chlorine isotope fractionation so that similar Λ are obtained. This unexpected result restrains the use of C−Cl isotope plots for distinguishing these reactions in the field and highlights the need to apply this approach with precaution and using complementary tools for identification of degradation mechanisms in the field (e.g., complementary hydrogen isotope analysis).

4. ENVIRONMENTAL SIGNIFICANCE

Carbon and chlorine isotope fractionation of CF during oxidation with heat-activated PS, by alkaline hydrolysis and by reductive dechlorination with Fe(0) was studied in batch experiments in order to explore the potential of CSIA for the identification of reaction mechanisms in the monitoring of remediation strategies at contaminated sites. For the first time, carbon isotope fractionation values (for heat-activated PS) and chlorine isotope fractionation values (for the three reactions) were determined. These new ε values increase the options of using CSIA for estimating the extent of contaminant degradation at field sites where remediation strategies are implemented that rely on induced abiotic transformations of CF. Based on the obtained ε values, it is likely that changes in isotope values in the field may be larger than 2‰ for carbon and 0.4‰ (for GC/IRMS instruments) or 2‰ (for GC/qMS instruments) for chlorine - these are the significant levels that have been suggested as reliable indicators of degradation.[34,81] Even with the relatively small carbon fractionation obtained for CF oxidation by PS (−8 ± 1‰) and chlorine isotope fractionation observed for Fe(0)-mediated reductive dechlorination (−3 ± 1‰), shifts in CF isotopic composition will be already detectable with a reasonable accuracy if the substrate is degraded by 20% and 25−50%, respectively.

Although only the reductive dechlorination showed significantly statistically different C−Cl isotope slope compared with the other two reactions (oxidation and alkaline hydrolysis), the dual isotope approach might still be used to identify different CF degradation mechanisms in the field, which would (or not necessarily) take place at the same time. For example, the coupling of two common treatments—ISCO and in situ bioremediation— has been shown not only to be feasible, but in many cases also to be able to provide a more efficient and extensive cleanup of contaminated sites.[82] In the case of PS, the anaerobic environment that is created following the consumption of the oxidant is ideal for CF microbial dehalogenation under sulfate reduction conditions to be enhanced. Enhanced CF bioremediation has also been observed when combining Fe(0) and methanogens that use the cathodic hydrogen generated by iron corrosion for cometabolic degradation of CF[83−85] or even better by dehalorespiring bacteria which are not inhibited at certain concentrations of CF.[29] Therefore, there would be an increasing number of case studies, where CF degradation due to PS application or Fe(0) barriers should be distinguished from biotic reductive dechlorination in the field. Although chlorine isotope fractionation during biotic CF dechlorination remains to be evaluated in detail, as well as the effect in CF degradation of Fe(0) aging or the presence of Fe(0) impurities such as graphite,[86] the dual C−Cl slopes obtained in the present work sets the grounds for the potential application of this approach

DOI: 10.1021/acs.est.7b00679
Environ. Sci. Technol. XXXX, XXX, XXX−XXX

for assessing if CF abiotic reductive dechlorination performed by Fe(0)-PRB or naturally occurring iron-bearing minerals would be or not distinguishable from microbial reductive dechlorination.

Although CF anaerobic biodegradation has been reported to occur mainly via cometabolic dechlorination or by dehalorespiration,[8] an alternative pathway was suggested in the presence of cobalamins and involving CF hydrolysis.[87,88] The mechanism of this reaction is not well-known, but it presumably involves the cobalamin-catalyzed conversion of CF to a monochlorocarbene, which would be subsequently hydrolyzed to formaldehyde. The produced formaldehyde could then be oxidized to CO or formate and finally to CO_2. The abiotic alkaline hydrolysis reaction characterized in the present study might be used as a reference system for this suggested CF biotic hydrolysis in future dual isotope-CSIA studies.

Finally, due to the significant difference between the C−Cl isotope slope of CF oxidation and reductive dechlorination, the dual isotope approach might be in addition useful for distinguishing between aerobic and anaerobic CF biodegradation pathways. CF aerobic biodegradation only occurs during oxidative cometabolism with other primary substrates such as methane, butane or toluene by oxygenase-expressing microorganisms.[8] The pathway of CF cooxidation starts by insertion of one oxygen atom into the molecule via H abstraction with phosgene as intermediate and final mineralization to chloride and CO_2. The chemical mechanism of CF oxidation is variable among the various existent monooxygenases, but the rate-limiting step is expected to be the cleavage of the C−H bond.

In conclusion, our study established an expedient base with carbon and chlorine isotope fractionation during three abiotic CF transformation mechanisms. Further research is needed in order to explore if other CF natural degradation pathways (for example naturally occurring iron-bearing minerals as well as aerobic and anaerobic degraders) might be similar to or different from the patterns generated in this study. Such information will allow connecting dual-plot slopes to known reaction mechanisms with the aim to distinguish different degradation processes in the field. This distinction would be important for better monitoring the success of remediation strategies at contaminated sites.

■ ASSOCIATED CONTENT

Supporting Information

The Supporting Information is available free of charge on the ACS Publications website at DOI: 10.1021/acs.est.7b00679.

Chemicals; analytical methods; further discussion in kinetics; calculation of AKIE values; calculation of isotope trend for DCM in the Fe(0) experiment; carbon and chlorine isotope fractionation patterns; further discussion in reaction pathways; comparison of ε and AKIE values for C and Cl isotopes in different studies (PDF)

■ AUTHOR INFORMATION

Corresponding Author

*Phone: +41 32 718 26 49; fax: +41 32 718 26 03; e-mail: clara.torrento@unine.ch.

ORCID

Clara Torrentó: 0000-0003-1480-2744

Jordi Palau: 0000-0001-9492-7306

Diana Rodríguez-Fernández: 0000-0002-2515-9945

Mònica Rosell: 0000-0003-1563-8595

Martin Elsner: 0000-0003-4746-9052

Notes

The authors declare no competing financial interest.

■ ACKNOWLEDGMENTS

This study was financed through the following projects: CGL2011-29975-C04-01 and CGL2014-57215-C4-1-R from the Spanish Government, 2014SGR1456 from the Catalan Government and a Marie Curie Career Integration Grant in the framework of the IMOTEC-BOX project (PCIG9-GA-2011-293808) within the European Union seventh Framework Programme. The experiments and analysis performed in Helmholtz Zentrum München by D. Rodríguez-Fernández were supported by the FPU2012/01615 contract. We want to thank the Scientific and Technological Centers of the University of Barcelona (CCiTUB) for their services. We thank the editor and three anonymous reviewers for comments that improved the quality of the manuscript.

■ REFERENCES

(1) Laturnus, F.; Haselmann, K. F.; Borch, T.; Gron, C. Terrestrial natural sources of trichloromethane (chloroform, CHCl3) - An overview. *Biogeochemistry* **2002**, *60*, 121−139.

(2) Albers, C. N.; Jacobsen, O. S.; Flores, E. M. M.; Pereira, J. S. F.; Laier, T. Spatial variation in natural formation of chloroform in the soils of four coniferous forests. *Biogeochemistry* **2011**, *103*, 317−334.

(3) Hunkeler, D.; Laier, T.; Breider, F.; Jacobsen, O. S. Demonstrating a natural origin of chloroform in groundwater using stable carbon isotopes. *Environ. Sci. Technol.* **2012**, *46*, 6096−6101.

(4) Rossberg, M.; Lendle, W.; Pfleiderer, G.; Tögel, A.; Torkelson, T. R.; Beutel, K. K. *Chloromethanes. Ullmann's Encyclopedia of Industrial Chemistry*, 2011.

(5) Zogorski, J. S.; Carter, J. M.; Ivahnenko, T.; Lapham, W. W.; Moran, M. J.; Rowe, B. L.; Squillace, P. J.; Toccalino, P. L. *The Quality of Our Nation'S Waters - Volatile Organic Compounds in the Nation'S Ground Water and Drinking-Water Supply Wells*; U.S. Geological Survey Circular 1292, 2006.

(6) Dobrzyńska, E.; Pośniak, M.; Szewczyńska, M.; Buszewski, B. Chlorinated volatile organic compounds: Old, however, actual analytical and toxicological problem. *Crit. Rev. Anal. Chem.* **2010**, *40*, 41−57.

(7) Agency for toxic substances and disease registry (ATSDR). Priority List of Hazardous Substances 2015, .http://www.atsdr.cdc.gov/spl/index.html.

(8) Cappelletti, M.; Frascari, D.; Zannoni, D.; Fedi et, S. Microbial degradation of chloroform. *Appl. Microbiol. Biotechnol.* **2012**, *96*, 1395−1409.

(9) Grostern, A.; Duhamel, M.; Dworatzek, S.; Edwards, E. A. Chloroform respiration to dichloromethane by a *Dehalobacter* population. *Environ. Microbiol.* **2010**, *12*, 1053−1060.

(10) Lee, M.; Low, A.; Zemb, O.; Koenig, J.; Michaelsen, A.; Manefield, M. Complete chloroform dechlorination by organochlorine respiration and fermentation. *Environ. Microbiol.* **2012**, *14*, 883−894.

(11) Chan, C. C. H.; Mundle, S. O. C.; Eckert, T.; Liang, X.; Tang, S.; Lacrampe-Couloume, G.; Edwards, E. A.; Sherwood-Lollar, B. Large carbon isotope fractionation during biodegradation of chloroform by *Dehalobacter* cultures. *Environ. Sci. Technol.* **2012**, *46*, 10154−10160.

(12) Tang, S.; Edwards, E. A. Identification of *Dehalobacter* reductive dehalogenases that catalyse dechlorination of chloroform, 1,1,1-trichloroethane and 1,1-dichloroethane. *Philos. Trans. R. Soc., B* **2013**, *368*, 20120318.

(13) Deshpande, N. P.; Wong, Y. K.; Manefield, M.; Wilkins, M. R.; Lee, M. Genome sequence of *Dehalobacter* UNSWDHB, a chloroform dechlorinating bacterium. *Genome Announc.* **2013**, *1*, e00720−13.

DOI: 10.1021/acs.est.7b00679
Environ. Sci. Technol. XXXX, XXX, XXX−XXX

Appendix A. Engineered Chloroform Transformation Reactions

(14) Ding, C.; Zhao, S.; He, J. A *Desulfitobacterium* sp. strain PR reductively dechlorinates both 1,1,1-trichloroethane and chloroform. *Environ. Microbiol.* **2014**, *16*, 3387−3397.
(15) Justicia-Leon, S. D.; Higgins, S.; Mack, E. E.; Griffiths, D. R.; Tang, S.; Edwards, E. A.; Löffler, F. E. Bioaugmentation with distinct *Dehalobacter* strains achieves chloroform detoxification in microcosms. *Environ. Sci. Technol.* **2014**, *48*, 1851−1858.
(16) Duhamel, M.; Wehr, S. D.; Yu, L.; Rizvi, H.; Seepersad, D.; Dworatzek, S.; Cox, E. E.; Edwards, E. A. Comparison of anaerobic dechlorinating enrichment cultures maintained on tetrachloroethene, trichloroethene, cis-dichloroethene and vinyl chloride. *Water Res.* **2002**, *36*, 4193−4202.
(17) Maymó-Gatell, X.; Nijenhuis, I.; Zinder, S. H. Reductive dechlorination of cis-1,2-dichloroethene and vinyl chloride by *Dehalococcoides ethenogenes*. *Environ. Sci. Technol.* **2001**, *35*, 516−521.
(18) Kenneke, J. F.; Weber, E. J. Reductive dehalogenation of halomethanes in iron- and sulfate-reducing sediments. 1. Reactivity pattern analysis. *Environ. Sci. Technol.* **2003**, *37*, 713−720.
(19) Huling, S. G.; Pivetz, B. E. *In Situ Chemical Oxidation-Engineering Issue*, EPA/600/R-06/072; U.S. Environmental Protection Agency Office of Research and Development, National Risk Management Research Laboratory: Cincinnati, OH, 2006.
(20) Huang, K. C.; Zhao, Z.; Hoag, G. E.; Dahmani, A.; Block, P. A. Degradation of volatile organic compounds with thermally activated persulfate oxidation. *Chemosphere* **2005**, *61*, 551−560.
(21) Waldemer, R. H.; Tratnyek, P. G.; Johnson, R. L.; Nurmi, J. T. Oxidation of chlorinated ethenes by heat-activated persulfate: Kinetics and products. *Environ. Sci. Technol.* **2007**, *41*, 1010−1015.
(22) Tsitonaki, A.; Petri, B.; Crimi, M.; Mosbaek, H.; Siegrist, R. L.; Bjerg, P. L. In situ chemical oxidation of contaminated soil and groundwater using persulfate: a review. *Crit. Rev. Environ. Sci. Technol.* **2010**, *40*, 55−91.
(23) Zhu, X.; Du, E.; Ding, H.; Lin, Y.; Long, T.; Li, H.; Wang, L. QSAR modeling of VOCs degradation by ferrous-activated persulfate oxidation. *Desalin. Water Treat.* **2016**, *57*, 1−15.
(24) Torrentó, C.; Audí-Miró, C.; Bordeleau, G.; Marchesi, M.; Rosell, M.; Otero, N.; Soler, A. The use of alkaline hydrolysis as a novel strategy for chloroform remediation: feasibility of using urban construction wastes and evaluation of carbon isotopic fractionation. *Environ. Sci. Technol.* **2014**, *48*, 1869−1877.
(25) Gillham, R. W.; OHannesin, S. F. Enhanced reduction of halogenated aliphatics by zero-valent iron. *Groundwater* **1994**, *32*, 958−967.
(26) Matheson, L. J.; Tratnyek, P. G. Reductive dehalogenation of chlorinated methanes by iron metal. *Environ. Sci. Technol.* **1994**, *28*, 2045−2053.
(27) Johnson, T. L.; Scherer, M. M.; Tratnyek, P. G. Kinetics of halogenated organic compound reduction by iron metal. *Environ. Sci. Technol.* **1996**, *30*, 2634−2640.
(28) Feng, J.; Lim, T.-T. Pathways and kinetics of carbon tetrachloride and chloroform reductions by nano-scale Fe and Fe/Ni particles: comparison with commercial micro-scale Fe and Zn. *Chemosphere* **2005**, *59*, 1267−1277.
(29) Lee, M.; Wells, E.; Wong, Y. K.; Koenig, J.; Adrian, L.; Richnow, H. H.; Manefield, M. Relative contributions of *Dehalobacter* and zerovalent Iron in the degradation of chlorinated methanes. *Environ. Sci. Technol.* **2015**, *49*, 4481−4489.
(30) O'Hannesin, S. F.; Gillham, R. W. Long-term performance of an in Situ "iron wall" for remediation of VOCs. *Groundwater* **1998**, *36*, 164−170.
(31) Wilkin, R. T.; Acree, S. D.; Ross, R. R.; Puls, R. W.; Lee, T. R.; Woods, L. L. Fifteen-year assessment of a permeable reactive barrier for treatment of chromate and trichloroethylene in groundwater. *Sci. Total Environ.* **2014**, *468−469*, 186−194.
(32) Zhang, W.-X. Nanoscale iron particles for environmental remediation: An overview. *J. Nanopart. Res.* **2003**, *5*, 323−332.
(33) Elsner, M.; Lacrampe-Couloume, G.; Mancini, S. A.; Burns, L.; Sherwood Lollar, B. Carbon isotope analysis to evaluate nanoscale Fe(0) treatment at a chlorohydrocarbon contaminated site. *Groundwater Monit. Rem.* **2010**, *30*, 79−95.
(34) Meckenstock, R. U.; Barbara Morasch, B.; Griebler, C.; Richnow, H. H. Stable isotope fractionation analysis as a tool to monitor biodegradation in contaminated aquifers. *J. Contam. Hydrol.* **2004**, *75*, 215−255.
(35) Elsner, M. Stable isotope fractionation to investigate natural transformation mechanisms of organic contaminants: principles, prospects and limitations. *J. Environ. Monit.* **2010**, *12*, 2005−2031.
(36) Mariotti, A.; Germon, J. C.; Hubert, P.; Kaiser, P.; Letolle, R.; Tardieux, A.; Tardieux, P. Experimental determination of nitrogen kinetic isotope fractionation: Some principles; illustration for the denitrification and nitrification processes. *Plant Soil* **1981**, *62*, 413−430.
(37) Elsner, M.; Zwank, L.; Hunkeler, D.; Schwarzenbach, R. P. A new concept linking observable stable isotope fractionation to transformation pathways of organic pollutants. *Environ. Sci. Technol.* **2005**, *39*, 6896−6916.
(38) Hofstetter, T. B.; Berg, M. Assessing transformation processes of organic contaminants by compound-specific stable isotope analyses. *TrAC, Trends Anal. Chem.* **2011**, *30*, 618−627.
(39) Mancini, S. A.; Hirschorn, S. K.; Elsner, M.; Lacrampe-Couloume, G.; Sleep, B. E.; Edwards, E. A.; Sherwood Lollar, B. Effects of trace element concentration on enzyme controlled stable isotope fractionation during aerobic biodegradation of toluene. *Environ. Sci. Technol.* **2006**, *40*, 7675−7681.
(40) Penning, H.; Cramer, C. J.; Elsner, M. Rate-dependent carbon and nitrogen kinetic isotope fractionation in hydrolysis of isoproturon. *Environ. Sci. Technol.* **2008**, *42*, 7764−7771.
(41) Renpenning, J.; Keller, S.; Cretnik, S.; Shouakar-Stash, O.; Elsner, M.; Schubert, T.; Nijenhuis, I. Combined C and Cl isotope effects indicate differences between corrinoids and enzyme (*Sulfurospirillum multivorans* PceA) in reductive dehalogenation of tetrachloroethene, but not trichloroethene. *Environ. Sci. Technol.* **2014**, *48*, 11837−11845.
(42) Renpenning, J.; Rapp, I.; Nijenhuis, I. Substrate hydrophobicity and cell composition influence the extent of rate limitation and masking of isotope fractionation during microbial reductive dehalogenation of chlorinated ethenes. *Environ. Sci. Technol.* **2015**, *49*, 4293−4301.
(43) Tobler, N. B.; Hofstetter, T. B.; Schwarzenbach, R. P. Carbon and hydrogen isotope fractionation during anaerobic toluene oxidation by *Geobacter metallireducens* with different Fe(III) phases as terminal electron acceptors. *Environ. Sci. Technol.* **2008**, *42*, 7786−7792.
(44) Vogt, C.; Cyrus, E.; Herklotz, I.; Schlosser, D.; Bahr, A.; Herrmann, S.; Richnow, H. H.; Fischer, A. Evaluation of toluene degradation pathways by two-dimensional stable isotope fractionation. *Environ. Sci. Technol.* **2008**, *42*, 7793−7800.
(45) Abe, Y.; Aravena, R.; Zopfi, J.; Shouakar-Stash, O.; Cox, E.; Roberts, J. D.; Hunkeler, D. Carbon and chlorine isotope fractionation during aerobic oxidation and reductive dechlorination of vinyl chloride and cis-1,2-dichloroethene. *Environ. Sci. Technol.* **2009**, *43*, 101−107.
(46) Audí-Miró, C.; Cretnik, S.; Otero, N.; Palau, J.; Shouakar-Stash, O.; Soler, A.; Elsner, M. Cl and C isotope analysis to assess the effectiveness of chlorinated ethene degradation by zero-valent iron: Evidence from dual element and product isotope values. *Appl. Geochem.* **2013**, *32*, 175−183.
(47) Cretnik, S.; Thoreson, K. A.; Bernstein, A.; Ebert, K.; Buchner, D.; Laskov, C.; Haderlein, S.; Shouakar-Stash, O.; Kliegman, S.; McNeill, K.; Elsner, M. Reductive dechlorination of TCE by chemical model systems in comparison to dehalogenating bacteria: Insights from dual element isotope analysis ($^{13}C/^{12}C$, $^{37}Cl/^{35}Cl$). *Environ. Sci. Technol.* **2013**, *47*, 6855−6863.
(48) Kuder, T.; van Breukelen, B. M.; Vanderford, M.; Philp, P. 3D-CSIA: Carbon, chlorine, and hydrogen isotope fractionation in transformation of TCE to ethene by a *Dehalococcoides* culture. *Environ. Sci. Technol.* **2013**, *47*, 9668−9677.
(49) Badin, A.; Buttet, G.; Maillard, J.; Holliger, C.; Hunkeler, D. Multiple dual C−Cl isotope patterns associated with reductive

DOI: 10.1021/acs.est.7b00679
Environ. Sci. Technol. XXXX, XXX, XXX−XXX

dechlorination of tetrachloroethene. *Environ. Sci. Technol.* **2014**, *48*, 9179−9186.
(50) Palau, J.; Cretnik, S.; Shouakar-Stash, O.; Höche, M.; Elsner, M.; Hunkeler, M. C and Cl isotope fractionation of 1,2-dichloroethane displays unique $\delta^{13}C/\delta^{37}Cl$ patterns for pathway identification and reveals surprising C−Cl bond involvement in microbial oxidation. *Environ. Sci. Technol.* **2014**, *48*, 9430−9437.
(51) Poulson, S. R.; Drever, J. I. Stable isotope (C, Cl, and H) fractionation during vaporization of trichloroethylene. *Environ. Sci. Technol.* **1999**, *33*, 3689−3694.
(52) Slater, G. F.; Ahad, J. M. E.; Sherwood Lollar, B.; Allen-King, R. M.; Sleep, B. E. Carbon isotope effects resulting from equilibrium sorption of dissolved VOCs. *Anal. Chem.* **2000**, *72*, 5669−5672.
(53) Wang, Y.; Huang, Y. S. Hydrogen isotopic fractionation of petroleum hydrocarbons during vaporization: Implications for assessing artificial and natural remediation of petroleum contamination. *Appl. Geochem.* **2003**, *18*, 1641−1651.
(54) Bouchard, D.; Hohener, P.; Hunkeler, D. Carbon isotope fractionation during volatilization of petroleum hydrocarbons and diffusion across a porous medium: a column experiment. *Environ. Sci. Technol.* **2008**, *42*, 7801−7806.
(55) Kuder, T.; Philp, P.; Allen, J. Effects of volatilization on carbon and hydrogen isotope ratios of MTBE. *Environ. Sci. Technol.* **2009**, *43*, 1763−1768.
(56) Jeannottat, S.; Hunkeler, D. Chlorine and carbon isotopes fractionation during volatilization and diffusive transport of trichloroethene in the unsaturated zone. *Environ. Sci. Technol.* **2012**, *46*, 3169−3176.
(57) Wanner, P.; Hunkeler, D. Carbon and chlorine isotopologue fractionation of chlorinated hydrocarbons during diffusion in water and low permeability sediments. *Geochim. Cosmochim. Acta* **2015**, *157*, 198−212.
(58) Hunkeler, D.; Meckenstock, R. U.; Sherwood Lollar, B.; Schmidt, T.; Wilson, J.; Schmidt, T.; Wilson, J. *A Guide for Assessing Biodegradation and Source Identification of Organic Ground Water Contaminants Using Compound Specific Isotope Analysis (CSIA)*, PA 600/R-08/148; US EPA: 2008; www.epa.gov/ada.
(59) Van Breukelen, B. M. Extending the Rayleigh equation to allow competing isotope fractionating pathways to improve quantification of biodegradation. *Environ. Sci. Technol.* **2007**, *41*, 4004−4010.
(60) Hunkeler, D.; Abe, Y.; Broholm, M. M.; Jeannottat, S.; Westergaard, C.; Jacobsen, C. S.; Aravena, R.; Bjerg, P. L. Assessing chlorinated ethene degradation in a large scale contaminant plume by dual carbon-chlorine isotope analysis and quantitative PCR. *J. Contam. Hydrol.* **2011**, *119*, 69−79.
(61) Wiegert, C.; Aeppli, C.; Knowles, T.; Holmstrand, H.; Evershed, R.; Pancost, R. D.; Macháčková, J.; Gustafsson, O. Dual carbon-chlorine stable isotope investigation of sources and fate of chlorinated ethenes in contaminated groundwater. *Environ. Sci. Technol.* **2012**, *46*, 10918−10925.
(62) Audí-Miró, C.; Cretnik, S.; Torrentó, C.; Rosell, M.; Shouakar-Stash, O.; Otero, N.; Palau, J.; Elsner, M.; Soler, A. C, Cl and H compound-specific isotope analysis to assess natural versus Fe(0) barrier-induced degradation of chlorinated ethenes at a contaminated site. *J. Hazard. Mater.* **2015**, *299*, 747−754.
(63) Badin, A.; Broholm, M. M.; Jacobsen, C. S.; Palau, J.; Dennis, P.; Hunkeler, D. Identification of abiotic and biotic reductive dechlorination in a chlorinated ethene plume after thermal source remediation by means of isotopic and molecular biology tools. *J. Contam. Hydrol.* **2016**, *192*, 1−19.
(64) Palau, J.; Jamin, P.; Badin, A.; Vanhecke, N.; Haerens, B.; Brouyère, S.; Hunkeler, D. Use of carbon-chlorine dual isotope analysis to assess the degradation pathways of 1,1,1-trichloroethane in groundwater. *Water Res.* **2016**, *92*, 235−243.
(65) Palau, J.; Shouakar-Stash, O.; Hunkeler, D. Carbon and chlorine isotope analysis to identify abiotic degradation pathways of 1,1,1-trichloroethane. *Environ. Sci. Technol.* **2014**, *48*, 14400−14408.
(66) Breider, F.; Hunkeler, D. Investigating chloroperoxidase-catalyzed formation of chloroform from humic substances using stable chlorine isotope analysis. *Environ. Sci. Technol.* **2014**, *48*, 1592−1600.
(67) Heckel, B.; Rodríguez-Fernández, D.; Torrentó, D.; Meyer, A.; Palau, J.; Domènech, C.; Rosell, M.; Soler, A.; Hunkeler, D.; Elsner, D. Compound-specific chlorine isotope analysis of tetrachloro-methane and trichloromethane by GC-IRMS vs. GC-qMS: Method development and evaluation of precision and trueness. *Anal. Chem.* **2017**, *89*, 3411−3420.
(68) Marchesi, M.; Aravena, R.; Sra, K. S.; Thomson, N. R.; Otero, N.; Soler, A.; Mancini, S. Carbon isotope fractionation of chlorinated ethenes during oxidation by Fe2+ activated persulfate. *Sci. Total Environ.* **2012**, *433*, 319−322.
(69) Marchesi, M.; Thomson, N. R.; Aravena, R.; Sra, K. S.; Otero, N.; Soler, A. Carbon isotope fractionation of 1,1,1-trichloroethane during base-catalyzed persulfate treatment. *J. Hazard. Mater.* **2013**, *260*, 61−66.
(70) Farrell, J.; Kason, M.; Melitas, N.; Li, T. Investigation of the long-term performance of zero-valent iron for reductive dechlorination of trichloroethylene. *Environ. Sci. Technol.* **2000**, *34*, 514−521.
(71) Neumann, A.; Hofstetter, T. B.; Skarpeli-Liati, M.; Schwarzenbach, R. P. Reduction of polychlorinated ethanes and carbon tetrachloride by structural Fe(II) in smectites. *Environ. Sci. Technol.* **2009**, *43*, 4082−4089.
(72) Gu, X. G.; Lu, S. G.; Li, L.; Qiu, Z. F.; Sui, Q.; Lin, K. F.; Luo, Q. S. Oxidation of 1,1,1-trichloroethane stimulated by thermally activated persulfate. *Ind. Eng. Chem. Res.* **2011**, *50*, 11029−11036.
(73) Xu, M. H.; Gu, X. G.; Lu, S. G.; Qiu, Z. F.; Sui, Q. Role of reactive oxygen species for 1,1,1-trichloroethane degradation in a thermally activated persulfate system. *Ind. Eng. Chem. Res.* **2014**, *53*, 1056−1063.
(74) Hine, J. Carbon dichloride as an intermediate in the basic hydrolysis of chloroform. A mechanism for substitution reactions at a saturated carbon atom. *J. Am. Chem. Soc.* **1950**, *72*, 2438−2445.
(75) Fells, I.; Moelwyn-Hughes, E. A. The kinetics of the hydrolysis of the chlorinated methanes. *J. Chem. Soc.* **1959**, 398−409.
(76) Hine, J.; Ehrenson, S. J. The effect of structure on the relative stability of dihalomethylenes. *J. Am. Chem. Soc.* **1958**, *80*, 824−830.
(77) Valiev, M.; Garrett, B. C.; Tsai, M.-K.; Kowalski, K.; Kathmann, S. M.; Schenter, G. K.; Dupuis, M. Hybrid approach for free energy calculations with high-level methods: Application to the S_N2 reaction of $CHCl_3$ and OH^- in water. *J. Chem. Phys.* **2007**, *127*, 051102−1−4.
(78) Aelion, C. M.; Hohëner, P.; Hunkeler, D.; Aravena, R. *Environmental Isotopes in Biodegradation and Bioremediation*; CRC Press: Boca Raton, FL, 450 p, 2010.
(79) Skell, P. S.; Hauser, C. R. The mechanism of beta-elimination with alkyl halides. *J. Am. Chem. Soc.* **1945**, *67*, 1661−1661.
(80) Zwank, L.; Elsner, M.; Aeberhard, A.; Schwarzenbach, R. P. Carbon isotope fractionation in the reductive dehalogenation of carbon tetrachloride at iron (hydr)oxide and iron sulfide minerals. *Environ. Sci. Technol.* **2005**, *39*, 5634−5641.
(81) Bernstein, A.; Shouakar-Stash, O.; Ebert, K.; Laskov, C.; Hunkeler, D.; Jeannottat, S.; Sakaguchi-Sader, K.; Laaks, J.; Jochmann, M. A.; Cretnik, S.; Jager, J.; Haderlein, S. B.; Schmidt, T. C.; Aravena, R.; Elsner, M. Compound-specific chlorine isotope analysis: A comparison of gas chromatography/isotope ratio mass spectrometry and gas chromatography/quadrupole mass spectrometry methods in an interlaboratory study. *Anal. Chem.* **2011**, *83*, 7624−7634.
(82) Sutton, N. B.; Grotenhuis, J. T. C.; Langenhoff, A. A. M.; Rijnaarts, H. H. M. Efforts to improve coupled in situ chemical oxidation with bioremediation: a review of optimization strategies. *J. Soils Sediments* **2011**, *11*, 129−140.
(83) Weathers, L. J.; Parkin, G. F.; Alvarez, P. J. Utilization of cathodic hydrogen as electron donor for chloroform cometabolism by a mixed, methanogenic culture. *Environ. Sci. Technol.* **1997**, *31*, 880−885.
(84) Novak, P.; Daniels, L.; Parkin, G. Enhanced dechlorination of carbon tetrachloride and chloroform in the presence of elemental iron

DOI: 10.1021/acs.est.7b00679
Environ. Sci. Technol. XXXX, XXX, XXX−XXX

and *Methanosarcina barkeri, Methanosarcina thermophila,* or *Methanosaeta concillii*. *Environ. Sci. Technol.* **1998**, *32*, 1438−1443.
(85) Gregory, K. B.; Mason, M. G.; Picken, H. D.; Weathers, L. J.; Parkin, G. F. Bioaugmentation of Fe (0) for the remediation of chlorinated aliphatic hydrocarbons. *Environ. Eng. Sci.* **2000**, *17*, 169−181.
(86) Támara, M. L.; Butler, E. C. Effects of iron purity and groundwater characteristics on rates and products in the degradation of carbon tetrachloride by iron metal. *Environ. Sci. Technol.* **2004**, *38*, 1866−1876.
(87) Becker, J. G.; Freedman, D. L. Use of cyanocobalamin to enhance anaerobic biodegradation of chloroform. *Environ. Sci. Technol.* **1994**, *28*, 1942−1949.
(88) Guerrero-Barajas, C.; Field, J. A. Riboflavin- and cobalamin-mediated biodegradation of chloroform in a methanogenic consortium. *Biotechnol. Bioeng.* **2005**, *89*, 539−550.

DOI: 10.1021/acs.est.7b00679
Environ. Sci. Technol. XXXX, XXX, XXX−XXX

B. Supporting Information of Chapter 2

B.1. Experimental section

	qMs-1 Munich	qMs-1 Munich	qMs-2 Neuchâtel	qMs-2 Neuchâtel
	CCl_4	**$CHCl_3$**	**CCl_4**	**$CHCl_3$**
Instrument manufacturer	Agilent	Agilent	Agilent	Agilent
GC	7890A (Agilent)	7890A (Agilent)	7890A (Agilent)	7890A (Agilent)
qMs	5975C qMS (Agilent)	5975C qMS (Agilent)	5975C qMS (Agilent)	5975C qMS (Agilent)
m/z	119 & 117	83 & 85	119 & 117	83 & 85
	most abundant fragments from fragment group II	most abundant fragments from fragment group I	most abundant fragments from fragment group II	most abundant fragments from fragment group I
EI (eV)	70	70	70	70
Dwell time (msec)	70	70	50	50
Flow (mL min)	1.4	1.4	1.2	1.2
Split	1:10	1:10	1:20	1:20
Column	Vocol column (30 m x 0.25 mm ID × 0.25 µm, Supelco)	Vocol column (30 m x 0.25 mm ID × 0.25 µm, Supelco)	DB-5 column (30 m x 0.25 mm ID × 0.25 µm, Agilent)	DB-5 column (30 m x 0.25 mm ID × 0.25 µm, Agilent)
Temperature program	start at 60°C (2 min), 8°C/min to 165°C (0 min), temperature ramp of 25°C/min to 220°C (1 min)	start at 60°C (2 min), 8°C/min to 165°C (0 min), temperature ramp of 25°C/min to 220°C (1 min)	start at 70°C (2 min), 20°C/min to 230°C (0 min)	start at 70°C (2 min), 20°C/min to 230°C (0 min)
Injection temperature	250°C	250°C	250°C	250°C
Injection technique	automated HS	automated HS	automated HS	automated HS
Injection vial	10mL (9ml Headspace + 1mL liquid)	10mL (9ml Headspace + 1mL liquid)	20mL (5ml Headspace + 15mL liquid)	20mL (5ml Headspace + 15mL liquid)
Agitator temperature	40°C	40°C	60°C	60°C
Autosampler	CombiPal (CTC Analytics)	CombiPal (CTC Analytics)	CombiPal (CTC Analytics)	CombiPal (CTC Analytics)
Peak integration	ChemStation Integrator	ChemStation Integrator	ChemStation Integrator	ChemStation Integrator
Software	ChemStation E.02.02.1431	ChemStation E.02.02.1431	ChemStation E.02.01.1177	ChemStation E.02.01.1177
Two-point calibration curve slope	0.91 ±0.03	1.6 ± 0.2	1.06 ±0.02	1.8 ± 0.2
m= number of x-y pairs of calibration curve	30	30	25	52
Concentration range	60-2600 µg/L	60-2400 µg/L	5-200 ug/L	10-840 ug/L

Table B 1. Setup of GC-qMS-1 (Munich) and GC-qMS-2 (Neuchâtel)

	IRMS CCl_4	IRMS $CHCl_3$
Instrument manufacturer	Thermo Fisher Scientific	Thermo Fisher Scientific
GC	Thermo Trace GC	Thermo Trace GC
IRMS	MAT 253	MAT 253
m/z	49 & 47	49 & 47
Flow (mL min)	1.4	1.4
Split	1:10	1:10
Column	Vocol column (30 m ×0.25 mm ID × 0.25 µm, Supelco)	Vocol column (30 m × 0.25 mm ID × 0.25 µm, Supelco)
Temperature program	start at 60°C (2 min), 8°C/min to 165°C (0 min), of 25°C/min to 220°C (1 min)	start at 60°C (2 min), 8°C/min to 165°C (0 min), of 25°C/min to 220°C (1 min)
Injection temperature	230°C	230°C
Injection technique	automated HS	automated HS
Injection vial	10mL (9ml Headspace + 1mL liquid)	10mL (9ml Headspace + 1mL liquid)
Agitator temperature	40°C	40°C
Autosampler	PAS Technology	PAS Technology
Peak integration	ISODAT 3.0	ISODAT 3.0
Software	ISODAT 3.0	ISODAT 3.0
Two-point calibration curve slope	0.87 ±0.02	1.5 ± 0.2
m= number of x-y pairs of calibration curve	20	20
Concentration range	20-2600 µg/L	20-2400 µg/L

Table B 2. Setup of GC-IRMS (Munich)

C. Supporting Information of Chapter 3

C.1. Experimental section

C.1.1. Materials & Methods

C.1.1.1. Chemicals

Chemicals used were tetrachloroethene (99.9%, Fluka and PPG Industries); trichloroethene (99.5% ACS grade, Dow Chemical and Sigma Aldrich), cis-dichloroethene (Dow Chemical and Sigma Aldrich); trichloromethane (Fluka and Alpha Aesar); glyme anhydrous (Sigma Aldrich); naphthalene (99%, Sigma Aldrich); pyrene (99%, Sigma Aldrich); sodium (99.9%, Sigma Aldrich); sodium formate (99%, Sigma Aldrich); sodium persulfate (98% Sigma Aldrich); sodium sulfide (Sigma Aldrich); graphene oxide (2mg/mL Sigma Aldrich); Tris(hydroxymethyl)-aminomethan (Roth); iron (Nano powder, Sigma Aldrich); hydrogen peroxide (Merck).

C.1.1.2. Reactions in an Organic Solvent

Reactions with Radical Anions of Naphthalene and Pyrene

For PCE and TCE six different stock solutions were prepared by dissolving neat chlorinated ethene in glyme (40 mL) to give concentrations between 20 mM and 49 mM (PCE) and between 22 mM and 56 mM (TCE). Naphthalene radical anion solutions were prepared using naphthalene (0.33 g, 2.5 mmol) dissolved in anhydrous glyme (20 mL) and sodium metal (0.083 g, 3.6 mmol) that had been cleaned on all sides so that it was shiny. The mixture was stirred for 2 hours in a glovebox (M. Braun, nitrogen atmosphere, less than 0.1 ppm oxygen). The resultant solution was filtered through a glass fiber filter in the glovebox and brought to a final volume of 25 mL. The same procedure was used to prepare pyrene radical anion solutions from pyrene (0.73 g, 3.6 mmol,) dissolved in anhydrous glyme and sodium metal (0.070 g, 3.0 mmol). Since these reactions cannot be assumed to necessarily produce quantitative amounts of radical anions, the effective concentration of the radical

anions in solution was determined by test reactions, based on their reactivity with each of the chlorinated ethenes.

Dechlorination Reactions

Each reaction was performed in 10 mL reaction vials on a stir plate using 1 mL of a given chlorinated ethene stock solution. To start the reactions, the freshly prepared radical anion solutions were added at room temperature inside the glovebox with 1 mL glass syringes, using pre-calculated volumes according to the results of test reactions. The brightly colored radical anion solutions bleached immediately upon addition to the reaction vials, which were quickly capped with PTFE coated crimp-caps.

According to the six different concentrations of the PCE and TCE solutions, each ratio resulted in a different extent of chlorinated ethene conversion. Each reaction was performed in duplicate, giving a total of twelve reaction solutions. Control reactions were prepared with an identical procedure, but with the addition of anhydrous glyme instead of radical anions to the chlorinated ethylene solution. For later concentration analysis, they served as corresponding "zero-conversion" concentrations for the respective conversion points.

To enable headspace analysis of the chlorinated target compounds, aliquots of the completed reaction mixtures (0.5 mL) were added to deionized water (4.5 mL) so that compounds could partition from the aqueous phase into the headspace for headspace sampling. These solutions were distributed in portions of 1 mL into five headspace vials of 10 mL total volume for subsequent analysis, and closed securely with PTFE-coated crimp caps.

C.1.2. Analytical Methods

Concentration Measurements

Aqueous samples were analyzed on an Agilent 7890A GC coupled to an Agilent 5975C quadrupole mass selective detector (Santa Clara, CA) equipped with a 30 m Vocol (Supelco) column of 0.25 mm inner diameter, with a film thickness of 1.5 µm operated with a He carrier gas flow of 1.6 mL/min. Automated headspace injections of 1 mL from 10 mL headspace vials containing 1 mL aqueous sample were carried out using a CombiPal

Autosampler (CTC Analytics). The injector temperature was 250 °C and the temperature program of the GC started at 40 °C for 2 min, was ramped at 10 °C min^{-1} to 80°C for 2 minutes, then ramped again at 30 °C min^{-1} to 180°C and finally held at 180 °C for 1 min. Concentrations were calculated using a 10-point calibration curve.

Stable Carbon Isotope Analysis

Compound Specific Isotope Analysis (CSIA) for carbon was conducted by injection of headspace samples on a GC-IRMS system (Thermo Fisher Scientific, Waltham, Massachusetts, USA) consisting of a Trace GC with a PAL autosampler (CTC Analytics), coupled to a MAT 253 IRMS through a GC/C III combustion interface. The gas chromatograph was equipped with a 60 m DB624 column of 0.32 mm inner diameter (Agilent, Santa Clara, California). The GC program started at 70 °C (2 min), increasing at 30 °C/min to 120 °C (9 min), and increasing at 30 °C/min to 220 °C (0 min). Delta values relative to the Vienna Pee Dee Belemnite (VPDB) international standard were evaluated by the instrument software against calibrated monitoring gas. The instrument isotope values were in a first step derived by the instrument's software, where samples were evaluated relative to a monitoring gas in each run. External standards of PCE ($\delta^{13}C$ of -28.0‰ ± 0.2‰), TCE ($\delta^{13}C$ TCE -27.1‰ ± 0.2‰), *cis*-DCE ($\delta^{13}C$ of -24.9‰ ± 0.2‰) and $CHCl_3$ ($\delta^{13}C$ of -48.4‰ ± 0.2‰) that had previously been characterized by EA-IRMS were run along with the samples as quality control. The resultant overall analytical uncertainty 2σ of carbon isotope measurements was ±0.5‰. The progress of dechlorination reactions was followed by evaluating the peak areas with respect to the "time zero" samples, to give the fractional conversion of reaction mixtures.

Stable Chlorine Isotope Analysis

Chlorine isotope analysis was performed according to a method adapted from Shouakar-Stash et al. [18, 19]. The measurements were conducted on a GC-IRMS system (Thermo Scientific, Waltham, Massachusetts, USA) consisting of a Trace GC that was connected to a MAT 253 IRMS with dual inlet system via a heated transfer line. The gas chromatograph was equipped with a 30 m VOCOL column (Supelco, Bellefonte, Pennsylvania, USA) with 0.25 mm inner diameter, a film thickness of 1.5 µm and operated with a He carrier gas at 1.4

ml/min. The GC program for PCE started at 85 °C (8 min) and increased at 60 °C/min to 205 °C (1 min). The GC program for TCE, cis-DCE and CF started at 50 °C (7 min), increasing at 60 °C/min to 70 °C (2.70 min) and at 80 °C/min to 140 °C (0.10 min). Instrument isotope values for chlorine measurements by IRMS were in a first step derived by the instrument's software, where samples were evaluated relative to a monitoring gas in each run. External standards were measured every ten samples for calibration of $\delta^{37}Cl$ values according to Bernstein et al. [19]. The conversion to delta values relative to the international reference Standard Mean Ocean Chloride (SMOC) was performed by an external two-point calibration analyzing PCE, TCE, cis-DCE and $CHCl_3$ standards. To form the regression for the 2 point calibration, the measured standard isotope values were plotted against the real isotope values of the standards. Afterwards, the measured sample values and standard values are corrected with the intercept and the slope of the regression. PCE standards (PCE – EIL -1 (Dow Chemicals) and PCE – EIL-2 (PPG Industries)) were used with a chlorine isotope signature ($\delta^{37}Cl$) of +0.29‰ and -2.52‰ [36]; TCE standards (TCE – EIL -1 (Dow Chemicals) and TCE – EIL-2 (PPG Industries)) with a chlorine isotope signature ($\delta^{37}Cl$) of +3.05‰ and -2.7‰ [19]; cis-DCE (cis-DCE -1 (Sigma Aldrich) and cis-DCE-2 (Chemos)) with a signature ($\delta^{37}Cl$) of 0.07‰ and -1.52‰ (determined according to Holt et al.[24] in the stable isotope laboratory of the University of Waterloo) and $CHCl_3$ ($CHCl_3$ -1 (Fluka) and $CHCl_3$-2 (Alpha Aesar)) with a signature ($\delta^{37}Cl$) of -3.02‰ and -5.41‰. The analytical uncertainty 2σ of chlorine isotopic measurements was ±0.2‰.

C.2. Results and Discussion

Control of the OS-SET reaction (CO_2 radical anions) with PCE and sodium persulfate, but without sodium formate to exclude that isotope values were influenced by a parallel reaction of PCE with sodium persulfate

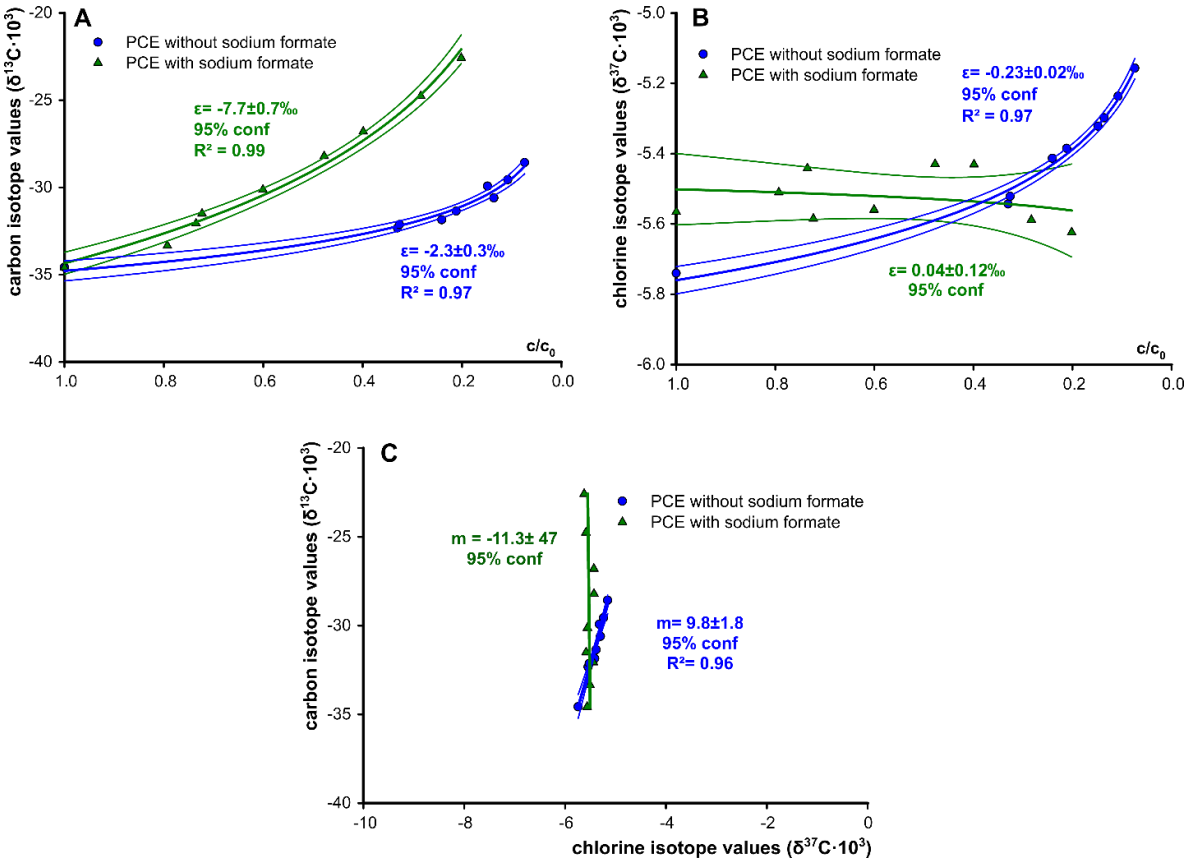

Figure C1 (A) enrichment factors of carbon for the control experiment of PCE reaction with and without sodium formate, were derived from the logarithmic fit of the change of 13 C isotope values and the concentration divided through the concentration at time point zero. (B) Enrichment factors of chlorine were generated on the same way (C) Dual element isotope plot of PCE reaction with and without sodium formate

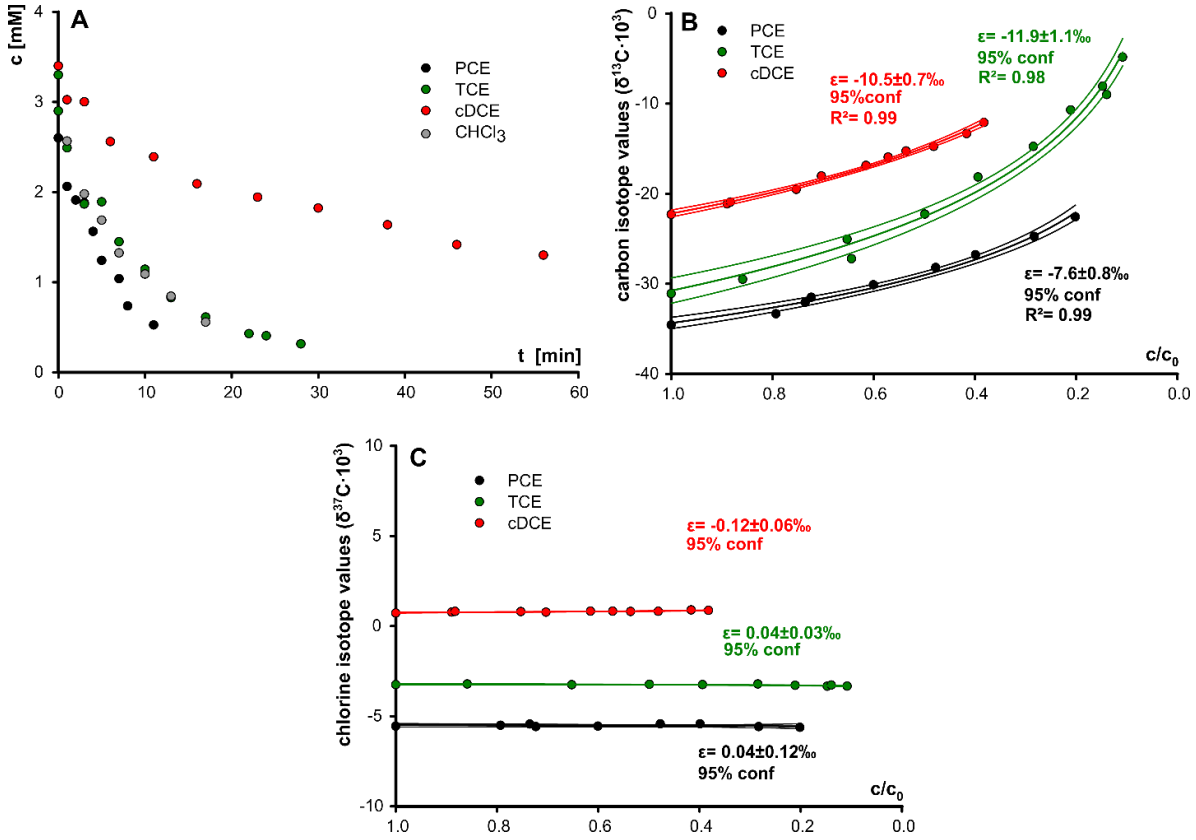

Figure C2 (A) Concentration vs time plot of the CO_2 radical anion experiments with PCE, TCE, cDCE and $CHCl_3$ (B) enrichment factors of carbon for the CO_2 radical anion experiments for PCE, TCE and cDCE were derived from the logarithmic fit of the change of 13 C isotope values and the concentration divided through the concentration at time point zero (C) Enrichment factors of chlorine were generated on the same way

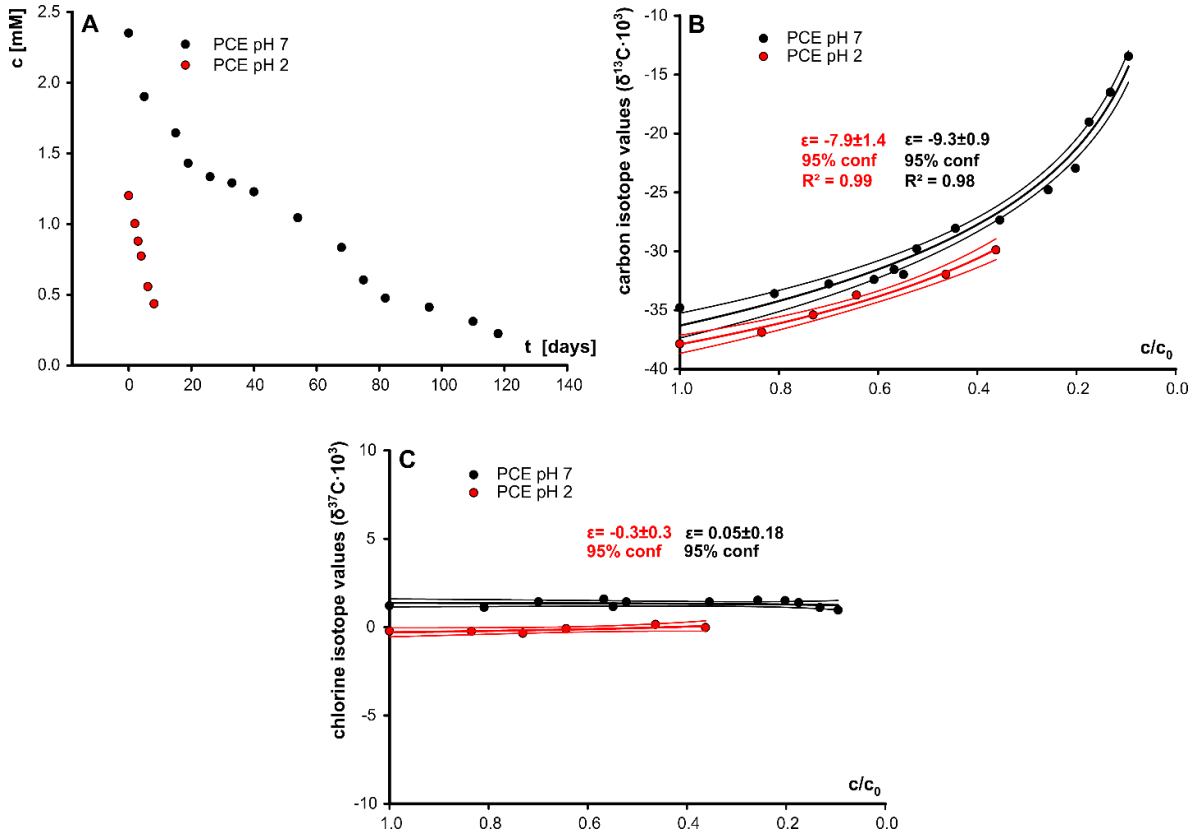

Figure C3 (A) Concentration vs time plot of the graphene oxide/sodium sulfide experiments with PCE at pH 2 and 7 (B) enrichment factor of carbon from the experiment with PCE at pH 7 and 2 (C) Enrichment factor of chlorine from the experiment with PCE at pH 7 and 2

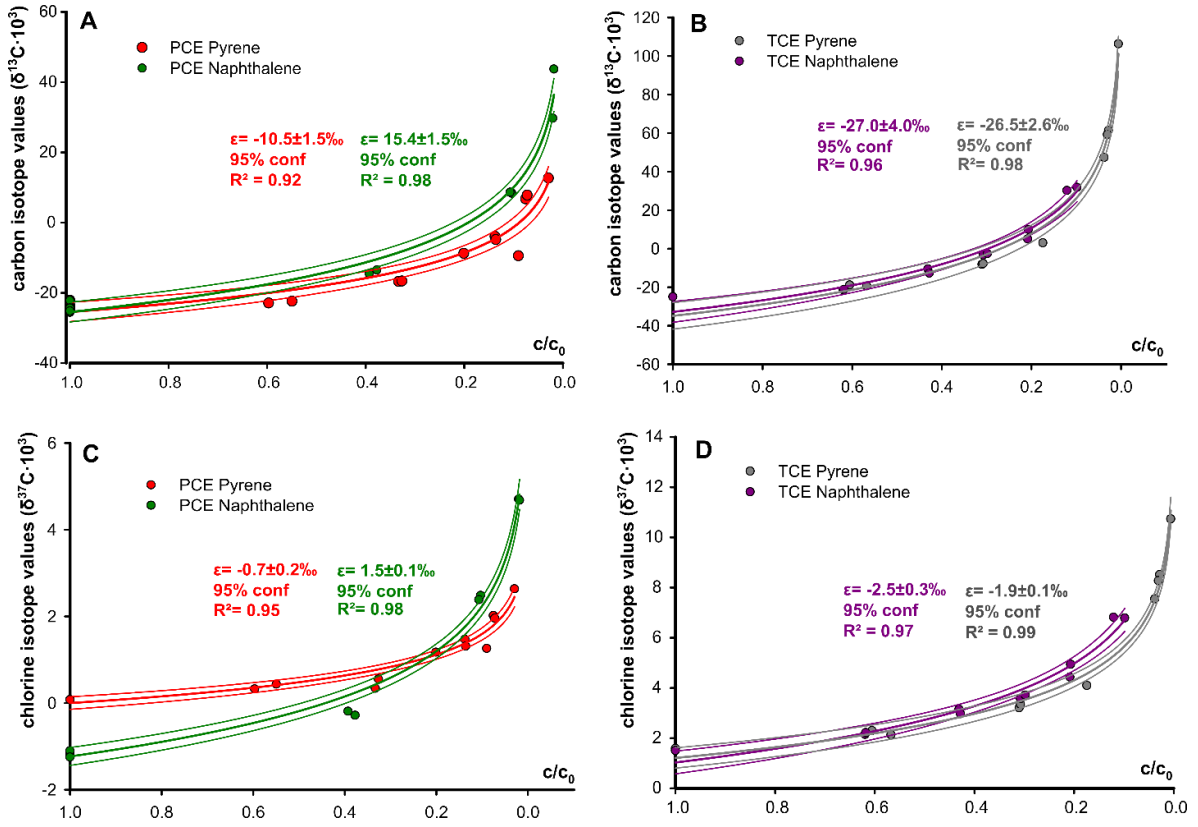

Figure C4 (A) Plot illustrates the enrichment factor of carbon for the experiment of PCE with pyrene- and naphthalene radical anions in organic solvent (B) Carbon enrichment factor of the TCE-pyrene and naphthalene radical anion experiment (C&D) Chlorine enrichment factors for the reaction of PCE (C) and TCE (D) with pyrene- and naphthalene radical anions

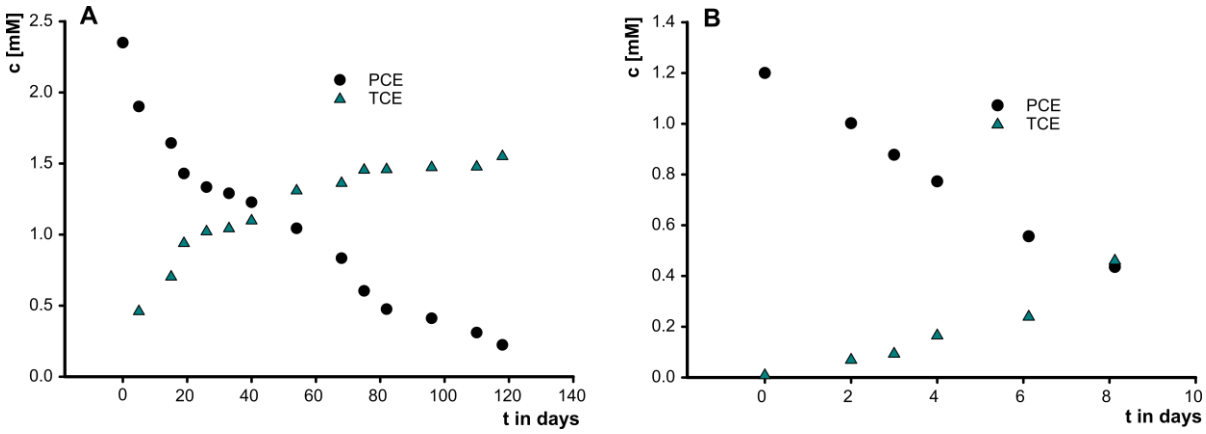

Figure C5 Concentration vs time plot of PCE degradation and TCE formation of the graphene oxide/sodium sulfide experiments at (A) pH 7 and (B) pH 2

D. Supporting Information of Chapter 4

D.1. Materials & Methods

D.1.1. Chemicals

Vitamin B_{12} (≥98%, Sigma Aldrich), tris(hydroxymethyl)-aminomethane, titanium(III)chloride ca. 15% (Merck), sodium citrate tribasic dihydrate (Sigma Aldrich), sodium carbonate (Sigma Aldrich), sodium hydroxide (Sigma Aldrich), hydrogen chloride 32wt. % (Sigma Aldrich), sodium phosphate dibasic (Sigma Aldrich), Disodium hydrogen phosphate dodecahydrate (Merck), deuterated water (Chemotrade), tetrachloroethene (99.9%, Fluka and PPG Industries); trichloroethene (99.5% ACS grade, Dow Chemical and Sigma Aldrich), cis-dichloroethene (Dow Chemical and Sigma Aldrich)

D.1.2. Kinetics, isotope effects and product formation in dehalogenation of chlorinated ethenes by Vitamin B_{12} at different pH.

The preparation of the Vitamin B_{12} degradation experiment was divided in three consecutive steps: *Preparation of buffered chlorinated ethene solutions* ***(solution 1)***. For the preparation of the stock solution 500 mL water and 27 mmol (54 mM) buffer was added to a beaker which was equipped with a stirrer. Depending on the desired pH value different buffers were used (TRIS buffer for pH 12-9; carbonate buffer for pH 8.5-6.5; phosphate buffer for pH 5.5-5.0). Subsequently, the pH value was adjusted to the chosen pH with appropriate amounts of 1 M HCl or 1 M NaOH. After the adjustment of the pH value, 495 mL of the solution were transferred to a 500 mL bottle which was also equipped with a stirrer and the solution was degassed with nitrogen. Subsequently, the degassed stock solution was transferred into an anoxic glovebox (MBRAUN; LABstar, Munich, Germany) with pure nitrogen atmosphere and the chosen chlorinated ethene was added.

<u>In the case of the PCE experiments</u> 76 µL (0.74 mmol; 1.5 mM)

For the TCE experiments 45 µL (0.5 mmol; 1.0 mM)

For the *cis*-DCE experiments 37 µL (0.49 mmol; 1.0 mM)

Preparation of Ti(III)citrate solutions ***(solution 2)***. In parallel, a titanium citrate solution was prepared by adding titanium(III)chloride (~15%; 15 mL; 18 mmol; 1.18 M) to a 100-mL two-headed flask equipped with a stirrer. The solution was diluted with 30 mL of water and degassed with nitrogen resulting in an eventual concentration of about 400 mM. During the preparation, the solution was kept the whole time under anoxic conditions. In the next step sodium citrate (9.8 g; 33.3 mmol; 740mM) was added to this solution together with 27 mmol (1.2 M) of the appropriate buffer. As mentioned above different buffers were used, depending on the desired pH value (TRIS buffer for pH 12-9; carbonate buffer for pH 8.5-6.5; phosphate buffer for pH 5.5-5.0). Consequently, the pH was adjusted.

Preparation of bottles containing Vitamin B_{12}.

After the preparation of the two solutions, Vitamin B_{12} was added to a 250-mL bottle, wrapped with aluminum foil and equipped with a stirrer and a mininert valve cap. Depending on the pH, different amounts of Vitamin B_{12} were added to the bottles to adjust the duration of the experiment:

In the case of PCE 20 mg (0.015 mmol in 245 mL; 61 μM) Vitamin B_{12} were added for each reaction, irrespective of pH.

In the case of TCE 15 mg (0.011 mmol in 135 mL; 81 μM) of Vitamin B_{12} were added for reactions at pH 12 and 11; 20 mg (0.015 mmol in 135 mL; 111 μM) Vitamin B_{12} for reactions at pH 9.5, 9.0 and 8.5; 40 mg (0.03 mmol in 135 mL; 222 μM) Vitamin B_{12} for reaction at pH 8.0, 7.5 and 7.0; 60 mg (0.044 mmol in 135 mL; 326 μM) Vitamin B_{12} for reactions at pH 6.5, 5.5 and 5.0.

For the radical trap experiments with TCE and d^7-isopropanol 30 mg (0.022 mmol in 135 mL; 163 μM) Vitamin B12 and d^7-isopropanol (1.5 mL; 20 mmol) were added.

In the case of *cis*-DCE 80 mg (0.059 mmol in 135 mL; 437 μM) were added for the reaction at pH 6.5,

Subsequently, aliquots of **solution 1** were added to the 250-mL bottle with Vitamin B_{12}:

In the case of PCE, 230 mL of the PCE buffer solution were used

In the case of TCE and *cis*-DCE 135 mL were used.

Each reaction was started by adding 15 mL of **solution 2**. Final concentrations in the reaction mixtures were:

In the case of the PCE experiments 1.4 mM (0.35 mmol)

For the TCE experiments 0.9 mM (0.14 mmol)

For the *cis*-DCE experiments 0.9 mM (0.13 mmol)

For PCE, samples of the reaction solution (0.5 mL) were removed at selected time points and injected into an 8 mL-vial containing a H_2O_2 solution (7 mL, 0.5 %) to stop the reaction. This protocol effectively quenched Ti(III) and destroyed the active form of Vitamin B_{12}, while leaving chlorinated products unaffected. Also, the absence of a deficit in the mass balance indicated that no bias from additional by-product formation was introduced (see Figure S7). For TCE and *cis*-DCE samples were taken from the headspace through the Mininert Caps of the bottles in regular intervals with a pressure lock syringe. For all samples concentration, carbon- and chlorine isotope measurements were conducted (see below).

D.1.3. Experiments to detect complex formation between Vitamin B12 and TCE by direct injection-mass spectrometry (DI-MS) and analysis of mass balance deficits

Mass spectrometric detection. (The whole procedure was performed in a glovebox (MBRAUN; LABstar, Munich, Germany) under anoxic conditions). To directly detect alkyl- and vinyl complexes by direct injection-mass spectrometry (DI-MS), two 5 mL aqueous solutions of TCE labeled with two ^{13}C atoms (2 µL; 0.011 mmol) were prepared at pH 11 and 3 (see above). To avoid decomposition of complexes by excess reduction agent, titanium citrate was avoided, and Vitamin B_{12} was instead pre-reduced using elemental Zn. To this end, the oxide layers of Zn shavings (1g; 15.3 mmol) were removed with HCl, the solution was neutralized with NaOH and the Zn shavings were washed with water. Afterwards, Vitamin B_{12} (30 mg; 0.022 mmol) was dissolved in 12 mL H_2O, the freshly cleaned Zn shavings were added and the solution was stirred for 12 hours to reduce cob(III)alamin to cob(I)alamin. For analysis by direct injection-mass spectrometry (DI-MS), six milliliter aliquots of this freshly prepared cob(I)alamin solution were added to each 12-mL vial, the vials were equipped with a stirrer, and the complex formation was started by adding 5 mL of the TCE solution to both vials. The samples for MS measurements were taken after 5 hours.

Mass balance deficits. For analysis of mass balance deficits, the cob(I)alamin solution was prepared as mentioned above, with the only exception that 104 mg (0.076 mmol) Vitamin B_{12} were dissolved in 20 mL water. Afterwards, aliquots of 10 mL cob(I)alamin solution were added to two 40-mL vials, wrapped with aluminum foil and equipped with a stirrer and a mininert valve cap. To start the reaction 10 mL of an oxygen-free TCE stock solution (3.8 mM; 17 µL in 50 mL) at pH 3 were added to the first 40-mL vial and 10 mL of an identical

stock solution at pH 11 were added to the second vial. In regular intervals two types of sample were removed at the same time: 0.1 mL headspace and 0.15 mL liquid samples. The headspace sample was analyzed by GC-MS immediately. The liquid sample was transferred into a 1 mL vial which already contained 0.8 mL oxygen free water to ensure anoxic conditions. Afterwards, the combined liquid sample was transferred into the purge and trap unit of the same GC-MS, purged for fifteen minutes and analyzed immediately after the headspace sample. Concentrations were calculated by preparing a 10-point calibration curve beforehand for each injection method (headspace and P&T, respectively).

D.1.4. Experiments in deuterated water

Reactions with deuterated water (99% purity) were conducted at pH 7.5 and 9. For the TCE stock solution (500mL; TCE: 40 µL; 0.44 mmol) deuterated water and 27 mmol buffer was used (pH 9 TRIS buffer, pH 7.5 carbonate buffer). To prepare the titanium citrate solution, the non-deuterated water in the titanium chloride solution (~15%; 15 mL) was carefully removed by heating under a nitrogen stream and replaced with deuterated water (45 mL). Sodium citrate (9.8 g; 33.3 mmol; 740 mM) was added, the pH was adjusted with Na_2CO_3. Subsequently, the same procedure was followed as described above.

D.1.5. Analytical Methods

Concentration Measurements

Reactions in water were evaluated by GC/MS analysis with a manual injection of 0.1 mL head-space samples using a Pressure lock syringe. Samples were injected into an Agilent 7890A GC coupled to an Agilent 5975C quadrupole MS. The column was a 60 m Q-Plot (Agilent, Santa Clara, California) column of 0.32 mm inner diameter operated with a helium carrier gas flow of 1.6 mL/min. The injector temperature was 250 °C and the temperature program of the GC started at 40 °C for 9 min, was ramped at 15 °C min^{-1} to 53°C for 2.7 minutes, then ramped at 13°C min^{-1} to 134°C, ramped again at 20°C to 200°C and finally held at 200 °C for 23 min. Concentrations were calculated using a 10-point calibration curve. For the Purge and Trap experiments the Agilent 7890A GC with 5975C quadrupole MS was

coupled to a purge and trap concentrator Tekmar Velocity XPTTM (Teledyne Tekmar, Mason (Ohio), USA) and the samples were purged for 15 minutes

Direct Aqueous Injection – High Resolution Mass Spectrometry Measurements

Samples for complex formation were transferred with a syringe pump by direct injection into an Orbitrap high resolution mass spectrometer (HRMS) detector equipped with electrospray ionization (ESI-HRMS, Thermo Exactive; Thermo Fisher Scientific, Waltham, Massachusetts, USA). Analyses of the reaction at low pH value were carried out in positive ionization mode and at high pH value in negative ionization mode.

Stable Carbon Isotope Analysis

For compound-specific isotope analysis (CSIA) of carbon, 0.1-1 mL headspace samples were manually injected through a Pressure lock syringe into a GC-IRMS system (Thermo Fisher Scientific, Waltham, Massachusetts, USA) consisting of a Trace GC coupled to a MAT 253 IRMS through a GC/C III combustion interface. The gas chromatograph was equipped with a 60 m Q-Plot column of 0.32 mm inner diameter (Agilent, Santa Clara, California). The GC program started at 40 °C for 9 min, was ramped at 15 °C min^{-1} to 53°C for 2.7 minutes, then ramped at 13°C min^{-1} to 134°C, ramped again at 20°C to 200°C and finally held at 200 °C for 23 min. Delta values relative to the Vienna Pee Dee Belemnite (VPDB) international standard were directly derived from the instrument software where calibrated monitoring gas was along with the samples. As quality control, external standards of PCE ($\delta^{13}C$ of -28.0 ±0.2‰), TCE ($\delta^{13}C$ TCE -27.1±0.2‰) and *cis*-DCE ($\delta^{13}C$ of -24.9±0.2‰) that had been characterized by EA-IRMS were run along with the samples. The overall analytical uncertainty 2σ of carbon isotope measurements was ±0.5‰.

Stable Chlorine Isotope Analysis

Chlorine isotope analysis was performed according to a method adapted from Shouakar-Stash et al. [18, 19]. For chlorine isotope measurements 0.1-1 mL of headspace sample were

manually injected into the GC-IRMS system (Thermo Scientific, Waltham, Massachusetts, USA), using a Pressure lock syringe. The GC-IRMS consisted of a Trace GC that was connected to a MAT 253 IRMS with dual inlet system via a heated transfer line. The GC was equipped with a 30 m VOCOL column (Supelco, Bellefonte, Pennsylvania, USA) with 0.25 mm inner diameter, a film thickness of 1.5 µm and operated with a He carrier gas flow of 1.4 ml/min. The GC program for PCE started at 85 °C (8 min) and increased at 60 °C/min to 205 °C (1 min). The GC program for TCE and *cis*-DCE started at 50 °C (7 min), increasing at 60 °C/min to 70 °C (2.70 min) and at 80 °C/min to 140 °C (0.10 min). In the first step instrument chlorine isotope values were derived through the instrument's software, where monitoring gas was measured against the samples in each run. Subsequently, these instrument isotope values $\delta^{37}Cl$ were subjected to an external two-point calibration relative to the international reference Standard Mean Ocean Chloride (SMOC) according to Bernstein et al.[19] by daily measurements of external standards of PCE, TCE and *cis*-DCE. The PCE standards had a chlorine isotope signature ($\delta^{37}Cl$) of +0.29‰ and -2.52‰; TCE standards a chlorine isotope signature ($\delta^{37}Cl$) of +3.05‰ and -2.7‰ and *cis*-DCE standards a signature ($\delta^{37}Cl$) of 0.07‰ and -1.52‰. The analytical uncertainty 2σ of chlorine isotopic measurements was ±0.2‰.

Stable Hydrogen Isotope Analysis

Compound-specific isotope analysis was performed according to a method adapted from Renpenning et al.[20]. For hydrogen isotope measurements 1 mL of headspace sample were manually injected into the GC-IRMS system (Thermo Scientific, Waltham, Massachusetts, USA), using a Pressure lock syringe. The GC-IRMS consisting of a Trace GC, coupled to a MAT 253 IRMS through a GC/C III combustion interface was operated with a pyrolysis module at 1400°C. A reactor filled with chromium was used in order to reduce the analyte to hydrogen gas without formation of HCl by-product [20]. The gas chromatograph was equipped with a 30 m Vocol column of 0.25 mm inner diameter and a film thickness of 1.5 µm (Supelco, Bellefonte, Pennsylvania, USA). The GC program started at 50 °C (6 min), increasing at 25 °C/min to 100 °C (4 min), and increasing at 30 °C/min to 140 °C (1 min). Analogous to chlorine isotope measurements, hydrogen isotope values were in a first step

derived by the instrument's software, where samples were evaluated relative to a monitoring gas in each run. Two external standards of TCE ($\delta^2H_{TCE\ 1}$ = 459‰ ± 5.0‰; $\delta^2H_{TCE\ 2}$ = -390‰ ± 5.0‰) were run along with the samples as quality control and for a two-point calibration. Standard isotope values had previously been characterized using a GC-IRMS and two organic reference materials[19, 20]. The resultant overall analytical uncertainty 2σ of hydrogen isotope measurements was ±5.0‰.

D.2. Results and Discussion

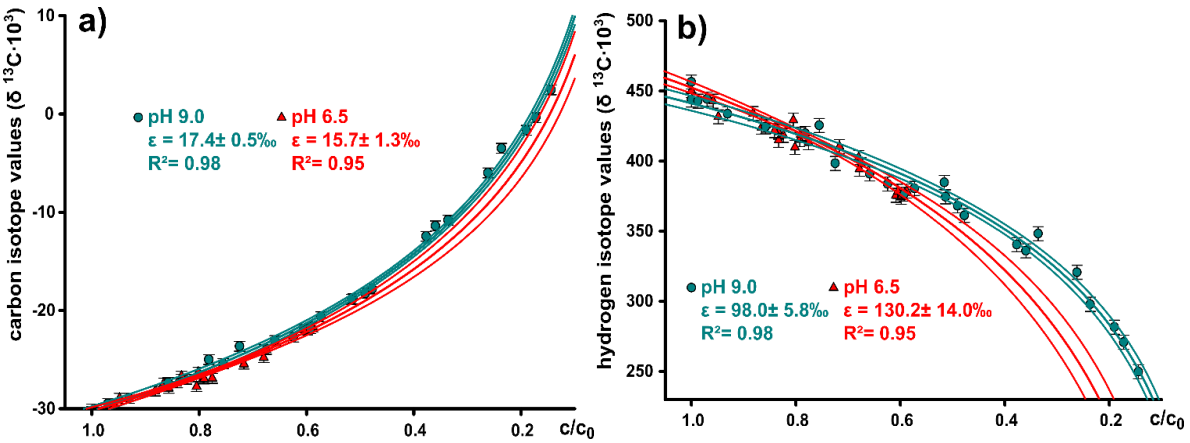

Figure D1. (a, b) enrichment factors of carbon and hydrogen for the for the reaction of TCE with Vitamin B12 at pH value 6.5 and 9 were derived from the logarithmic fit of the change of $^{13}C/\ ^{2}H$ isotope values and the concentration divided through the concentration at time point zero.

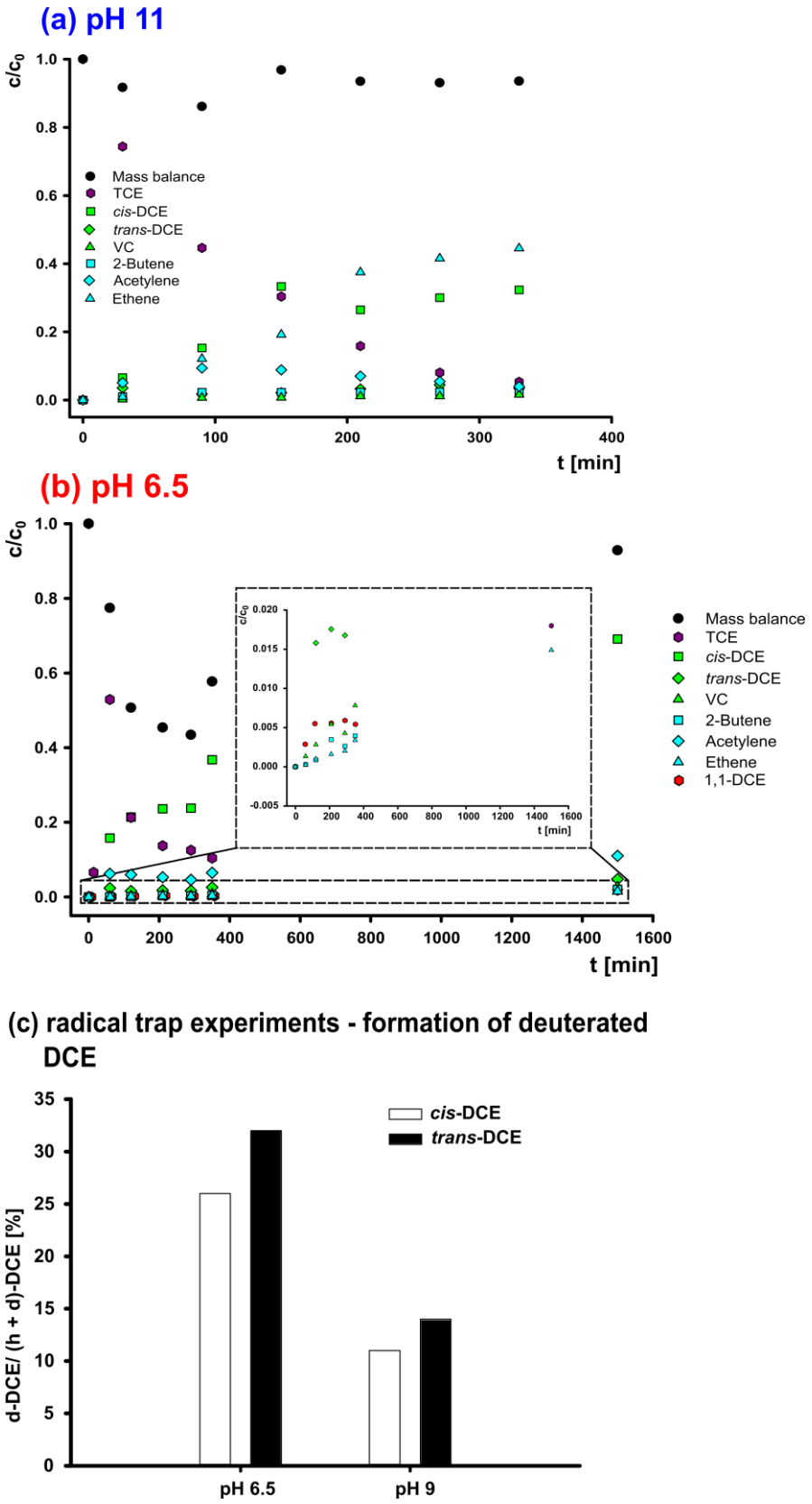

Figure D2. (a, b) Concentration-time plots of the reaction of TCE with Vitamin B12 at pH 11 and 6.5 (c) Incorporation of deuterium in radical trap experiments with d^7-isopropanol gives evidence of more dichlorovinyl radicals at steady state at pH 6.5 compared to pH 9.

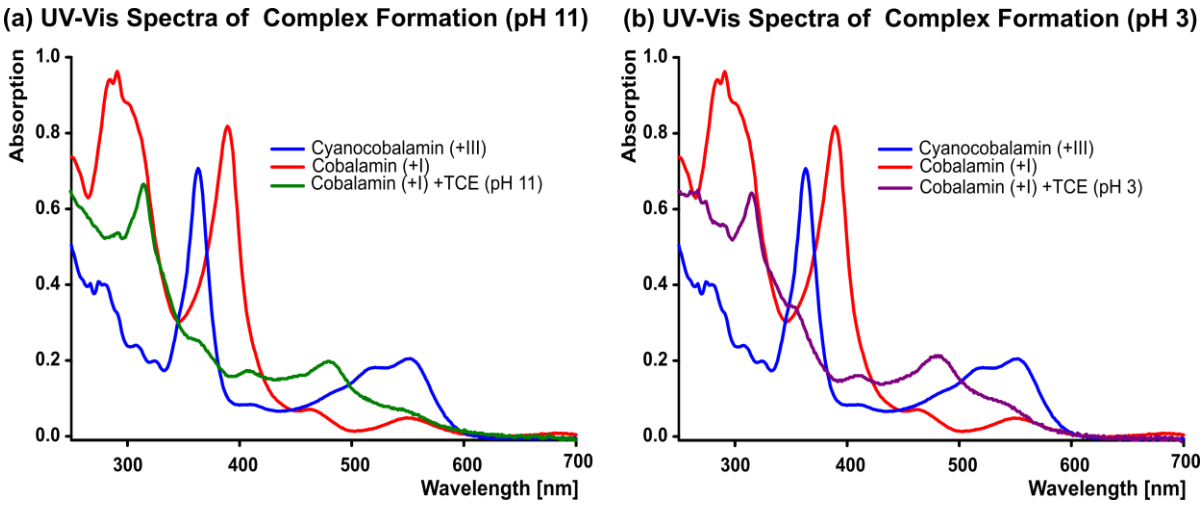

Figure D3. UV-Vis spectra of complex formation at pH value 3 and 11

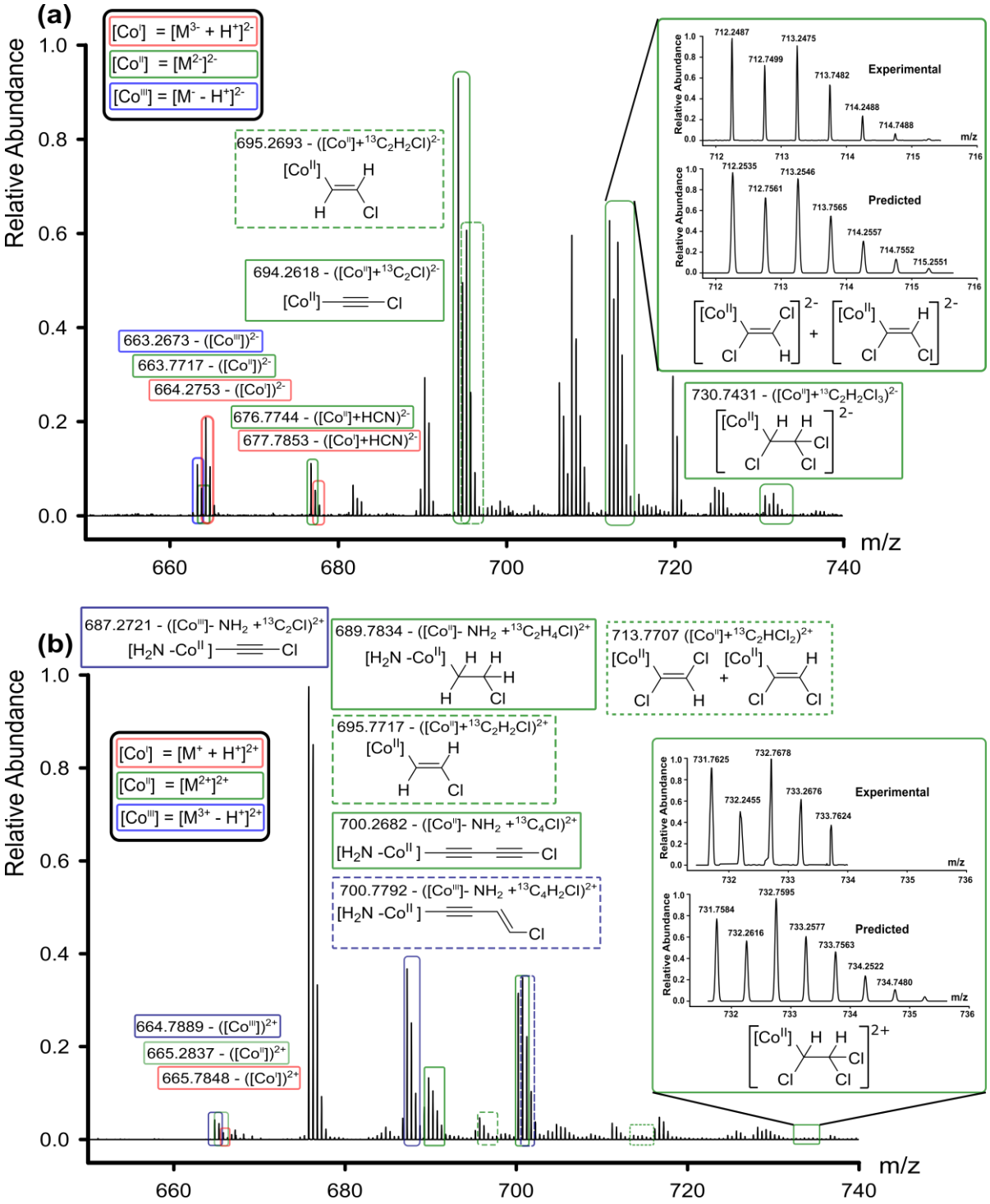

Figure D4. Mass spectra give evidence of cob(II)alamin vinyl- (5, 6) and alkyl-complexes (4) in stoichiometric reaction of TCE with pre-reduced Vitamin B_{12}. Mass spectra of the reaction of double ^{13}C-labeled TCE with Vitamin B_{12} at pH value 11 (panel a, measurement in double negative mode) and 2 (panel b, measurement in double positive mode). [Co^x] stands for cob(x)alamin, where x is the oxidation state. [Co^x]+$C_uH_vCl_w$ stands for alkyl-, vinyl- and acetylene complexes of Vitamin B_{12}, whereas [Co^x]-NH_2 represents cob(x)alamin from which a NH_2 group of the porphyrin ring was eliminated by fragmentation in the mass spectrometer. Blue boxes are drawn around Co(III) complexes, green boxes around Co(II) complexes and red boxes around Co(I) species (only Vitamin

B_{12}, no complexes). Dashed or solid boxes do not have a specific meaning, but are drawn to better distinguish peak multiplets of different structures. Note that the spectra are recorded in double positive or double negative mode so that a difference in m/z of 0.5 corresponds to a difference in one atomic mass unit.

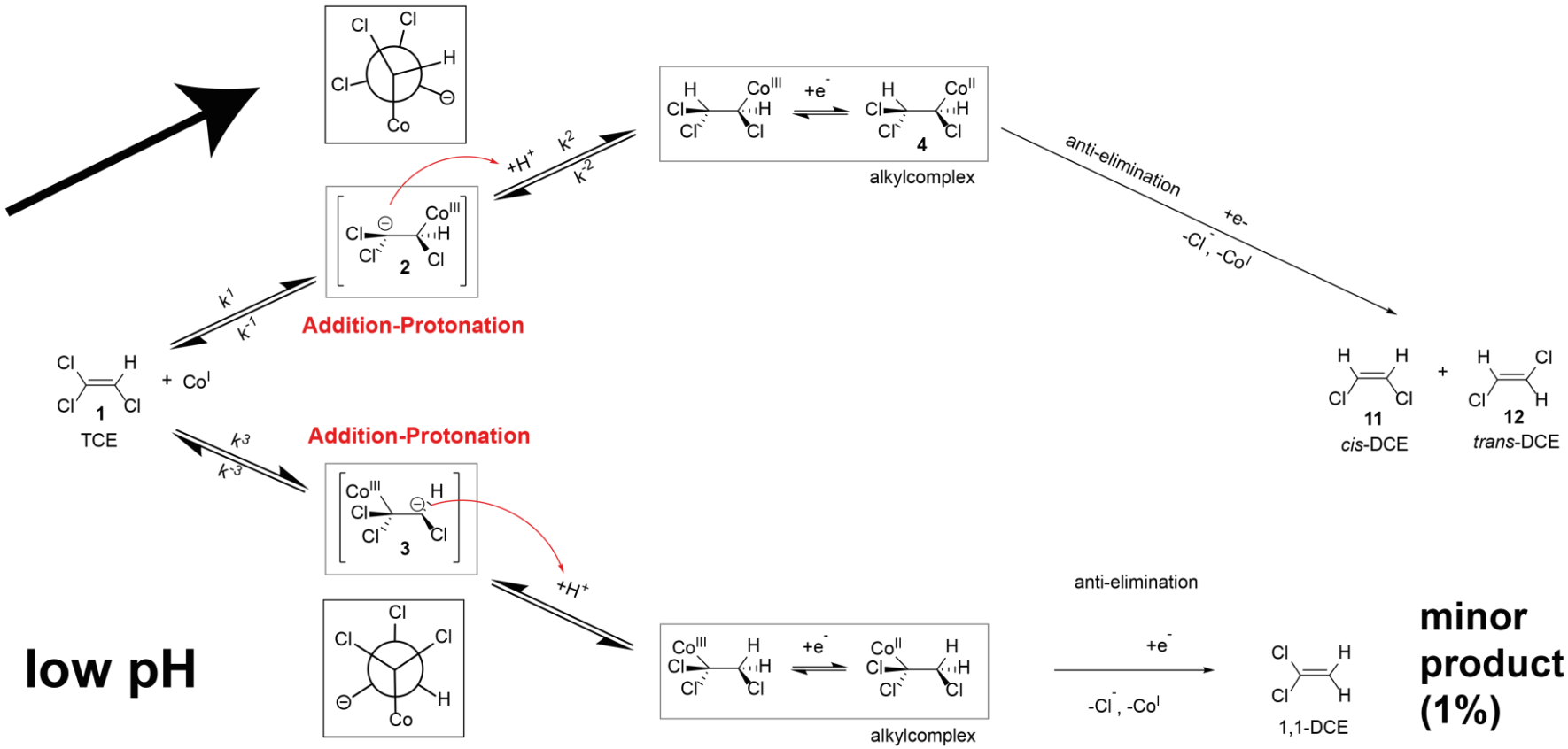

Scheme D1: The reaction scheme illustrates the attack of cob(I)alamin at the vicinal and geminal position with subsequent protonation for both pathways and possible product formation (endmember for low pH value)

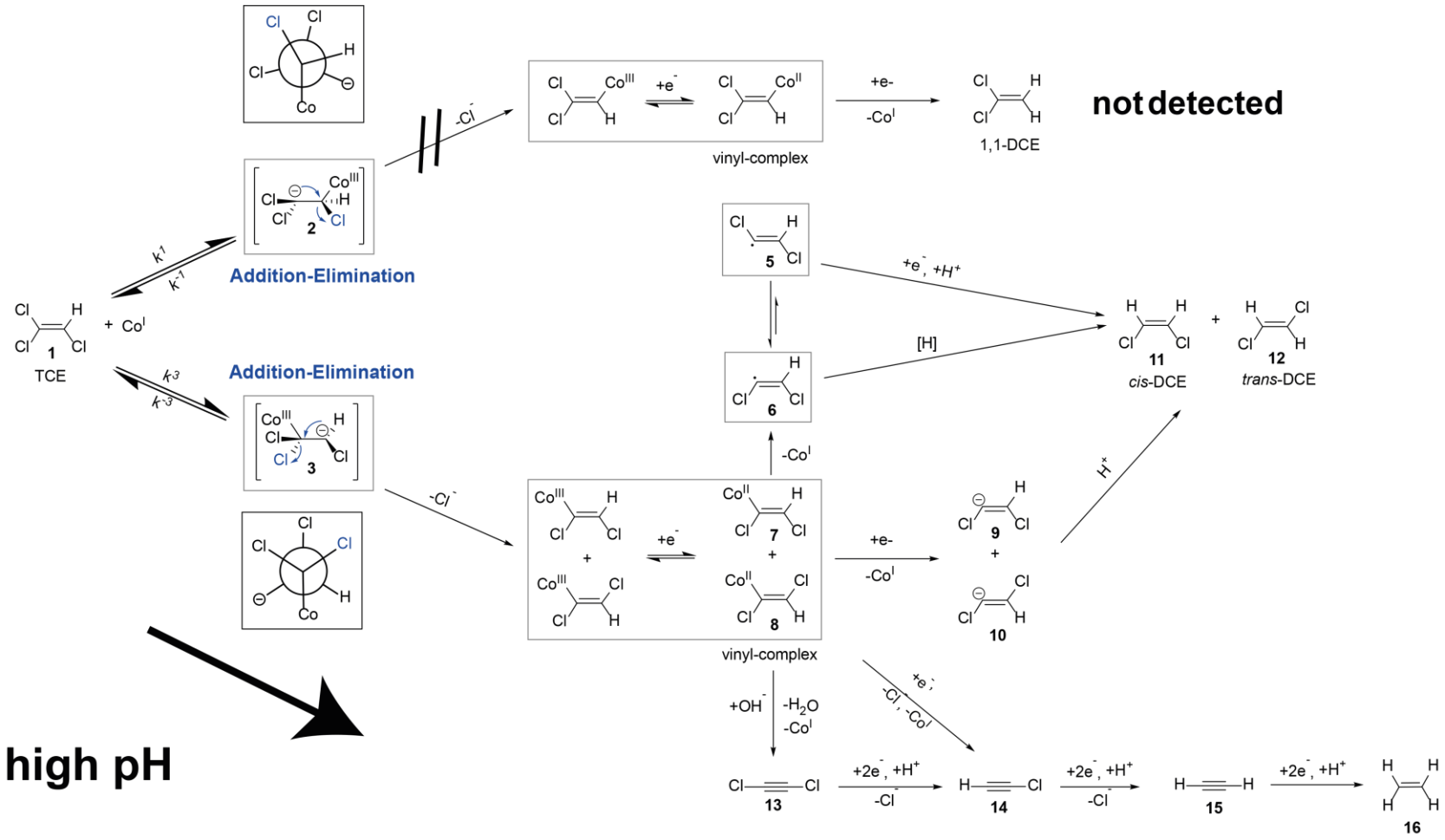

Scheme D2: The reaction scheme illustrates the attack of cob(I)alamin at the vicinal and geminal position with subsequent elimination of chloride for both pathways and possible product formation (endmember for high pH value)

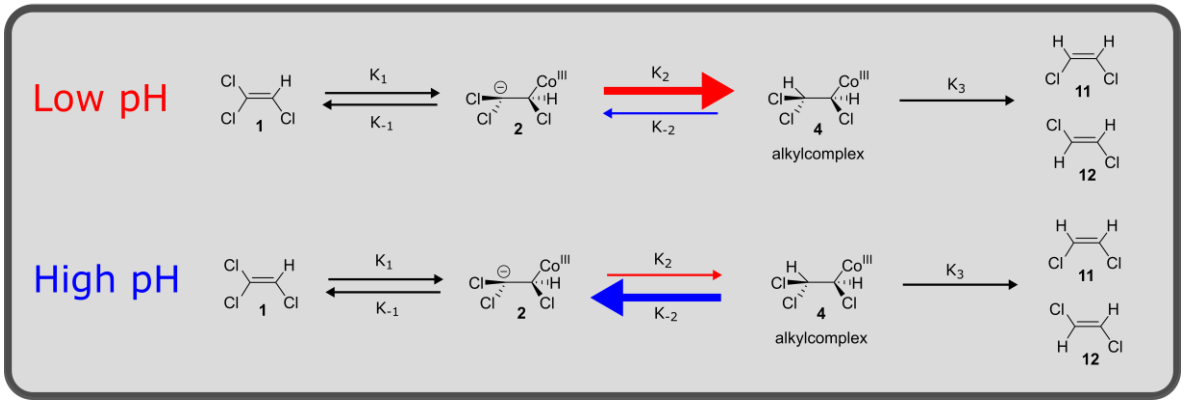

Figure D5. Rate determining step of the addition-protonation pathway changes with the pH value

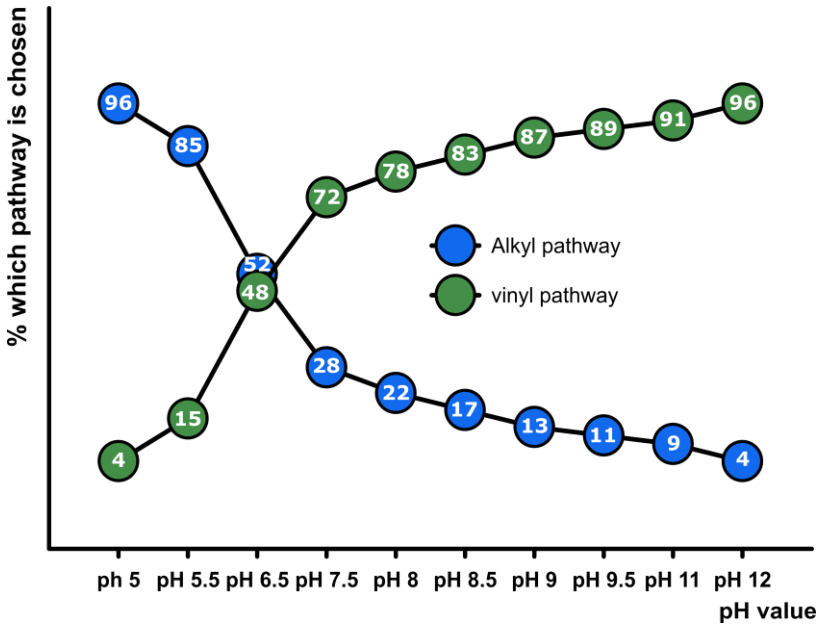

Figure D6. Proportional distribution which pathway is chosen is calculated using the chlorine enrichment of *cis*-DCE and the changes of chlorine isotope values for each reaction.

The calculation of the proportional distribution which pathway is chosen is based on the assumption that PCE is only degraded via addition-elimination and cis-DCE only via addition-protonation. Further, to achieve a comparison of chlorine isotope effects between PCE, TCE and *cis*-DCE on an equal basis, the PCE and *cis*-DCE isotope enrichment factors ($\varepsilon^{37}Cl$) were corrected for the effect of non-reacting positions and intramolecular competition[101] as follows. Since a primary position-specific chlorine isotope effect is "diluted" in the molecular average according to the number of Cl atoms (n = 4 in the case of

PCE (C_2Cl_4), n=3 in the case of TCE (C_2HCl_3) and n = 2 in the case of *cis*-DCE ($C_2H_2Cl_2$)[22], the chlorine isotope enrichment factor of the PCE reduction at pH 11 (ε^{37}Cl = -4.2 ‰) was multiplied by 4/3 (ε^{37}Cl (PCE adjusted) = -5.6 ‰) and for cis-DCE reduction at pH 6.5 (ε^{37}Cl = -1.5 ‰) by 2/3 (ε^{37}Cl (*cis*-DCE adjusted) = 1.0 ‰). The calculated enrichment factors would be observed when TCE is only degraded via the addition-elimination or addition-protonation pathway.

The proportional distribution is calculated by the following equations.

$$\varepsilon_{Cl}(addition-elimination) = \varepsilon_{Cl}(measured) - \varepsilon_{Cl}\ (cis-DCE\ adjusted) \quad (1)$$

$$\%(addition-elimination) = \frac{\varepsilon_{Cl}(addition-elimination)}{\varepsilon_{Cl}(PCE\ adjusted)-\varepsilon_{Cl}(cis-DCE\ adjusted)} \quad (2)$$

$$\%(addition-protonation) = 100\% - \%(addition-elimination) \quad (3)$$

Here ε^{37}Cl (measured) is the total chlorine enrichment factor, which is presented in Figure 2b (e.g. at pH 6.5: -3.2 ± 0.2) and ε^{37}Cl (addition-elimination) is the chlorine enrichment part of the addition-elimination pathway.

Strictly speaking, the proposed correction only works if an isotope effect occurs in only one of several molecular positions (for example, in the case of a primary isotope effects if secondary isotope effects at other positions are absent, or in the case of a secondary isotope effect if it occurs in only one position). Since this cannot necessarily be taken for granted – especially in the case of *cis*-DCE – the calculations proposed here must be considered as tentative approximation.

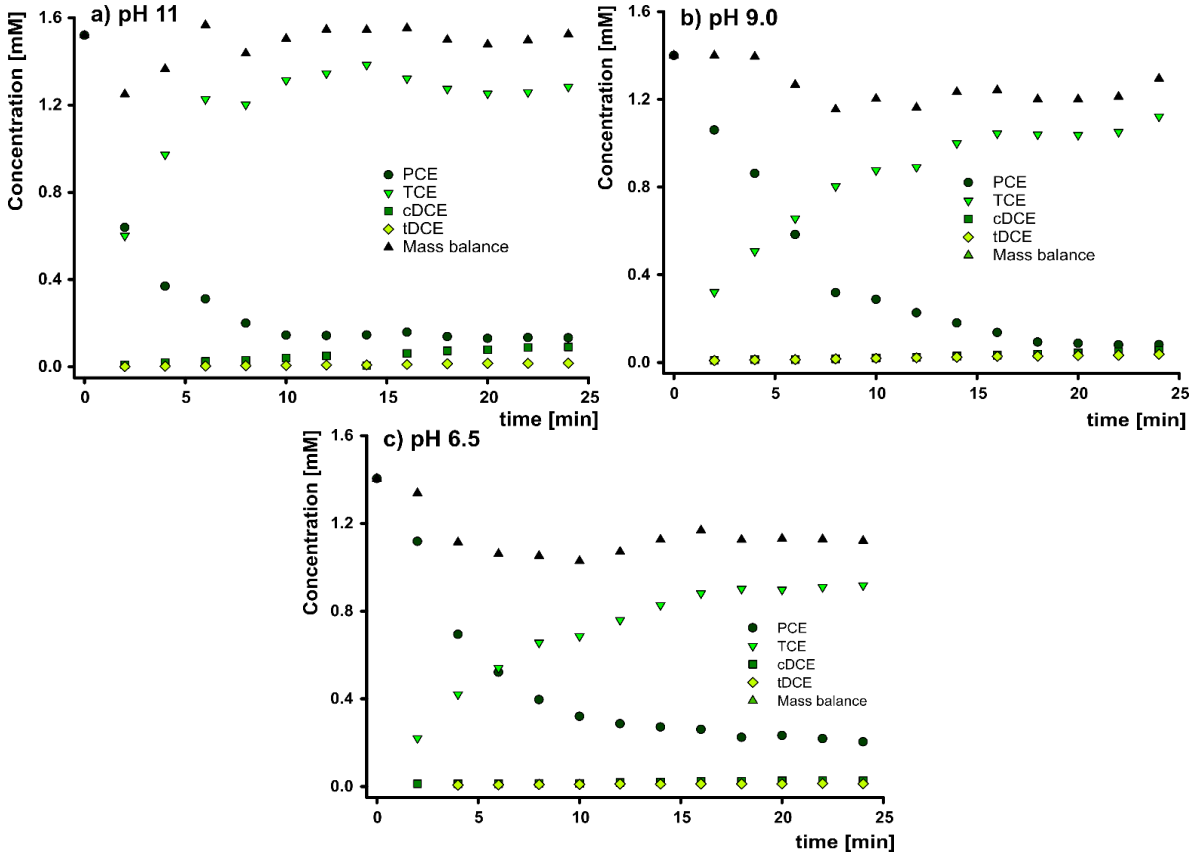

Figure D7. (a, b, c) Concentration-time plots of the reaction of PCE with Vitamin B12 at pH 11, 9 and 6.5

Abbreviations

% .... per centum (Latin) – percent; parts per hundred

‰ ..... pro mille (Latin) – per mil; parts per thousand

µg..... microgram; 1µg = $1 \cdot 10^{-6}$ g

µL ..... microliter; 1 µL = $1 \cdot 10^{-6}$ L

µmol..... micromole; 1 µmol = $1 \cdot 10^{-6}$ mol

AKIE..... Apparent Kinetic Isotope Effect

CAS ..... Chemical Abstracts Service

CCl_4 ..... tetrachloromethane

cDCE ..... *cis*-dichloroethene

CEs ..... Chlorinated Ethenes

CH_4 ..... methane

$CHCl_3$ ..... trichloromethane

CH_2Cl_2 ..... dichloromethane

CH_3Cl ..... chloromethane

cm ..... centimeter; $10 \cdot 10^{-2}$ m

CMs ..... Chlorinated methanes

CSIA ..... Compound-specific Stable Isotope Analysis

d ..... day

DFT..... density functional theory

DOI..... Digital Object Finder

Dr. rer. nat..... doctor rerum naturalium (Latin) – Doctor of Natural Science

Dr. .....Doktor (German) – Doctor, equivalent to PhD

e.g. .....exempli gratia (Latin) – for example

EA .....Elemantal Analysis

EIE.....equilibrium isotope effect

et al. .....et alii (Latin) – and others

FID .....Flame Ionization Detector

g.....gram; 1 g = $1 \cdot 10^{-3}$ kg

GC .....Gas Chromatography

GC-qMS .....Gas Chromatography – quadropol Mass Spectrometer

h.....hour; 1h = 60 min

HPLC .....High Performance Liquid Chromatography

IS-SET.....Inner-Sphere Single Electron Transfer

IRMS .....Isotope Ratio Mass Spectrometry

K.....Kelvin

kg.....kilogram

KIE .....kinetic isotope effect

L .....Liter

LC.....Liquid Chromatography

M .....molar; 1 mol·L^{-1}

mg.....milligram; 1 mg = $1 \cdot 10^{-6}$ kg

min .....minute; 1 min = 60 s

mL .....milliliter; 1 mL = $1 \cdot 10^{-3}$ L

mM .....millimolar; 1 mM = $1 \cdot 10^{-3}$ M

mmol .....millimol; 1 mmol = $1 \cdot 10^{-3}$ mol

mol ..... mole

MS ..... Mass Spectrometry

m/z ..... ratio of molecular (or atomic) mass to the charge number of the ion

NMR ..... Nuclear Magnetic Resonance Spectroscopy

OS-SET ..... Outer-Sphere Single Electron Transfer

P&T ..... Purge and Trap

PCE ..... tetrachloroethene

pH ..... potential Hydrogenii (Latin) – decimal logarithm of the reciprocal of the hydrogen activity in water

pK_a ..... logarithmic from of the acid dissociation constant K_a; $pK_a = -\log_{10} K_a$

ppm ..... parts per million; 1 ppm = $1 \cdot 10^{-6}$

ref ..... reference

rpm ..... rounds per minute

s ..... second

SIM ..... Selected Ion Mode

TCE ..... Trichloroethene

UV ..... ultraviolet

VC ..... vinyl chloride

vs ..... versus (Latin) – compared to; against

V-PDB ..... Vienna PeeDee Belemnite

V-SMOC ..... Vienna Standard Mean Ocean Water

ZPE ..... zero-point energy

ZVI.....zero valent iron

References

1. Oki, T.; Kanae, S., Global hydrological cycles and world water resources. *Science* **2006,** *313*, (5790), 1068-1072.
2. Fetzner, S., Bacterial dehalogenation. *Applied Microbiology and Biotechnology* **1998,** *50*, (6), 633-657.
3. Gossett, J. M., Fishing for microbes. *Science* **2002,** *298*, (5595), 974-975.
4. Moran, M. J.; Zogorski, J. S.; Squillace, P. J., Chlorinated Solvents in Groundwater of the United States. *Environ. Sci. Technol.* **2007,** *41*, (1), 74-81.
5. U.S. EPA *Assessment of the Potential Impacts of Hydraulic Fracturing for Oil and Gas on Drinking Water Resources*; Washington, DC,, 2015.
6. Henschler, D., Toxicity of Chlorinated Organic Compounds: Effects of the Introduction of Chlorine in Organic Molecules. *Angewandte Chemie International Edition in English* **1994,** *33*, (19), 1920-1935.
7. Holliger, C.; Wohlfarth, G.; Diekert, G., Reductive dechlorination in the energy metabolism of anaerobic bacteria. *FEMS Microbiology Reviews* **1998,** *22*, (5), 383-398.
8. Ellis, D. E.; Lutz, E. J.; Odom, J. M.; Buchanan, R. J.; Bartlett, C. L.; Lee, M. D.; Harkness, M. R.; DeWeerd, K. A., Bioaugmentation for Accelerated In Situ Anaerobic Bioremediation. *Environ. Sci. Technol.* **2000,** *34*, (11), 2254-2260.
9. Krone, U. E.; Laufer, K.; Thauer, R. K.; Hogenkamp, H. P. C., Coenzyme F430 as a possible catalyst for the reductive dehalogenation of chlorinated C1 hydrocarbons in methanogenic bacteria. *Biochemistry* **1989,** *28*, (26), 10061-10065.
10. Krone, U. E.; Thauer, R. K.; Hogenkamp, H. P. C., Reductive dehalogenation of chlorinated C1-hydrocarbons mediated by corrinoids. *Biochemistry* **1989,** *28*, (11), 4908-4914.
11. Egli, C.; Tschan, T.; Scholtz, R.; Cook, A. M.; Leisinger, T., Transformation of tetrachloromethane to dichloromethane and carbon dioxide by Acetobacterium woodii. *Applied and Environmental Microbiology* **1988,** *54*, (11), 2819-2824.
12. Morrill, P. L.; Lacrampe-Couloume, G.; Slater, G. F.; Sleep, B. E.; Edwards, E. A.; McMaster, M. L.; Major, D. W.; Lollar, B. S., Quantifying chlorinated ethene degradation during reductive dechlorination at Kelly AFB using stable carbon isotopes. *Journal of Contaminant Hydrology* **2005,** *76*, (3-4), 279-293.
13. Lojkasek-Lima, P.; Aravena, R.; Shouakar-Stash, O.; Frape, S. K.; Marchesi, M.; Fiorenza, S.; Vogan, J., Evaluating TCE Abiotic and Biotic Degradation Pathways in a Permeable Reactive Barrier Using Compound Specific Isotope Analysis. *Ground Water Monitoring and Remediation* **2012,** *32*, (4), 53-62.
14. Arnold, W. A.; Roberts, A. L., Pathways and kinetics of chlorinated ethylene and chlorinated acetylene reaction with Fe(O) particles. *Environ. Sci. Technol.* **2000,** *34*, (9), 1794-1805.
15. Elsner, M.; Chartrand, M.; VanStone, N.; Lacrampe Couloume, G.; Sherwood Lollar, B., Identifying Abiotic Chlorinated Ethene Degradation: Characteristic Isotope Patterns in Reaction Products with Nanoscale Zero-Valent Iron. *Environ. Sci. Technol.* **2008,** *42*, (16), 5963-5970.
16. Smidt, H.; de Vos, W. M., Anaerobic microbial dehalogenation. *Annual Review of Microbiology* **2004,** *58*, 43-73.

17. Meyer, A. H.; Penning, H.; Elsner, M., C and N isotope fractionation suggests similar mechanisms of microbial atrazine transformation despite involvement of different Enzymes (AtzA and TrzN). *Environ. Sci. Technol.* **2009,** *43*, (21), 8079-8085.
18. Shouakar-Stash, O.; Drimmie, R. J.; Zhang, M.; Frape, S. K., Compound-specific chlorine isotope ratios of TCE, PCE and DCE isomers by direct injection using CF-IRMS. *Appl. Geochem.* **2006,** *21*, (5), 766-781.
19. Bernstein, A.; Shouakar-Stash, O.; Ebert, K.; Laskov, C.; Hunkeler, D.; Jeannottat, S.; Sakaguchi-Söder, K.; Laaks, J.; Jochmann, M. A.; Cretnik, S.; Jager, J.; Haderlein, S. B.; Schmidt, T. C.; Aravena, R.; Elsner, M., Compound-Specific Chlorine Isotope Analysis: A Comparison of Gas Chromatography/Isotope Ratio Mass Spectrometry and Gas Chromatography/Quadrupole Mass Spectrometry Methods in an Interlaboratory Study. *Anal. Chem.* **2011,** *83*, (20), 7624-7634.
20. Renpenning, J.; Kümmel, S.; Hitzfeld, K. L.; Schimmelmann, A.; Gehre, M., Compound-Specific Hydrogen Isotope Analysis of Heteroatom-Bearing Compounds via Gas Chromatography–Chromium-Based High-Temperature Conversion (Cr/HTC)–Isotope Ratio Mass Spectrometry. *Anal. Chem.* **2015,** *87*, (18), 9443-9450.
21. Hoefs, J., *Stable Isotope Geochemistry*. Springer-Verlag: Berlin, 1997.
22. Elsner, M.; Zwank, L.; Hunkeler, D.; Schwarzenbach, R. P., A new concept linking observable stable isotope fractionation to transformation pathways of organic pollutants. *Environ. Sci. Technol.* **2005,** *39*, (18), 6896-6916.
23. Brand, W. A., High precision isotope ratio monitoring techniques in mass spectrometry. *Journal of Mass Spectrometry* **1996,** *31*, (3), 225-235.
24. Holt, B. D.; Sturchio, N. C.; Abrajano, T. A.; Heraty, L. J., Conversion of chlorinated volatile organic compounds to carbon dioxide and methyl chloride for isotopic analysis of carbon and chlorine. *Anal. Chem.* **1997,** *69*, (14), 2727-2733.
25. Shouakar-Stash, O.; Drimmie, R. J., Online methodology for determining compound-specific hydrogen stable isotope ratios of trichloroethene and 1,2-cis-dichloroethene by continuous-flow isotope ratio mass spectrometry. *Rapid Communications in Mass Spectrometry* **2013,** *27*, (12), 1335-1344.
26. Kuder, T.; Philp, P., Demonstration of Compound-Specific Isotope Analysis of Hydrogen Isotope Ratios in Chlorinated Ethenes. *Environ. Sci. Technol.* **2013,** *47*, (3), 1461-1467.
27. Wiedemeier, T. H.; Rifai, H. S.; Newell, C. J.; Wilson, J. T., *Natural attenuation of fuels and chlorinated solvents in the subsurface*. John Wiley & Sons: New York, N.Y., 1999.
28. Hunkeler, D.; Meckenstock, R. U.; Sherwood Lollar, B.; Schmidt, T.; Wilson, J.; Schmidt, T.; Wilson, J. *A Guide for Assessing Biodegradation and Source Identification of Organic Ground Water Contaminants using Compound Specific Isotope Analysis (CSIA)*; PA 600/R-08/148 | December 2008 | www.epa.gov/ada; US EPA: Oklahoma, USA, 2008.
29. Meckenstock, R. U.; Morasch, B.; Griebler, C.; Richnow, H. H., Stable isotope fractionation analysis as a tool to monitor biodegradation in contaminated acquifers. *J.Contam.Hydrol.* **2004,** *75*, (3-4), 215-255.
30. Blessing, M.; Schmidt, T. C.; Dinkel, R.; Haderlein, S. B., Delineation of Multiple Chlorinated Ethene Sources in an Industrialized Area: A Forensic Field Study Using Compound-Specific Isotope Analysis. *Environ. Sci. Technol.* **2009,** *43*, (8), 2701-2707.
31. Mancini, S. A.; Ulrich, A. E.; Lacrampe-Couloume, G.; Sleep, B.; Edwards, E. A.; Sherwood Lollar, B., Carbon and hydrogen isotopic fractionation during anaerobic biodegradation of benzene. *Applied and Environmental Microbiology* **2003,** *69*, (1), 191-198.

32. Kuder, T.; Wilson, J. T.; Kaiser, P.; Kolhatkar, R.; Philp, P.; Allen, J., Enrichment of stable carbon and hydrogen isotopes during anaerobic biodegradation of MTBE: microcosm and field evidence. *Environ. Sci. Technol.* **2005,** *39*, (1), 213-220.
33. Kuntze, K.; Kozell, A.; Richnow, H. H.; Halicz, L.; Nijenhuis, I.; Gelman, F., Dual Carbon–Bromine Stable Isotope Analysis Allows Distinguishing Transformation Pathways of Ethylene Dibromide. *Environ. Sci. Technol.* **2016,** *50*, (18), 9855-9863.
34. Penning, H.; Sorensen, S. R.; Meyer, A. H.; Aamand, J.; Elsner, M., C, N, and H Isotope Fractionation of the Herbicide Isoproturon Reflects Different Microbial Transformation Pathways. *Environ. Sci. Technol.* **2010,** *44*, (7), 2372-2378.
35. Cretnik, S.; Thoreson, K. A.; Bernstein, A.; Ebert, K.; Buchner, D.; Laskov, C.; Haderlein, S.; Shouakar-Stash, O.; Kliegman, S.; McNeill, K.; Elsner, M., Reductive Dechlorination of TCE by Chemical Model Systems in Comparison to Dehalogenating Bacteria: Insights from Dual Element Isotope Analysis (13C/12C, 37Cl/35Cl). *Environ. Sci. Technol.* **2013,** *47*, (13), 6855-6863.
36. Renpenning, J.; Keller, S.; Cretnik, S.; Shouakar-Stash, O.; Elsner, M.; Schubert, T.; Nijenhuis, I., Combined C and Cl Isotope Effects Indicate Differences between Corrinoids and Enzyme (Sulfurospirillum multivorans PceA) in Reductive Dehalogenation of Tetrachloroethene, But Not Trichloroethene. *Environ. Sci. Technol.* **2014,** *48*, (20), 11837–11845.
37. Palau, J.; Cretnik, S.; Shouakar-Stash, O.; Höche, M.; Elsner, M.; Hunkeler, D., C and Cl Isotope Fractionation of 1,2-Dichloroethane Displays Unique δ13C/δ37Cl Patterns for Pathway Identification and Reveals Surprising C–Cl Bond Involvement in Microbial Oxidation. *Environ. Sci. Technol.* **2014,** *48*, (16), 9430-9437.
38. Kuder, T.; van Breukelen, B. M.; Vanderford, M.; Philp, P., 3D-CSIA: Carbon, Chlorine, and Hydrogen Isotope Fractionation in Transformation of TCE to Ethene by a Dehalococcoides Culture. *Environ. Sci. Technol.* **2013,** *47*, (17), 9668-9677.
39. Wiegert, C.; Aeppli, C.; Knowles, T.; Holmstrand, H.; Evershed, R.; Pancost, R. D.; Macháčková, J.; Gustafsson, Ö., Dual Carbon-Chlorine Stable Isotope Investigation of Sources and Fate of Chlorinated Ethenes in Contaminated Groundwater. *Environ. Sci. Technol.* **2012,** *46*, (20), 10918-10925.
40. Hunkeler, D.; Abe, Y.; Broholm, M. M.; Jeannottat, S.; Westergaard, C.; Jacobsen, C. S.; Aravena, R.; Bjerg, P. L., Assessing chlorinated ethene degradation in a large scale contaminant plume by dual carbon-chlorine isotope analysis and quantitative PCR. *Journal of Contaminant Hydrology* **2011,** *119*, (1-4), 69-79.
41. Badin, A.; Broholm, M. M.; Jacobsen, C. S.; Palau, J.; Dennis, P.; Hunkeler, D., Identification of abiotic and biotic reductive dechlorination in a chlorinated ethene plume after thermal source remediation by means of isotopic and molecular biology tools. *Journal of Contaminant Hydrology* **2016,** *192*, 1-19.
42. Wiegert, C.; Mandalakis, M.; Knowles, T.; Polymenakou, P. N.; Aeppli, C.; Macháčková, J.; Holmstrand, H.; Evershed, R. P.; Pancost, R. D.; Gustafsson, Ö., Carbon and Chlorine Isotope Fractionation During Microbial Degradation of Tetra- and Trichloroethene. *Environ. Sci. Technol.* **2013,** *47*, (12), 6449-6456.
43. vanWarmerdam, E. M.; Frape, S. K.; Aravena, R.; Drimmie, R. J.; Flatt, H.; Cherry, J. A., Stable chlorine and carbon isotope measurements of selected chlorinated organic solvents. *Appl. Geochem.* **1995,** *10*, (5), 547-552.
44. Zwank, L.; Berg, M.; Elsner, M.; Schmidt, T. C.; Schwarzenbach, R. P.; Haderlein, S. B., New evaluation scheme for two-dimensional isotope analysis to decipher biodegradation processes: application to groundwater contamination by MTBE. *Environ. Sci. Technol.* **2005,** *39*, (4), 1018-1029.

45. Shouakar-Stash, O.; Frape, S. K.; Drimmie, R. J., Stable hydrogen, carbon and chlorine isotope measurements of selected chlorinated organic solvents. *Journal of Contaminant Hydrology* **2003,** *60*, (3-4), 211-228.
46. Holt, B. D.; Heraty, L. J.; Sturchio, N. C., Extraction of chlorinated aliphatic hydrocarbons from groundwater at micromolar concentrations for isotopic analysis of chlorine. *Environmental Pollution* **2001,** *113*, (3), 263-269.
47. Numata, M.; Nakamura, N.; Koshikawa, H.; Terashima, Y., Chlorine isotope fractionation during reductive dechlorination of chlorinated ethenes by anaerobic bacteria. *Environ. Sci. Technol.* **2002,** *36*, (20), 4389-4394.
48. Van Acker, M.; Shahar, A.; Young, E. D.; Coleman, M. L., GC/multiple collector-ICPMS method for chlorine stable isotope analysis of chlorinated aliphatic hydrocarbons. *Anal. Chem.* **2006,** *78*, (13), 4663-4667.
49. Zakon, Y.; Halicz, L.; Gelman, F., Isotope Analysis of Sulfur, Bromine, and Chlorine in Individual Anionic Species by Ion Chromatography/Multicollector-ICPMS. *Anal. Chem.* **2014,** *86*, (13), 6495-6500.
50. Sakaguchi-Soder, K.; Jager, J.; Grund, H.; Matthaus, F.; Schuth, C., Monitoring and evaluation of dechlorination processes using compound-specific chlorine isotope analysis. *Rapid Communications in Mass Spectrometry* **2007,** *21*, (18), 3077-3084.
51. Aeppli, C.; Holmstrand, H.; Andersson, P.; Gustafsson, O., Direct compound-specific stable chlorine isotope analysis of organic compounds with quadrupole GC/MS using standard isotope bracketing. *Anal. Chem.* **2010,** *82*, (1), 420-426.
52. Jin, B.; Laskov, C.; Rolle, M.; Haderlein, S. B., Chlorine Isotope Analysis of Organic Contaminants Using GCâ€“qMS: Method Optimization and Comparison of Different Evaluation Schemes. *Environ. Sci. Technol.* **2011,** *45*, (12), 5279-5286.
53. Palau, J.; Shouakar-Stash, O.; Hunkeler, D., Carbon and Chlorine Isotope Analysis to Identify Abiotic Degradation Pathways of 1,1,1-Trichloroethane. *Environ. Sci. Technol.* **2014,** *48*, (24), 14400-14408.
54. Breider, F.; Hunkeler, D., Investigating Chloroperoxidase-Catalyzed Formation of Chloroform from Humic Substances Using Stable Chlorine Isotope Analysis. *Environ. Sci. Technol.* **2014,** *48*, (3), 1592-1600.
55. Hitzfeld, K. L.; Gehre, M.; Richnow, H.-H., A novel online approach to the determination of isotopic ratios for organically bound chlorine, bromine and sulphur. *Rapid Communications in Mass Spectrometry* **2011,** *25*, (20), 3114-3122.
56. Renpenning, J.; Hitzfeld, K. L.; Gilevska, T.; Nijenhuis, I.; Gehre, M.; Richnow, H. H., Development and Validation of an Universal Interface for Compound-Specific Stable Isotope Analysis of Chlorine (Cl-37/Cl-35) by GC-High-Temperature Conversion (HTC)-MS/IRMS. *Anal. Chem.* **2015,** *87*, (5), 2832-2839.
57. Schimmelmann, A.; Qi, H.; Coplen, T. B.; Brand, W. A.; Fong, J.; Meier-Augenstein, W.; Kemp, H. F.; Toman, B.; Ackermann, A.; Assonov, S.; Aerts-Bijma, A. T.; Brejcha, R.; Chikaraishi, Y.; Darwish, T.; Elsner, M.; Gehre, M.; Geilmann, H.; Gröning, M.; Hélie, J.-F.; Herrero-Martín, S.; Meijer, H. A. J.; Sauer, P. E.; Sessions, A. L.; Werner, R. A., Organic Reference Materials for Hydrogen, Carbon, and Nitrogen Stable Isotope-Ratio Measurements: Caffeines, n-Alkanes, Fatty Acid Methyl Esters, Glycines, l-Valines, Polyethylenes, and Oils. *Anal. Chem.* **2016,** *88*, (8), 4294-4302.
58. Slater, G.; Sherwood Lollar, B.; Allen King, R.; O'Hannesin, S. F., Isotopic fractionation during reductive dechlorination of trichloroethene by zero-valent iron: influence of surface treatment. *Chemosphere* **2002,** *49*, 587-596.

59. Elsner, M.; Couloume, G. L.; SherwoodLollar, B., Freezing To Preserve Groundwater Samples and Improve Headspace Quantification Limits of Water-Soluble Organic Contaminants for Carbon Isotope Analysis. *Anal. Chem.* **2006,** *78*, (21), 7528-7534.
60. Torrentó, C.; Audí-Miró, C.; Bordeleau, G.; Marchesi, M.; Rosell, M.; Otero, N.; Soler, A., The Use of Alkaline Hydrolysis As a Novel Strategy for Chloroform Remediation: The Feasibility of Using Construction Wastes and Evaluation of Carbon Isotopic Fractionation. *Environmental Science & Technology* **2014,** *48*, (3), 1869-1877.
61. Palau, J.; Soler, A.; Teixidor, P.; Aravena, R., Compound-specific carbon isotope analysis of volatile organic compounds in water using solid-phase microextraction. *Journal of Chromatography A* **2007,** *1163*, (1–2), 260-268.
62. Coplen, T. B.; Brand, W. A.; Gehre, M.; Groning, M.; Meijer, H. A. J.; Toman, B.; Verkouteren, R. M., New guidelines for delta C-13 measurements. *Anal. Chem.* **2006,** *78*, (7), 2439-2441.
63. Elsner, M.; Hunkeler, D., Evaluating Chlorine Isotope Effects from Isotope Ratios and Mass Spectra of Polychlorinated Molecules. *Anal. Chem.* **2008,** *80*, (12), 4731-4740.
64. Rayleigh, J. W. S., Theoretical Considerations respecting the Separation of Gases by Diffusion and Similar Processes. *Philosophical Magazine* **1896,** *42*, 493-498.
65. Bernstein, A.; Shouakar-Stash, O.; Ebert, K.; Laskov, C.; Hunkeler, D.; Jeannottat, S.; Sakaguchi-Soder, K.; Laaks, J.; Jochmann, M. A.; Cretnik, S.; Jager, J.; Haderlein, S. B.; Schmidt, T. C.; Aravena, R.; Elsner, M., Compound-Specific Chlorine Isotope Analysis: A Comparison of Gas Chromatography/Isotope Ratio Mass Spectrometry and Gas Chromatography/Quadrupole Mass Spectrometry Methods in an Interlaboratory Study. *Anal. Chem.* **2011,** *83*, (20), 7624-7634.
66. Hunkeler, D.; Elsner, M., Principles and Mechanisms of Isotope Fractionation. In *Environmental Isotopes in Biodegradation and Bioremediation*, Aelion, C. M.; Hohener, P.; Hunkeler, D.; Aravena, R., Eds. CRC Press: Boca Raton, London, New York, 2010.
67. Carter, J. M.; Lapham, W. W.; Zogorski, J. S., Occurrence of volatile organic compounds in aquifers of the United States. *Journal of the American Water Resources Association* **2008,** *44*, (2), 399-416.
68. Schwarzenbach, R. P.; Gschwend, P. M.; Imboden, D. M., *Environmental Organic Chemistry*. second edition ed.; John Wiley & Sons, Inc.: New Jersey, 2003; p 1313.
69. Löffler, F. E.; Edwards, E. A., Harnessing microbial activities for environmental cleanup. *Curr. Opin. Biotechnol.* **2006,** *17*, (3), 274-284.
70. Scherer, M. M.; Richter, S.; Valentine, R. L.; Alvarez, P. J. J., Chemistry and microbiology of permeable reactive barriers for in situ groundwater clean up. *Crit. Rev. Environ. Sci. Technol.* **2000,** *30*, (3), 363 - 411.
71. Tratnyek, P. G.; Scherer, M. M.; Johnson, T. L.; Matheson, L. J., Permeable Reactive Barriers of Iron and Other Zero-Valent Metals. In *Chemical Degradation Methods for Wastes and Pollutants*, Tarr, M. A., Ed. Marcel Dekker, Inc.: New York, Basel, 2003; pp 371-421.
72. Elsner, M.; Hofstetter Thomas, B., Current Perspectives on the Mechanisms of Chlorohydrocarbon Degradation in Subsurface Environments: Insight from Kinetics, Product Formation, Probe Molecules, and Isotope Fractionation. In *Aquatic Redox Chemistry*, American Chemical Society: 2011; Vol. 1071, pp 407-439.
73. Taube, H., Rates and Mechanisms of Substitution in Inorganic Complexes in Solution. *Chemical Reviews* **1952,** *50*, (1), 69-126.
74. Savéant, J.-M., Single Electron Transfer and Nucleophilic Substitution. In *Adv. Phys. Org. Chem.*, Bethell, D., Ed. Academic Press: 1990; Vol. Volume 26, pp 1-130.

75. Marcus, R. A., Electron Transfer Reactions in Chemistry: Theory and Experiment (Nobel Lecture). *Angewandte Chemie International Edition in English* **1993,** *32*, (8), 1111-1121.
76. Eberson, L., *Electron Transfer Reactions in Organic Chemistry*. Springer Verlag Berlin, 1987.
77. Rosokha, S. V.; Kochi, J. K., Fresh Look at Electron-Transfer Mechanisms via the Donor/Acceptor Bindings in the Critical Encounter Complex. *Acc. Chem. Res.* **2008,** *41*, (5), 641-653.
78. Kliegman, S.; McNeill, K., Dechlorination of chloroethylenes by cob(i)alamin and cobalamin model complexes. *Dalton Trans.* **2008,** *0*, (32), 4191-4201.
79. Glod, G.; Angst, W.; Holliger, C.; Schwarzenbach, R. P., Corrinoid-mediated reduction of tetrachloroethylene, trichloroethylene and trichlorofluoroethane in homogeneoues aqueous solution: reaction kinetics and reaction mechanisms. *Environ. Sci. Technol.* **1997,** *31*, (1), 253-260.
80. Kliegman, S.; McNeill, K., Reconciling Disparate Models of the Involvement of Vinyl Radicals in Cobalamin-Mediated Dechlorination Reactions. *Environ. Sci. Technol.* **2009,** *43*, (23), 8961-8967.
81. Shey, J.; van der Donk, W. A., Mechanistic studies on the vitamin B-12-catalyzed dechlorination of chlorinated alkenes. *J. Am. Chem. Soc.* **2000,** *122*, (49), 12403-12404.
82. Parthasarathy, A.; Stich, T. A.; Lohner, S. T.; Lesnefsky, A.; Britt, R. D.; Spormann, A. M., Biochemical and EPR-Spectroscopic Investigation into Heterologously Expressed Vinyl Chloride Reductive Dehalogenase (VcrA) from Dehalococcoides mccartyi Strain VS. *J. Am. Chem. Soc.* **2015,** *137*, (10), 3525-3532.
83. Payne, K. A. P.; Quezada, C. P.; Fisher, K.; Dunstan, M. S.; Collins, F. A.; Sjuts, H.; Levy, C.; Hay, S.; Rigby, S. E. J.; Leys, D., Reductive dehalogenase structure suggests a mechanism for B12-dependent dehalogenation. *Nature* **2015,** *517*, (7535), 513-516.
84. Bommer, M.; Kunze, C.; Fesseler, J.; Schubert, T.; Diekert, G.; Dobbek, H., Structural basis for organohalide respiration. *Science* **2014,** *346*, (6208), 455-458.
85. Matheson, L. J.; Tratnyek, P. G., Reductive Dehalogenation of Chlorinated Methanes by Iron Metal. *Environ. Sci. Technol.* **1994,** *28*, 2045-2053.
86. Chen, S. W.; Fan, D. M.; Tratnyek, P. G., Novel Contaminant Transformation Pathways by Abiotic Reductants. *Environmental Science & Technology Letters* **2014,** *1*, (10), 432-436.
87. Lim, D.-H.; Lastoskie, C. M.; Soon, A.; Becker, U., Density Functional Theory Studies of Chloroethene Adsorption on Zerovalent Iron. *Environ. Sci. Technol.* **2009,** *43*, (4), 1192-1198.
88. Lim, D.-H.; Lastoskie, C. M., Density Functional Theory Studies on the Relative Reactivity of Chloroethenes on Zerovalent Iron. *Environ. Sci. Technol.* **2009,** *43*, (14), 5443-5448.
89. Scherer, M. M.; Balko, B. A.; Tratnyek, P. G., The Role of Oxides in Reduction Reactions at the Metal-Water Interface. In *Mineral-Water Interfacial Reactions*, American Chemical Society: 1999; Vol. 715, pp 301-322.
90. Scherer, M. M.; Balko, B. A.; Gallagher, D. A.; Tratnyek, P. G., Correlation analysis of rate constants for dechlorination by zero-valent iron. *Environ. Sci. Technol.* **1998,** *32*, (19), 3026-3033.
91. Kohn, T.; Arnold, W. A.; Roberts, A. L., Reactivity of substituted benzotrichlorides toward granular iron, Cr(II), and an iron(II) porphyrin: A correlation analysis. *Environ. Sci. Technol.* **2006,** *40*, (13), 4253-4260.

92. Luo, J.; Hu, J.; Wei, X.; Fu, L.; Li, L., Dehalogenation of persistent halogenated organic compounds: A review of computational studies and quantitative structure–property relationships. *Chemosphere* **2015,** *131*, 17-33.
93. Abe, Y.; Aravena, R.; Zopfi, J.; Parker, B.; Hunkeler, D., Evaluating the fate of chlorinated ethenes in streambed sediments by combining stable isotope, geochemical and microbial methods. *Journal of Contaminant Hydrology* **2009,** *107*, (1-2), 10-21.
94. Audí-Miró, C.; Cretnik, S.; Otero, N.; Palau, J.; Shouakar-Stash, O.; Soler, A.; Elsner, M., Cl and C isotope analysis to assess the effectiveness of chlorinated ethene degradation by zero-valent iron: Evidence from dual element and product isotope values. *Appl. Geochem.* **2013,** *32*, (0), 175-183.
95. Melander, L.; Saunders, W. H., *Reaction rates of isotopic molecules*. John Wiley: New York, 1980; p 331.
96. Wolfsberg, M.; Van Hook, W. A.; Paneth, P., *Isotope Effects in the Chemical, Geological and Bio Sciences*. Springer: Dordrecht, Heidelberg, London, New York, 2010.
97. Kohen, A.; Limbach, H.-H., *Isotope Effects in Chemistry and Biology*. CRC Press / Taylor and Francis: Boca Raton, FL, 2006; p 1074.
98. Elsner, M., Stable isotope fractionation to investigate natural transformation mechanisms of organic contaminants: principles, prospects and limitations. *J. Environ. Monit.* **2010,** *12*, (11), 2005-2031.
99. Vogt, C.; Dorer, C.; Musat, F.; Richnow, H.-H., Multi-element isotope fractionation concepts to characterize the biodegradation of hydrocarbons — from enzymes to the environment. *Curr. Opin. Biotechnol.* **2016,** *41*, 90-98.
100. Abe, Y.; Aravena, R.; Zopfi, J.; Shouakar-Stash, O.; Cox, E.; Roberts, J. D.; Hunkeler, D., Carbon and Chlorine Isotope Fractionation during Aerobic Oxidation and Reductive Dechlorination of Vinyl Chloride and cis-1,2-Dichloroethene. *Environ. Sci. Technol.* **2009,** *43*, (1), 101-107.
101. Cretnik, S.; Bernstein, A.; Shouakar-Stash, O.; Löffler, F.; Elsner, M., Chlorine Isotope Effects from Isotope Ratio Mass Spectrometry Suggest Intramolecular C-Cl Bond Competition in Trichloroethene (TCE) Reductive Dehalogenation. *Molecules* **2014,** *19*, (5), 6450-6473.
102. Badin, A.; Buttet, G.; Maillard, J.; Holliger, C.; Hunkeler, D., Multiple Dual C–Cl Isotope Patterns Associated with Reductive Dechlorination of Tetrachloroethene. *Environ. Sci. Technol.* **2014,** *48*, (16), 9179-9186.
103. Buchner, D.; Behrens, S.; Laskov, C.; Haderlein, S. B., Resiliency of Stable Isotope Fractionation (δ13C and δ37Cl) of Trichloroethene to Bacterial Growth Physiology and Expression of Key Enzymes. *Environ. Sci. Technol.* **2015,** *49*, 13230−13237.
104. Rosso, J. A.; Bertolotti, S. G.; Braun, A. M.; Mártire, D. O.; Gonzalez, M. C., Reactions of carbon dioxide radical anion with substituted benzenes. *Journal of Physical Organic Chemistry* **2001,** *14*, (5), 300-309.
105. Fu, H.; Zhu, D., Graphene Oxide-Facilitated Reduction of Nitrobenzene in Sulfide-Containing Aqueous Solutions. *Environ. Sci. Technol.* **2013,** *47*, (9), 4204-4210.
106. Karim, M. R.; Hatakeyama, K.; Matsui, T.; Takehira, H.; Taniguchi, T.; Koinuma, M.; Matsumoto, Y.; Akutagawa, T.; Nakamura, T.; Noro, S.-i.; Yamada, T.; Kitagawa, H.; Hayami, S., Graphene Oxide Nanosheet with High Proton Conductivity. *J. Am. Chem. Soc.* **2013,** *135*, (22), 8097-8100.
107. Hatakeyama, K.; Tateishi, H.; Taniguchi, T.; Koinuma, M.; Kida, T.; Hayami, S.; Yokoi, H.; Matsumoto, Y., Tunable Graphene Oxide Proton/Electron Mixed Conductor that Functions at Room Temperature. *Chemistry of Materials* **2014,** *26*, (19), 5598-5604.

108. Hatakeyama, K.; Islam, M. S.; Michio, K.; Ogata, C.; Taniguchi, T.; Funatsu, A.; Kida, T.; Hayami, S.; Matsumoto, Y., Super proton/electron mixed conduction in graphene oxide hybrids by intercalating sulfate ions. *Journal of Materials Chemistry A* **2015,** *3*, (42), 20892-20895.
109. Follett, A. D.; McNeill, K., Reduction of Trichloroethylene by Outer-Sphere Electron-Transfer Agents. *J. Am. Chem. Soc.* **2005,** *127*, (3), 844-845.
110. Elsner, M.; Jochmann, M. A.; Hofstetter, T. B.; Hunkeler, D.; Bernstein, A.; Schmidt, T. C.; Schimmelmann, A., Current challenges in compound-specific stable isotope analysis of environmental organic contaminants. *Anal. Bioanal. Chem.* **2012,** *403*, (9), 2471-2491.
111. Koppenol, W. H.; Rush, J. D., Reduction potential of the carbon dioxide/carbon dioxide radical anion: a comparison with other C1 radicals. *The Journal of Physical Chemistry* **1987,** *91*, (16), 4429-4430.
112. Totten, L. A.; Roberts, A. L., Calculated One- and Two-Electron Reduction Potentials and Related Molecular Descriptors for Reduction of Alkyl and Vinyl Halides in Water. *Crit. Rev. Environ. Sci. Technol.* **2001,** *31*, (2), 175-221.
113. Eberson, L.; Shaik, S. S., Electron-transfer reactions of radical anions: do they follow outer- or inner-sphere mechanisms? *J. Am. Chem. Soc.* **1990,** *112*, (11), 4484-4489.
114. Hammond, G. S., A Correlation of Reaction Rates. *J. Am. Chem. Soc.* **1955,** *77*, (2), 334-338.
115. Northrop, D. B., Steady-State Analysis of Kinetic Isotope Effects in Enzymatic Reactions. *Biochem.* **1975,** *14*, (12), 2644-2651.
116. Hayes, J. M., Fractionation of carbon and hydrogen isotopes in biosynthetic processes. *Rev. Mineral. Geochem.* **2001,** *43*, 225-277.
117. Pause, L.; Robert, M.; Saveant, J. M., Reductive cleavage of carbon tetrachloride in a polar solvent. An example of a dissociative electron transfer with significant attractive interaction between the caged product fragments. *J. Am. Chem. Soc.* **2000,** *122*, (40), 9829-9835.
118. Costentin, C.; Robert, M.; Saveant, J. M., Successive removal of chloride ions from organic polychloride pollutants. Mechanisms of reductive electrochemical elimination in aliphatic gem-polychlorides, alpha,beta-polychloroalkenes, and alpha,beta-polychloroalkanes in mildly protic medium. *J. Am. Chem. Soc.* **2003,** *125*, (35), 10729-10739.
119. Costentin, C.; Robert, M.; Saveant, J. M., Fragmentation of aryl halide pi anion radicals. Bending of the cleaving bond and activation vs driving force relationships. *J. Am. Chem. Soc.* **2004,** *126*, (49), 16051-16057.
120. Costentin, C.; Robert, M.; Saveant, J.-M., Does Catalysis of Reductive Dechlorination of Tetra- and Trichloroethylenes by Vitamin B12 and Corrinoid-Based Dehalogenases Follow an Electron Transfer Mechanism? *J. Am. Chem. Soc.* **2005,** *127*, (35), 12154-12155.
121. Costentin, C.; Robert, M.; Savéant, J.-M., Does Catalysis of Reductive Dechlorination of Tetra- and Trichloroethylenes by Vitamin B12 and Corrinoid-Based Dehalogenases Follow an Electron Transfer Mechanism? *J. Am. Chem. Soc.* **2005,** *127*, (35), 12154-12155.
122. Bylaska, E. J.; Dupuis, M.; Tratnyek, P. G., One-Electron-Transfer Reactions of Polychlorinated Ethylenes: Concerted and Stepwise Cleavages. *The Journal of Physical Chemistry A* **2008,** *112*, (16), 3712-3721.
123. Carter, J. M.; Lapham, W. W.; Zogorski, J. S., Occurrence of Volatile Organic Compounds in Aquifers of the United States1. *J. Am. Water Resour. Assoc.* **2008,** *44*, (2), 399-416.

124. Fincker, M.; Spormann, A. M., Biochemistry of Catabolic Reductive Dehalogenation. *Annual Review of Biochemistry* **2017,** *86*, (1), 357-386.
125. Yan, J.; Simsir, B.; Farmer, A. T.; Bi, M.; Yang, Y.; Campagna, S. R.; Loffler, F. E., The corrinoid cofactor of reductive dehalogenases affects dechlorination rates and extents in organohalide-respiring Dehalococcoides mccartyi. *ISME J.* **2016,** *10*, 1092-1101.
126. Kunze, C.; Bommer, M.; Hagen, W. R.; Uksa, M.; Dobbek, H.; Schubert, T.; Diekert, G., Cobamide-mediated enzymatic reductive dehalogenation via long-range electron transfer. *Nat. Commun.* **2017,** *8*, 15858.
127. McCauley, K. M.; Wilson, S. R.; van der Donk, W. A., Synthesis and characterization of chlorinated alkenylcobaloximes to probe the mechanism of vitamin B-12-catalyzed dechlorination of priority pollutants. *Inorg. Chem.* **2002,** *41*, (2), 393-404.
128. Fritsch, J. M.; Retka, N. D.; McNeill, K., Synthesis, Structure, and Unusual Reactivity of b-Halovinyl Cobalt Porphyrin Complexes. *Inorg. Chem.* **2006,** *45*, (5), 2288-2295.
129. Rich, A. E.; DeGreeff, A. D.; McNeill, K., Synthesis of (chlorovinyl)cobaloxime complexes, model complexes of proposed intermediates in the B12-catalyzed dehalogenation of chlorinated ethylenes. *Chem. Commun.* **2002,** *0*, (3), 234-235.
130. Jones, P. G.; Yang, L.; Steinborn, D., (cis-1,2-Dichlorovinyl)bis(dimethylglyoximato-N,N')(pyridine-N)cobalt(III) Chloroform Solvate, [Co(dmgH)2(py)(CCl=CHCl)].CHCl3. *Acta Crystallogr., Sect. C: Cryst. Struct. Commun.* **1996,** *52*, (10), 2399-2402.
131. McCauley, K. M.; Pratt, D. A.; Wilson, S. R.; Shey, J.; Burkey, T. J.; Van Der Donk, W. A., Properties and reactivity of chlorovinylcobalamin and vinylcobalamin and their implications for vitamin B12-catalyzed reductive dechlorination of chlorinated alkenes. *J. Am. Chem. Soc.* **2005,** *127*, (4), 1126-1136.
132. McCauley, K. M.; Wilson, S. R.; van der Donk, W. A., Characterization of Chlorovinylcobalamin, A Putative Intermediate in Reductive Degradation of Chlorinated Ethylenes. *J. Am. Chem. Soc.* **2003,** *125*, (15), 4410-4411.
133. Fritsch, J. M.; McNeill, K., Aqueous Reductive Dechlorination of Chlorinated Ethylenes with Tetrakis(4-carboxyphenyl)porphyrin Cobalt. *Inorg. Chem.* **2005,** *44*, (13), 4852-4861.
134. Glod, G.; Brodmann, U.; Werner, A.; Holliger, C.; Schwarzenbach, R. P., Cobalamin-mediated reduction of *cis*- and *trans*-dichloroethene, and vinylchloride in homogeneous aqueous solution: reaction kinetics and mechanistic considerations. *Environ. Sci. Technol.* **1997,** *31*, (11), 3154-3160.
135. Cooper, M.; Wagner, A.; Wondrousch, D.; Sonntag, F.; Sonnabend, A.; Brehm, M.; Schüürmann, G.; Adrian, L., Anaerobic Microbial Transformation of Halogenated Aromatics and Fate Prediction Using Electron Density Modeling. *Environ. Sci. Technol.* **2015,** *49*, (10), 6018-6028.
136. Liao, R.-Z.; Chen, S.-L.; Siegbahn, P. E. M., Unraveling the Mechanism and Regioselectivity of the B12-Dependent Reductive Dehalogenase PceA. *Chem. - Eur. J.* **2016,** *22*, (35), 12391-12399.
137. Johannissen, L. O.; Leys, D.; Hay, S., A common mechanism for coenzyme cobalamin-dependent reductive dehalogenases. *Phys. Chem. Chem. Phys.* **2017,** *19*, (8), 6090-6094.
138. Schmitz, R. P. H.; Wolf, J.; Habel, A.; Neumann, A.; Ploss, K.; Svatos, A.; Boland, W.; Diekert, G., Evidence for a Radical Mechanism of the Dechlorination of Chlorinated Propenes Mediated by the Tetrachloroethene Reductive Dehalogenase of Sulfurospirillum multivorans. *Environ. Sci. Technol.* **2007,** *41*, (21), 7370-7375.

139. Ji, L.; Wang, C.; Ji, S.; Kepp, K. P.; Paneth, P., Mechanism of Cobalamin-Mediated Reductive Dehalogenation of Chloroethylenes. *ACS Catalysis* **2017,** *7*, (8), 5294-5307.
140. Lesage, S.; Brown, S.; Millar, K., A different mechanism for the reductive dechlorination of chlorinated ethenes: Kinetic and spectroscopic evidence. *Environ. Sci. Technol.* **1998,** *32*, (15), 2264-2272.
141. Pratt, D. A.; Van Der Donk, W. A., On the role of alkylcobalamins in the vitamin B12-catalyzed reductive dehalogenation of perchloroethylene and trichloroethylene. *Chem. Commun.* **2006,** *0*, (5), 558-560.
142. Sessions, A. L., Isotope-ratio detection for gas chromatography. *J. Sep.Sci* **2006,** *29*, 1946-1961.
143. McKelvie, J. R.; Hyman, M. R.; Elsner, M.; Smith, C.; Aslett, D. M.; Lacrampe-Couloume, G.; Sherwood Lollar, B., Isotopic Fractionation of Methyl tert-Butyl Ether Suggests Different Initial Reaction Mechanisms during Aerobic Biodegradation. *Environ. Sci. Technol.* **2009,** *43*, (8), 2793-2799.
144. Hofstetter, T. B.; Berg, M., Assessing transformation processes of organic contaminants by compound-specific stable isotope analysis. *TrAC, Trends Anal. Chem.* **2011,** *30*, (4), 618-627.
145. Matthews, D. E.; Hayes, J. M., Isotope-Ratio-Monitoring Gas Chromatography-Mass Spectrometry. *Anal. Chem.* **1978,** *50*, (11), 1465-1473.
146. Uppal, R.; Incarvito, C. D.; Lakshmi, K. V.; Valentine, A. M., Aqueous Spectroscopy and Redox Properties of Carboxylate-Bound Titanium. *Inorg. Chem.* **2006,** *45*, (4), 1795-1804.
147. Lexa, D.; Saveant, J. M., The electrochemistry of vitamin B12. *Acc. Chem. Res.* **1983,** *16*, (7), 235-243.
148. Lexa, D.; Saveant, J. M.; Zickler, J., Electrochemistry of vitamin B12. 2. Redox and acid-base equilibria in the B12a/B12r system. *J. Am. Chem. Soc.* **1977,** *99*, (8), 2786-2790.
149. Gan, Y.; Yu, T.; Zhou, A.; Liu, Y.; Yu, K.; Han, L., Variability in the carbon isotope fractionation of trichloroethene on its reductive dechlorination by vitamin B12. *Environ. Sci.: Processes Impacts* **2014,** *16*, (8), 1882-1888.
150. Slater, G. F.; Sherwood Lollar, B.; Lesage, S.; Brown, S., Carbon isotope fractionation of PCE and TCE during dechlorination by vitamin B12. *Groundwater Monit. Rem.* **2003,** *23*, (4), 59-67.
151. Cichocka, D.; Siegert, M.; Imfeld, G.; Andert, J.; Beck, K.; Diekert, G.; Richnow, H.-H.; Nijenhuis, I., Factors controlling the carbon isotope fractionation of tetra- and trichloroethene during reductive dechlorination by Sulfurospirillum ssp. and Desulfitobacterium sp. strain PCE-S. *FEMS Microbiol. Ecol.* **2007,** *62*, (1), 98-107.
152. Nonnenberg, C.; van der Donk, W. A.; Zipse, H., Reductive Dechlorination of Trichloroethylene: A Computational Study. *J. Phys. Chem. A* **2002,** *106*, (37), 8708-8715.
153. Lexa, D.; Sayeant, J. M.; Zickler, J., Electrochemistry of vitamin B12. 5. Cyanocobalamins. *J. Am. Chem. Soc.* **1980,** *102*, (8), 2654-2663.
154. Rappoport, Z., Nucleophilic Vinylic Substitution. *Adv. Phys. Org. Chem.* **1969,** *7*, 1-114.
155. Pratt, D. A.; Van Der Donk, W. A., Theoretical investigations into the intermediacy of chlorinated vinylcobalamins in the reductive dehalogenation of chlorinated ethylenes. *J. Am. Chem. Soc.* **2005,** *127*, (1), 384-396.
156. Shey, J.; McGinley, C. M.; McCauley, K. M.; Dearth, A. S.; Young, B. T.; van der Donk, W. A., Mechanistic Investigation of a Novel Vitamin B12-Catalyzed Carbon-Carbon Bond Forming Reaction, the Reductive Dimerization of Arylalkenes. *J. Org. Chem.* **2002,** *67*, (3), 837-846.

157. Marlier, J. F., Multiple isotope effects on the acyl group transfer reactions of amides and esters. *Acc. Chem. Res.* **2001,** *34*, (4), 283-290.
158. Heckel, B.; Cretnik, S.; Kliegman, S.; Shouakar-Stash, O.; McNeill, K.; Elsner, M., Reductive Outer-Sphere Single Electron Transfer Is an Exception Rather than the Rule in Natural and Engineered Chlorinated Ethene Dehalogenation. *Environ. Sci. Technol.* **2017,** *51*, (17), 9663-9673.
159. Lee, M.; Wells, E.; Wong, Y. K.; Koenig, J.; Adrian, L.; Richnow, H. H.; Manefield, M., Relative Contributions of Dehalobacter and Zerovalent Iron in the Degradation of Chlorinated Methanes. *Environ. Sci. Technol.* **2015,** *49*, (7), 4481-4489.
160. Chan, C. C. H.; Mundle, S. O. C.; Eckert, T.; Liang, X.; Tang, S.; Lacrampe-Couloume, G.; Edwards, E. A.; Sherwood Lollar, B., Large Carbon Isotope Fractionation during Biodegradation of Chloroform by Dehalobacter Cultures. *Environ. Sci. Technol.* **2012,** *46*, (18), 10154-10160.
161. Churchill, D. G.; Janak, K. E.; Wittenberg, J. S.; Parkin, G., Normal and Inverse Primary Kinetic Deuterium Isotope Effects for C−H Bond Reductive Elimination and Oxidative Addition Reactions of Molybdenocene and Tungstenocene Complexes: Evidence for Benzene σ-Complex Intermediates. *J. Am. Chem. Soc.* **2003,** *125*, (5), 1403-1420.
162. Jones, W. D., Isotope Effects in C−H Bond Activation Reactions by Transition Metals. *Acc. Chem. Res.* **2003,** *36*, (2), 140-146.
163. Bengali, A. A.; Schultz, R. H.; Moore, C. B.; Bergman, R. G., Activation of the C-H Bonds in Neopentane and Neopentane-d12 by (.eta.5-C5(CH3)5)Rh(CO)2: Spectroscopic and Temporal Resolution of Rhodium-Krypton and Rhodium-Alkane Complex Intermediates. *J. Am. Chem. Soc.* **1994,** *116*, (21), 9585-9589.
164. Casey, C. P.; Singer, S. W.; Powell, D. R.; Hayashi, R. K.; Kavana, M., Hydrogen Transfer to Carbonyls and Imines from a Hydroxycyclopentadienyl Ruthenium Hydride: Evidence for Concerted Hydride and Proton Transfer. *J. Am. Chem. Soc.* **2001,** *123*, (6), 1090-1100.
165. Casey, C. P.; Johnson, J. B., Kinetic isotope effect evidence for the concerted transfer of hydride and proton from hydroxycyclopentadienyl ruthenium hydride in solvents of different polarities and hydrogen bonding ability. *Canadian Journal of Chemistry* **2005,** *83*, (9), 1339-1346.
166. Thalén, L. K.; Zhao, D.; Sortais, J.-B.; Paetzold, J.; Hoben, C.; Bäckvall, J.-E., A Chemoenzymatic Approach to Enantiomerically Pure Amines Using Dynamic Kinetic Resolution: Application to the Synthesis of Norsertraline. *Chem. - Eur. J.* **2009,** *15*, (14), 3403-3410.
167. Samec, J. S. M.; Bäckvall, J.-E., Ruthenium-Catalyzed Transfer Hydrogenation of Imines by Propan-2-ol in Benzene. *Chem. - Eur. J.* **2002,** *8*, (13), 2955-2961.
168. Whitesides, G. M.; Gaasch, J. F.; Stedronsky, E. R., Mechanism of thermal decomposition of dibutylbis(triphenylphosphine)platinum(II). *J. Am. Chem. Soc.* **1972,** *94*, (15), 5258-5270.
169. Alexanian, E. J.; Hartwig, J. F., Mechanistic Study of β-Hydrogen Elimination from Organoplatinum(II) Enolate Complexes. *J. Am. Chem. Soc.* **2008,** *130*, (46), 15627-15635.
170. Ljungdahl, T.; Bennur, T.; Dallas, A.; Emtenäs, H.; Mårtensson, J., Two Competing Mechanisms for the Copper-Free Sonogashira Cross-Coupling Reaction. *Organometallics* **2008,** *27*, (11), 2490-2498.
171. Shi, Z.; Li, B.; Wan, X.; Cheng, J.; Fang, Z.; Cao, B.; Qin, C.; Wang, Y., Suzuki–Miyaura Coupling Reaction by PdII-Catalyzed Aromatic C□H Bond Activation Directed by an N-Alkyl Acetamino Group. *Angewandte Chemie International Edition* **2007,** *46*, (29), 5554-5558.

172. Seregin, I. V.; Ryabova, V.; Gevorgyan, V., Direct Palladium-Catalyzed Alkynylation of N-Fused Heterocycles. *J. Am. Chem. Soc.* **2007,** *129*, (25), 7742-7743.
173. Mandal, A. B.; Lee, G.-H.; Liu, Y.-H.; Peng, S.-M.; Leung, M.-k., Formation of 4-Methylphenanthrenes in Palladium-Catalyzed Annulation of Diethyl 2,2‘-Diiodo-4,4‘-biphenyldicarboxylate with Internal Alkynes, Using Methyl Nitrobenzoates as the Methylating Agent. *J. Org. Chem.* **2000,** *65*, (2), 332-336.
174. Goj, L. A.; Widenhoefer, R. A., Mechanistic Studies of the Cycloisomerization of Dimethyl Diallylmalonate Catalyzed by a Cationic Palladium Phenanthroline Complex. *J. Am. Chem. Soc.* **2001,** *123*, (45), 11133-11147.
175. Takacs, J. M.; Clement, F.; Zhu, J.; Chandramouli, S. V.; Gong, X., Catalytic Palladium-Mediated Bisdiene Carbocyclizations: Bisdiene to Enediene Cycloisomerizations. *J. Am. Chem. Soc.* **1997,** *119*, (25), 5804-5817.
176. Cheong, P. H.-Y.; Morganelli, P.; Luzung, M. R.; Houk, K. N.; Toste, F. D., Gold-Catalyzed Cycloisomerization of 1,5-Allenynes via Dual Activation of an Ene Reaction. *J. Am. Chem. Soc.* **2008,** *130*, (13), 4517-4526.
177. Ragaini, F.; Rapetti, A.; Visentin, E.; Monzani, M.; Caselli, A.; Cenini, S., Synthesis of Indoles by Intermolecular Cyclization of Unfunctionalized Nitroarenes and Alkynes, Catalyzed by Palladium−Phenanthroline Complexes. *J. Org. Chem.* **2006,** *71*, (10), 3748-3753.
178. Yip, W.-P.; Yu, W.-Y.; Zhu, N.; Che, C.-M., Alkene cis-Dihydroxylation by [(Me3tacn)(CF3CO2)RuVIO2]ClO4 (Me3tacn = 1,4,7-Trimethyl-1,4,7-triazacyclononane): Structural Characterization of [3 + 2] Cycloadducts and Kinetic Studies. *J. Am. Chem. Soc.* **2005,** *127*, (41), 14239-14249.
179. Bernasconi, C. F.; Flores, F. X.; Kittredge, K. W., Physical Organic Chemistry of Transition Metal Carbene Complexes. 7.1 Kinetics of Hydrolysis of (CO)5MC(OR)Ph (M = Cr, W; R = Me, Et) and (CO)5Cr(OMe)CHCHPh in Aqueous Acetonitrile. *J. Am. Chem. Soc.* **1997,** *119*, (9), 2103-2110.
180. Bernasconi, C. F.; Leyes, A. E., Physical Organic Chemistry of Transition Metal Carbene Complexes. 9.1 Thermodynamic and Kinetic Acidity of (2-Oxacyclopentylidene)pentacarbonylchromium(0) in Aqueous Acetonitrile. *J. Am. Chem. Soc.* **1997,** *119*, (22), 5169-5175.
181. Chinchilla, R.; Nájera, C., The Sonogashira Reaction: A Booming Methodology in Synthetic Organic Chemistry. *Chemical Reviews* **2007,** *107*, (3), 874-922.
182. Wang, X.; Song, Y.; Qu, J.; Luo, Y., Mechanistic Insights into the Copper-Cocatalyzed Sonogashira Cross-Coupling Reaction: Key Role of an Anion. *Organometallics* **2017,** *36*, (5), 1042-1048.
183. Labinger, J. A., Tutorial on Oxidative Addition. *Organometallics* **2015,** *34*, (20), 4784-4795.

Curriculum Vitae

BENJAMIN MATTHÄUS HECKEL

born on 14th.of September 1986 in Füssen

QUALIFICATION

Since 01.2018	Postdoc at the Technical University Munich
	Investigating Reaction Mechanisms and Isotope Effects of Halogenated Hydrocarbons
	Specialization: Organic-Analytical Chemistry
2014-2017	PhD student at the Helmholtz-Center Munich
	Investigating Mechanisms of Reductive Chlorinated Hydrocarbon Degradation
	Specialization: Organic-Analytical Chemistry
	Supervisor: Prof. Dr. Martin Elsner
2010-2013	Postgraduate studies in Chemistry at the University Postdam
	Specialization: Organic & Polymer Chemistry
	Master Thesis at 3M Technical Ceramics (formerly ESK Ceramics) Topic:
	Synthese von Bornitrid über eine 2-Stufen-Synthese und eine Hoch-temperatur Direktsynthese.
	Supervisor: Prof. Dr. Andreas Taubert and Dr. Martin Engler
2007-2010	Undergraduate studies in Chemistry at the University Postdam
	Specialization: Organic & Polymer Chemistry
	Bachelor Thesis: Asymmetrische Photo-Dehydro-Diels-Alder Reaktion. Supervisor: Prof. Dr. Pablo Wessig
2006	A-level at the Gymnasium Füssen

2017: Heckel, B.; Rodríguez-Fernández, D.; Torrentó, C.; Meyer, A.; Palau, J.; Domènech, C.; Rosell, M.; Soler, A.; Hunkeler, D.; Elsner, M.; Compound-specific Chlorine Isotope Analysis of Tetrachloromethane and Trichloromethane by GC-IRMS vs. GC-qMS: Method Development and Evaluation of Precision and Trueness, *Anal. Chem.* **2017**, 89, 3411−3420

2017: Torrentó, C.; Palau, P.; Rodríguez-Fernández, D.; Heckel, B.; Meyer, A.; Domènech, C.; Rosell, M.; Soler, A.; Elsner, M.; Hunkeler, D.; Carbon and Chlorine Isotope Fractionation Patterns Associated with Different Engineered Chloroform Transformation Reactions, *Environ. Sci. Technol.* **2017**, 51 (11), 6174-6184

2017: Heckel, B.; Cretnik, S.; Kliegman, S.; Shouakar-Stash, O.; McNeill, K.; Elsner, M., Reductive Outer-Sphere Single Electron Transfer Is an Exception Rather than the Rule in Natural and Engineered Chlorinated Ethene Dehalogenation. *Environ. Sci. Technol.* **2017,** *51*, (17), 9663-9673.

2018: Heckel, B.; McNeill, K.; Elsner, M., Chlorinated Ethene Reactivity with Vitamin B12 Is Governed by Cobalamin Chloroethylcarbanions as Crossroads of Competing Pathways; *ACS Catal.* **2018**, 8, 3054−3066